



Are extracellular particles mediators of chemotherapy resistance in head and neck cancer?

Helal Ghadeer Alanazi

A thesis submitted in partial fulfilment of the requirements for the degree of
Doctor of Philosophy

The University of Sheffield

Faculty of Medicine, Dentistry and Health

School of Clinical Dentistry

November 2023

Acknowledgements

I would like to express my heartfelt gratitude to my late parents, whose unwavering support and prayers during their lifetime laid the foundation for all of my accomplishments. I would also like to express my deepest appreciation to my home country, Saudi Arabia, and my sponsor, Prince Sattam bin Abdulaziz University, whose generous support and funding were pivotal in my graduate studies journey.

I am immensely grateful to my supervisor, Dr. Stuart Hunt, whose steadfast guidance has been instrumental from the very beginning of my PhD journey. His commitment to regular weekly group meetings, monthly supervisory sessions, and an ever-welcoming open-door approach for his students has profoundly shaped my academic growth. Moreover, whenever research obstacles arose, Dr. Hunt's vast knowledge and experience have been a beacon, illuminating the path to solutions with unwavering patience and expertise. It is difficult to find words that truly encapsulate my appreciation for his enduring support and academic mentorship.

A special word of thanks goes to Dr. Helen Colley, my second supervisor, for her commitment and the considerable effort she made to provide support and sage advice, even during her own challenging times.

Many thanks to my academic advisor professor Daniel Lambert for his unlimited support.

My journey, which began in the USA in 2013 and culminates in the UK, would not have been the same without my supportive companions, who have been pillars of support. To my family, my wife Norah, and my children Lojain, Aleen, Sultan, Meshari, and Somow, your love and patience have been my constant source of strength. Norah, in particular, deserves special acknowledgment for her support and for caring for our family with such grace.

I must also express my heartfelt thanks to the Hunt's group—Dr. Karima, Dr. Wenyi, and Dr. Cathy for their encouragement and solidarity throughout this journey.

I am equally grateful to my friends and rest of my family in my back home, and my friends in the school, Faisal, Adel, and Alhassan for their ceaseless support, and to the technical team, Jason and Brenka, for their indispensable assistance.

A big thank you to my colleague, Dr. Asma Elhowati, for her willingness to lend a hand whenever needed, and to all the students on the third floor for fostering a positive and enjoyable atmosphere.

To everyone who has contributed to my journey, your collective support has been the bedrock of my success, and I am eternally grateful.

Abbreviations list

| Abbreviation | Definition |
|--------------|-----------------------------------------------------------------------|
| Δ HGS | Hepatocyte growth factor-regulated tyrosine kinase substrate knockout |
| Δ MVP | Major vault protein knockout |
| μ M | Micromolar |
| ANOVA | Analysis of variance |
| APAF1 | Apoptotic protease activating factor 1 |
| ASO | Antisense oligonucleotide |
| ATP | Adenosine triphosphate |
| BCA | Bovine serum albumin |
| BM | Bone marrow |
| BSA | Bovine serum albumin |
| CAFs | Cancer-associated fibroblasts |
| Cas9 | CRISPR-associated protein 9 |
| CDDP | Cisplatin |
| cDNA | Complementary DNA |
| CisplatinR | Cisplatin resistant cell line |
| CRISPR Cas9 | Clustered regularly interspaced short palindromic repeats |
| CTR1 | Copper transporter 1 |
| DMEM | Dulbecco Modified Eagle Medium |
| DMSO | Dimethyl sulfoxide |
| DNA | Deoxyribonucleic acid |
| DTX | Docetaxel |
| ECL | Enhanced Chemiluminescence |

| | |
|-------|--------------------------------------------------------------|
| ECM | Extracellular matrix |
| EDTA | Ethylenediaminetetraacetic acid |
| EMT | Epithelial to mesenchymal transition |
| EPs | Extracellular particles |
| ESCRT | Endosomal sorting complex required for transport |
| EVs | Extracellular vesicles |
| FBS | Foetal bovine serum |
| FLIP | FLICE-like inhibitory protein |
| FAK | Focal Adhesion Kinase |
| FU | Fluorouracil |
| GAPDH | Glyceraldehyde 3-phosphate dehydrogenase |
| GST | Glutathione S-transferases |
| HDL | High-Density Lipoproteins |
| HER-2 | Human epidermal growth factor receptor 2 |
| HGS | Hepatocyte growth factor-regulated tyrosine kinase substrate |
| HIV-1 | Human immunodeficiency virus-1 |
| HNC | Head and neck cancer |
| HNSCC | Head and neck squamous cell carcinoma |
| HPV | Human papillomavirus |
| HRP | Horseradish Peroxidase |
| IC50 | Half-maximal inhibitory concentration |
| IL | Interleukin |
| ILVs | Intraluminal vesicles |
| ISEV | International Society for Extracellular Vesicles |

| | |
|-----------|----------------------------------------------------------------|
| kDa | Kilodaltons |
| LDL | Low-Density Lipoproteins |
| LRP | Lung resistance-related protein |
| MHC | Major histocompatibility complex |
| MiRNAs | Small non-coding RNA molecules |
| MISEV2018 | Minimal information for studies of extracellular vesicles 2018 |
| MMR | Mismatch repair |
| mRNA | Messenger RNA |
| mTOR | Mechanistic target of rapamycin |
| MTT | 3-[4,5-dimethylthiazol-2-yl]-2,5 diphenyl tetrazolium bromide |
| MVB | Multivesicular bodies |
| MVE | Multivesicular endosome |
| MVP | Major vault protein |
| NaB | Sodium butyrate |
| NaCl | Sodium chloride |
| NER | Nucleotide excision repair |
| NTA | Nanoparticle Tracking Analysis |
| OSCC | Oral squamous cell carcinoma |
| PBS | Phosphate-buffered saline |
| PDAC | Pancreatic ductal adenocarcinoma |
| P-GP | P-glycoprotein |
| PI | Propidium iodide |
| PTKs | Protein tyrosine kinases |
| PS | phosphatidyl serine |

| | |
|----------|------------------------------------------------------------|
| qPCR | Quantitative polymerase chain reaction |
| RIPA | Radioimmunoprecipitation assay buffer |
| rRNA | Ribosomal RNA |
| RNA | Ribonucleic acid |
| RNase | Ribonucleases |
| RPMI | Roswell Park Memorial Institute |
| RT-PCR | Reverse transcription-polymerase chain reaction |
| SAGE | Serial analysis of gene expression |
| SDS-PAGE | Sodium dodecyl sulphate-polyacrylamide gel electrophoresis |
| siRNA | Small interfering RNA |
| SMVs | shed microvesicles |
| snRNP | Small nuclear ribonucleoproteins |
| SRPs | Signal recognition particles |
| STDV | Standard deviation |
| TBS | Tris-buffered saline |
| TBST | Tris-buffered saline Tween-20 |
| TEM | Transmission electron microscopy |
| TEMED | Tetramethyl ethylenediamine |
| TEP1 | Telomerase-associated protein 1 |
| TME | Tumour microenvironment |
| TracrRNA | Trans-activating crRNA |
| TSG101 | Tumour Susceptibility Gene 101 protein |
| UBAP1 | Ubiquitin associated protein 1 |
| UEV | Ubiquitin E2 variant |

| | |
|----------|----------------------------------------------------------|
| UF-dFBS | Ultra-filtered EV-depleted FBS |
| UIM | Ubiquitin interaction motif |
| UKEV | UK Society for Extracellular Vesicles |
| V-domain | V-central proline-rich domain |
| VE | Vascular endothelial |
| VEGF | Vascular endothelial growth factor |
| Vfa1 | Vps four-associated 1 |
| VHS | Vps-27, HGS and STAM |
| VPARP | Vault polymerase |
| Vps | Vacuolar protein sorting associated protein |
| VSE | Vps4 stimulatory element |
| VSL | Vta1 SBP1 LIP5 |
| Vta1 | Vacuolar protein sorting-associated protein Vta1 homolog |
| vtRNA | Vault RNA |
| WT | Wild type |
| ATM | Ataxia telangectasia |

| | |
|---------------------------------------------------------------------------|----------|
| Contents | |
| Abstract | 1 |
| Chapter 1 Introduction | 3 |
| 1.1 Head and neck cancer | 3 |
| 1.2 Oral squamous cell carcinoma | 4 |
| 1.3 Treatment of HNC | 5 |
| 1.3.1 Molecular mechanisms of cisplatin action against tumour cells. | 7 |
| 1.3.1.1 Apoptosis activation in cisplatin treated cancer cells | 8 |
| 1.3.2 Molecular mechanisms of resistance to cisplatin..... | 9 |
| 1.3.3 Tumour microenvironment and resistance to chemotherapy | 10 |
| 1.4 Extracellular Vesicles (EVs)..... | 12 |
| 1.4.1 Discovery of Extracellular vesicles | 12 |
| 1.4.2 Nomenclature of EVs..... | 13 |
| 1.4.3 Types of Extracellular Vesicles | 14 |
| 1.4.3.1 Exosomes | 14 |
| 1.4.3.2 Microvesicles (MVs) | 17 |
| 1.4.3.3 Apoptotic bodies | 18 |
| 1.4.4 Molecular cargo of EVs | 19 |
| 1.4.4.1 Lipid and carbohydrate | 19 |
| 1.4.4.2 Proteins | 20 |
| 1.4.4.3 Nucleic acid | 21 |
| 1.4.5 Function of EVs: | 22 |

| | |
|-----------------------------------------------------------------------------------|-----------|
| 1.4.5.1 Function of EVs in normal physiology | 22 |
| 1.4.5.2 Function of EVs in cancer..... | 24 |
| 1.4.6 Role of extracellular vesicles in resistance to chemotherapeutic drugs..... | 28 |
| 1.4.7 Other extracellular particles | 29 |
| 1.5 The vault particle | 30 |
| 1.5.1 Vault components | 32 |
| 1.5.2 The function of vaults | 32 |
| 1.5.2.1 MVP..... | 33 |
| 1.5.2.2 TEP1 | 36 |
| 1.5.2.3 PARP4..... | 36 |
| 1.5.2.4 Vault RNA | 37 |
| 1.6 Hypothesis and project aims | 39 |
| Chapter 2 Materials and methods | 40 |
| 2.1 General consumables | 40 |
| 2.2 Cell lines | 40 |
| 2.3 Cell culture and passage..... | 40 |
| 2.3.1 Cell counting | 41 |
| 2.3.2 Cell line storage | 41 |
| 2.3.3 Monolayer cell seeding | 42 |
| 2.4 Generating cisplatin resistant cell lines (Cisplatin ^R)..... | 42 |
| 2.5 Cisplatin treatment | 43 |

| | |
|----------------------------------------------------------------------------------------------------------|----|
| 2.6 MTT assay | 43 |
| 2.6.1 IC50 value | 44 |
| 2.7 Extracellular particle methods | 44 |
| 2.7.1 Preparation of EV-depleted FBS | 44 |
| 2.7.2 Cell culture conditioned medium | 45 |
| 2.7.3 Differential centrifugation | 45 |
| 2.7.4 Characterization of nanoparticles by nanoparticle tracking analysis..... | 46 |
| 2.8 Protein methods | 48 |
| 2.8.1 Protein harvesting: | 48 |
| 2.8.2 Protein quantification :..... | 49 |
| 2.8.3 Sodium dodecyl sulfate-polyacrylamide gel electrophoresis (SDS-PAGE) and protein transfer | 50 |
| 2.8.4 Western blotting:..... | 52 |
| 2.8.5 Membrane stripping and preservation: | 52 |
| 2.9 RNA methods..... | 53 |
| 2.9.1 RNA extraction: | 53 |
| 2.9.2 RNA quantification | 54 |
| 2.9.3 Reverse transcription | 54 |
| 2.9.3.1 Total RNA..... | 54 |
| 2.9.4 Quantitative polymerase chain reaction (qPCR)..... | 56 |
| 2.9.4.1 Multiplex qPCR for transcript expression | 56 |
| 2.9.4.2 Data analysis | 57 |

| | | |
|---------------------------------------------------------------------------------------|------------------------------------------------------------------------------------------------------------------------------------------|-----------|
| 2.10 | VtRNA1-1 antisense oligonucleotide transfection | 58 |
| 2.11 | Transmission electron microscopy: | 59 |
| 2.12 | Apoptosis detection by flow Cytometry: | 59 |
| 2.13 | Cell cycle phases detection by flow cytometry..... | 60 |
| 2.14 | Assessment of Cell Proliferation and doubling time | 61 |
| 2.15 | Statistical analysis | 62 |
| Chapter 3 Effect of cisplatin treatment on extracellular particle release..... | | 63 |
| 3.1 | Introduction:..... | 63 |
| 3.2 | Aim of this chapter: | 64 |
| 3.3 | Results..... | 65 |
| 3.3.1 | Cell line viability in response to cisplatin treatment..... | 65 |
| 3.3.2 | Determination of the IC50 values for the H357 and FaDu cell lines following a 24-hour and 48-hour incubation period with cisplatin. | 66 |
| 3.3.3 | Determination of the proportion of apoptotic HNC cells after treated with cisplatin. | 71 |
| 3.3.4 | FBS depletion by ultrafiltration: | 74 |
| 3.3.5 | Effect of cisplatin treatment on extracellular particles release from H357 and FaDu | 76 |
| 3.3.5.1 | Assessment of extracellular particle protein markers | 79 |
| 3.4 | Discussion | 81 |
| 3.4.1 | HNC cell viability in response to cisplatin treatment | 81 |
| 3.4.2 | Cisplatin-induced apoptosis in HNC cell lines | 83 |

| | |
|--------------------------------------------------------------------------------------------------------------------|------------|
| 3.4.3 Characterisation of extracellular particle release in HNC cell lines in response to cisplatin treatment..... | 87 |
| Chapter 4 Effect of blocking extracellular particle release on cisplatin sensitivity..... | 90 |
| 4.1 Introduction:..... | 90 |
| 4.2 Aim of this chapter: | 91 |
| 4.3 Results..... | 92 |
| 4.3.1 Validation of HGS knockout in H357 cell line by qPCR and western blotting | 92 |
| 4.3.2 Evaluating the growth rate and doubling time of WT and Δ HGS cell lines | 94 |
| 4.3.3 Determining live, apoptotic, and dead cells in response to cisplatin treatment after depletion of HGS | 101 |
| 4.3.4 Validation of MVP knockout in H357 cell line by qPCR and western blotting... | 105 |
| 4.3.5 Evaluating the growth rate and doubling time of WT and Δ MVP cell lines | 107 |
| 4.3.6 The impact of MVP depletion on cisplatin-induced extracellular particle release | 109 |
| 4.3.7 Determining live, apoptotic, and dead cells in response to cisplatin treatment after depletion of MVP..... | 114 |
| 4.3.8 vtRNA1-1 antisense knockdown in Δ MVP cell line | 118 |
| 4.4 Discussion..... | 120 |
| 4.4.1 Characterisation Δ HGS and Δ MVP cell lines..... | 120 |
| 4.4.2 Impact cisplatin treatment on Δ HGS and Δ MVP cell lines | 121 |
| Chapter 5 Are extracellular particles mediators of cisplatin resistance in head and neck cancer? | 125 |

| | |
|---------------------------------------------------------------------------------------------------------------------------------|------------|
| 5.1 Introduction..... | 125 |
| 5.2 Aim of this chapter: | 125 |
| 5.3 Results:..... | 127 |
| 5.3.1 Generation of a cisplatin resistant HNC cell line..... | 127 |
| 5.3.2 Characterisation of the cisplatin resistant cell line | 127 |
| 5.3.2.1 Cisplatin ^R cell morphology and growth characteristics | 127 |
| 5.3.2.2 Viability of cisplatin ^R and WT cell lines following cisplatin exposure..... | 129 |
| 5.3.2.3 Comparing live, apoptotic, and dead cells in response to cisplatin treatment in Cisplatin ^R and WT..... | 131 |
| 5.3.2.4 Analysis of cell cycle using flow cytometry | 134 |
| 5.3.2.5 Cellular mechanisms of cisplatin resistance | 136 |
| 5.3.2.6 Cellular expression of vault particle components and HGS | 138 |
| 5.3.3 Impact of cisplatin treatment on EP release from WT and cisplatin ^R cell lines .. | 140 |
| 5.3.4 Can EPs derived from cisplatin ^R HNC cells transfer cisplatin resistance?..... | 144 |
| 5.4 Discussion..... | 146 |
| 5.4.1 Cisplatin ^R cells show reduced proliferation rate | 146 |
| 5.4.2 Cisplatin ^R cell line has reduced sensitivity to cisplatin and reduced expression of CTR1 influx pump | 147 |
| 5.4.3 Cisplatin ^R cells release fewer EPs after cisplatin treatment..... | 148 |
| 5.4.4 EPs from cisplatin ^R HNC cells can transfer cisplatin resistance | 149 |
| Chapter 6 General Discussion: | 151 |
| 6.1 Extracellular particles and chemotherapy resistance | 151 |

| | |
|-----------------------------------------------------------------------------------------|------------|
| 6.2 Extracellular particles as targets to resensitize chemotherapy-resistant cells..... | 152 |
| 6.3 Monitoring Cancer Through Circulating Extracellular Vesicles | 153 |
| 6.4 Limitations and future work..... | 155 |
| 6.4.1 Limitations | 155 |
| 6.4.2 Future work | 156 |
| References:..... | 158 |

List of figures

| | |
|------------------------------------------------------------------------------------------------------------|-----|
| Figure 1.1. Cisplatin activation in aqueous solution..... | 7 |
| Figure 1.2 Tumour microenvironment..... | 12 |
| Figure 1.3 Extracellular vesicle biogenesis. | 16 |
| Figure 1.4 Model of protein sorting in MVB intraluminal vesicles. | 18 |
| Figure 1.5 The extracellular vesicle cargo..... | 22 |
| Figure 1.6 EVs transfer proteins and nucleic acid. | 24 |
| Figure 1.7 EVs are mediators of intercellular communication within the tumour microenvironment..... | 27 |
| Figure 1.8 Visualization and composition of vault particles. | 31 |
| Figure 2.1 Diagram illustrating differential centrifugation..... | 46 |
| Figure 3.1 Viability of H357 cell line after cisplatin treatment..... | 67 |
| Figure 3.2 Viability of FaDu cell line after cisplatin treatment. | 68 |
| Figure 3.3 Assessment of apoptosis in H357 cell line after cisplatin treatment. | 72 |
| Figure 3.4 Assessment of apoptosis in FaDu cell line after cisplatin treatment. | 73 |
| Figure 3.5 Depletion of particles from FBS..... | 75 |
| Figure 3.6 Impact of cisplatin on extracellular particle release in H357 cell line. | 77 |
| Figure 3.7 Impact of cisplatin on extracellular particle release in FaDu cell line. | 78 |
| Figure 3.8 Detection of EV and vault particle markers in EP pellets derived from H357 and FaDu cells. | 80 |
| Figure 4.1 Evaluating the successful knockout of HGS protein from the H357 cell line..... | 93 |
| Figure 4.2 Growth curve of H357 WT and Δ HGS cell lines. | 95 |
| Figure 4.3 Effect of HGS depletion on EP release post cisplatin treatment. | 98 |
| Figure 4.4 Detection of EV and vault particle markers present in EP pellets post cisplatin treatment. | 100 |

| | |
|--------------------------------------------------------------------------------------------------------------------------------------------|-----|
| Figure 4.5 Flow cytometry analysis of cisplatin-induced responses in H357WT and Δ HGS cell lines. | 104 |
| Figure 4.6 Evaluating the successful knockout of MVP protein from the H357 cell line. | 106 |
| Figure 4.7 Growth curve of H357 WT and Δ MVP cell lines. | 108 |
| Figure 4.8 Effect of MVP depletion on EP release post cisplatin treatment. | 111 |
| Figure 4.9 Detection of EV and vault particle markers present in EP pellets post cisplatin treatment. | 113 |
| Figure 4.10 Flow cytometry analysis of cisplatin-induced responses in H357 WT and Δ MVP cell lines. | 117 |
| Figure 4.11 Preliminary experiment to test efficiency of antisense oligonucleotide knockdown of vtRNA1-1 expression. | 119 |
| Figure 5.1 Morphology and growth characteristics of H357 WT and cisplatin ^R cell lines. . | 128 |
| Figure 5.2 Metabolic activity/cell viability assessment of cisplatin ^R and WT post cisplatin treatment. | 130 |
| Figure 5.3 Flow cytometry analysis of cisplatin-induced apoptosis in WT and cisplatin ^R cell lines. | 133 |
| Figure 5.4 Cell cycle analysis for WT and cisplatin ^R cell lines post cisplatin exposure. | 135 |
| Figure 5.5 Detection of proteins involved in cisplatin resistance by western blotting. | 137 |
| Figure 5.6 Cellular transcript expression of vault components and HGS..... | 139 |
| Figure 5.7 Impact of cisplatin treatment on EP release from cisplatin ^R and WT cell lines... | 141 |
| Figure 5.8 Detection of EV and vault particle markers derived from WT and cisplatin ^R cells following cisplatin treatment. | 143 |
| Figure 5.9 Investigation of role of extracellular particles in mediating cisplatin resistance. | 145 |

List of tables

| | |
|------------------------------------------------------------------------------------------------------------------------------|----|
| Table 1.1. HNC morbidity and mortality, combined from 185 countries of the world in 2018 (Bray et al, 2018). | 4 |
| Table 1.2 Categorisation of extracellular vesicle types. | 16 |
| Table 2.1 Setting of ZetaView instrument | 48 |
| Table 2.2 Composition of protein lysis buffer | 49 |
| Table 2.3 The components and quantity to make two 12% SDS-PAGE gels | 51 |
| Table 2.4 Buffers and reagents used in SDS-PAGE and western blotting | 51 |
| Table 2.5 Lists of antibodies used in western blotting..... | 53 |
| Table 2.6 Composition of RT-PCR master mix..... | 55 |
| Table 2.7 Setting of RT-PCR profile | 55 |
| Table 2.8 TaqMan probes used in this study | 56 |
| Table 2.9 Composition of Real-time PCR master mix | 57 |
| Table 2.10 Setting of Real-time PCR two-step cycling conditions | 57 |
| Table 2.11 ASO transfection reaction volumes per well of a 24-well plate | 58 |
| Table 2.12 Composition of Annexin V incubation reagent | 60 |
| Table 3.1 H357 IC ₁₀ , IC ₅₀ and IC ₉₀ values after 24-hour incubation with cisplatin..... | 69 |
| Table 3.2 H357 IC ₁₀ , IC ₅₀ and IC ₉₀ values after 48-hour incubation with cisplatin. | 69 |
| Table 3.3 FaDu IC ₁₀ , IC ₅₀ and IC ₉₀ values after 24-hour incubation with cisplatin. | 69 |
| Table 3.4 FaDu IC ₁₀ , IC ₅₀ and IC ₉₀ values after 48-hour incubation with cisplatin. | 70 |
| Table 3.5 Cisplatin concentrations that were chosen for experiments: | 70 |

Abstract

Head and neck cancer (HNC) is a term that describes malignancies that arise in areas such as the mouth and lips, larynx, pharynx, salivary glands, nose, paranasal sinus, and nasopharynx. HNC usually occurs after exposure to carcinogenic factors such as alcohol, tobacco, and human papilloma virus (HPV). Moreover, this type of cancer has a high recurrence rate at the primary site after treatment. Cisplatin is a cornerstone in the chemotherapeutic treatment of HNC, utilized for its ability to induce cancer cell death. However, resistance to cisplatin remains a significant challenge, reducing its efficacy. There is evidence that extracellular particles (EPs) such as extracellular vesicles (EVs) and vault particles mediate resistance to chemotherapy in some cancer types. However, little is known of their relative contribution, especially in HNC. Given the pivotal role of cisplatin in HNC treatment, it was hypothesized that EPs released from HNC cells exposed to cisplatin facilitate chemotherapy resistance by exporting cisplatin or by mediating intercellular communication with neighbouring cells. To test this hypothesis, MTT assay was used to determine the concentration of cisplatin required to reduce cell viability by 50% (IC₅₀) in H357 and FaDu HNC cell lines. EV deficient (H357 Δ HGS) and vault particle deficient (H357 Δ MVP) were utilised to explore their contribution to cisplatin resistance. A cisplatin-resistant H357 cell line (cisplatin^R) was generated by prolonged exposure to increasing concentrations of cisplatin, and putative proteins involved in resistance were quantified by western blotting. The proportion of cells undergoing apoptosis in response to cisplatin treatment was determined by flow cytometry. The concentration of EPs in cell line conditioned medium and ultracentrifugation pellets were determined by nanoparticle tracking analysis (NTA). EPs pellets were characterised by western blotting to detect EV (CD63 and TSG101) and vault particle (MVP) markers.

Apoptosis was triggered in the H357 cell line following treatment with cisplatin, but not in the FaDu cell line. Treatment of H357 with cisplatin also resulted in increased release of EPs, which included EV and vault particles. Despite releasing fewer EPs in response to cisplatin treatment, the EV deficient cell line (H357 Δ HGS) showed no significant difference in cisplatin sensitivity, whereas the vault particle deficient cell line (H357 Δ MVP) was more resistant to cisplatin treatment. The cisplatin^R

cell line showed increased viability and reduced apoptosis but released fewer EPs following cisplatin treatment.

The findings suggest that the differential release of EPs in response to cisplatin treatment might contribute to the variability in chemotherapy resistance among HNC cell lines. Specifically, vault particles may play a more crucial role than previously understood in mediating resistance to cisplatin. This insight into the mechanistic underpinnings of cisplatin resistance in HNC cells could guide the development of novel therapeutic strategies aimed at enhancing cisplatin sensitivity by targeting the release or function of specific EPs.

Chapter 1 Introduction

1.1 Head and neck cancer

Head and neck cancer (HNC) encompass a variety of tumours that typically arise from the squamous cells lining the mucosal surfaces within the head and neck region (Chow, 2020). These cancers commonly affect areas such as the nasal cavity, nasopharynx, paranasal sinuses, oral cavity, oropharynx, hypopharynx, larynx, lip, and salivary glands (summarised in Table 1.1) (Chow, 2020; Rezende et al., 2010). HNC was ranked as the seventh most prevalent cancer globally in 2018, comprising 3% of total cancer cases (Bray et al., 2018; Siegel et al., 2016). In the United Kingdom, there has been a significant increase of 33% in the incidence of these cancers since the early 1990s (Cancer Research UK, 2020). Data from 2017 showed 12,238 new cases, while deaths in 2018 numbered 4,077 as reported by Cancer Research UK (2018). Annually, HNCs account for about 2% of cancer-related mortalities globally (*Head and Neck Cancers Statistics*, 2017). Common signs of these malignancies may include a non-healing wound or sore, a neck lump, difficulty swallowing, or unexplained bleeding or pain. Established risk factors for HNC development include tobacco use, which increases the risk of oral cavity and pharynx cancers by 4-5 times and laryngeal cancers by 10 times compared to non-smokers (Johnson et al., 2020). Additional risks involve genetic factors, alcohol use, suboptimal nutrition, and infectious agents (Blot et al., 1988; Gillison et al., 2008; Goldenberg et al., 2004) Specifically, HPV type 16 has been implicated as an etiological factor for these cancers (zur Hausen & de Villiers, 1994). Within Europe, an estimated 73% of oropharyngeal cancer instances are attributed to HPV, and the virus is also present in 12% of cancers of the oral cavity, hypopharynx, and larynx (Mehanna et al., 2013).

Table 1.1. Rate of HNC morbidity and mortality cases in 2018, combined from 185 countries of the world (Bray et al, 2018).

| Cancer site | Morbidity in 2018 | Mortality in 2018 |
|------------------|-------------------|-------------------|
| Lip, oral cavity | 354,864 | 177,384 |
| Larynx | 177,422 | 94,771 |
| Nasopharynx | 129,079 | 72,987 |
| Oropharynx | 92,887 | 51,005 |
| Hypopharynx | 80,608 | 34,984 |
| Salivary glands | 52,799 | 22,176 |

1.2 Oral squamous cell carcinoma

Oral squamous cell carcinoma (OSCC) is the most common type among head and neck cancers, accounting for more than 90% of cases (Perdomo et al., 2016). OSCC can arise in any part of the oral cavity's mucosa, with the tongue and floor of the mouth being the most commonly affected areas (Duray et al., 2012; Kouketsu et al., 2016). OSCC predominately affects men who are in their fifties and sixties, and its risk is considerably increased by the use of tobacco, alcohol, and betel quid (Petti, 2009). Recent trends indicate a concerning increase in OSCC incidence among younger individuals. The exact impact of traditional risk factors such as tobacco and alcohol use within this age group remains elusive. This ambiguity might stem from the hypothesis that younger individuals have had less time to accumulate exposure to these risk factors, traditionally linked to OSCC development. Despite this, the rising incidence suggests that other elements, possibly including genetic predispositions, viral infections such as HPV, or novel environmental and lifestyle factors, might play a significant role. (Kaminagakura et al., 2012). Although HPV infection has a well-established link with oropharyngeal cancer, its role in OSCC development remains a subject of debate. High-risk HPV strains, particularly (HPV-16/18) have been more closely connected with OSCC, and the number of OSCC cases involving these HPV strains

has been increased (Jiang & Dong, 2017). The survival outcomes for individuals diagnosed with OSCC are disappointingly low, hovering between 50-60%, which is largely attributed to the advanced stage of the disease at the time of diagnosis, despite the presence of advanced therapeutic options such as surgical intervention, radiation therapy, and chemotherapy (Blatt et al., 2017).

1.3 Treatment of HNC

The management of head and neck cancer (HNC) typically necessitates a multidisciplinary approach, incorporating surgery, radiation, and chemotherapy. Chemotherapy plays a pivotal role in the treatment of patients with locally advanced forms of the disease, aiming to reduce tumour size and the risk of metastasis. Among various strategies, chemotherapy utilized as induction therapy or in conjunction with radiotherapy (chemo-radiotherapy) prior to definitive loco-regional therapy has shown promising outcomes. Numerous randomized trials have explored the efficacy of different combinations of chemotherapy and radiotherapy treatments, highlighting the significant role of such interventions in enhancing patient survival (Posner, 2005).

In the realm of induction chemotherapy, the combination of fluorouracil (FU) and cisplatin (CDDP) has been identified as beneficial for patients with locally advanced HNC, contributing to tumour reduction and a decreased metastatic rate. A landmark randomized trial further indicated that augmenting this regimen with docetaxel (DTX) – forming a TPF (docetaxel, cisplatin, and fluorouracil) induction chemotherapy – significantly improves survival outcomes compared to the standard FU and CDDP regimen, thus setting a new benchmark in HNC treatment (Lorch et al., 2011). Despite these advancements, challenges such as high rates of recurrence, metastasis, and mortality persist, partly due to the emergence of chemotherapy resistance, particularly against agents like CDDP.

A comprehensive longitudinal study over 6.0 years (72.2 months) has underscored the superiority of the TPF regimen over the standard PF (cisplatin and fluorouracil) treatment in managing head and neck cancer. The findings revealed that patients receiving TPF experienced significantly extended median survival times of 70.6 months (95% CI: 49.0–89.0 months) compared to 34.8 months

(95% CI: 22.6–48.0 months) for those on the PF regimen ($p=0.014$). The five-year overall survival (OS) rates further affirmed the efficacy of TPF, with 52% survival in the TPF group versus 42% in the PF group, translating to a 26% reduction in mortality risk (HR= 0.74, 95% CI: 0.58–0.94) (Lorch et al., 2011).

Additionally, progression-free survival (PFS) was markedly improved in the TPF-treated cohort, registering at 38.1 months (95% CI: 19.3–66.1 months) against 13.2 months in the PF group (95% CI: 10.6–20.7 months; HR= 0.75, 95% CI: 0.60–0.94). Subgroup analyses based on tumour location highlighted that patient with hypopharyngeal and laryngeal cancers benefited significantly from TPF, with improved OS and PFS (PFS HR= 0.68, 95% CI: 0.47–0.98), although the survival difference was not statistically significant ($p=0.11$), likely due to the role of salvage surgeries post-progression.

For individuals with oropharyngeal primary tumours, TPF demonstrated a significantly enhanced comparative survival benefit over time when juxtaposed with PF ($p=0.045$), where the median OS for PF stood at 64.7 months and was yet to be reached for the TPF arm (HR= 0.69, 95% CI: 0.48–0.99). No significant difference in OS was observed for patients with oral cavity tumours.

The study also revealed that TPF's benefits were particularly pronounced in patients with Stage IV tumours, showcasing a marked improvement in overall survival over a five-year period compared to the PF regimen ($p=0.03$). This distinct advantage was not observed among patients with Stage III disease ($p=0.26$), underscoring the importance of tailoring treatment strategies to individual patient profiles and disease characteristics (Lorch et al., 2011).

1.3.1 Molecular mechanisms of cisplatin action against tumour cells.

Cisplatin is an inorganic compound with square planar structure, which reacts with DNA to induce DNA damage or irreversible cell death. In its natural conformation, cisplatin is neutral and requires activation through a series of chemical transformation processes that involves the aquation of the cisplatin *cis*-chloro ligand position for it to interact with DNA (Figure 1.1) (Rezaee et al., 2013).

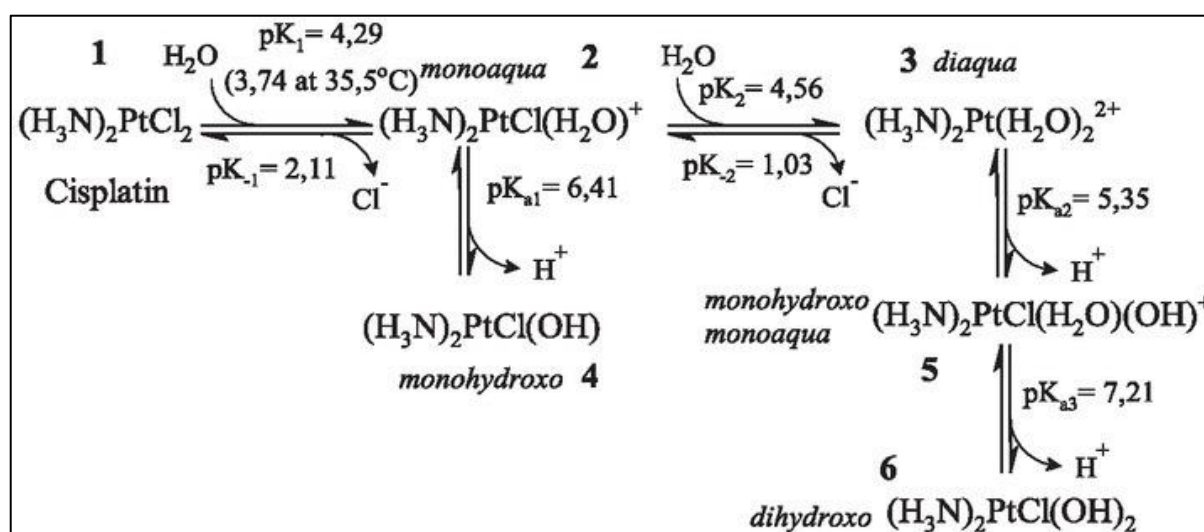


Figure 1.1. Cisplatin activation in aqueous solution.

Interaction between (1) cisplatin and water molecule cause displacement of one chloride ion to form a (2) mono-aqua derivative, the reaction is repeated for the second chloride forming (3) a di-aqua derivative due to the stronger bond formed between metal and nitrogen compared to the metal and chloride ion. The aqua species formed has high acidity at pH 7 causing complete deprotonation (4) as a monohydroxo and (6). Adapted from (Davies et al., 2000).

The aquation reaction is a spontaneous event taking place within the cytoplasm, aided by the low concentration of chloride ions. This results in the creation of highly reactive mono- and bi-aquated forms of cisplatin (Michalke, 2010). The toxicity of cisplatin to tumour cells can be attributed to the interaction between the nucleophilic nitrogen at position seven of the purine bases in DNA, leading to crosslinks within and between DNA strands, and forming DNA-DNA adducts and DNA-protein interactions (Siddik, 2003). Notably, the ApG and CpG crosslinks are the most recognised DNA lesions, primarily responsible for cisplatin-induced cytotoxicity. Furthermore, the reactivity of the aquated cisplatin molecule in the cytoplasm renders it susceptible to reactions with various endogenous

compounds, such as those involved in maintaining redox balance, thus inducing oxidative stress that also contributes to DNA damage (Wang et al., 2021).

DNA lesions or damage, like those caused by cisplatin, are repaired through different pathways. Examples include the nucleotide excision repair (NER) pathway, which is primarily responsible for removing cisplatin-induced DNA adducts, and the mismatch repair (MMR) pathway (Duan et al., 2020; H. Zhu et al., 2016). Typically, when a lesion is encountered, the cell cycle halts in the S and G2 phases, activating the DNA repair protein p53 and initiating the DNA damage response pathway to restore DNA integrity. In instances where the damage is extensive and irreparable, the cells within the tumor environment are destined for apoptotic cell death (Aubrey et al., 2018).

1.3.1.1 Apoptosis activation in cisplatin treated cancer cells

P53 is a short lived tumour suppressor that plays a central role in maintaining genome integrity. Upon treatment with cisplatin, the creation of DNA adducts and oxidative stress often lead to excessive DNA damage which signals activation of ataxia telangectasia (ATM) and Rad3-related (ATR) proteins, which leads to phosphorylation of p53. Once stabilised, p53 takes on the role of inducing the transcriptional expression of various proteins. These include cell cycle proteins like p21, pro-apoptotic proteins such as Bax, and DNA repair proteins such as GADD45 (Basu & Krishnamurthy, 2010). Moreover, it has been discovered that p53 induces apoptosis in cells treated with cisplatin by degrading FLICE-like inhibitory protein (FLIP), a protein typically known to bind death receptors and inhibit executioner caspases. Additionally, p53 associates with the anti-apoptotic/survival protein Bcl2, which has the effect of neutralising its activity in binding Bax, thus enhancing apoptosis (Abedini et al., 2010).

Beyond the activation of apoptosis mediated by p53, the tyrosine kinase c-Abl has a noteworthy part to play. It's capable of transitioning between the cytoplasm and nucleus in response to DNA damage caused by cytotoxic agents. Evidence from numerous studies has pointed out that for the induction of apoptosis resulting from DNA damage, the nuclear localisation of c-Abl is crucial (Barilà et al., 2003; Yoshida et al., 2005). Furthermore, c-Abl is implicated in cisplatin-induced apoptosis. Mice deficient in the nuclear signal of the c-Abl localisation motif were found to have reduced apoptosis in renal tubule cells where cisplatin was concentrated (Sridevi et al., 2013). Imatinib, an inhibitor of c-Abl, has also

been found to prevent cisplatin-induced apoptosis in both laboratory and living organism environments (Kim et al., 2013). All of these findings suggest that cisplatin appears to instigate the transition of c-Abl from the cytoplasm to the nucleus to provoke apoptosis.

1.3.2 Molecular mechanisms of resistance to cisplatin.

One of the underlying molecular mechanisms that give rise to CDDP resistance in tumour cells is a decrease in its intracellular bioavailability or accumulation. This is further enhanced by an increased sequestration of cisplatin by metallothioneins, glutathione, and other nucleophilic scavengers within the cytoplasm. The Copper transporter 1 (CTR1) is a transmembrane protein that facilitates the internal transport of cisplatin. This protein can boost the translocation of cisplatin into the cell and its cytotoxicity when copper is present. However, tumour cells have adapted to lower the expression of CTR1 under clinically relevant concentrations of cisplatin (Kalayda et al., 2012).

Furthermore, multidrug-resistant proteins such as MRP1, MRP2, and MRP3, with special emphasis on MRP2, are part of the ABC ATPase family of proteins that play a significant role in the efflux of cisplatin out of cancer cells. There have been previous reports indicating that the expression level of MRP2 could serve as a prognostic factor in assessing the cancer cell response to cisplatin treatment (Korita et al., 2010; Yamasaki et al., 2011). Additionally, copper-extruding P-type ATPases, ATP7A and ATP7B, are another set of proteins found to be upregulated in cisplatin-resistant cancer cells (Huo et al., 2016).

As stated earlier, the reactivity of aquated cisplatin allows for a nucleophilic attack by cytoplasmic molecules such as GSH and metallothioneins, leading to the sequestration of cisplatin out of the cytoplasm. This has been observed in cisplatin-resistant cancer cells derived from ovarian cancer patients before and after the acquisition of resistance (Ishikawa, 1992).

Alongside these mechanisms that predispose cisplatin for sequestration, there are proteins that identify DNA adducts of all types and trigger DNA repair pathways for the cell to recover genomic integrity. However, these proteins and their associated pathways often exhibit hyperactivation in

cisplatin resistance, granting the cells the capacity to repair the damage rapidly or withstand a high level of damage without initiating any apoptotic mechanisms (Galluzzi et al., 2018). For example, the excision repair cross-complementing rodent repair deficiency, complementation group 1 (ERCC1), is a DNA endonuclease in the NER pathway that, in conjunction with ERCC4, forms a heterodimer that excises DNA at the 5' of cisplatin-induced DNA adducts. The expression of ERCC1 has been shown to positively correlate with NER proficiency and negatively correlate with cancer cell survival in various cancers (Galluzzi et al., 2018). Moreover, ERCC1 is involved in DNA inter-strand adduct repair, which is found to be deficient in cisplatin-sensitive cells but enhanced in cisplatin-resistant tumour cells (Usanova et al., 2010).

1.3.3 Tumour microenvironment and resistance to chemotherapy

The tumour microenvironment (TME) is a multi-faceted ecosystem of various cell types, including tumour cells, immune cells, fibroblasts, and extracellular components, such as growth factors, enzymes, and signalling molecules (Figure 1.2) (Hinshaw & Shevde, 2019). What influences tumour fate is the relationships between all these various components of the TME. The tissue architecture is characterised by interactions between extracellular matrix (ECM) and cell. The TME therefore modulates the typical architecture by signalling the progress of tumours and metastases through cell adhesion molecules, tissue reshaping via metalloproteinases, as well as the hypoxic environment (Lunt et al., 2009). The TME's role in the progression of tumours, metastasis and therapy resistance is well demonstrated in the literature (Son et al., 2016). ECM has been proposed to provide protection against apoptosis induced by chemotherapy in small cell lung cancer and other cancers (Hazlehurst & Dalton, 2001). It has been suggested that integrin-mediated signal transduction, including Protein Tyrosine Kinases (PTKs)-dependent mechanisms, may provide protection against apoptosis through activation by an ECM ligand. The TME promotes the interaction of cancer cells and stromal cells, resulting in appropriate ECM interactions. Excessive accumulation of dense and rigid ECM, which often encapsulates tumour cell clusters and may serve as a shield, is thought to protect the cells from therapeutic agents. This effect is directly associated with a decreased supply of oxygen, nutrients, and metabolites, which are affected by this barrier. Increased hypoxia and metabolic stress contribute to pathways that trigger anti-apoptotic

and drug resistance mechanisms. Finally, through integrin and Focal Adhesion Kinase (FAK)-signalling, cell-ECM interaction and increased tissue stiffness can directly contribute to tumour chemoresistance (Henke et al., 2020). Clearly, a greater understanding of the molecular mechanisms contributing to cisplatin resistance will provide targets for agents that can modulate cisplatin resistance and improve chemotherapy efficacy (Sherman-Baust et al., 2003). Serial analysis of gene expression (SAGE) revealed a large number of genes that are expressed in response to cisplatin resistance. Collagen VI, an ECM protein with growth factor-like properties, is abundantly expressed in cisplatin-resistant cells which has been shown *in vitro* to significantly increase cisplatin resistance in ovarian cancer cells. Importantly, ovarian tumour staining with a collagen VI antibody reveals areas of high concentration of collagen VI *in vivo* and shows that the tumour cells express collagen VI. Collagen VI RNA levels in tumours have been associated with tumour grade, a predictor of prognosis in ovarian cancer. These results indicate that in the presence of chemotherapeutic drugs, tumour cells may modulate their microenvironment to favour survival (Sherman-Baust et al., 2003). Cellular communication in the TME is accomplished by various signalling networks, including paracrine and juxtacrine interactions (Li & Nabet, 2019). Paracrine signalling includes the production of secreted molecules such as cytokines, growth factors, chemokines and extracellular vesicles (EVs) (Li & Nabet, 2019; Milane et al., 2015). EVs are membrane-enclosed particles that contain proteins, nucleic acids and metabolites (Leidal & Debnath, 2020), which act as signalling agents to modulate the TME. EVs, with their capacity to alter the TME and distant sites, play a major role in tumour progression and metastasis (Kahlert & Kalluri, 2013).

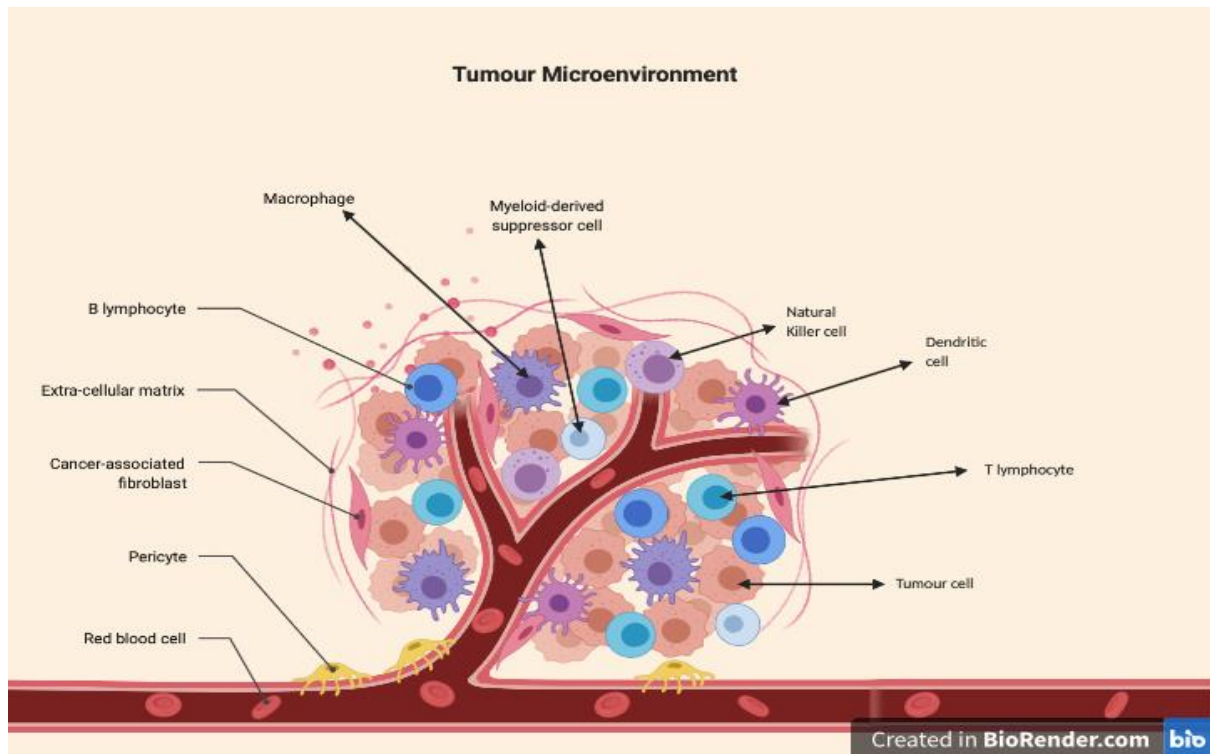


Figure 1.2 Tumour microenvironment.

Tumours include neoplastic cells, immune, stromal and endothelial cells found in an extracellular matrix, coexisting together. The tumour niche is a complex system of vascular supply and exposure to numerous growth factors (Illustration generated using Biorender software).

1.4 Extracellular Vesicles (EVs)

1.4.1 Discovery of Extracellular vesicles

The consensus in the scientific community is that extracellular vesicles (EVs) were first identified by a scientist named Rosemary Johnston in 1987. Johnston's work was focused on examining the behaviour of the transferrin receptor during the development of reticulocytes in sheep. Employing methods like transmission electron microscopy (TEM) and immunogold labelling, she provided evidence showing the transfer of receptors from the cell membrane into multivesicular bodies (MVBs). Subsequently, as these MVBs fused with the cell's plasma membrane, the receptors were released from the cell in the form of vesicles. (Johnstone et al., 1987). This is often thought of as the start of a newly discovered field of research. However, the term "exosomes" was used for the first time in a 1981 study to describe vesicles with diameters between 500 and 1000 nm, which were also accompanied by small

vesicles with diameter of 40 nm (Trams et al., 1981). The authors suggested that all vesicles would be called exosomes. After initially being thought of as a cellular waste disposal system, EVs were recognised to have an important role in intercellular transfer of mRNA and miRNA (Ratajczak et al., 2006; Valadi et al., 2007). A pivotal advancement in the study of extracellular vesicles (EVs) occurred with the finding that cancer cells emit a substantially higher volume of EVs compared to non-cancerous cells (Logozzi et al., 2009; Taylor et al., 2008). This discovery has propelled a surge in EV research, with a growing body of investigators exploring the roles of EVs in various aspects of health and disease.

1.4.2 Nomenclature of EVs

EVs are discharged into the extracellular environment from many different cell types that have been studied (Théry et al., 2001), including but not limited to: cytotoxic T cells, B lymphocytes (Harding et al., 2013), and neoplastic cells (van Niel et al., 2001). The nomenclature in the field of EV research can be complicated, with some researchers naming EVs based on their cell or tissue origin. For example, cardiosomes are released from cardiomyocytes (Chaturvedi et al., 2015), prostate cell-derived exosomes are called prostrasomes (Vlaeminck-Guillem, 2018), immunogenic EVs are called tolerosomes, and cancer-derived EVs are known as oncosomes (Minciacchi et al., 2015). More recently the International Society for Extracellular Vesicles (ISEV) has supported the use of a common EV nomenclature (Théry et al., 2018). One of the main challenges in the field is the overlapping size and other physical properties of EV subpopulations, as current abilities to isolate them from the biological fluids or cell culture medium are unable to produce pure populations of the various EV types. In the most recent ISEV position paper, researchers are encouraged to use operational terminology for EV subtypes referring to physical characteristics of EVs, such as size (small EVs (sEVs), medium EVs (mEVs), and large EVs (lEVs)) and biological structure (CD63, CD81, Annexin A5-positive EVs etc.). According to conditions or source of the cells (hypoxic EVs, podocyte EVs, apoptotic bodies, large oncosomes) ought to replace terms such as microvesicles and exosomes. (Théry et al., 2018). ISEV has recommended that the term EVs should be used where the biogenesis is unknown.

1.4.3 Types of Extracellular Vesicles

The literature refers to several types of EVs. However, according to their biogenesis, three different subpopulations of EVs exist: exosomes, microvesicles and apoptotic bodies/EVs (Figure 1.3). Also, see table 1.2 for a summary of physical EV characteristics.

1.4.3.1 Exosomes

Originally, the term "exosomes" referred to vesicles of various sizes (40-1000 nm) produced by cells (Trams et al., 1981) and smaller vesicles (30-100 nm) derived from endosomes (Johnstone et al., 1987). Safaei et al. (2005b) suggested a size range of 50 nm to 200 nm for exosomes. For a long time, exosomes were believed to have a cup-shaped morphology when viewed by TEM (Rapooso et al., 1996). However, later studies using cryo-electron microscopy revealed a spherical shape (Almgren et al., 2000), with the cup shape being an artifact caused by drying during TEM sample preparation (Conde-Vancells et al., 2008). Exosome density has been determined to be between 1.13 g/ml to 1.19 g/ml (Escola et al., 1998; Raposo et al., 1996), although Theyry et al. (2001) reported a density range of 1.10 g/ml to 1.21 g/ml. Recently, exomeres, a new type of particle potentially related to EVs, have been identified, ranging between 30 and 50 nm and possibly contaminating exosome preparations (Chen et al., 2019).

Exosomes are generated through the multivesicular body/endosome (MVB/MVE) pathway, with the Endosomal Sorting Complex Required for Transport (ESCRT) playing a crucial role in their biogenesis (Figure 1.4). Typically, proteins are mono-ubiquitinated to be recognized by ESCRT-0 machinery, and proteins from ESCRT-I, II, and III are sequentially recruited to the early endosomal membrane, where they regulate cargo loading and membrane invagination to form intraluminal vesicles

(Y. Zhang et al., 2019). The resulting MVB can either be trafficked to the lysosome for degradation or fuse with the plasma membrane to release exosomes (Figure 1.6) (Yellon & Davidson, 2014).

Table 1.2 Categorisation of extracellular vesicle types.

The table summarizes characteristics commonly used to classify EVs. Listed are the three types of EVs that are most studied. Adapted from Théry et al. (2009).

| Feature | Exosomes | Microvesicles | Apoptotic bodies |
|-----------------------------------|---------------|-----------------|-------------------------------|
| Size | 50-150 nm | 100-1000 nm | 50-1000 nm |
| Density | 1.13-1.19g/mL | ND | 1.16-1.28 g/mL |
| Appearance by electron microscope | Cup shape | Irregular shape | Heterogenous |
| Sedimentation | 100,000 g | 10,000 g | 1200 g, 10,000 g or 100,000 g |
| Intracellular origin | Endosomes | Plasma membrane | ND |

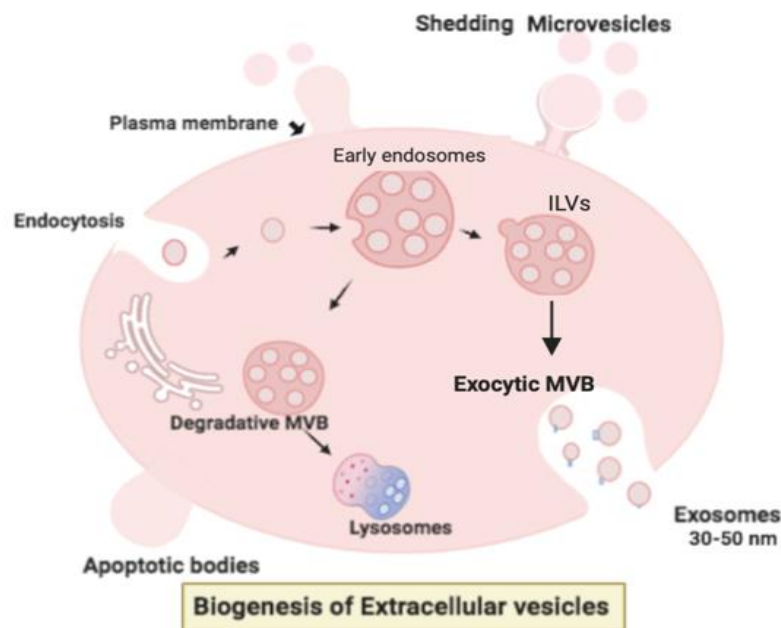


Figure 1.3 Extracellular vesicle biogenesis.

Microvesicles (MVs) are generated through the outward budding of the cell's plasma membrane. While exosomes originate as small vesicles that are created from the inward folding of the membrane of early endosomes, which contain intraluminal vesicles (ILVs), ultimately leading to the formation of multivesicular bodies (MVBs). These MVBs can either fuse with the plasma membrane, discharging the ILVs as exosomes into the extracellular milieu, or they can converge with lysosomes where they are degraded. In the context of cell death through apoptosis, the resultant vesicles are referred to as apoptotic bodies or EVs. Created with BioRender.com.

Exosomes can also form in the absence of ESCRT. Although ESCRT-independent mechanisms are not well-defined, mammalian cells lacking main ESCRT components can still form MVBs and exosomes (Stuffers et al., 2009). These mechanisms rely on lipids, often investigated through disrupting lipid biogenesis, such as ceramide (Trajkovic et al., 2008). Exosomes are rich in cholesterol, an essential component of MVBs. ESCRT-independent MVB formation is supported by evidence that cells depleted of four ESCRT subunits can still produce CD63-positive MVBs (Stuffers et al., 2009). However, it remains unclear whether MVBs designated for degradation or fusion with the plasma membrane are distinct forms of MVBs. This biogenesis cycle from MVBs is typical only for exosomes.

1.4.3.2 Microvesicles (MVs)

Microvesicles, also known as shedding vesicles, microparticles or ectosomes, have diameters ranging from 100-1000 nm and are generated through the regulated release of the plasma membrane via outward budding (Cocucci et al., 2009; EL Andaloussi et al., 2013). Microvesicle density is not well-defined (Castellana et al., 2009), but they are estimated to sediment at centrifugal speeds of 10,000 xg (Heijnen et al., 1999). They appear heterogeneous in morphology when observed by TEM (Antonyak et al., 2011; Heijnen et al., 1999). The biogenesis of microvesicles differs from that of exosomes. Generally, local lipids and proteins are redistributed as a result of the plasma membrane's external blebbing, this process is accompanied by a perpendicular repositioning and concentration of protein and nucleic acid contents within the area of the emerging microvesicle. (Figure 1.6). However, the molecular mechanisms behind this process remain unclear (D'Souza-Schorey & Clancy, 2012). Microvesicle biogenesis starts with membrane curvature, which is potentially induced at the site of the future microvesicle by protein-driven local forces (Muralidharan-Chari et al., 2010). The generation of membrane curvature is thought to stem from the accumulation of proteins, where the interplay among these proteins exerts a force that facilitates the bending of the membrane (Stachowiak et al., 2012). Notably, proteins that are part of the endosomal system and the ESCRT (Endosomal Sorting Complex Required for Transport) machinery have been associated with the formation of microvesicles.

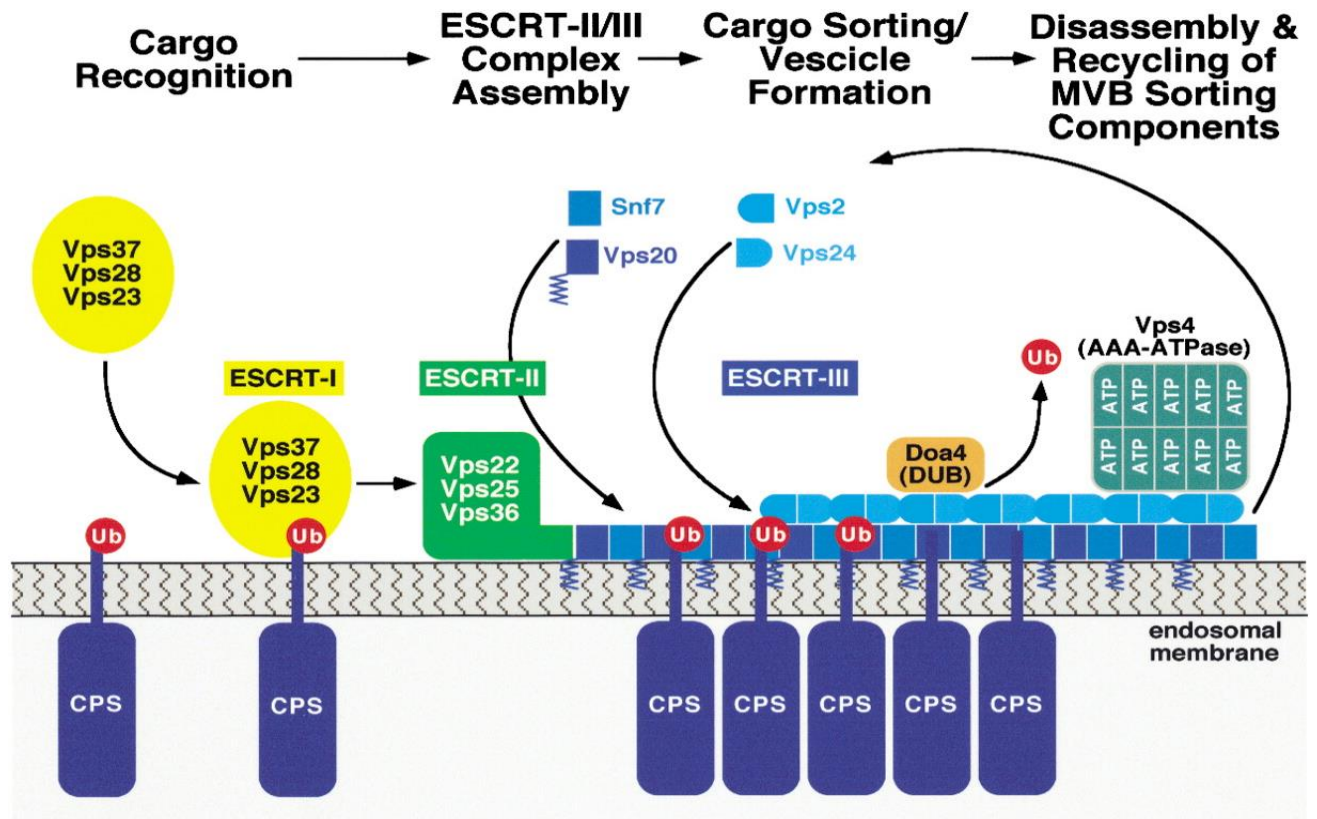


Figure 1.4 Model of protein sorting in MVB intraluminal vesicles.

Within the endosome, ESCRT-I identifies the ubiquitinated CPS, subsequently activating the function of ESCRT-II in assembling and oligomerizing the small coiled-coil proteins, leading to the formation of ESCRT-III. This ESCRT-III protein assembly then segregates and concentrates CPS into a specific endosomal subdomain, which subsequently invaginates to produce a vesicle. The deubiquitinating enzyme, Doa4, associates with ESCRT-III, facilitating the removal of the ubiquitin label from the cargo before its incorporation into the MVB vesicle. Once MVB sorting concludes, the AAA-type ATPase Vps4 is drawn to ESCRT-III, causing the protein complex to detach from the membrane. Taken from (Babst et al., 2002).

1.4.3.3 Apoptotic bodies

Cells undergoing apoptosis exclusively release apoptotic bodies, also known as EVs, which are noticeably larger and exhibit more variability in size, ranging from 100 to 5000 nm. These structures are packed with pieces of genomic DNA, cellular cytoplasm, and organelles. It's been proposed that apoptotic bodies may serve to transport "find-me" and "eat-me" signals from dying cells, thereby recruiting macrophages and immature phagocytes to facilitate the process of cellular clearance (Depraetere, 2000; Ravichandran, 2010). Local phagocytosis, driven by macrophage receptors, is also a pathway for the clearance of these bodies (Savill, 1997). The signals dispatched may comprise various

chemokines, such as C-X3-C motif chemokine ligand 1, and nucleotides like ATP and uridine 5' triphosphate (Elliott et al., 2009; Truman et al., 2008).

A pivotal change in the membrane of apoptotic cells is the translocation of phosphatidylserine to the external layer of the lipid bilayer, marking the cells for Annexin V binding and aiding in their recognition by phagocytes (Martínez & Freyssinet, 2001). Additionally, alterations at the membrane's surface include the exposure of thrombospondin and C3b binding sites (Friedl et al., 2002; Takizawa et al., 1996), which along with Annexin V are now established as standard markers for identifying apoptotic bodies.

Apoptotic bodies are a heterogeneous group, believed to consist of at least two main subsets (Hauser et al., 2017). Considering their more random packaging of contents, some apoptotic bodies may be more nucleotide-rich while others may primarily encase cytoplasm, leading to variations in density and distinctive sets of markers that can be detected. Such variability underscores the need for nuanced methods in their separation and identification. Their significant size disparity means that apoptotic bodies often might be isolated alongside other EV types due to co-purification.

1.4.4 Molecular cargo of EVs

Despite there being EV subtypes, many studies have shown that they contain similar molecular cargo, which are sorted into the EV during biogenesis (Johnstone, 2006; Théry et al., 2002), namely lipids, proteins, and nucleic acids (Figure 1.5).

1.4.4.1 Lipid and carbohydrate

EV membranes are composed of lipids such as cholesterol, sphingolipid, phosphoglyceride, ceramide, and phosphatidylserine (Zheng et al., 2014). Although their structure and sizes may vary, their composition is generally representative of the parent cells. As such, the cholesterol-to-phospholipid ratio in vesicle membranes is similar to that of the cell membrane (Vidal et al., 1989). Nonetheless, specific differences exist, such as the lack of enrichment with lysophosphatidic acid in the lipid bilayer, which is often associated with MVBs where exosomes are generated (Brouwers et al., 2013; Llorente et al., 2013). EVs also contain numerous carbohydrates, including polylectosamine,

mannose, glycoprotein, and glycan (Batista et al., 2011). The distribution of lipids in vesicle membranes closely resembles that of lipid rafts, which are implicated in exosome formation (Matsuo et al., 2004). A comparison of the physical properties of EV membranes and cell membranes using techniques such as fluorescence anisotropy, nuclear magnetic resonance, and electron spin resonance has revealed that the membranes of these vesicles exhibit increased fluidity and rapid "flip-flop" motion between layers (Brouwers et al., 2013).

1.4.4.2 Proteins

EVs can carry active proteins and enzymes, as well as membrane trafficking and CD antigen proteins like CD9, CD63, CD81, and CD82 (Andreu & Yáñez-Mó, 2014). Notably, they contain major histocompatibility complexes (MHC) such as MHC class I and II, fusion proteins (annexins, GTPases, and flotillin), heat-shock proteins (Hsp70, Hsp90), ESCRT subunits, proteins involved in MVB biogenesis (TSG101, Alix), and lipid-related proteins and phospholipases (Zheng et al., 2014). The specific cargo packaging likely requires some guiding machinery, but our understanding of such a system remains incomplete. Analysing this system is challenging due to the heterogeneity of vesicles and variations in their production throughout a cell's life cycle. One study by Tauro et al.'s investigation into extracellular vesicles from the LIM1863 colon carcinoma cell line reveals the release of two exosome populations with distinct origins, basolateral and apical. Using immunocapture methods, they distinguish these groups by their unique protein compositions, with basolateral vesicles featuring proteins like early endosome antigen 1 and ADP-ribosylation factor, and apical vesicles containing markers such as CD63 and mucin 13. This differentiation suggests a sophisticated form of cellular messaging, potentially enabling targeted communication with specific cells or tissues. (Tauro et al., 2013).

Biogenesis of all vesicle types begins with plasma membrane modifications. The concept of lipid rafting is a potential mechanism for the arrangement of certain areas and their associated membrane proteins. Proteins such as stomatin, GM1, and flotillin-1 have been linked to the lipid raft areas identified in vesicles (Gassart et al., 2003). The occurrence of post-translational modification within vesicles strongly supports the existence of a deliberate sorting mechanism since rafts interact

with various protein forms. The idea of rafts exchanging membrane properties, which enables the curvature attributes necessary for vesicle formation, might suggest that entire rafts are incorporated into vesicles, carrying their anchored proteins as well (Gassart et al., 2003).

Ubiquitination is the most common method for cells to transport proteins through degradation pathways, typically by packaging them into lysosome-bound vesicles with the assistance of ESCRT complexes (Figure 1.4). One study investigating the ubiquitination role in EV proteins found that MHC-II complexes are not ubiquitinated (Gauvreau et al., 2009), implying the existence of two distinct mechanisms for protein sorting into MVBs. Further research indicated that immature dendritic cells use the ubiquitin-dependent process, leading to receptor degradation. In contrast, after cell activation, the ubiquitin-independent strategy was employed, and vesicles carrying the MHC-II complex that could interact with T cells were released from the cells (Buschow et al., 2009).

1.4.4.3 Nucleic acid

EVs are believed to carry substantial amounts of nucleic acids, necessitating a unique mechanism for packaging them into vesicles (Bhome et al., 2018). Various sized vesicles were separated using serial centrifugation, revealing that apoptotic bodies contained high concentrations of ribosomal RNA (rRNA), while exosomes held small amounts and microvesicles had negligible quantities (Crescitelli et al., 2013). These differences not only indicated the presence of a preferential packaging system but also encouraged further differentiation among vesicle subtypes.

Vesicular nucleic acids primarily consist of RNA, including microRNA (miRNA) and messenger RNA (mRNA) molecules. MiRNAs are small non-coding RNA molecules involved in post-transcriptional gene regulation and are frequently dysregulated in numerous diseases, including cancer (Kosaka et al., 2013). Sequence cluster analysis led to the hypothesis that RNA contains a signalling motif necessary for vesicle-mediated release from cells. This hypothesis has recently been demonstrated for miRNA, with specific signal motifs (GGAG and CCCU) commonly identified in miRNAs exported in EVs (Bhome et al., 2018) , as well as several longer motifs found in miRNAs enriched in cells (Villarroya-Beltri et al., 2013).

Moreover, it was shown that the ribonuclear protein hnRNP A2B1 could recognize this motif, possibly sorting these miRNAs into vesicles once they have been sumoylated (Villarroya-Beltri et al., 2013). However, an alternative mechanism has been proposed, in which endogenous RNAs modulate miRNA packaging into vesicles (Squadrito et al., 2014). Thus, it is plausible that multiple sorting mechanisms exist.

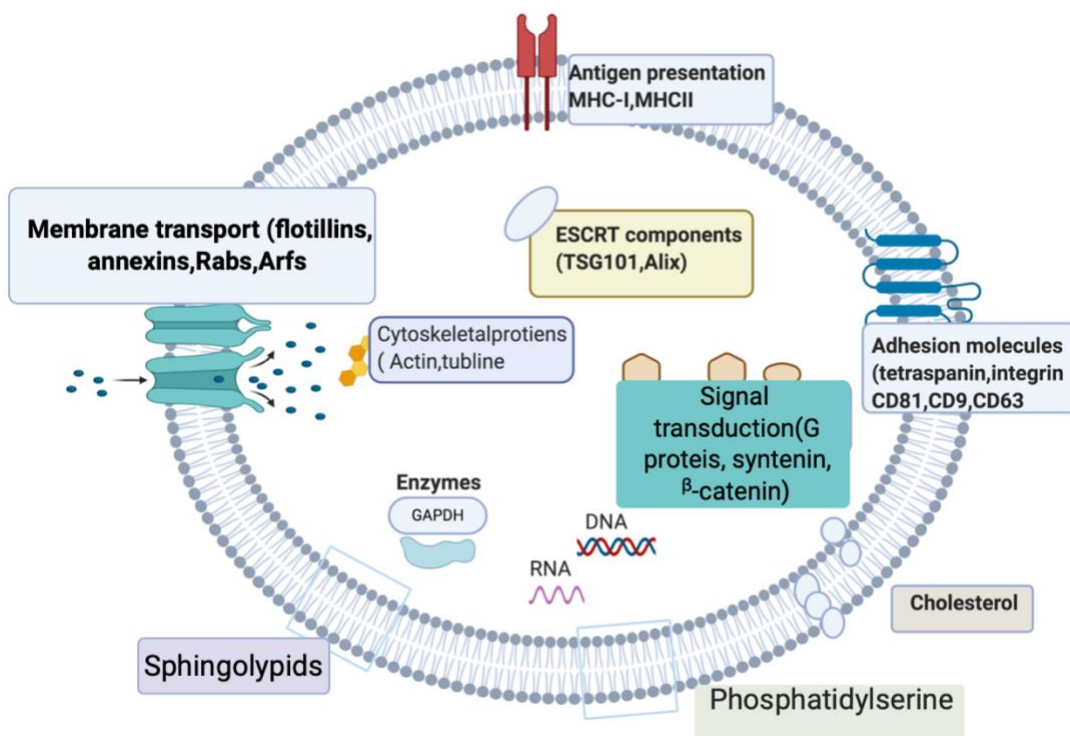


Figure 1.5 The extracellular vesicle cargo.

EVs contain a wide variety of molecular cargo including protein, lipid, and nucleic acid. Created with BioRender.com

1.4.5 Function of EVs:

1.4.5.1 Function of EVs in normal physiology

EVs have been found in various biological fluids, such as cerebrospinal fluid (Marzesco et al., 2005; Street et al., 2012), saliva (Palanisamy et al., 2010), blood (Alberro et al., 2021), bronchoalveolar fluid (Admyre et al., 2003), urine (Sato et al., 1990), nasal fluid (Lässer et al., 2011), and synovial fluid (György et al., 2012). The presence of EVs in diverse body fluids suggests their involvement in

numerous normal processes. For example, urinary EVs have been implicated in the elimination of lipids and various cellular proteins (van Balkom et al., 2011) and potentially play a role in signalling along nephrons (Knepper & Pisitkun, 2007).

Berckmans et al. (2011) found that EVs transfer tissue factor in saliva, which could lead to blood clotting, indicating that EVs may be an evolutionary mechanism involved in wound healing (Berckmans et al., 2011). EVs isolated from synovial fluid have been proposed as key mediators and suppliers of molecules necessary for cell surface adhesion (Skriner et al., 2006). EVs can also transport proteins essential for the male reproductive system (Sullivan et al., 2005) and contribute to the transfer of immunity from mother to developing foetus. Immunocompetent EVs have been discovered in breast milk, emphasizing their role in immunity (Admyre et al., 2007).

EVs have been extensively studied in the coagulation process, showing that increased aggregation of platelet-derived EVs enhances thrombin formation and induces thrombosis (Chen et al., 2013; Suades et al., 2012). EVs are widely utilized by the immune system, with mature dendritic cell derived EVs acting as initiators of immune responses (Segura et al., 2005). In mice, keratinocyte derived EVs play a similar role (Kotzerke et al., 2013). T-regulatory cell-generated EVs help suppress pathogenic T-helper cells through their miRNA cargo (Okoye et al., 2014). One of the most significant roles of EVs during pregnancy is their function as mediators between the foetus and mother (Arck & Hecher, 2013; Chua et al., 1991). Marrow cell derived EVs can modulate prosurfactant B expression in marrow cells during lung injury, allowing for repair (Aliotta et al., 2007). EVs have also been implicated in bone calcification. They play a crucial role in the bone remodelling microenvironment, with bone derived EVs containing osteogenic proteins like bone morphogenetic protein and alkaline phosphatase, which are essential for this process (Golub, 2009). These EVs can transport and facilitate the delivery of substances such as bone morphogenetic protein, sialoprotein, and Vascular Endothelial Growth Factor (VEGF) directly to bone tissue (Nahar et al., 2008). Furthermore, it has been demonstrated that EVs from hepatocytes are capable of transferring proteins to the liver (Conde-Vancells et al., 2008, 2010), which are involved in the liver's response to injury (Royo et al., 2013) and in the regulation of normal cellular proliferation (Lee et al., 2008).

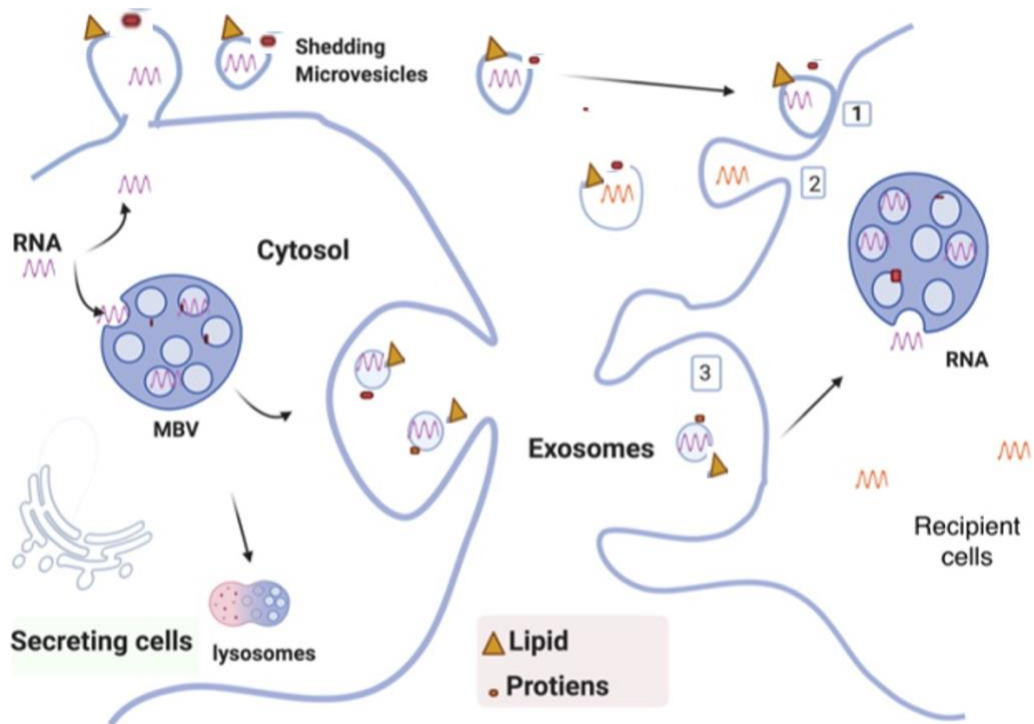


Figure 1.6 EVs transfer proteins and nucleic acid.

Transmembrane proteins and the associated membrane proteins are integrated into Shedding microvesicles (SMVs) or into the ILVs of MBVs. These exosomes and SMVs, with various sizes, either attach at the recipient cell's plasma membrane or are endocytosed by these cells and then release the material within the target cells, or these vesicles merge with the target cell's plasma. All of these mechanisms contribute to the introduction of proteins and nucleic acid into the recipient cell's cytosol or membrane. This process is thought to be involved in chemotherapy resistance as the cell cannot lyse the drug substances and aims to get rid of them by excreting the EVs. In addition, these vesicles may bundle nucleic acids and proteins in the cells. This cargo carrying information on drug resistance can then be passed by EVs to the target cells to confer drug resistance to those cells (Safaei et al., 2005). In addition to tumour growth and metastasis, this pathway also includes intracellular signalling by EVs involving inflammation, immune inhibition. Created with BioRender.com.

1.4.5.2 Function of EVs in cancer

The burgeoning field of EV research is fuelled by the understanding that these vesicles can mediate the exchange of information between donor and recipient cells, rendering them vital tools for exploring biological processes, both normal and aberrant. In the context of cancer, EVs secreted by tumours are thought to critically influence the stromal environment of solid tumours (Becker et al., 2016). Extensive research has shown that EVs emitted by tumours can affect adjacent cells, driving oncogenic processes like angiogenesis, transformation of fibroblasts (Chowdhury et al., 2014; Mineo

et al., 2012; Webber et al., 2015), modulating non-cancerous cell behaviour (Skog, Würdinger, van Rijn, Meijer, Gainche, Sena-Esteves, et al., 2008), or transferring oncogenic molecules to more indolent cancer cells (Al-Nedawi et al., 2008), thus supporting tumour expansion and spread at the original tumour site.

EVs are also strongly linked to the establishment of metastatic sites. A seminal study by Peinado et al. demonstrated increased melanoma expansion and metastatic load in mice implanted with BM progenitors conditioned by metastatic melanoma exosomes through a so-called "education" mechanism. The Met proto-oncogene was elevated in aggressive melanoma cells, and its horizontal transference from melanoma exosomes to bone marrow (BM) cells was a key factor in fostering BM cell multiplication and, consequentially, metastasis (Peinado et al., 2012). In pancreatic cancer, it was found that conditioning mice with PDAC cell-derived exosomes predisposed them to liver metastases. This study elucidated the sequence of events leading to metastatic niche formation in the liver, starting with PDAC exosomes being incorporated by liver Kupffer cells. These exosomes horizontally transferred MIF to the Kupffer cells, inducing them to secrete TGF- β , which in turn prompted fibronectin production by hepatic stellate cells, thus initiating fibrosis. The subsequent fibronectin layer then attracted bone marrow-derived macrophages and neutrophils to the liver, culminating in the establishment of a pre-metastatic niche (Costa-Silva et al., 2015).

Research has also indicated that malignant breast cancer cell-derived EVs can be assimilated by less aggressive tumour cells, which can be located either nearby or at distant *in vivo* sites. An investigation into the mRNA content of these EVs revealed a concentration of genes linked to cell migration. Introducing EVs from metastatic breast cancer cells into non-metastatic cells *in vivo* experiments utilizing the Cre-LoxP system to trace the uptake of extracellular vesicles (EVs) from highly metastatic MDA-MB-231 breast cancer cells by less metastatic T47D cells demonstrated a significant influence on tumour cell behaviour. The study, conducted in a mouse model, revealed that the transfer of EVs facilitates the communication of functional mRNA between cells, notably enhancing the migratory and metastatic capabilities of the recipient T47D cells. Through the use of intravital imaging and genetic markers, this process was visualized and quantified (Zomer et al., 2015). Importantly, the exchange of EVs is a two-way street, as illustrated by studies indicating that cancer-

associated fibroblasts can enhance the migratory and metastatic tendencies of breast cancer cells via EV release (Luga et al., 2012). A compelling piece of research also suggested that exosomes may play a role in determining the specific organs that tumours metastasize to. This organ specificity is driven by tumour-derived exosomes that are internalized by cells particular to the target organ, with certain integrins directing the vesicles to these cells. In this study, it was revealed that the integrins $\alpha 6\beta 4$ and $\alpha 6\beta 1$ on exosomes from breast cancer are crucial for lung metastasis, as they mediate uptake by S100A4-positive fibroblasts and surfactant protein C-positive epithelial cells within the lung tissue. Similarly, the presence of $\alpha v\beta 5$ on pancreatic cancer exosomes was shown to advance liver metastasis through their fusion with Kupffer cells (Costa-Silva et al., 2015).

In summary, this body of research sheds light on some of the ways EVs contribute to tumour progression (Figure 1.7). The various mechanisms through which EVs participate in cancer development and metastasis highlight their significance in understanding the complex nature of tumour growth and dissemination. By studying these mechanisms, researchers can gain valuable insights into potential therapeutic targets and strategies for combating cancer.

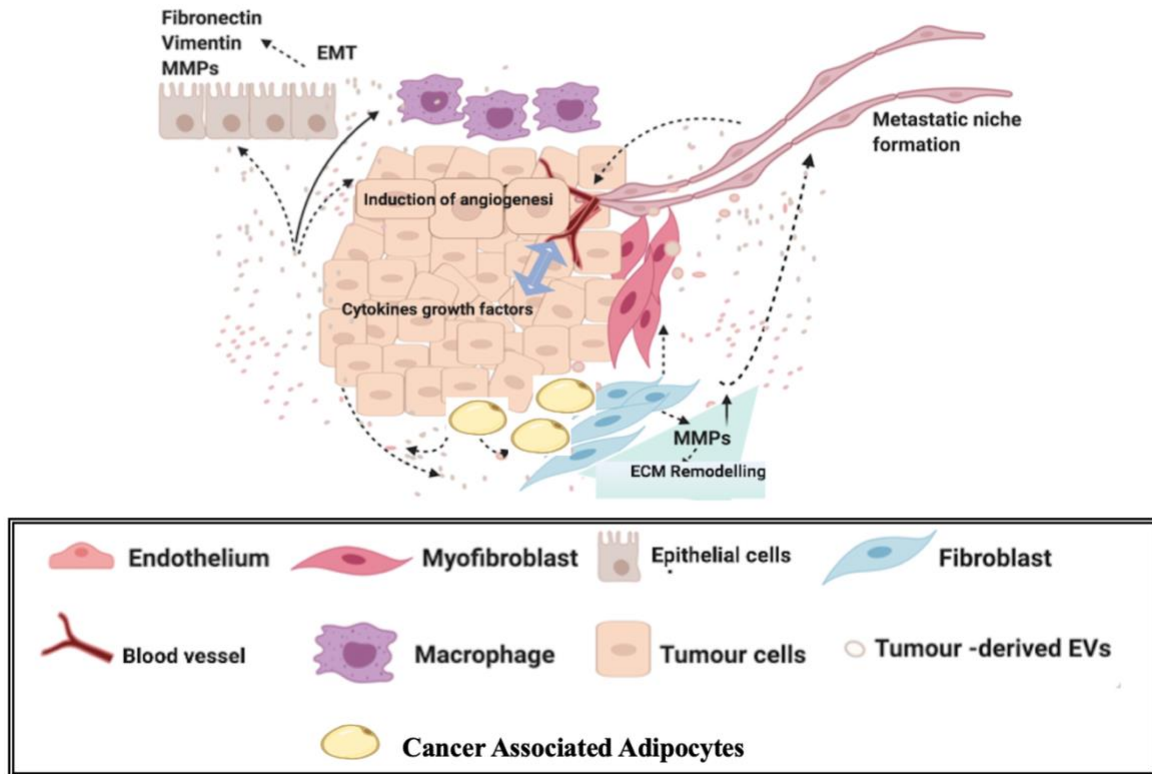


Figure 1.7 EVs are mediators of intercellular communication within the tumour microenvironment.

EVs are commonly seen as facilitators in the tumour-promoting dialogue between cancer cells, neighbouring cells, and infiltrating immune cells. The diagram provides a streamlined representation of how tumour-derived EVs contribute to the transformation of fibroblasts into myofibroblasts, which subsequently leads to the secretion of matrix metalloproteinases (MMPs) and the degradation of the extracellular matrix (ECM). Additionally, tumour EVs play a role in activating tumour-associated macrophages to release growth factors, which in turn stimulate angiogenesis and create an inflammatory microenvironment. Furthermore, these EVs can disrupt the balance of the immune system by inducing changes that contribute to immunosuppression, thereby offering protection to the tumour (interaction between EVs and the immune system not depicted). As the tumour expands, its metabolic needs surpass the capacity of its blood supply, resulting in increased hypoxia. To counteract this, the tumour emits angiogenic factors along with EVs that encourage the formation of new blood vessels to compensate for the low oxygen levels. Primary tumour-derived EVs also activate epithelial cells to emit factors involved in epithelial-mesenchymal transition (EMT), leading to decreased adhesion among tumour cells, remodelling of the ECM, and new blood vessel formation, all of which are processes that ultimately assist in the dissemination of tumour cells to distant sites.

1.4.6 Role of extracellular vesicles in resistance to chemotherapeutic drugs

EVs have been found to contribute to drug resistance in cancer treatment through multiple pathways. They can also aid in the transmission of resistance within the TME. For instance, high concentrations of cisplatin have been detected in EVs, as evidenced by research on platinum resistance in ovarian cancer cells. In response to cisplatin treatment, cells significantly increase the secretion and release of EVs containing high concentrations of cisplatin (Safaei et al., 2005). It is believed that the EVs absorb the drug and eliminate it through the urine. Furthermore, EVs may play a role in transferring resistance to Herceptin (trastuzumab), an antibody-based therapy. It has been shown that tumour cell lines with overexpression of the human epidermal growth factor receptor 2 (HER-2) generate EVs containing the HER-2 molecule, which can bind to and sequester trastuzumab from target cells (Ciravolo et al., 2012).

Vesicle transfer has been demonstrated to mediate resistance systematically across a cell population. By transmitting the ABCB1 (MDR-1)/P-glycoprotein (P-GP) multidrug resistance transporter, prostate cancer cells resistant to docetaxel can confer resistance to cells susceptible to both doxorubicin and docetaxel (Corcoran et al., 2012). Docetaxel resistance was observed via EV transfer in a breast cancer model, with a group revealing the transfer of miRNAs such as miR-100, miR-222, and miR-30a. Interestingly, these miRNAs affect the vesiculation of the membrane (Chen et al., 2014; Mineo et al., 2012), leading to increased vesicle production similar to the response of ovarian cancer cells to cisplatin. The same group also described the vesicle-mediated transmission of the P-GP transporter to sensitive cells as a mechanism that induces resistance (Lv et al., 2014).

Drug resistance is not solely transmitted among cancer cells. Healthy cells have also been found to transfer resistance to cancer cells by transporting proteins and miRNA through vesicles. EVs produced by stromal cells have been shown to regulate numerous pathways such as P38, P53, and AKT (Sousa et al., 2015), although the precise mechanism remains to be determined.

As normal cells surround and transport crucial components to cancer cells, it is likely that a signal from the tumour cells to the healthy cells occurs initially. This communication might alter the healthy cell's vesicle production, changing the cargo, surface targeting, and quantity produced to meet the

demands of the cancer cells. It is possible that the substances transferred by healthy cells are produced in larger amounts or are not secreted at all by cancer cells. A recent study reported that by increasing the expression of the zinc finger protein SNAIL (Snail), transformed fibroblasts could mediate resistance to gemcitabine and transfer this resistance to cancer cells (Richards et al., 2017). Cancer-associated fibroblasts (CAFs) undergo significant modifications compared to their normal counterparts, and these changes may encompass variations in vesicle secretion, similar to what is observed during the differentiation processes of stem cells, monocytes, and colon cancer cells. (Medina & Ghahary, 2010). In a specific model focusing on differentiating stem cells and monocytes, it was observed that the cells undergoing differentiation released extracellular vesicles (EVs) that contained 14-3-3 proteins. These proteins have the capability to activate dermal fibroblasts. (Medina & Ghahary, 2010). When colon cancer cell lines were treated with sodium butyrate, they released more EVs, and these EVs had distinct phenotypic effects on recipient cells (Lucchetti et al., 2017). Yeung et al. (2016) study linked miR-21 transfer from adipocytes and CAFs to cancer. Upon binding to apoptotic protease activating factor 1 (APAF1), the transferred miR-21 induced resistance to paclitaxel (Yeung et al., 2016). Cancer-associated adipocytes, like CAFs, are shown to be influenced by cancer cells in ways that alter EV production.

In summary, extracellular vesicles play a crucial role in drug resistance in cancer treatment by transmitting resistance within the tumour microenvironment and mediating resistance systematically across cell populations. Both cancer cells and healthy cells contribute to the transfer of resistance via the transport of proteins and miRNA through vesicles. Understanding these mechanisms could be essential for developing more effective cancer treatments and overcoming drug resistance.

1.4.7 Other extracellular particles

Extracellular particles (EPs) encompass a diverse range of entities that play crucial roles in cellular communication, transport, and various physiological processes (Malkin & Bratman, 2020). Among these are exomeres, which are smaller than exosomes and are involved in protein and lipid transport. Supermeres, another category, are larger complexes that have distinct protein and lipid

compositions. Additionally, lipid particles, such as High-Density Lipoproteins (HDL) and Low-Density Lipoproteins (LDL), are critical for cholesterol transport (Malkin & Bratman, 2020; Q. Zhang et al., 2021). Vault particles present another type of EP. These barrel-shaped structures, primarily composed of the major vault protein (MVP), have been implicated in multidrug resistance and other cellular processes, making them an intriguing subject of study (Kickhoefer et al., 1998).

1.5 The vault particle

Vault particles were first observed in 1986 when they were found mixed in with clathrin-coated vesicles from rat liver (Kedersha & Rome, 1986). They were named vaults because they looked like the vaulted ceilings seen in cathedrals. These barrel-shaped particles are actually huge ribonucleoprotein complexes (Figure 1.8), weighing 13 million Daltons and measuring about 35 nm by 65 nm (Kedersha et al., 1990; Kong et al., 1999). This makes them about three times larger than ribosomes found in eukaryotic cells, and ten times bigger than other ribonucleoproteins like signal recognition particles (SRPs) or small nuclear ribonucleoproteins (snRNP)(Batey et al., 2000) .

Interestingly, these large particles were unnoticed for quite a while due to a technical issue (Rome et al., 1991). The contrast stains typically used for electron microscopy, namely osmium tetroxide and uranyl acetate, work well with charged components of membranes and nucleic acids, but not so well with vault particles which are mostly made up of protein and have less RNA. This means that these particles nearly disappear when viewed through a transmission electron microscope using these stains. The particles only became visible after a purification process and using a different staining method (Figure 1.8) (Kedersha & Rome, 1986).

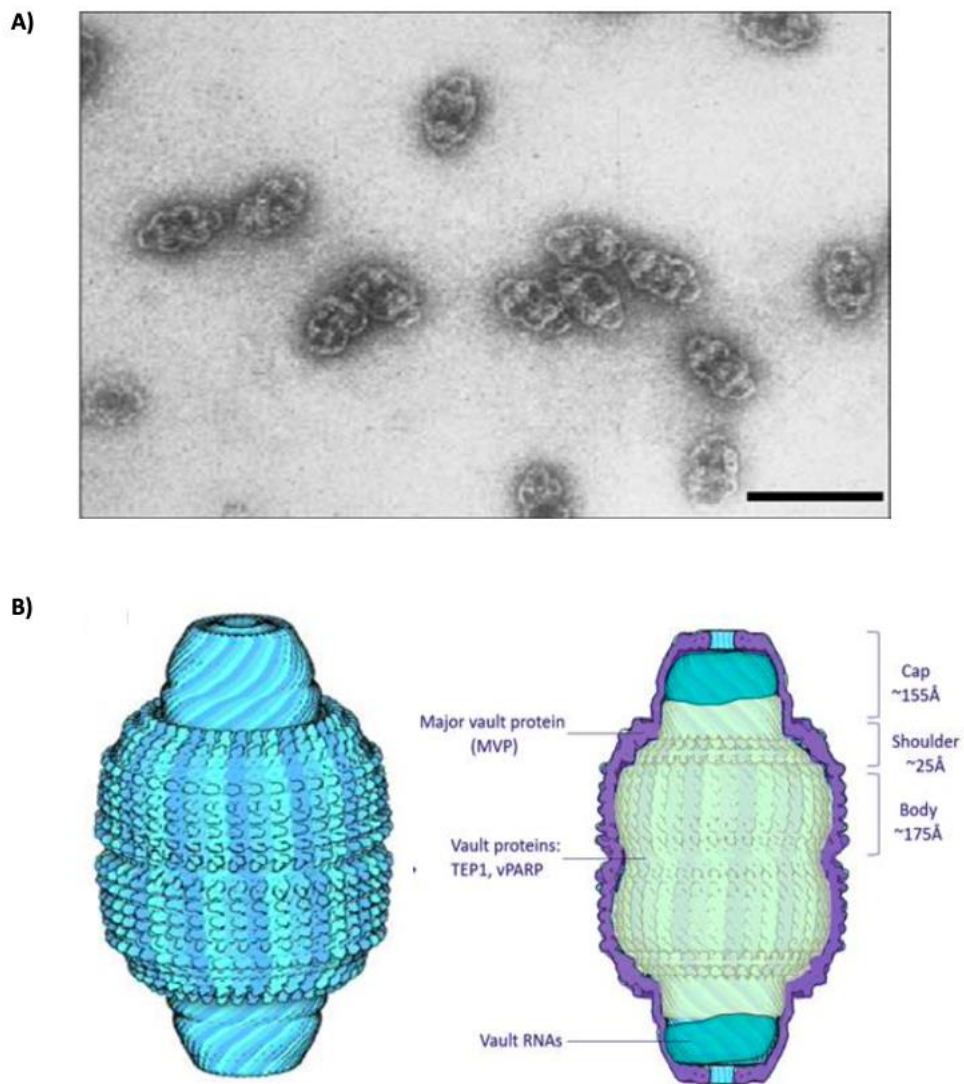


Figure 1.8 Visualization and composition of vault particles.

A) In the electron microscopy image, the structure of vault particles is visible, with a scale bar indicating 100 nm located in the lower left corner. The image is reproduced with permission, under license number 1146890-1 (Kedersha & Rome, 1986). B) The diagrammatic illustration outlines the constituent molecules of a vault particle, which encompasses MVP, TEP1, PARP4/vPARP, and vtRNAs.

These vault-like structures have been found in a wide variety of eukaryotic species, from mammals to fish to slime mould to protozoa (Kedersha et al., 1990; Rome et al., 1991). But they may

not be a core part of all eukaryotic cells as they weren't found in baker's yeast, nematode worm, fruit flies, or the plant known as *Arabidopsis thaliana* (Kickhoefer et al., 1996).

1.5.1 Vault components

Vaults found in mammals are composed of at least four unique elements, which include three large proteins and a few small non-coding RNA molecules (Kedersha & Rome, 1986). The primary component of vaults is a protein referred to as the major vault protein (MVP), which accounts for over 70% of the total mass of the vault complex. The two remaining proteins found in vaults are smaller. One has a molecular weight of 193 kDa and contains an activity called poly (ADP-ribose) polymerase (PARP), hence it is referred to as vault PARP (VPARP), p193 or PARP4 (Kickhoefer, Siva, et al., 1999). The other protein, with a molecular weight of 240 kDa, appears to be the same as the telomerase-associated protein 1 (TEP1 or p240). This particular component of the vault is also part of another ribonucleoprotein complex, the telomerase complex. Vault RNA (vtRNA) contributes ~5% to the vault mass (Kedersha & Rome, 1986). It's been proposed that a single vault particle is made up of 96 molecules of MVP, 8 molecules of PARP4, 2 molecules of TEP1 (Kickhoefer et al., 1996), and at least 6 molecules of vtRNA (Kong et al., 2000). Observations highlighted that the significant molar prevalence of Major Vault Protein (MVP) compared to minor vault proteins differs from the typical composition seen in other ribonucleoproteins. This pattern is more closely aligned with the makeup of coated vesicles or the molecular redundancy found in cytoskeletal configurations, such as microtubules and stress fibers, or seen within specific viruses. While it's not confirmed, there's a fascinating theory suggesting that these vault particles may have evolved from a virus that had a symbiotic relationship with the host, also known as a viral endosymbiont (Kedersha et al., 1991).

1.5.2 The function of vaults

Despite significant progress in understanding the structure and individual components of vaults, their exact role within cells remains unknown. Given their unique hollow barrel-like form and their

location within cells, many researchers have suggested that they might be involved in intracellular transport.

The observed partial overlap in spatial distribution between vaults and cytoskeletal structures could imply that vaults are either mobilized via the cytoskeleton network or contribute to the maintenance of cytoskeletal integrity. Supporting evidence for this proposition comes from studies in the electric ray *Torpedo*, which demonstrated vault transport within axons from the cell body to nerve terminals (Herrmann et al., 1996; Li et al., 1999). Detailed microscopic analyses suggested a strong link between vaults and synaptic vesicles in the nerve terminals of the electric organ. The researchers theorised that substances destined for secretion may associate with vaults and travel along microtubules to synaptic vesicles (Herrmann et al., 1998). This cytoskeleton-mediated transport could allow vaults to ferry cargo to and from specific locations within the cell. However, more research is needed to validate this transport system, possibly by examining the effects of drugs that influence actin and microtubules, the energy requirements of the transport process, and the role of molecular motors.

The possibility of vaults being involved in nucleocytoplasmic transport comes from observations in rat fibroblasts. Some vaults were found near the nuclear membrane, often close to the nuclear pore complex (Chugani et al., 1993). However, the initial idea that vaults might be the long-sought central plugs has been mostly dismissed. The central plug is now commonly seen as material passing through the nuclear pore, rather than a distinct entity. The observations could indicate that vaults dock at the cytoplasmic side of the nuclear pore complex to pick up or drop off cargo. Potential cargo could include ribosomes, as MVP has been found alongside ribosomes in developing sea urchin embryos. Additionally, MVP has been found in conjunction with the human oestrogen receptor, with oestrogen treatment increasing the association of MVP with the oestrogen receptor in nuclear extracts (Abbondanza et al., 1998). It's important to note that potential vault cargo might not only be inside the vault complex but could also be attached to its exterior. The functions of the vault particles are discussed here, taking into consideration the specific roles played by each of their components. MVP

MVP, the primary structural element of vaults, is crucial for their assembly. When MVP function is inhibited, the formation of vault particles is disrupted (Berger et al., 2009). The assembly of vaults is primarily influenced by the presence of Major Vault Protein (MVP), as opposed to the lesser

roles played by other vault proteins such as TEP1 and PARP4. This implies that the existence of MVP at normal levels is a critical prerequisite for the formation of vault particles, according to findings by (Kickhoefer et al., 1998). Nonetheless, studies by Mossink et al. (2002) revealed that mice lacking MVP (MVP (-/-)) did not display any noticeable defects, suggesting a complexity in the role of MVP in physiological processes (Mossink et al., 2002).

Several studies highlight that MVP has multifaceted roles in biological processes. Notably, MVP is connected with preventing cell death in aging human cells. Decreasing MVP levels leads to a drop in the protective protein Bcl-2 and an increase in the c-Jun protein in these cells (Ryu et al., 2008). Additionally, reducing MVP has been found to trigger cell death in various cell types, including macrophages and cells from lung, liver, and breast cancers (Bai et al., 2019; H. M. Lee et al., 2017; Pasillas et al., 2015). MVP on the cell surface is also implicated in enhancing the growth and spread of liver cancer cells, possibly by activating several cellular pathways (Lee et al., 2017). Furthermore, a higher abundance of MVP corresponds with reduced levels of certain proteins involved in DNA repair mechanisms, suggesting vaults' potential involvement in these processes (Lloret et al., 2009). Recent investigations also point to MVP's roles in combating obesity and artery-related issues, influencing bone breakdown, and its association with viral interactions and disease development (Ben et al., 2013; W. Wang et al., 2020; Yuan et al., 2021).

Vault particles, particularly the MVP component, have been associated with drug resistance in lung cancer due to its heightened expression levels (Scheper et al., 1993). This overexpression has been noted across several cancer cell lines that show resistance to multiple drugs (Schroeijers et al., 2000). Recent research linked MVP to worse outcomes in patients with a specific breast cancer subtype, triple-negative breast cancer (TNBC). This study revealed MVP's role in driving resistance to chemotherapy in TNBC cells, primarily through activation of the Akt pathway and the promotion of a cellular transformation process called epithelial to mesenchymal transition (EMT), which was influenced by the Notch1 protein's binding to MVP promoter regions (Xiao et al., 2019). Furthermore, MVP was originally referred to as the lung resistance-related protein (LRP), stemming from its significance identified in a specific lung cancer cell line, SW-1573, in the 1990s (Scheper et al., 1993). An intriguing observation was that the resistance of certain cells to chemotherapy drugs like doxorubicin could be

traced back to increased MVP expression when exposed to sodium butyrate (NaB). This heightened MVP expression led to the drugs being shifted from the cell nucleus to the cytoplasm (Kitazono et al., 2001). Similar findings in throat cancer cells underscored MVP's ability to induce drug resistance by moving these agents away from their primary targets in the nucleus (Cheng et al., 2000). Later research indicated that in the SW-620 cell line, MVP heightened expression could be triggered by a variety of stress factors, including NaB, through a specific cellular pathway (Ikeda et al., 2008). Additionally, a study that targeted individual vault proteins underscored MVP's critical role, along with another protein, PARP4, in ensuring cell survival in drug-resistant scenarios (Wojtowicz et al., 2017).

MVP has been identified as playing a role in the movement of chemotherapy drugs between the nucleus and cytoplasm by aiding the creation of cytoplasmic vesicles. In some less-sensitive cancer cells, there's a noticeable shift of these drugs to specific vesicles in the cytoplasm, which are found to be associated with MVP (Meschini et al., 2002). MVP, when produced in abundance by adipocytes near tumours, has also been found to assist in the transport of doxorubicin-laden EVs within breast cancer cells (Lehuédé et al., 2019). Research further indicates suppression of MVP can halt the movement of doxorubicin into lysosomes, suggesting MVP plays a pivotal role in reinforcing tumour cells' drug resistance (Herlevsen et al., 2007). However, findings about MVP's involvement in drug resistance have been mixed. For instance, MVP-deficient mice didn't show heightened sensitivity to multiple drugs in specific cell types, contradicting the expected role of MVP in drug resistance (Mossink et al., 2002). In lung cancer cells, while a link between MVP expression and resistance to one drug, cisplatin, was seen, such a relationship wasn't observed for other drugs like doxorubicin (Berger et al., 2009). Similarly, despite MVP's overproduction in an ovarian cancer cell line, resistance to several drugs was not detected (Scheffer et al., 1995). In a different context, within dendritic cells, MVP was found to overlap with the lysosomal marker CD63, a molecule frequently associated with late endosomes or multivesicular bodies, often seen as standard EV markers (Schroeijsers et al., 2002). Additional work in colon cancer cells revealed MVP's role in sorting specific miRNA cargoes within EVs, which appeared to boost tumour development (Teng et al., 2017). These findings hint at MVP's potential significance in the inner workings and intercellular transport related to vesicles and their selective cargo allocation.

1.5.2.1 TEP1

TEP1 is a protein linked with telomerase. Beyond its role as a secondary vault protein, this 290 kDa protein is also a key element of another ribonucleoprotein complex that assists in creating new telomerases at the ends of chromosomes (Kickhoefer, Stephen, et al., 1999; Saito et al., 1997). TEP1 collaborates with telomerase RNA and the enzymatic protein telomerase reverse transcriptase (TERT) in mammalian cells, bolstering the functionality of the complex. Yet, in mTEP1^{-/-} mouse models, there weren't any notable changes in telomerase RNA levels or activity (Kickhoefer et al., 2001; Liu et al., 2000). Notably, even though TEP1 is a part of two ribonucleoprotein assemblies, there's no recorded telomerase activity linked to vault particles. This hints at TEP1's potential involvement in promoting the structure or formation of ribonucleoprotein within vaults (Kickhoefer, Stephen, et al., 1999).

Kickhoefer et al. (2001) emphasized TEP1's role in bolstering the stability of vtRNAs within vault particles (Kickhoefer et al., 2001). Detailed 3D visualizations of vaults demonstrated that when mTEP1 is lacking in mice, the resulting vaults, though structurally sound, have less dense caps. Notably, mTEP1^{-/-} mouse-produced vaults entirely lacked vtRNA. This was in line with the vtRNA found in the leftover fractions from vault purifications (Kickhoefer et al., 2001). TEP1 interactions with vtRNAs or telomerase hinge on its Tetrahymena p80 similarity region, crucial for guiding TEP1 to vaults during their formation (Poderycki et al., 2005).

In a more recent examination of ovarian cancer tissue from untreated patients, TEP1 expression, along with MVP and PARP4, was seen to be notably reduced at the mRNA level in cancerous samples, in contrast to healthy ones. However, it was increased at the protein level (Szaflarski et al., 2013). This inconsistency in vault protein expression levels was linked to the altered regulation of other proteins connected to multidrug resistance in advanced tumours. This highlighted the significance of post-transcriptional oversight of vault proteins in the context of cancer-associated drug resistance (Szaflarski et al., 2013).

1.5.2.2 PARP4

PARP4 possesses a domain similar to the poly (adenosine diphosphate-ribosyl) transferase, although it doesn't directly interact with DNA because it lacks the N-terminal DNA binding domain.

This suggests that its transferase functionality might depend on interactions with other proteins (Kickhoefer, Siva, et al., 1999). Notably, the polymerase action of PARP4 was deemed non-essential for integrating the glutathione S-transferases (GST)-tagged-C-terminal portion of PARP4 into vault-like structures in *E. coli*, which were formed by protein C-tagged human MVP (Zheng et al., 2004). Even though PARP4 activity appeared unrelated to MVP's capacity to self-assemble vault-like particles, its potential role in boosting MVP-driven drug resistance has been underscored in cell lines resistant to multiple drugs (Wojtowicz et al., 2017). Moreover, an imaging study that utilized green fluorescent protein (GFP)-tagged MVP in a NSCLC cell line revealed an almost full overlap of tubular vault structures in the cytoplasm with PARP4 proteins (van Zon et al., 2003). Collectively, these findings point towards the potential structural importance of secondary vault proteins in the formation and fortification of the vault assembly.

1.5.2.3 Vault RNA

Vault particles contain short polymerase III transcripts named vtRNAs (Kedersha & Rome, 1986). These vtRNAs display a conserved polymerase III promoter, but vary in length across species, ranging between 86 and 141 nucleotides. They all have a shared stem-loop secondary structure (van Zon et al., 2003). While mice and rats possess one vtRNA, bullfrogs have two, and humans possess four distinct vtRNA paralogs, encoded by specific genes. Another vtRNA found on the X chromosome in humans is generally considered a pseudogene (Stadler et al., 2009; van Zon et al., 2001).

Interestingly, nuclease treatments that disrupt vtRNA don't impact the assembly of the vault complex, suggesting that vtRNA plays a functional, but not structural, role in vaults (Kedersha et al., 1991). Research has linked elevated levels of vtRNA expression with resistance to chemotherapy in certain human cancer cell lines, such as glioblastoma, leukaemia, and osteocarcinoma (Gopinath et al., 2010). Additionally, studies indicate a close interaction between vtRNA 1-1 and a specific splicing factor, with implications for cell sensitivity to chemotherapy (Chen et al., 2018). Other studies reveal that vtRNAs can directly bind to chemotherapy drugs, potentially aiding in their removal from cells (Gopinath et al., 2005). Beyond chemotherapy resistance, vtRNAs have roles in preventing cell death and inhibiting anti-viral immunity, with some particularly associated with cancer development

processes (Ahn et al., 2018; Amort et al., 2015; Golec et al., 2019; F. Li et al., 2015). Notably, the majority of vtRNA doesn't bind to the vault particle, implying other potential roles (Kickhoefer et al., 2002). Some vtRNA not associated with vaults have been found in separate smaller ribonucleoprotein particles, and recent research has started to uncover their role in autophagy (Horos, Büscher, Kleinendorst, et al., 2019; Horos, Büscher, Sachse, et al., 2019).

Multiple proteins have been identified that bind to vtRNAs. Their affinity to these proteins, for instance, SRSF2, can be modified post-transcriptionally (Sajini et al., 2019). Regulatory activities of vtRNA1-1 arise from certain modifications, which lead to the creation of small vtRNA fragments (svRNAs) that have their own regulatory effects (Hussain et al., 2013; Sajini et al., 2019). These svRNAs are produced in a specific manner and have been shown to regulate certain target genes. Deep RNA sequencing from certain cells has shown multiple svRNA clusters. Specific svRNAs have been associated with drug resistance (Persson et al., 2009), while others have a functional role in cell differentiation (Sajini et al., 2019). Additional vtRNA modifications have been documented, and distinct vtRNA profiles in different EV subsets have been reported (Bellingham et al., 2012; Lässer et al., 2016; Lunavat et al., 2015; Nolte-'t Hoen et al., 2012). The packaging of vtRNA and its fragments into EVs remains a topic of study, with one protein, YBX1, being identified as crucial in transporting small RNA molecules, including vtRNAs, into EVs from specific cells (Shurtleff et al., 2017).

1.6 Hypothesis and project aims

The hypothesis suggests that extracellular particles released from HNC cells, when exposed to chemotherapeutic agents like cisplatin, undergo alterations in their molecular cargo. This change potentially facilitates chemotherapy resistance in neighbouring or naïve cells. To explore this hypothesis, the project will aim to address the following objectives: (“We hypothesised” has been deleted to avoid using (we and our), and this approach was applied throughout the thesis)

1. HNC cell lines will be treated with cisplatin and dose-response determined by MTT assay and flow cytometry.
2. Cells will be treated with sub-lethal doses of cisplatin and conditioned medium will be characterised by nanoparticle tracking analysis to assess EV size and concentration.
3. Extracellular particles will be isolated from conditioned medium by ultracentrifugation and further characterised by western blotting for common EV markers such as CD63 and TSG101, and MVP for vault particles.
4. Cell lines that are EV and vault particle-deficient will be utilised to explore the role of these extracellular particles in HNC response to cisplatin treatment.
5. Naïve cells will be treated with EVs derived from a cisplatin resistant cell line (cisplatin^R) and susceptibility of naïve cells to the drug determined by flow cytometry.

Chapter 2 Materials and methods

2.1 General consumables

The chemicals and reagents used in the laboratory were ordered from Merck, which was previously known as Sigma-Aldrich. Molecular biology reagents, unless specified otherwise, were purchased from Thermo Fisher Scientific.

2.2 Cell lines

In this study, two commercially available human head and neck squamous cell carcinoma (HNSCC) cell lines were used: FaDu (ATCC, HTB-43TM), derived from a pharynx squamous cell carcinoma of a 56-year-old Caucasian male (Rangan, 1972), and H357 (ECACC, 06092004), originally isolated from a 74-year-old male patient with a squamous cell carcinoma of the tongue (Yeudall et al., 1993). CRISPR/Cas9 genome edited derivatives of the H357 cell line, H357 MVP KO and H357 HGS KO, were created by Miss Xinming Liu and Miss Wenyi Jiang, respectively. FaDu cells were cultured in Roswell Park Memorial Institute (RPMI) 1640 medium, while H357 cells (and derivatives) were cultured in Dulbecco Modified Eagle Medium (DMEM) containing 1000 mg/L glucose. Both culture media were supplemented with 2 mM L-glutamine and 10% (v/v) foetal bovine serum (FBS) to provide necessary nutrients and support optimal cell growth.

2.3 Cell culture and passage

The cell lines in this study were routinely cultured in T75 (75 cm²) tissue culture flasks under optimal conditions. Upon reaching approximately 70-80% confluence, monolayers were washed twice with 10 ml of sterile Dulbecco's phosphate-buffered saline (PBS) to remove any residual medium. Subsequently, 3 ml of 0.25% trypsin/EDTA solution was added to the monolayer, and the flask was incubated at 37°C for 5 minutes in a 5% (v/v) CO₂ humidified environment to facilitate cell detachment. During this time, an inverted light microscope was used to monitor the dissociation of cells from the flask surface.

Upon complete cell detachment, the trypsin was neutralized by adding 7 ml of pre-warmed complete medium to the flask. The cell suspension was then collected and centrifuged at 123 xg for 5 minutes using a benchtop centrifuge (Harrier 18/80, MSE, UK) to pellet the cells. After discarding the supernatant, the cell pellet was resuspended in a fresh volume of complete medium, as required, and transferred to a new T75 tissue culture flask. The cells were subsequently placed in a 37°C incubator with a humidified environment containing 5% (v/v) CO₂ to promote growth.

This passaging procedure was repeated when the monolayers reached approximately 70-80% confluence to ensure optimal cell growth and viability. Furthermore, cells were maintained within a 20-passage window to minimize the risk of phenotypic drift and maintain the consistency of experimental results. Cell lines were routinely tested for mycoplasma contamination.

2.3.1 Cell counting

In instances where a specific cell number was required for experiments, cells were trypsinised as above (section 2.3) and resuspended in 10 ml of fresh growth medium as to accurately determine the cell concentration, 10 µl of the cell suspension was pipetted beneath the coverslip of a glass haemocytometer (Neubauer Improved Hemocytometer). Utilizing an inverted light microscope (Nikon, ECLIPSE, TS100, Tokyo, Japan) at 10x objective magnification, the number of cells in each of the four corner quadrants of the haemocytometer, each consisting of 16 squares was carefully counted.

Subsequently, the values obtained from the four corner quadrants were averaged, and the mean count was multiplied by 1×10^4 to calculate the cell concentration in cells per milliliter. The required number of cells was then pelleted at 123 xg for 5 minutes before resuspension in the desired volume of pre-warmed complete medium, ready for seeding into the cell culture vessel.

2.3.2 Cell line storage

Cells were trypsinised and counted as above (section 2.3.1). Afterward, they were centrifuged to form a pellet. This pellet was then mixed in a solution containing 90% (v/v) FBS and 10% (v/v) dimethyl sulfoxide (DMSO), ensuring a final concentration of 1×10^6 cells per milliliter. Each 1 ml

portion of this cell mixture was placed into cryogenic vials. These vials were first kept at -80°C overnight using a Mr. FrostyTM container and subsequently stored in liquid nitrogen.

2.3.3 Monolayer cell seeding

Cells were trypsinised and counted as mentioned in section (2.3.1.) Following trypsinization and enumeration, cells were prepared for seeding into various culture vessels, including 96-well plates, 6-well plates, T25, and T75 flasks. The cell suspension was adjusted to achieve specific seeding densities suitable for each vessel type. For example, a typical seeding density for the 96-well plates was 1×10^4 cells per well, with 100 μl of the cell suspension dispensed into each well. This standardized approach ensured a consistent cell distribution across all vessel types, providing a reliable foundation for assessing treatment effects. After seeding, the culture vessels were placed in an incubator set at 37°C with a humidified 5% (v/v) CO_2 atmosphere. The overnight incubation allowed cells to firmly attach to the surface of the respective vessels and establish a uniform monolayer. This step was vital for ensuring the consistency and reproducibility of subsequent experimental procedures, especially when evaluating the cytotoxic impacts of agents like cisplatin on HNC cell lines.

2.4 Generating cisplatin resistant cell lines (Cisplatin^R)

The H357 and FaDu cell lines underwent long-term treatment with the chemotherapy agent cisplatin. To prepare a stock solution of cisplatin, 30 mg of cisplatin powder was dissolved in 100 ml of 0.9% (w/v) NaCl, yielding a 1 mM solution. The stock solution was subsequently sterilized using a 0.2 μm Millex[®] syringe filter. This suspension was either utilized immediately or aliquoted into 1 ml portions, shielded from light, and stored at -20°C for future use. The treatment strategy was designed to start at a low, sub-lethal dose of 0.5 μM cisplatin. Following this initial dose, the concentration was systematically increased in increments of 0.5 μM with the aim of reaching the determined IC₅₀ value. Both cell lines were routinely passaged as described (section 2.3) in the presence of cisplatin. However, it is pertinent to note that the FaDu cell line did not achieve the desired IC₅₀ concentration, leading to the exclusive use of the H357 line for subsequent experiments.

2.5 Cisplatin treatment

The 1 mM cisplatin stock solution prepared as above (section 2.4) was further diluted in cell culture medium to obtain a series of working concentrations: 0.02 μM , 1 μM , 2 μM , 5 μM , 10 μM , 20 μM , 100 μM , and 200 μM .

Pre-seeded 96-well plates (1×10^4 cells/well), as described previously (section 2.3.3), containing 100 μl of culture medium per well, were treated with 100 μl of each cisplatin concentration. This process resulted in final cisplatin concentrations of 0.01 μM , 0.5 μM , 1 μM , 2.5 μM , 5 μM , 10 μM , 50 μM , and 100 μM in the wells. Additionally, a vehicle control group was treated with a volume of 0.9% (w/v) NaCl equivalent to the maximum cisplatin concentration, ensuring a valid comparison for the experimental groups. The cells were incubated with cisplatin for 24 and 48 hours at 37°C in a humidified incubator with 5% (v/v) CO₂, ready for downstream cell viability testing.

2.6 MTT assay

The 3-(4,5-dimethylthiazolyl-2-yl)-2,5-diphenyl tetrazolium bromide (MTT) assay was employed to assess cell metabolic activity as an indication of viability following treatment with cisplatin as above (section 2.5). Cells were treated with the drug for 24 and 48 hours, after which the culture medium was removed, and 100 μl of freshly prepared MTT dye (0.5 mg/ml in PBS) was added to each well. The plate was then incubated at 37°C and 5% CO₂ for 2 hours, allowing viable cells to reduce MTT to formazan, which generated a purple colour. Following incubation, the MTT solution was carefully aspirated, and 50 μl of acidified isopropanol was added to each well to solubilize the formazan crystals. The optical density (OD) of the solubilized formazan was measured at a wavelength of 570 nm (OD₅₇₀ nm) using an Infinite® M200 PRO NanoQuant plate reader (TECAN) in conjunction with Magellan software, with a reference wavelength of 630 nm to account for background absorbance. The absorbance data obtained from the plate reader was transferred to an Excel spreadsheet for further analysis, including the calculation of percentage cell viability and statistical comparisons between treated and control groups.

2.6.1 IC50 value

The absorbance values obtained from the MTT assay as above (section 2.6) were processed using Microsoft Excel to determine the percentage cell viability. Each absorbance value was normalized to the average absorbance of the vehicle control group, providing relative cell viability values for the treated samples. Subsequently, the mean and standard deviation of these relative values were calculated for each treatment group. The data were then plotted as dose-response curves using GraphPad Prism 9 software (GraphPad Inc, San Diego, CA, USA), which facilitated the visualization and analysis of the relationship between cisplatin concentrations and cell viability.

Nonlinear regression analysis was performed using the dose-response inhibition model to fit the experimental data and better understand the cytotoxic effects of cisplatin on the cell lines. From this analysis, half-maximal inhibitory concentration (IC50) values were calculated, which represented the drug concentration required to reduce cell viability by 50%.

2.7 Extracellular particle methods

2.7.1 Preparation of EV-depleted FBS

FBS was depleted of extracellular vesicles (EVs) through ultrafiltration, following a method adapted from Kornilov R et al. (2018). The process involved filtering FBS through 0.2 μm filters to remove any particulate contaminants (Kornilov et al., 2018). The filtered FBS was then loaded into the upper chamber of Amicon Ultra-15 centrifugal filter units, featuring a 100 kDa molecular weight cut-off. Subsequently, the samples were centrifuged at $3,000 \times g$ for 2 hours at 4°C , which allowed the smaller molecules (<100 kDa) to pass through the filter membrane while retaining the larger molecules/particles (such as EVs) in the upper chamber. The flow-through collected in the lower chamber represented ultrafiltered EV-depleted FBS (UF-dFBS). To ensure sterility, UF-dFBS was filtered once more through 0.2 μm filters before immediate use or storage at -20°C .

2.7.2 Cell culture conditioned medium

Cells were treated with trypsin and subsequently enumerated (section 2.3.1). In order to determine the particle concentration released by these cells, 2.5×10^5 of them were seeded in each well of a 6-well plate in 2 ml of standard growth medium. These were then allowed to attach overnight. The next day, the spent medium was discarded, and each well was washed twice with PBS. Following the wash, 2 ml of fresh growth medium supplemented with 10% (v/v) UF-dFBS was added to each well. After another overnight incubation, the medium was subjected to centrifugation at $300 \times g$ for 10 minutes, ensuring the detachment of any free-floating cells. The resulting conditioned medium was promptly cooled on ice in preparation for Nanoparticle Tracking Analysis (NTA) (section 2.7.4). Where larger volumes of conditioned medium were required, 2×10^6 cells were seeded in a T75 culture flask along with 10 ml of low-glucose DMEM and allowed to attach for a period of 24 hours. Post-adherence, the old growth medium was removed, and the cells were washed twice with PBS. The cells were then incubated with 6 ml of fresh growth medium supplemented with 10% (v/v) UF-dFBS. After incubating for an additional 24 hours, the medium was once again centrifuged at $300 \times g$ for 10 minutes to pellet any unattached cells. The supernatant harvested from this process was then processed by differential centrifugation (section 2.7.3).

2.7.3 Differential centrifugation

The conditioned medium (section 2.7.2) was subjected to a series of centrifugation steps (Figure 2.1), based on the methodology outlined by Théry et al. (2006), aiming to isolate EVs. Initially, this medium was centrifuged at $2000 \times g$ for a duration of 15 minutes, yielding a pellet. The supernatant was then subjected to a second round of centrifugation at $10,000 \times g$ for 30 minutes using an OHAUS FRONTIER™ 5000 SERIES MULTI PRO. Subsequently, the supernatant underwent centrifugation at $100,000 \times g$ for 1 hour using a Beckman Coulter Optima TLX ultracentrifuge equipped with a TLA-100.4 rotor. This was followed by a wash using PBS and another centrifugation at the same speed for 1 hour. All centrifugation steps took place at 4°C . The resultant pellets, derived from varied centrifugation speeds, were reconstituted in either 50 μl of PBS or a lysis buffer, making them suitable for Nanoparticle

Tracking Analysis (section 2.7.4) and western blot (section 2.8.4) experiments. These prepared samples were preserved at a temperature of -20°C .

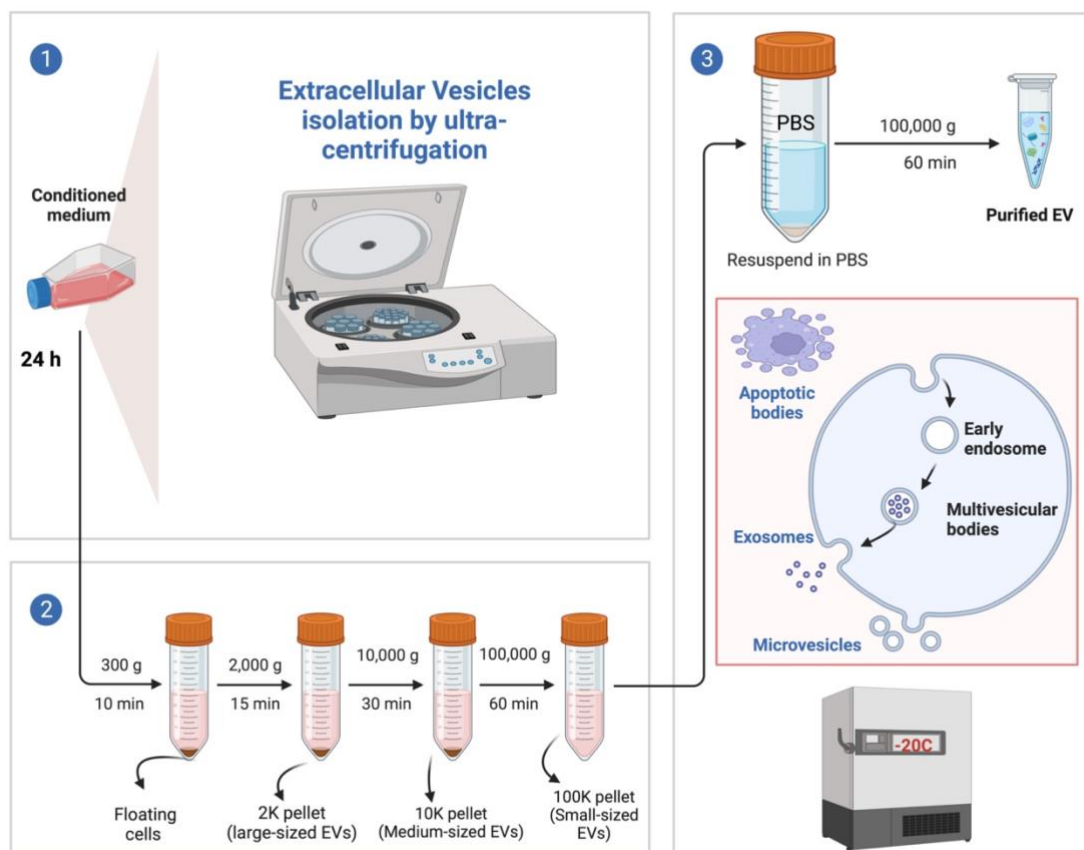


Figure 2.1Diagram illustrating differential centrifugation.

In T75 flasks, 2 million cells were seeded in normal medium. After a day, the medium was switched to EV- free medium. This medium was then spun at different speeds: first $300 \times g$ for 10 minutes, then $2000 \times g$ for 15 minutes, next $10,000 \times g$ for 30 minutes, and lastly $100,000 \times g$ for 1 hour. The separated particles, or pellets, were washed with PBS and spun again at $100,000 \times g$ for 1 hour. The diagram was created using BioRender.

2.7.4 Characterization of nanoparticles by nanoparticle tracking analysis

Nanoparticle tracking analysis (NTA) was conducted using a ZetaView nanoparticle tracking video microscope PMX-120 (Particle Metrix GmbH). This instrument detects particles within selected size ranges across 11 positions in the sample cell, following the manufacturer's recommended settings (Table 2.1), and tracks their Brownian motion. This enables the measurement of particle size and concentration in the solution. In accordance with the company's instructions, the ZetaView instrument

was calibrated using polystyrene particles of a known average size of 100 nm, diluted at a ratio of 1:250,000 in Milli-Q water. The instrument was then thoroughly washed three times with 5 ml of Milli-Q water prior to sample loading.

Cell culture conditioned medium (section 2.7.2) and EV pellets (Figure 2.1) were analysed using the ZetaView instrument. Samples were initially diluted with Milli-Q water to achieve a concentration ranging between 10^6 and 10^7 particles/ml, with the dilution factors noted for subsequent calculation of original concentrations. A 3 ml aliquot of the diluted sample was injected into the sample cell using a syringe, followed by image acquisition and automatic outlier analysis by the instrument. The sample cell was thoroughly washed three times, or until no particles were detected, with 5 ml of Milli-Q water prior to loading the next sample. Measurements for small (~100 nm) particles in the samples were performed using the settings provided (Table 2.1). The concentration and size distribution data generated by the instrument were used for further analysis. When measuring particles in conditioned media from different cell lines, the volumes of recovered media and cell counts were also recorded to facilitate normalization of particle numbers.

Table 2.1 Setting of ZetaView instrument

| Parameters | Settings for small particles (~100 nm) |
|--------------------|-----------------------------------------------|
| Sensitivity | 70 |
| Shutter | 70 |
| Minimum Brightness | 25 pixels |
| Maximum Brightness | 255 pixels |
| Minimum Area | 20 pixels |
| Maximum Area | 500 pixels |
| Trace length | 15 |
| Framerate | 30 frames per second (fps) |
| Position | 11 |
| Cycles | 3 |

2.8 Protein methods

2.8.1 Protein harvesting:

Cells were seeded in 6-well plates or T25 flasks, following previously mentioned procedures (section 2.3.3). After rinsing the cell twice with PBS, they were solubilised using 50 μ l or 100 μ l of protein lysis buffer (table 2.2). These cell lysates were then relocated to new microfuge tubes and chilled for 30 minutes, followed by a brief 10-minute room temperature exposure to break down nucleic acids. The lysates were clarified by centrifugation at 13,000 \times g for 5 minutes and the supernatant, was transferred to another microfuge tube. It was then either stored at -20°C or directly subjected to further analysis.

Table 2.2 Composition of protein lysis buffer

| Component | Volume | Final concentration |
|------------------------------------------------------------------|---------------|--------------------------------------------------------------------------------------------|
| Pierce™ Universal Nuclease for cell lysis | 0.5 µl | 250 U/µl |
| 7× cOmplete™, Mini, EDTA-free Protease Inhibitor Cocktail | 143 µl | 1X |
| 10× RIPA buffer | 100 µl | 0.5 M Tris-HCL, 1.5 M Sodium Chloride (NaCl), 2.5% deoxycholic acid, 10% NP-40, 10 mM EDTA |
| Distilled water | 756.5 µl | |
| Total | 1 ml | |

2.8.2 Protein quantification:

The BCA Protein Assay Kit by Pierce (Thermo Fisher Scientific, 23227) was utilized as per the provided guidelines. Bovine serum albumin (BSA) standards were prepared in protein lysis buffer to achieve varying concentrations (ranging from 0 to 2 mg ml⁻¹). To align the samples' absorbance with the standard curve, they were diluted either 5-fold or 10-fold using the same buffer. For the assay, 10 µl of either the sample or the standard was combined with 200 µl of the assay reagent (a mixture of solutions A and B in a 50:1 ratio) in a 96-well plate, in duplicate. After sealing, the plate was warmed at 37°C for 30 minutes. Subsequent colour change (at 562 nm absorbance) was assessed using a TECAN Infinite M200 microplate reader. A standard curve was constructed, mapping absorbance to BSA levels, which then informed a polynomial formula to determine the protein content in the samples.

2.8.3 Sodium dodecyl sulphate-polyacrylamide gel electrophoresis (SDS-PAGE) and protein transfer

Proteins underwent separation using 12% SDS-PAGE. The gel components are itemised below (Table 2.3), and all associated buffers were formulated in-house (Table 2.4). The resolving gel was poured between two glass plates and topped with isopropanol. Upon solidifying, the isopropanol layer was rinsed off with distilled water. The stacking gel was subsequently added atop the resolving gel, and a 15-well comb was placed. Once solidified, the comb was removed, and the wells thoroughly rinsed with distilled water. The gel was then set in a tank containing 1× SDS-PAGE running buffer. Typically, 10-40 µg of cell lysate was used for general protein analysis, while EVs protein assessment was based on equivalent volumes of lysate. Depending on the loading buffer concentration, lysates were diluted in either 10 µl or 20 µl of dH₂O. Diluted samples were mixed with respective loading buffers, with 20 µl samples paired with 5 µl of 5× loading buffer (National Diagnostics, EC-887) and 10 µl samples with 10 µl of 2× buffer (National Diagnostics, EC-886). These samples were then heated to 95°C for 5 minutes and loaded into the gel alongside 5 µl of Precision Plus Protein Dual Colour Standards (Bio-Rad, 1610394). Electrophoresis was conducted initially at 100-120 V, and upon sample entry into the gel, the voltage was adjusted to 120-150 V for an hour.

Table 2.3 The components and quantity to make two 12% SDS-PAGE gels

| | Reagent | Volume |
|----------------------|----------------------------------------------|---------------|
| Stacking gel | 40% Acrylamide | 0.975 ml |
| | Upper tris buffer | 2.1 ml |
| | dH ₂ O | 4.725 ml |
| | 10% (v/v) Ammonium persulfate solution (APS) | 100 µl |
| | Tetramethyl ethylenediamine (TEMED) | 10 µl |
| Resolving gel | 40% Acrylamide | 3 ml |
| | Lower tris buffer | 2.5 ml |
| | dH ₂ O | 4.3 ml |
| | 10% (v/v) Ammonium persulfate solution (APS) | 200 µl |
| | TEMED | 5 µl |

Table 2.4 Buffers and reagents used in SDS-PAGE and western blotting

| Buffer | Concentration | pH |
|--------------------------------------|--------------------------------------------------------|-----------|
| Upper Tris buffer | 1500 mM Tris base, 14 mM Sodium dodecyl sulphate (SDS) | 8.8 |
| Lower Tris buffer | 545 mM Tris base, 14 mM SDS | 6.8 |
| 1× SDS-PAGE running buffer | 25 mM Tris base, 192 mM glycine, 3 mM SDS | 8.3 |
| 1× TBS buffer | 20 mM Tris base, 150 mM NaCl | 7.6 |
| 1× TBS Tween-20 buffer (TBST) | As above with 0.1% (v/v) Tween-20 | 7.6 |
| Blocking buffer | As above with 5% (w/v) skimmed milk powder | — |

2.8.4 Western blotting:

Following the electrophoresis process (section 2.8.3), the stacking gel was removed. The proteins that had separated on the resolving gel were then carefully arranged onto an Amersham Protran 0.45 μm nitrocellulose membrane (Merck, Germany), situated between six filter papers. Special attention was given to eliminate any trapped air bubbles with a roller. The proteins were subsequently transferred via the Trans-Blot Turbo Transfer system (Bio-Rad, USA) with settings at 1 A, 25 V for 30 minutes. The nitrocellulose membranes were then blocked using a solution of tris-buffered saline (TBS) supplemented with 0.1% (v/v) Tween-20 (TBST) and 5% (w/v) skimmed milk powder, for 1 hour. These membranes were then subjected to an overnight incubation at 4°C with the chosen primary antibodies (Table 2.5). Following this, the membranes were washed three times with 1 \times TBST for 15 minutes, before being treated with a corresponding secondary antibody (Table 2.5) mixed in the blocking solution, kept at ambient temperature for 60 minutes. Once the membrane was washed again as above, the bound antibody complexes were detected using either PierceTM ECL Substrate (Bio-Rad, 1705061) or WESTAR SUPERNOVA (Cyanagen, XLS3), contingent on protein density. Post a 5-minute substrate immersion, membranes were either captured on a C-DiGit Blot Scanner (Li-Cor, USA) or exposed to CL-XPosure X-ray sheets (Thermo Fisher Scientific, UK) in a dark room. The resulting films were processed and stabilized with an Xograph Compact X4 apparatus (Xograph Imaging Systems, UK).

2.8.5 Membrane stripping and preservation:

When reusing membranes became necessary, the antibodies adhering to them were stripped using the RestoreTM western blot stripping solution (Thermo Fisher Scientific, 21059). This involved shaking the membrane in 10 to 20 ml of the stripping solution at ambient temperature for a period between 10 and 15 minutes. Subsequent to this, the membrane underwent three washing cycles with 1 \times TBST, each lasting 10 minutes. Once cleaned, the membrane was re-blocked and subjected to probing as described earlier (section 2.8.4). For preservation, the membrane was immersed in 1 \times TBST and securely encased

in a plastic pouch to ensure its moist state. This allowed it to be stored at 4°C for a duration extending up to two weeks.

Table 2.5 Lists of antibodies used in western blotting

| Antibody | Catalogue No. | Primary/ Secondary | Host species | Antibody type | Dilution | Molecular weight |
|---------------------------------------|--------------------------|--------------------|--------------|---------------|------------|------------------|
| Anti-HGS | ab155539 (Abcam) | Primary | Rabbit | Polyclonal | 1 in 1000 | 110 kDa |
| Anti-MVP | ab175239 (Abcam) | Primary | Rabbit | Monoclonal | 1 in 2000 | 99 kDa |
| Anti-TSG101 | ab125011 (Abcam) | Primary | Mouse | Monoclonal | 1 in 1000 | 44 kDa |
| Anti-CD63 | ab134045 (Abcam) | Primary | Rabbit | Monoclonal | 1 in 1000 | 26 kDa |
| Anti-ATP7A | Sc-376467 | Primary | Mouse | Monoclonal | 1 in 500 | 178 kDa |
| Anti-ATP7B | Sc-373964 | Primary | Mouse | Monoclonal | 1 in 500 | 165 kDa |
| Anti-RRBP1 | ab95983(Abcam) | Primary | Rabbit | Polyclonal | 1 in 1000 | 109 kDa |
| Anti-CTR1 | Ab129067 (Abcam) | Primary | Rabbit | Monoclonal | 1 in 1000 | 21 kDa |
| Anti-β actin | A1978 (Sigma-Aldrich) | Primary | Mouse | Monoclonal | 1 in 10000 | 42 kDa |
| Mouse Horseradish peroxidase (HRP) | A25112 (Abbkine) | Secondary | Goat | Polyclonal | 1 in 3000 | 50 kDa |
| Rabbit HRP | A25022 (Abbkine) | Secondary | Mouse | Monoclonal | 1 in 3000 | 50 kDa |

2.9 RNA methods

To prevent contamination by ribonucleases (RNase), all RNA-related procedures were conducted using RNase-free pipette tips, tubes, and nuclease-free water that had been properly filtered.

2.9.1 RNA extraction:

RNA was isolated from monolayers (section 2.3.3) using the Monarch® Total RNA Mini Preparation Kit (New England Biolabs, T2010S). Cells were rinsed thrice with PBS, followed by the addition of 350 µl of lysis solution to each well. The cell layers were then gently scraped and gathered in the lysis solution. All specimens passed through columns designed for genomic DNA exclusion. Following a 30-second centrifugation at 13,000 ×g, the filtrate, enriched with RNA, was preserved. An equal volume of 100% ethanol was introduced to the filtrate and lightly mixed. To bind the RNA from the solution, the mix was then centrifuged through an RNA purification column at 13,000 ×g for 30

seconds. The column was rinsed using 500 μ l of wash solution, followed by an on-column DNase I procedure to eliminate any lingering genomic DNA. By combining 5 μ l DNase I with 75 μ l DNase I reaction buffer and allowing it to sit on top of each column at ambient temperature for 15 minutes, the removal was executed. Subsequently, 500 μ l RNA priming solution was added to each column and spun at 13,000 \times g for 30 seconds. The columns underwent two more washes using the wash solution and were centrifuged at the same rate for 30 seconds and then 2 minutes. The purified RNA was then eluted into RNase-free tubes with 100 μ l of nuclease-free water. Aliquots of the RNA samples were then stored at -80 $^{\circ}$ C for future use.

2.9.2 RNA quantification

The NanoDropTM 1000 UV-VIS spectrophotometer (Thermo Fisher Scientific, USA) was employed to determine the concentration and purity of RNA. Adhering to the manufacturer's guidelines, 1 μ l of the isolated RNA was placed between the device's optical pedestals, using nuclease-free water as a blank.

2.9.3 Reverse transcription

2.9.3.1 Total RNA

Using the High-Capacity cDNA Reverse Transcription Kit from Applied Biosystems (reference 4368814), RNA was transcribed into complementary DNA (cDNA). Post quantification with NanoDrop (section 2.9.2), 100 ng of the total RNA, in a 10 μ l volume, was combined with a 10 μ l reaction master mix (Table 2.6) This mixture was then processed in the Applied BiosystemsTM 2720 Thermal Cycler, following the prescribed protocols from the manufacturer (Table 2.7). Stored samples were kept at -20 $^{\circ}$ C when not in immediate use.

Table 2.6 Composition of RT-PCR master mix

| Components | High capacity cDNA reverse transcription |
|-------------------------------------------|-------------------------------------------------|
| 10× RT Buffer | 2 µl |
| 25× dNTP Mix (100 mM) | 0.8 µl |
| 10× RT Random Primers | 2 µl |
| MultiScribe™ Reverse Transcriptase | 1 µl |
| Nuclease-free H₂O | 4.2 µl |
| Template RNA | 10 µl |
| Total per reaction | 20 µl |

Table 2.7 Setting of RT-PCR profile

| High-Capacity cDNA reverse transcription | |
|-------------------------------------------------|-------------|
| Temperature | Time |
| 25°C | 10 minutes |
| 37°C | 120 minutes |
| 85°C | 5 minutes |
| 4°C | Hold |

2.9.4 Quantitative polymerase chain reaction (qPCR)

2.9.4.1 Multiplex qPCR for transcript expression

The analysis of transcript expression was conducted employing TaqMan primer/probes as detailed in Table 2.8. The multiplex reactions were set up according to specifications provided in Table 2.9, with the Glyceraldehyde 3-phosphate dehydrogenase (GAPDH) serving as the endogenous control. For accurate results, every sample was tested in triplicate using a Rotor-Gene Q 2 plex real-time PCR instrument, manufactured by QIAGEN in Germany. The procedure followed a two-step program, as outlined in Table 2.10, and data acquisition was done from both green and yellow fluorescence channels. The cycle threshold was determined at 0.04, from which the Ct values were derived for subsequent data interpretation.

Table 2.8 TaqMan probes used in this study

| Target (reporter) | Gene name | Assay ID |
|--------------------------|--------------------------------------------------------------|-----------------|
| HGS | Hepatocyte growth factor-regulated tyrosine kinase substrate | Hs00610371_m1 |
| MVP | Major vault protein | Hs00911188_m1 |
| TEP1 | Telomerase associated protein1 | Hs00200091_m1 |
| PARP4 | Poly(ADP-ribose) polymerase family member4 | Hs00173105_m1 |
| vtRNA1-1 | Vault RNA 1-1 | Hs03676993_s1 |
| GAPDH | Glyceraldehyde 3-phosphate dehydrogenase | Hs99999905_m1 |

Table 2.9 Composition of Real-time PCR master mix

| Component | Multiplex qPCR |
|----------------------------------|----------------|
| 2× qPCRBio Probe Blue Mix Lo-ROX | 5 µl |
| RNase free water | 3.5 µl |
| TaqMan test probe | 0.5 µl |
| cDNA templates | 0.5 µl |
| GAPDH probe | 0.5 µl |
| Total per reaction | 10 µl |

Table 2.10 Setting of Real-time PCR two-step cycling conditions

| | Steps | Temperature | Time |
|----------|-----------------------------|-------------|------------|
| | PCR initial activation step | 95°C | 10 minutes |
| Combined | Denaturing | 95°C | 10 seconds |
| | Amplification | 60°C | 45 seconds |

2.9.4.2 Data analysis

Once Ct values were derived as detailed in (section 2.9.4), the ΔC_t was used by taking the difference between the Ct value of the target gene and that of the endogenous control. The fold change in expression was then determined using the $2^{-\Delta C_t}$ method, as described by Rizzacasa et al. (2019).

2.10 VtRNA1-1 antisense oligonucleotide transfection

The sequence for a predesigned DNA antisense oligonucleotide (ASO) to target vtRNA1-1 (5'-TGTTTCAATTAAAGAACTGT-3') was taken from Amort et al. (2015) and ordered from Integrated DNA Technologies. The ASO was reconstituted in 50 μ l IDTE buffer (pH 7.5) to give a final concentration of 100 μ M. This was diluted in IDTE buffer (pH 7.5) to produce a 10 μ M working stock. Cells were seeded into a 24-well plate at 1×10^5 cells per well and incubated overnight. Transfection mixtures were assembled in sterile tubes (volumes for 1 well shown in Table 2.11) and incubated at room temperature for 20 minutes. Transfection mixture was added dropwise to wells containing cells overlaid with 450 μ l growth medium. Cells were incubated for 24-48 hours before RNA extraction for subsequent qPCR analysis.

Table 2.11 ASO transfection reaction volumes per well of a 24-well plate

| Final ASO concentration (nM) | Volume of OptiMEM (μ l) | Volume of TransIT oligo reagent (μ l) | Volume of 10 μ M ASO (μ l) |
|------------------------------|------------------------------|--------------------------------------------|-------------------------------------|
| 0 | 47 | 3 | 0 |
| 50 | 44.5 | 3 | 2.5 |
| 75 | 43.24 | 3 | 3.76 |
| 100 | 42 | 3 | 5 |
| 200 | 37 | 3 | 10 |

2.11 Transmission electron microscopy:

For transmission electron microscopy analysis, a volume of 5 microlitres from the EV samples was placed on carbon-prepped copper grids, which had previously been discharged, for an incubation period of 5 minutes. Excess liquid was drained prior to staining procedure with a 1% solution of phosphotungstic acid at a pH level of 7.2, lasting for one minute. Thereafter, the grids experienced two successive washes in distilled water, each lasting a minute. The imaging phase was executed using the Tecnai T12 Spirit transmission electron microscope by FEI, which operated at a voltage setting of 80 kV. All resulting images were captured digitally with the Gatan Orius 1000B camera, and further processed utilizing the Gatan digital micrograph software.

2.12 Apoptosis detection by flow Cytometry:

Cellular apoptosis levels were assessed using the TACS™ Annexin V-FITC Apoptosis Detection Kit (R&D Systems, 4830-01-K). 2.5×10^5 cells / well were seeded in 6-well plates (section 2.3) with standard growth medium and then kept in a 37°C, 5% CO₂ humidified environment for 24 hours. Post this period, cells underwent a double rinse with PBS, followed by trypsinization using 0.5 ml trypsin for each well. The cells were then counted (section 2.3.1), suspended in 1.5 ml medium, and subjected to centrifugation at 300 ×g for 5 minutes at ambient temperature. Cells were washed in cold PBS + 1% (w/v) BSA and centrifuged again at the same speed for 5 minutes. The cell pellets were then treated with Annexin V incubation reagent (Table 2.12) at a volume of 100 µl for every 1×10^5 cells, and this was followed by a 15-minute incubation in a dark, cold environment. 400 µl of 1× Binding Buffer solution, derived from a 1:10 dilution of 10× Binding Buffer with distilled water, was used for rinsing the cells post-incubation. Using the LSR II Flow Cytometer (BD Bioscience, UK), the fluorescence intensity of these cells was assessed. A total of 1×10^4 events were recorded for each sample. This machine operates on dual lenses, recording forward (FSC-A) and side (SSC-A) light scatter. The excitation wavelengths were set to 530 nm (for Annexin V) and 660 nm (for Propidium iodide). Data from the flow cytometry was analysed using the FlowJo software (version V10), cell populations were distinguished based on their viability, apoptosis, and death using the FSC / SSC gating strategy.

Table 2.12 Composition of Annexin V incubation reagent

| Component | Volume |
|------------------------------|---------------|
| 10× Binding Buffer | 10 µl |
| Propidium iodide (PI) | 10 µl |
| TACS Annexin V-FITC | 1 µl |
| Distilled water | 79 µl |
| Total | 100 µl |

2.13 Cell cycle phases detection by flow cytometry

In this study, the H357 WT and cisplatin^R cell lines were utilized. The methodology initiated with cells being seeded at a density of 2.5×10^5 cells/well in a 6-well plate and allowed to adhere overnight. Subsequent to this, cells were treated with 0.9% NaCl as a control and with 14 µM of cisplatin, based on the determined IC₅₀. The samples were then incubated at 37°C in a 5% CO₂ environment for a duration of 24 hours. subsequently washed in FACS buffer composed of 100 mM PBS, 0.1% BSA. Between 5×10^5 and 1×10^6 cells were then transferred to an Eppendorf tube, ensuring consistent cell numbers across tubes to maintain uniform staining intensity. The cells were then fixed using ice-cold 70% ethanol, with the ethanol being added via a Pasteur pipette while vortexing—a crucial step. Post-fixation, cells were left at 4°C for a minimum of 30 minutes. Following this, cells were centrifuged at approximately 492 xg for 5 minutes. It's noteworthy that post-ethanol fixation, a slightly higher centrifugal force might be required due to the flocculent nature of the cells. After

centrifugation, the cells were washed twice with FACS buffer, ensuring the pellet, which might adhere to the side of the microcentrifuge tube, was retained.

Subsequently, 50 µl of RNase (100 µg/ml; Sigma) was added to the cells, followed by an incubation period at room temperature or 37°C for 15 minutes. This was succeeded by the addition of 300 µl of PI, achieving a final concentration of 50 µg/ml. The cells were then incubated for a minimum of 1 hour at room temperature. Some cell types might necessitate a more extended incubation, potentially overnight, for optimal staining. Once stained, the samples were stored for up to a week at 4°C, shielded from light. It's essential not to wash the samples before analysis. The final step involved analysing the samples using flow cytometry, collecting 10,000 events for each sample.

2.14 Assessment of Cell Proliferation and doubling time

To evaluate cellular growth over a designated period, a methodology outlined by Marayati et al. (2022) was employed. Cell lines were seeded at a density of 5×10^4 cells in each well of 6-well plates, supplemented with standard growth medium. These cells were then subjected to a 37°C environment with a 5% CO₂ atmosphere, for durations of 24, 48, 72, or 96 hours. After each incubation period and three washes with PBS, cells in each well were treated with 0.5 ml of trypsin for detachment. Following this, the cells were re-suspended in 1.5 ml of growth medium and subsequently quantified using a haemocytometer. The rate of cell growth, or doubling time, was then determined using a specific calculation as follow:

Growth rate:

$$r = \frac{\ln\left(\frac{N(t)}{N_0}\right)}{t}$$

$$\text{Doubling time} = \frac{\ln(2)}{r}$$

Or:

$$\text{Doubling time} = t \times \frac{\log(2)}{\log(N(t)) - \log(N_0)}$$

Where:

- $N(t)$ = the number of cells at time t
- N_0 = the number of cells at time 0
- r = growth rate
- t = time (in hours)

2.15 Statistical analysis

Data are presented as mean \pm standard deviation (mean \pm STDV). Both Student's t-test and ANOVA were employed to determine the statistical relevance of the findings for pairwise and more than two comparisons, respectively. A p-value below 0.05 was considered indicative of significance. Each experiment was performed on three separate occasions, unless otherwise stated. To visually represent statistical significance in the results, specific notations were used: 'ns' for not significant and *P<0.05, **P<0.01, ***P<0.001, and ****P<0.0001 for respective p-values. All graphical representations and related analyses were conducted using Graphpad Prism (Version 10.0).

Chapter 3 Effect of cisplatin treatment on extracellular particle release

3.1 Introduction:

Head and neck cancers (HNCs) are a complex group of malignancies that arise from various anatomical sites within the head and neck region, including the oral cavity, pharynx, and larynx. Globally, HNCs account for over 650,000 new cases and 330,000 deaths annually, making it a significant public health concern (Shang et al., 2021). The primary modalities of treatment for HNCs include surgery, radiation, and chemotherapy, often used in combination to achieve optimal outcomes. Cisplatin, a platinum-based chemotherapeutic agent, has been at the forefront of HNC treatment for several decades. Its mechanism of action primarily involves the formation of DNA adducts, leading to DNA damage and subsequent cell death (Kanno et al., 2021). While cisplatin has shown significant therapeutic benefits, a substantial proportion of patients either do not respond to treatment or develop resistance over time. This resistance can be intrinsic, present before treatment, or acquired after exposure to the drug. The mechanisms underlying cisplatin resistance in HNCs are multifaceted and not entirely understood. Factors such as increased drug efflux, enhanced DNA repair mechanisms, and evasion of apoptosis have been proposed (Kanno et al., 2021). However, recent evidence suggests a novel player in this intricate puzzle: extracellular particles (EPs) (Lucotti et al., 2022).

EPs, encompassing: exosomes, microvesicles, apoptotic bodies, exomeres (Zhang et al., 2018), and vault particles (Jeppesen et al., 2019), and other structures, are released into the extracellular environment by various cell types. These EPs play crucial roles in cell-to-cell communication by transferring lipids, proteins, and nucleic acids between cells. In the context of cancer, EPs have been implicated in promoting tumour growth, invasion, angiogenesis, and immune evasion (Kim et al., 2002).

Recent studies have begun to unravel the potential role of EPs in mediating chemotherapy resistance. For instance, EPs can sequester chemotherapeutic drugs, reducing their availability to tumour cells. They can also transfer drug-resistance genes or proteins between tumour cells, thereby spreading the resistance phenotype (Steinbichler et al., 2019). Given the emerging significance of EPs

in chemotherapy resistance, understanding their dynamics in response to cisplatin treatment is of paramount importance. Do HNC cells alter their EP release profile upon exposure to cisplatin? This is the main question that this chapters seeks to address.

3.2 Aim of this chapter:

To investigate the impact of cisplatin treatment on the release and characteristics of extracellular particles from HNC cell lines H357 and FaDu.

Objectives:

- Conduct MTT assays to ascertain the cisplatin IC50 values of squamous cell carcinoma cell lines H357 and FaDu, aiming to determine their sensitivity to the drug and suitable cisplatin concentrations for follow on experiments.
- Utilize flow cytometry to quantify the proportion of apoptotic cells in H357 and FaDu cell lines post-cisplatin treatment.
- Measure the concentration of extracellular particles released from H357 and FaDu cell lines post-cisplatin treatment, using conditioned medium, to gauge the impact of chemotherapy on particle release.
- Isolate extracellular particles through differential centrifugation and subsequently profile extracellular vesicles and vault particle markers via western blotting, aiming to characterize the composition of the released particles.

3.3 Results

3.3.1 Cell line viability in response to cisplatin treatment

The hypothesis is that the number of EPs released from cisplatin-treated HNC cells would increase, and the type of EP may be altered compared to untreated controls. To test this hypothesis, it was important to first determine the cisplatin sensitivity or resistance profiles of the H357 and FaDu cell lines. Both cell lines were cultured in 75 cm² tissue culture flasks under standardized conditions. Subsequently, cells were seeded into 96-well plates with 1×10^4 cells/ well, with a 24-hour adhesion window preceding cisplatin exposure. The drug's cytotoxicity was assessed at 24 and 48-hour intervals using an MTT assay across a cisplatin concentration gradient (0.01 to 100 μ M) to generate dose-response curves.

Across all three replicate experiments and for each time point, no significant difference was observed between the vehicle and the normal culture medium controls (Figure 3.1/3.2, A and B).

For the H357 cell line, a dose-dependent decrease in cell viability was observed with increasing cisplatin concentrations. At the lowest concentration of 0.01 μ M cisplatin for 24 hours, cell viability remained largely unaltered, registering an average survival rate of $101.2 \pm 12.78\%$. However, as the concentration increased to 10 μ M, there was a marked reduction to $73.15 \pm 9.47\%$. This decline was even more pronounced at the 100 μ M concentration, decreasing to $6.32 \pm 1.02\%$. When the exposure duration was extended to 48 hours, the average cell viability was $110.1 \pm 11.3\%$ for 0.01 μ M, $31.54 \pm 4.06\%$ for 10 μ M, and $5.91 \pm 0.41\%$ for the 100 μ M concentration (Figure 3.1. C, D).

The FaDu cell line exhibited a parallel trend. A 24-hour exposure to 0.01 μ M cisplatin resulted in an average cell survival of $100.7 \pm 6.60\%$. This was decreased to $53.33 \pm 8.44\%$ at 10 μ M and further reduced to $3.92 \pm 2.61\%$ at 100 μ M. Extending the exposure to 48 hours, the cell viability for 0.01 μ M was $100.64 \pm 12.53\%$, $29.12 \pm 9.69\%$ for 10 μ M, and $1.66 \pm 0.94\%$ for the 100 μ M concentration (Figure 3.2. C, D).

Comparatively, both cell lines demonstrated heightened sensitivity to cisplatin as the concentration increased. The 48-hour exposure generally yielded lower viability percentages than the 24-hour exposure, underscoring the time-dependent cytotoxic effects of cisplatin. Notably, while both cell lines

exhibited a similar trend in response to the drug, the H357 cells appeared slightly more resistant than the FaDu cells at certain concentrations, especially during the 48-hour incubation.

In conclusion, these findings emphasize the potent cytotoxic effects of cisplatin on HNC cell lines. The observed dose- and time-dependent decline in cell viability demonstrates the importance of empirically determining cisplatin doses for further experiments.

3.3.2 Determination of the IC₅₀ values for the H357 and FaDu cell lines following a 24-hour and 48-hour incubation period with cisplatin.

The dose-response curves were used to calculate the IC₅₀, which represented the cisplatin concentration causing a 50% reduction in cell viability. For the H357 cell line, the IC₅₀ values post 24 and 48-hour cisplatin exposures were determined to be 14 μ M and 6.0 μ M, respectively (Table 3.1 and Table 3.2). In contrast, the FaDu cell line exhibited IC₅₀ values of 11 μ M after 24 hours (Table 3.3) and 5.4 μ M post a 48-hour exposure (Table 3.4). The IC₁₀ and IC₉₀ values were also calculated and presented alongside the IC₅₀ values (Tables 3.1 – 3.4). Based on the IC₅₀ values were determined the concentrations of cisplatin to use in future experiments. In addition to the IC₅₀ dose, doses of 0.5x IC₅₀ and 2x IC₅₀ were also selected for use (Table 3.5).

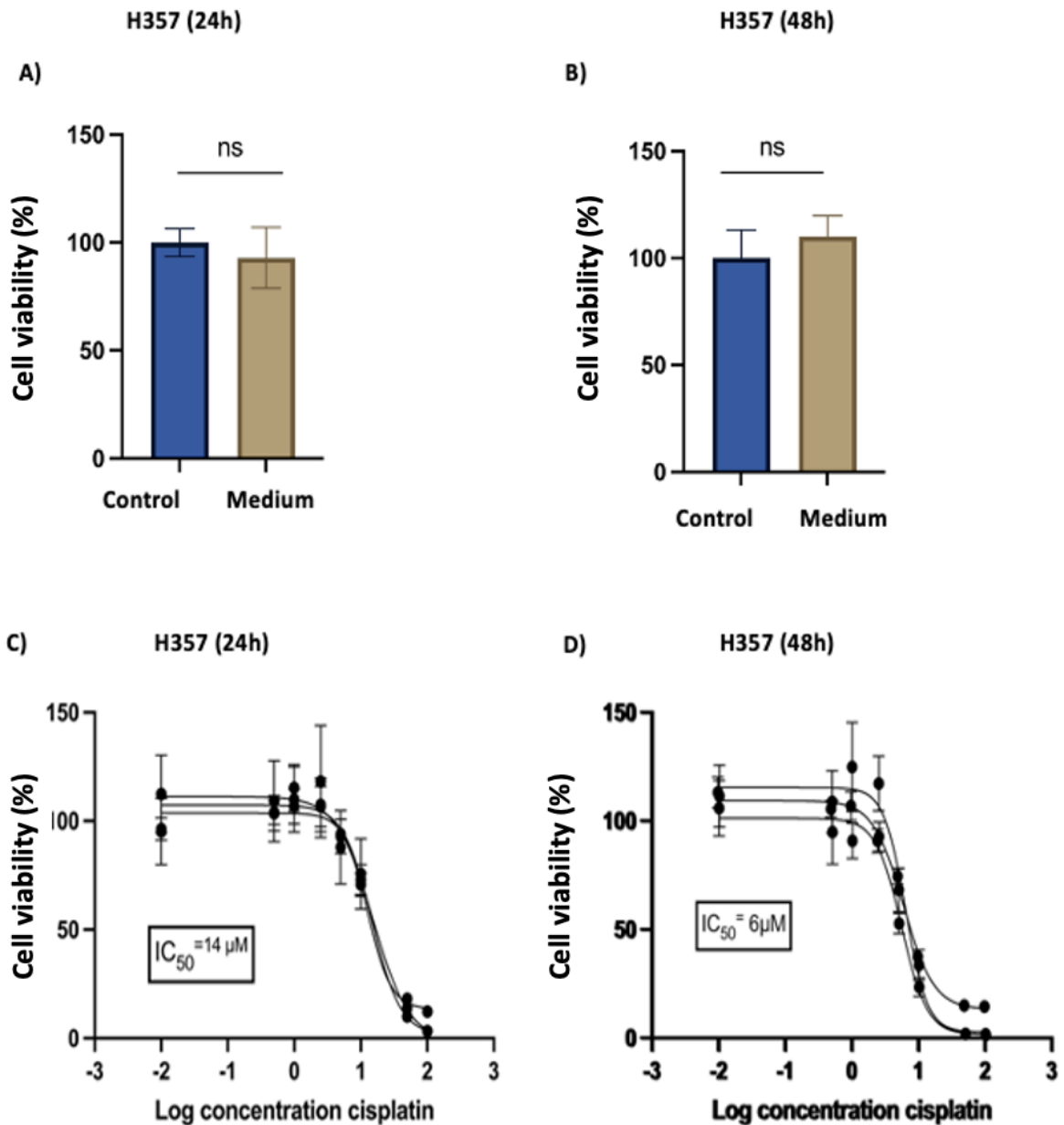


Figure 3.1 Viability of H357 cell line after cisplatin treatment.

Cellular metabolic activity and viability were assessed by comparing cells incubated with the vehicle control, 0.9% NaCl (control) to those cultured in standard growth medium (Medium), 24 hours (A) and 48 hours (B). Following this, cells were plated at a density of 1×10^4 cells/well in 96-well plates and treated with a gradient of cisplatin concentrations (0.01 to 100 μM) or a vehicle control (0.9% NaCl) for the same durations. The MTT assay then assessed cell metabolic activity/viability, and the resulting dose-response curves were plotted, documenting the effects of the cisplatin treatment over 24 (C) and 48 hours (D). Percentage cell survival was calculated relative to the vehicle control.

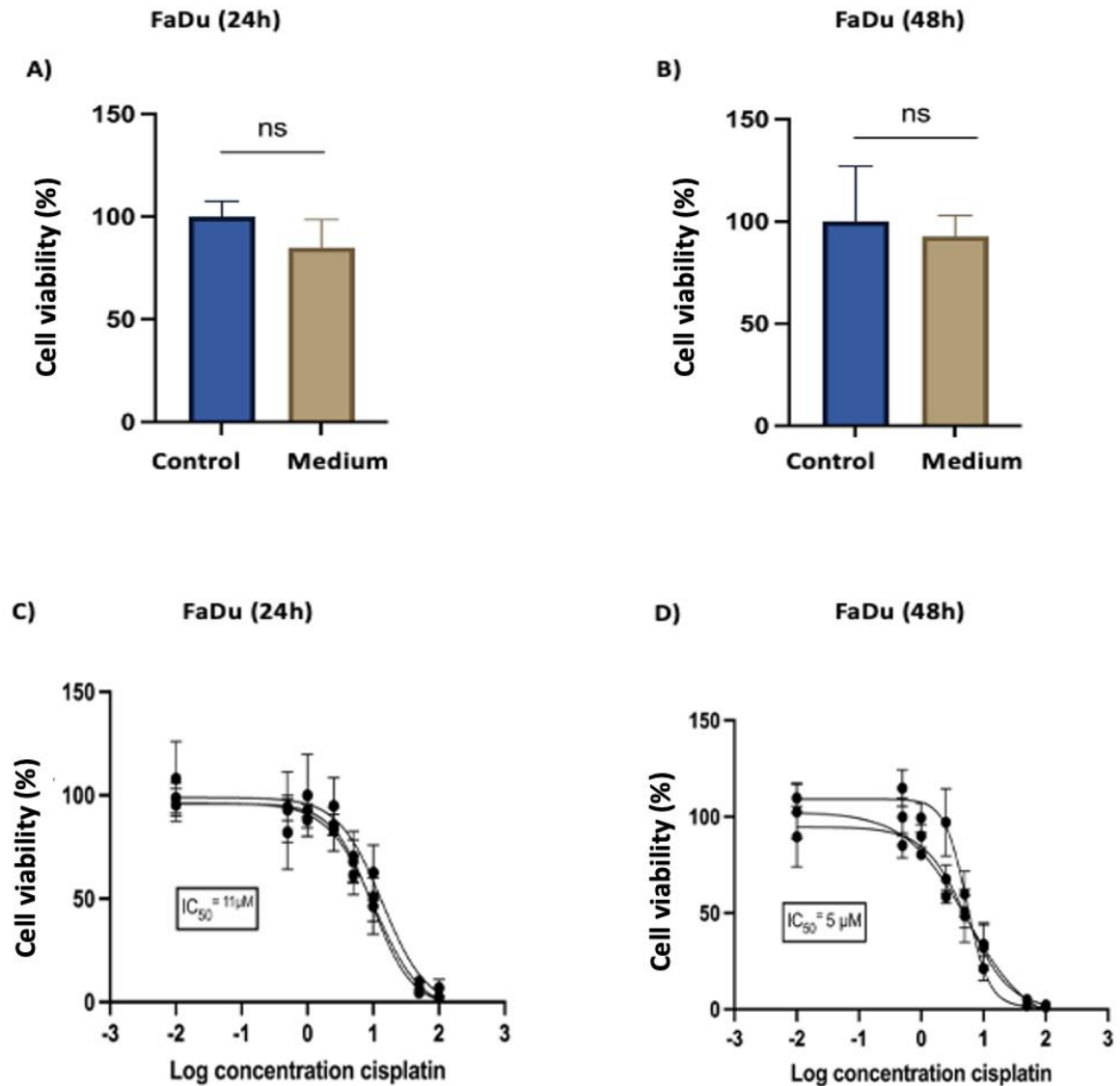


Figure 3.2 Viability of FaDu cell line after cisplatin treatment.

Cellular metabolic activity and viability were assessed by comparing cells incubated with the vehicle control 0.9% NaCl (control) to those cultured in standard growth medium (Medium), 24 hours (A) and 48 hours (B). Following this, cells were plated at a density of 1×10^4 cells/well in 96-well plates and treated with a gradient of cisplatin concentrations (0.01 to 100 μM) or a vehicle control (0.9% NaCl) for the same durations. The MTT assay then assessed cell metabolic activity/viability, and the resulting dose-response curves were plotted, documenting the effects of the cisplatin treatment over 24 (C) and 48 hours (D). Percentage cell survival was calculated relative to the vehicle control.

Table 3.1 H357 IC₁₀, IC₅₀ and IC₉₀ values after 24-hour incubation with cisplatin.

| Number of repeat | IC ₁₀ values (μM) | IC ₅₀ values (μM) | IC ₉₀ values (μM) |
|------------------|------------------------------|------------------------------|------------------------------|
| R1 | 5.14 | 12.60 | 30.89 |
| R2 | 4.93 | 14.70 | 43.9 |
| R3 | 3.81 | 15.21 | 60.83 |
| Average | 4.62 | 14.17 | 45.21 |
| (+/- SD) | 0.71 | 1.38 | 15.01 |

Table 3.2 H357 IC₁₀, IC₅₀ and IC₉₀ values after 48-hour incubation with cisplatin.

| Number of repeat | IC ₁₀ values (μM) | IC ₅₀ values (μM) | IC ₉₀ values (μM) |
|------------------|------------------------------|------------------------------|------------------------------|
| R1 | 1.93 | 6.10 | 19.33 |
| R2 | 2.77 | 6.31 | 14.39 |
| R3 | 2.06 | 5.45 | 14.40 |
| Average | 2.25 | 5.95 | 16.04 |
| (+/- SD) | 0.45 | 0.45 | 2.84 |

Table 3.3 FaDu IC₁₀, IC₅₀ and IC₉₀ values after 24-hour incubation with cisplatin.

| Number of repeat | IC ₁₀ values (μM) | IC ₅₀ values (μM) | IC ₉₀ values (μM) |
|------------------|------------------------------|------------------------------|------------------------------|
| R1 | 2.52 | 13.75 | 75.12 |
| R2 | 1.72 | 10.48 | 63.85 |
| R3 | 2.09 | 9.76 | 45.49 |
| Average | 2.11 | 11.32 | 61.48 |
| (+/- SD) | 14.95 | 2.12 | 14.95 |

Table 3.4 FaDu IC₁₀, IC₅₀ and IC₉₀ values after 48-hour incubation with cisplatin.

| Number of repeat | IC ₁₀ values (μM) | IC ₅₀ values (μM) | IC ₉₀ values (μM) |
|------------------|------------------------------|------------------------------|------------------------------|
| R1 | 0.94 | 5.41 | 31.18 |
| R2 | 0.44 | 5.43 | 67.10 |
| R3 | 2.19 | 5.42 | 13.39 |
| Average | 1.19 | 5.41 | 37.22 |
| (+/- SD) | 0.90 | 0.01 | 27.36 |

Table 3.5 Cisplatin concentrations that were chosen for experiments:

| H357 | FaDu |
|-------------------------------------|-------------------------------------|
| Cisplatin concentration (μM) | Cisplatin concentration (μM) |
| Vehicle control 0.9% NaCl | Vehicle control 0.9% NaCl |
| 7 μM (0.5x IC ₅₀) | 5.5 μM (0.5x IC ₅₀) |
| 14 μM (IC ₅₀) | 11 μM (IC ₅₀) |
| 28 μM (2x IC ₅₀) | 22 μM (2x IC ₅₀) |

3.3.3 Determination of the proportion of apoptotic HNC cells after treated with cisplatin.

To evaluate the proportion of apoptotic cells in HNC cell lines following cisplatin treatment at the concentrations decided above (Table 3.5), flow cytometry was employed, utilizing dual labelling with Annexin V-FITC and propidium iodide (PI). A key indicator of cellular apoptosis is the externalization of phosphatidyl serine (PS) on the cell membrane. Under normal conditions, PS remains confined to the inner surface of the plasma membrane, a process maintained by the amino-phospholipid translocase (Züllig et al., 2007). However, during apoptosis, this phospholipid distribution loses its asymmetry due to enzyme activity disruption, leading to the external manifestation of PS. Annexin V, a phospholipid-binding protein that binds to PS in the presence of calcium, can be tagged with the fluorescent marker FITC. PI is a membrane impermeant DNA-binding dye that is usually excluded from viable cells. Therefore, dual staining with annexin V and PI enables the differentiation between live (Annexin V⁻/PI⁻), apoptotic (Annexin V⁺/PI⁻) and dead cells (PI⁺).

Representative scatter plots are shown to illustrate how cell populations were selected (Figure 3.3 and Figure 3.4 panels A-D). For H357 cells treated with the control (0.9% NaCl), the mean apoptotic cell percentage was $0.57\% \pm 0.47\%$ (Figure 3.3. E), while for cisplatin concentrations of $7\ \mu\text{M}$, $14\ \mu\text{M}$, and $28\ \mu\text{M}$, the percentages were $2.18\% \pm 0.80\%$, $7.54\% \pm 2.29\%$, and $14.7\% \pm 2.32\%$, respectively. In contrast, the FaDu cell line exhibited apoptotic percentages of $1.0\% \pm 0.42\%$ (control), $1.93\% \pm 0.67\%$ ($5.5\ \mu\text{M}$), $3.80\% \pm 1.95\%$ ($11\ \mu\text{M}$), and $4.35\% \pm 1.89\%$ ($22\ \mu\text{M}$) (Figure 3.4. E). Notably, in H357 cells, significant differences in live, apoptotic, and dead cell populations were observed at $14\ \mu\text{M}$ and $28\ \mu\text{M}$ concentrations compared to the control, while the $7\ \mu\text{M}$ concentration showed no significant difference (Figure 3.3. E). Conversely, for FaDu cells, no significant differences were observed across most concentrations, except for a notable difference in live cells at the $28\ \mu\text{M}$ concentration when compared with the control (Figure 3.4. E).

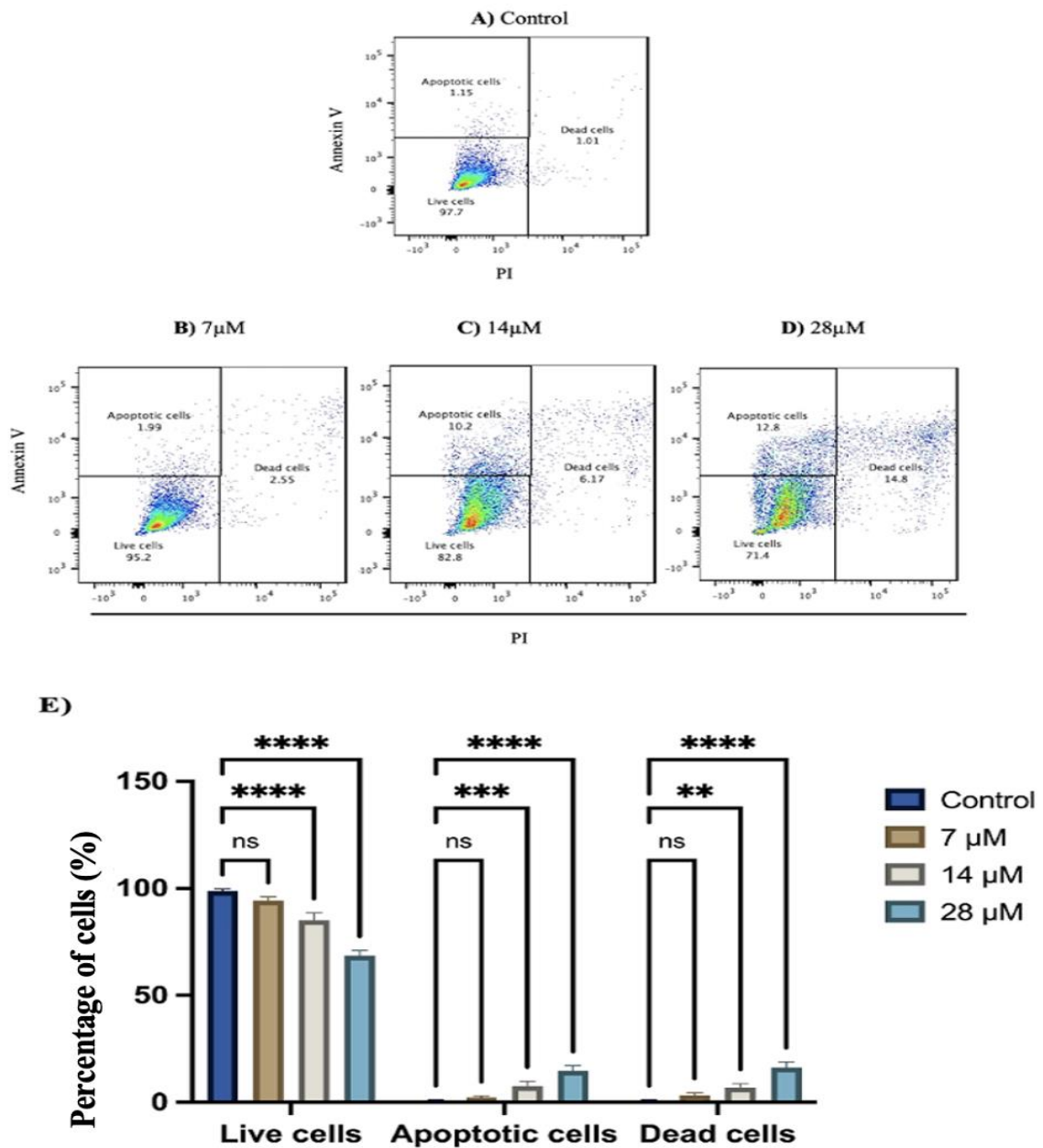


Figure 3.3 Assessment of apoptosis in H357 cell line after cisplatin treatment.

The proportions of apoptotic and dead cells were determined using flow cytometry, post-staining with Annexin V-FITC and PI. H357 cell line (2.5×10^5 cells/6-well) was incubated in medium for a duration of 24 hours and treated with different concentration of cisplatin for another 24h. Representative scatter plots showcasing PI (X-axis) against Annexin V (Y-axis) are depicted in panels A-D. The percentages of viable, apoptotic, and dead cells are presented in panel E. The percentage of live, apoptotic and dead cells within each individual sample was calculated following gating to select single cells. The presented values represent the average from four biological replicates \pm SD. Significance levels are indicated as follows: ns=not significant, ** = $p < 0.01$, *** = $p < 0.001$, **** = $p < 0.0001$, determined via two-way ANOVA.

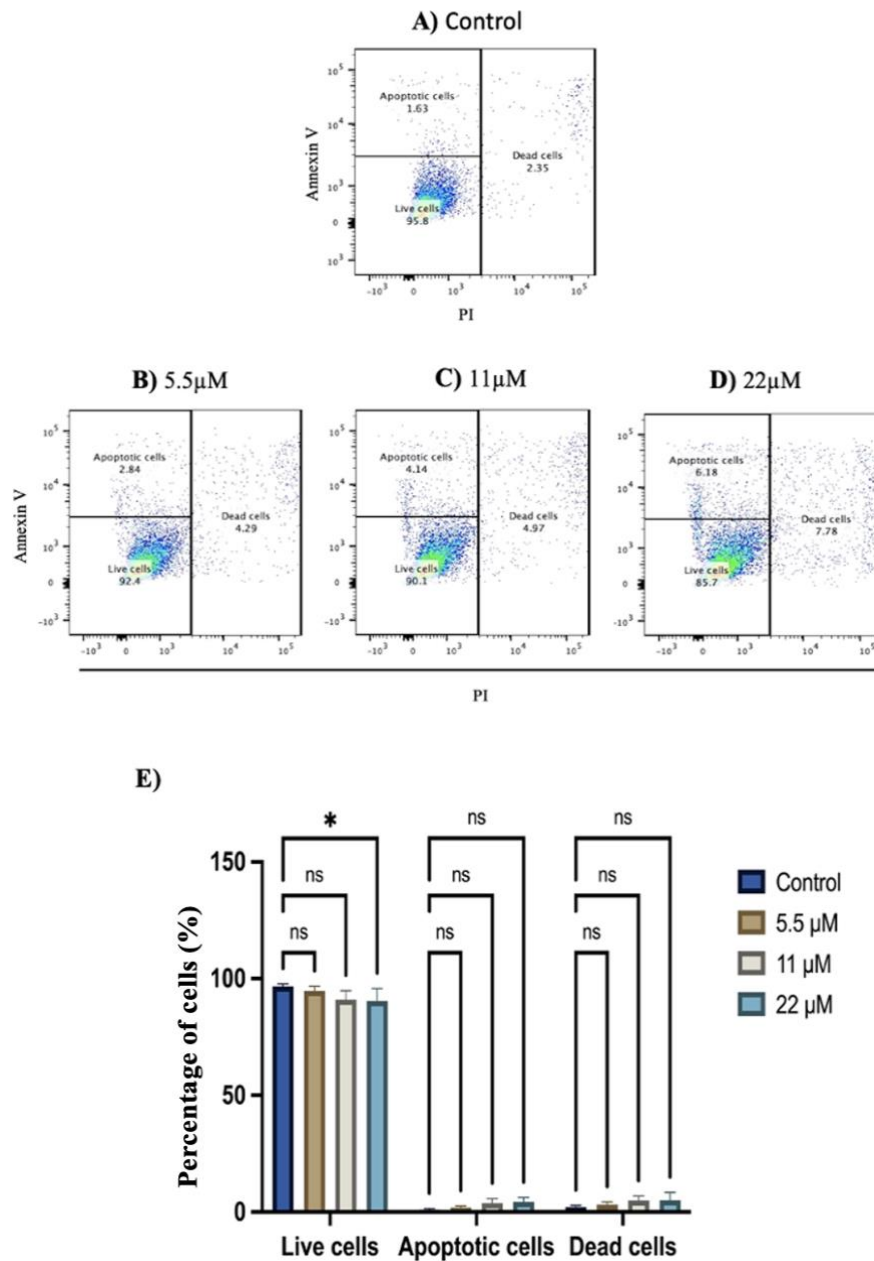


Figure 3.4 Assessment of apoptosis in FaDu cell line after cisplatin treatment.

The proportions of apoptotic and dead cells were determined using flow cytometry, post-staining with Annexin V-FITC and PI. FaDu cell line (2.5×10^5 cells/6-well) was incubated in medium for a duration of 24 hours and treated with different concentration of cisplatin for another 24h. Representative scatter plots showcasing PI (X-axis) against Annexin V (Y-axis) are depicted in panels A-D. The percentages of viable, apoptotic, and dead cells are presented in panel E. The percentage of live, apoptotic and dead cells within each individual sample was calculated following gating to select single cells. The presented values represent the average from four biological replicates \pm SD. Significance levels are indicated as follows: ns=not significant, * = $p < 0.05$ determined via two-way ANOVA.

3.3.4 FBS depletion by ultrafiltration:

For experiments involving EPs, it was crucial to ensure that the foetal bovine serum (FBS) utilized in cell culture media was devoid of endogenous particles, as there is the potential for endogenous particles present in foetal bovine serum (FBS) to interfere with the experimental outcomes. To address this, an ultrafiltration method was used to deplete the FBS of these particles (Kornilov et al., 2018). Standard FBS underwent centrifugation using Amicon ultra-15 centrifugal filters and the resultant filtrate was termed UF-dFBS. Growth medium was supplemented with standard FBS or UF-dFBS and particle concentration was determined by nanoparticle tracking analysis (NTA). The regular FBS was found to contain approximately 2.5×10^9 particles/ml. In contrast, the UF-dFBS contained significantly fewer particles 9.6×10^6 particles/ml. Serum-free medium contained no detectable particles. However, medium supplemented with 10% regular FBS had a particle concentration of 2.5×10^8 particles/ml, which was significantly higher compared to the medium containing 10% UF-dFBS, which contained 3.2×10^6 particles /ml (Figure 3.5). Thus, indicating that the ultrafiltration procedure depleted a large proportion of the endogenous particles from FBS, making it appropriate for subsequent experiments.

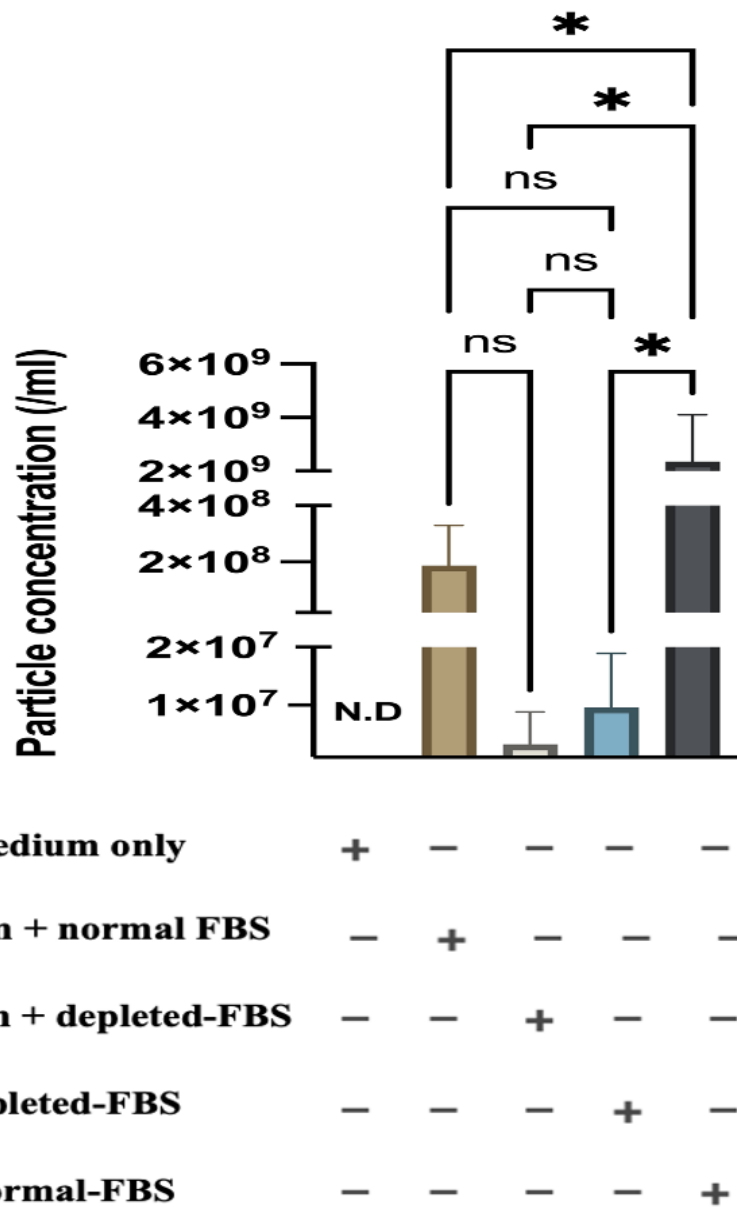


Figure 3.5 Depletion of particles from FBS.

RPMI medium was prepared in three variations: serum-free; with 10% standard FBS; and with 10% UF-dFBS. Additionally, both UF-dFBS and regular FBS were compared. To assess the particle concentration of these samples, Nanoparticle Tracking Analysis (NTA) was conducted using a Zetaview instrument. The presented data is an average derived from three separate experiments (n=3), with error bars representing standard deviation. Significance level is indicated as follows: * = p < 0.05 determined via one-way ANOVA.

3.3.5 Effect of cisplatin treatment on extracellular particles release from H357 and FaDu

To investigate the impact of cisplatin on the release of EPs from HNC cell lines, H357 and FaDu were treated with the cisplatin concentrations previously determined based on their IC50 values (Table 3.5). H357 cells were treated with cisplatin concentrations of 7 μ M, 14 μ M, and 28 μ M (Figure 3.6), while the FaDu cells received treatments of 5.5 μ M, 11 μ M, and 22 μ M (Figure 3.7). Additionally, a vehicle control group for both cell lines was maintained with 0.9% NaCl. After a 24-hour incubation with cisplatin, the medium was replaced with medium supplemented with UF-dFBS for an additional 24 hours. Post-treatment, the conditioned medium from each cell line was subjected to NTA to quantify the small particles. These quantifications were then normalized to the cell count for each respective well.

The number of particles released per cell for H357 treated with vehicle control, 7 μ M, 14 μ M, and 28 μ M cisplatin was 6.6×10^2 , 3.06×10^3 , 4.12×10^3 and 1.38×10^4 respectively. When the H357 cell line was treated with 28 μ M cisplatin there was a significant 21-fold increase in particle release compared to the control. However, there was no significant difference for the other concentrations tested (Figure 3.6 A). Analysis of the mean particle diameter revealed no statistically significant differences across the tested cisplatin concentrations (Figure 3.6 B).

In contrast, the FaDu cell line did not display any significant differences in EP release across all tested cisplatin concentrations when compared with the control (Figure 3.7 A). The number of particles released per cell for FaDu treated with vehicle control, 5.5 μ M, 11 μ M, and 22 μ M cisplatin was 1.63×10^3 , 2.22×10^3 , 1.30×10^3 and 3.26×10^3 , respectively. There were also no significant differences in the mean particle diameter for the different cisplatin concentrations (Figure 3.7 B).

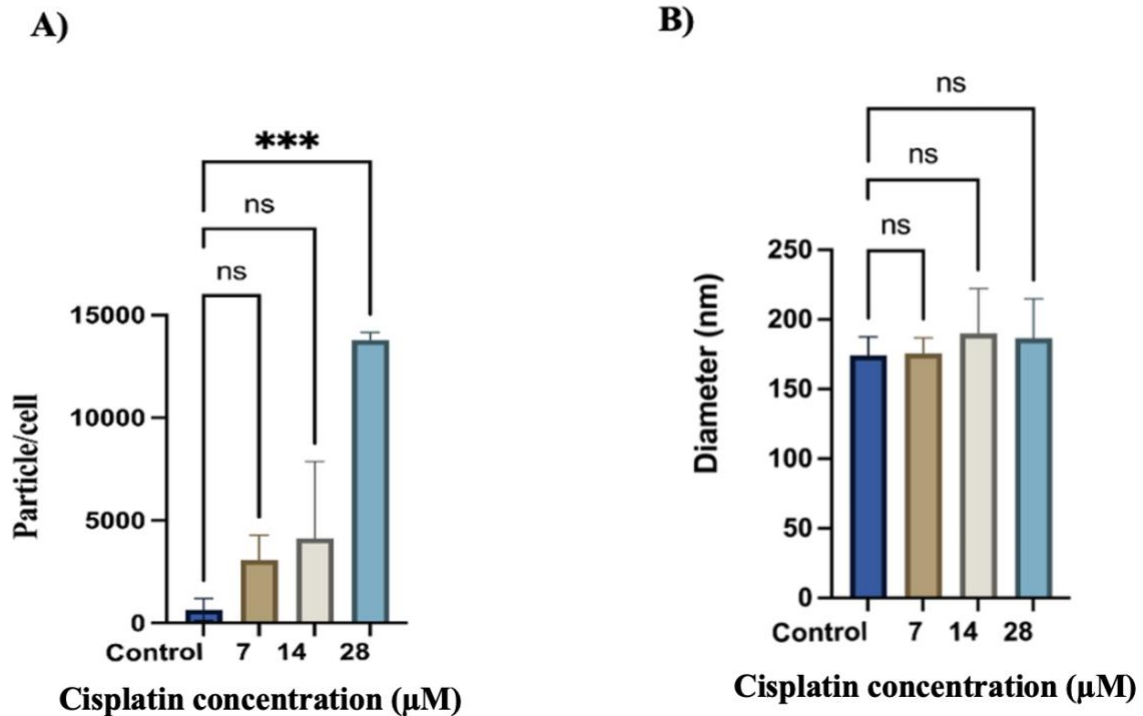


Figure 3.6 Impact of cisplatin on extracellular particle release in H357 cell line.

Cells were seeded at 2.5×10^5 cells/6-well and allowed to adhere. Cells were incubated with cisplatin for 24 h followed by replacement to medium supplemented with UF-dFBS and incubation for 24 h. Particle concentration in the conditioned medium was quantified using NTA and subsequently normalized based on cell counts (A). The mean particle diameter was also determined (B). The presented data represent the average of three biological replicates, with error bars indicating the standard deviation (SD). Statistical significance was determined using one-way ANOVA, with ns= not significant and *** indicating $P < 0.0001$.

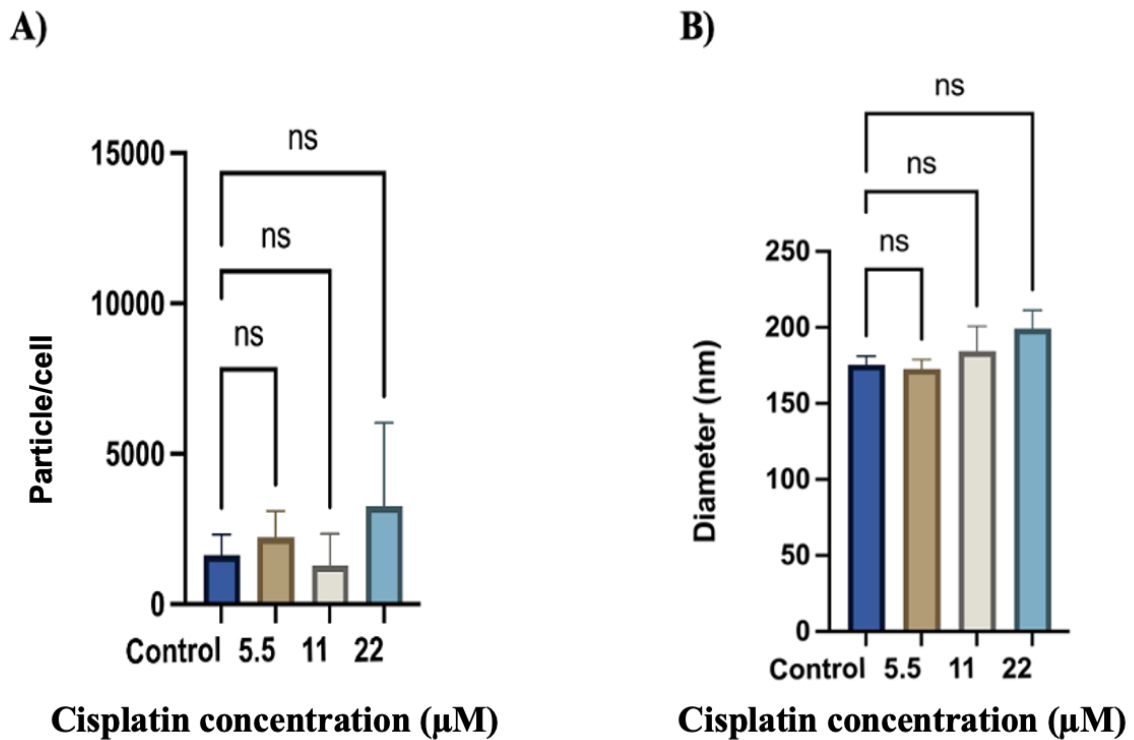


Figure 3.7 Impact of cisplatin on extracellular particle release in FaDu cell line.

Cells were seeded at 2.5×10^5 cells/6-well and allowed to adhere. Cells were incubated with cisplatin for 24 h followed by replacement to medium supplemented with UF-dFBS and incubation for 24 h. Particle concentration in the conditioned medium was quantified using NTA and subsequently normalized based on cell counts (A). The mean particle diameter was also determined (B). The presented data represent the average of three biological replicates, with error bars indicating the standard deviation (SD). Statistical significance was determined using one-way ANOVA, with ns= not significant.

3.3.5.1 Assessment of extracellular particle protein markers

To further characterise the EPs present in cell line conditioned medium after cisplatin treatment, particles were pelleted by ultracentrifugation at 100,000 x *g* for 1 hour. The pelleted EPs were solubilised in RIPA buffer. This was followed by western blot analysis to identify specific markers, namely Tumour Susceptibility Gene 101 protein (TSG101) and CD63, associated with extracellular vesicles, and MVP for vault particles. CD63, a member of the tetraspanin family, is predominantly found in EVs. This is due to the specific microdomains they create, known as tetraspanin-enriched microdomains (TEMs). These TEMs engage with a variety of signalling proteins and play a crucial role in the formation of EVs (Andreu & Yáñez-Mó, 2014). As an integral part of the ESCRT-I complex, TSG101 is pivotal in modulating vesicular transport. It interacts with ubiquitinated cargo proteins, facilitating their sorting into multivesicular bodies (MVBs).

H357 and FaDu cell lines underwent treatment with distinct concentrations of cisplatin, as detailed in Table 3.5. Subsequent analysis via western blotting revealed the presence of specific markers within the pelleted particles. Notably, markers characteristic of EVs (CD63 and TSG101), as well as the marker indicative of vault particles (MVP), were consistently detected across all tested cisplatin concentrations (Figure 3.8. A and B). There was an increase in MVP band intensity for EP derived from H357 and FaDu treated with the highest concentration of cisplatin. There was also a decrease in TSG101 band intensity in the same samples. There was no discernible pattern for CD63 for H357 derived EPs, whereas CD63 band intensity increased in EP derived from FaDu treated with the highest cisplatin concentration.

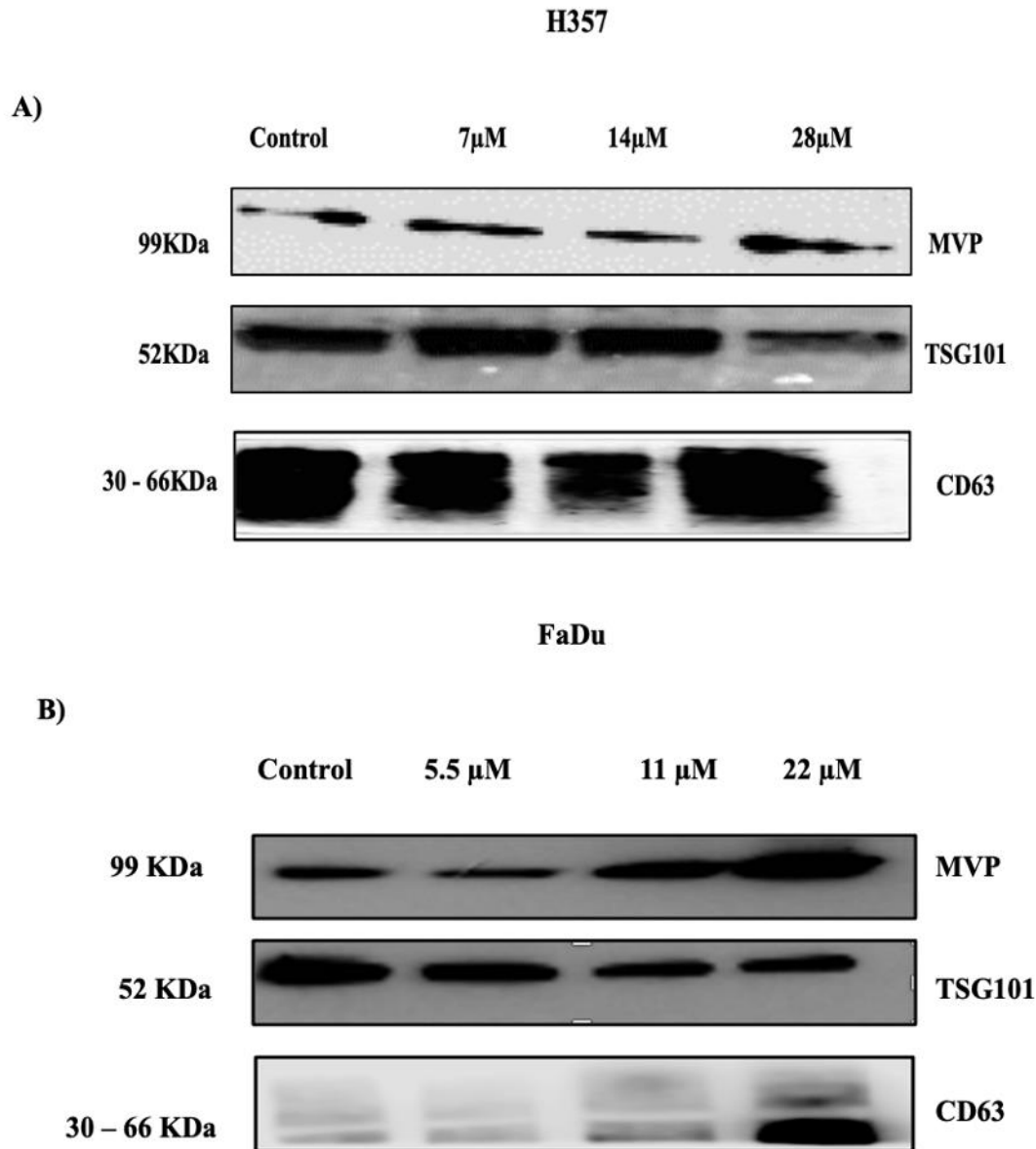


Figure 3.8 Detection of EV and vault particle markers in EP pellets derived from H357 and FaDu cells.

Cells were seeded at 2×10^6 cells/75 cm² flask and allowed to adhere. Monolayers were treated with cisplatin for 24 h and then medium was replaced to that supplemented with UF-dFBS and incubated for a further 24 h. Extracellular particles were pelleted by ultracentrifugation at $100 \times 10^3 \times g$ for 1 h, followed by washing in PBS and recentrifugation at $100,000 \times g$ for 1 h. The resulting EP pellets were then solubilised in RIPA buffer. Equal volumes of EP lysate were separated by SDS-PAGE and subsequently transferred onto a nitrocellulose membrane in preparation for western blotting. After blocking, these membranes were incubated with primary antibodies overnight at 4°C. Following a series of washes, the membranes were exposed to HRP-linked secondary antibodies at room temperature for 1 h. After a brief 5-minute incubation with a luminescent substrate, the membranes were exposed to X-ray film. The images are representative of three independent experiments.

3.4 Discussion

3.4.1 HNC cell viability in response to cisplatin treatment

The MTT assay, a widely accepted method for assessing cell metabolism as an indirect measure of viability, revealed a clear correlation between increasing cisplatin concentrations and reduced cell viability. This dose-dependent cytotoxicity is consistent with findings from studies such as the one by Hong et al., which showed that the level of cell viability and apoptosis induced by cisplatin was affected by its concentration, revealing a mechanism for dose-dependent cell death (Hong et al., 2012). Moreover, the cytotoxicity of cisplatin varies among different cell lines due to differences in drug uptake into the cells (Eichholtz-Wirth & Hietel, 1986), which might explain the slight variations in sensitivity between the H357 and FaDu cell lines. This observation suggests that intrinsic cellular factors, such as DNA repair mechanisms or drug influx/efflux pumps might influence the sensitivity of these cell lines to cisplatin (Welters et al., 1998). For instance, a study by Welters et al. (1997) highlighted that cellular platinum levels are positively correlated with cisplatin-induced growth inhibition in HNC *in vitro* (Welters et al., 1997). Another study by Mandic et al. (2005) reported that the loss of nuclear p53 signal correlates with cisplatin resistance in HNC (Mandic et al., 2005), further underscoring the importance of understanding the molecular underpinnings of cisplatin sensitivity and resistance in HNC cell lines.

The extended exposure to cisplatin, from 24 to 48 hours, further reduced cell viability, underscoring the time-dependent cytotoxic effects of the drug. This phenomenon has been observed in other studies as well, where prolonged exposure to cisplatin led to enhanced DNA damage and subsequent cell death (Schmidt & Chaney, 1993).

The determination of IC₅₀ values for cisplatin in H357 and FaDu cell lines provides crucial insights into the sensitivity or resistance profiles of these HNC cell lines. IC₅₀ values, representing the concentration of cisplatin required to reduce cell viability by 50%, serve as a standard metric to gauge the efficacy of chemotherapeutic agents. The sensitivity of HNC cell lines to cisplatin, as indicated by IC₅₀ values, can be influenced by a myriad of factors, including genetic mutations, protein expression profiles, and the duration of drug exposure. In this study, the H357 cell line demonstrated IC₅₀ values

of 14 μM and 6 μM after 24 and 48-hour exposures, respectively. The FaDu cell line exhibited similar sensitivities with IC50 values of 11 μM and 5 μM for the same durations. These findings align closely with a previous study that reported a common IC50 value of 15 μM for the OSCC cell lines H357, SCC9, and SCC4 (Mohapatra et al., 2021). Interestingly, on study observed an IC50 value of 6 μM for FaDu cells after 72-hour cisplatin incubation, which is very similar to the 48 hour IC50 value (Yang et al., 2019). It would expect the 72-hour IC50 to be much lower than the 48-hour IC50. The reason for this discrepancy is unclear.

Furthermore, other studies on OSCC cell lines revealed a broad spectrum of cisplatin sensitivities (Khoo et al., 2019 ; Shriwas et al., 2021). While the H103 cell line had IC50 values closely resembling these findings (15 μM for 24 hours and 4.57 μM for 48 hours), the H314 cell line exhibited a stark resistance with IC50 values of 200 μM and 100 μM for the respective durations. This variation in sensitivity was further exemplified by the H103/cisD2 cell line, which, after repeated cisplatin treatments, showed a heightened IC50 value of 150 μM . Such variations underscore the multifaceted nature of cellular responses to cisplatin, as also highlighted by Bauer et al. (2007) and Martens-de Kemp et al. (2013). The former emphasized the role of genetic factors, such as wild-type p53 and high Bcl-xL levels, in influencing cisplatin resistance, while the latter identified DNA-bound platinum as a crucial determinant of cisplatin sensitivity. The comparison between the dosages of cisplatin used in vitro and those administered in clinical settings requires careful examination due to the intrinsic differences in dosage calculation and application methods. Clinically, cisplatin dosages are determined based on body mass, a methodology that inherently considers the patient's physiological capabilities for drug absorption and metabolism (Wang et al., 2021). In contrast, in vitro experiments focus on measuring cisplatin concentrations that was determined IC50 based on MTT assay or a similar assay (He et al., 2016), which presents a fundamental challenge for establishing direct comparisons between these two approaches.

Moreover, the pharmacokinetics of cisplatin within patients introduce variables not present in laboratory conditions. Upon administration, cisplatin is subject to bodily processes such as renal excretion and faces challenges in uniformly reaching all areas of complex 3D human tissues (Ried et al., 2015; Zhang et al., 2021). These factors significantly influence the drug's effectiveness and its ability

to penetrate tumours, where distribution is further impeded by the physical and biological complexities of these tissues.

In the laboratory, studies typically involve treating monolayer cell cultures with anti-cancer drugs, a method that fails to mimic the complex 3D structure of human tumours and does not account for the metabolic processes affecting drug distribution and excretion in the body. Consequently, the dosages applied in vitro are significantly lower than those used in clinical practice (Gupta et al., 2022; Tchoryk et al., 2019). This difference highlights the limitations of directly comparing in vitro concentrations with clinical dosages and emphasizes the importance of a careful interpretation of how cisplatin operates within the complex biological environment of the human body.

This analysis highlights the critical methodological and physiological distinctions between in vitro and clinical uses of cisplatin, pointing out the difficulties in directly comparing dosages between these environments. It stresses the need for careful consideration when extrapolating laboratory findings to clinical contexts, ensuring that such interpretations are conducted with careful examination and attention to detail.

In conclusion, while the findings are in line with several studies, they also highlight the variability in HNC cell line sensitivity to cisplatin, which may relate to the complex interplay of genetic, molecular, and temporal factors.

3.4.2 Cisplatin-induced apoptosis in HNC cell lines

Apoptosis, characterized by nuclear chromatin condensation, cytoplasmic organelle compaction, and cell surface changes, plays a pivotal role in tissue modelling during vertebrate development. The induction of apoptosis by chemotherapeutic agents, including cisplatin, has been proposed as a primary mode of cell death. Given the significance of apoptosis in drug-induced cytotoxicity, understanding its underlying mechanisms is crucial for the development of more effective chemotherapeutic strategies (Kaufmann & Earnshaw, 2000).

The cytotoxic effects of cisplatin on HNC cell lines were evaluated using flow cytometry, focusing on the induction of apoptosis. The externalization of phosphatidyl serine (PS) on the cell membrane serves as a hallmark of apoptosis. This phenomenon is consistent with previous findings

where PS externalization was noted during apoptosis due to enzyme activity disruption, leading to the external manifestation of PS (Mirnikjoo et al., 2009; Züllig et al., 2007). The dual staining with Annexin V and PI, as employed in this study, provides a robust method to differentiate between live, apoptotic, and dead cells.

In the present study, H357 cells exhibited a dose-dependent increase in apoptosis upon cisplatin treatment. Specifically, significant differences in apoptotic cell populations were observed at 14 μ M and 28 μ M concentrations compared to the control. This is consistent with the known cytotoxic effects of cisplatin, which is believed to induce apoptosis through the platination of DNA, leading to the formation of intrastrand and interstrand cross-links (Eastman, 1991; Roberts & Friedlos, 1987; Roberts & Thomson, 1979). Such DNA damage can result in a slowdown in S-phase transit, followed by a G2 block (Fraval & Roberts, 1979; Sorenson et al., 1990). Cells may either overcome this G2 block and continue to cycle or remain arrested and eventually undergo cell death.

Interestingly, the FaDu cell line showed a negligible response to cisplatin treatment, with no significant differences in apoptotic percentages across most concentrations. This suggests potential cell line-specific differences in sensitivity to cisplatin, which could be attributed to variations in DNA repair mechanisms, cell cycle checkpoints, or other cellular processes. The differential apoptotic responses between the H357 and FaDu cell lines might be attributed to the unique genetic and molecular profiles of each cell line. For instance, a study on HL-60 cells revealed that cisplatin-induced apoptosis involved the downregulation of BCL2 and upregulation of BCL2L12 genes (Floros et al., 2003). Furthermore, Qin and Ng (2002) highlighted that cisplatin induced apoptosis in hepatoma cells via both p53-dependent and -independent pathways. This suggests that multiple molecular pathways might be at play in the observed apoptotic responses in H357 and FaDu cells.

Previous studies have demonstrated the induction of apoptosis in various cell lines upon cisplatin treatment. For instance, the KM-1 oral squamous cell carcinoma cell line exposed to cisplatin showed that while most cells underwent apoptosis, a small fraction exhibited necrosis (Ita & Murakami, 1998). This suggests that cisplatin can induce both apoptotic and necrotic cell death, depending on the cell type and treatment conditions.

Furthermore, studies on L1210 cells have shown that higher doses of cisplatin lead to rapid cell death through apoptosis, while lower doses result in a G2 block, with cells either overcoming this block or eventually dying without undergoing apoptosis (Sorenson et al., 1990). This dual mechanism of cell death underscores the complexity of cisplatin's cytotoxic effects and highlights the importance of dose and cell type in determining the cellular response.

In conclusion, the present study has illuminated the complex apoptotic effects of cisplatin on HNC cell lines, revealing significant insights into the drug's cytotoxic mechanisms. Through meticulous investigation, it was observed that the H357 and FaDu cell lines exhibit differential responses to cisplatin treatment, a phenomenon that underscores the paramount importance of cell-specific factors in determining drug efficacy. This differential sensitivity highlights the intricate, multifaceted nature of cisplatin's action at the molecular level, potentially attributable to variations in DNA repair mechanisms, cell cycle checkpoints, and other critical cellular processes. The broader scientific literature corroborates the findings, suggesting that cisplatin exerts its cytotoxic effects through diverse mechanisms, which could elucidate the observed differences in cisplatin-induced apoptosis between these two cell lines.

Moreover, the study encountered a notable discrepancy between the outcomes of MTT and flow cytometry assays when evaluating the IC_{50} values and apoptotic rates within these cell lines. This discrepancy can be primarily attributed to the inherent differences in the methodologies and biological implications of these assays (Sazonova et al., 2022). While the MTT assay serves as an indirect measure of cell viability by quantifying cellular metabolic activity, it does not distinguish among the specific pathways leading to cell death, such as apoptosis, necrosis, or autophagy (Siewewerts et al., 1995). Conversely, flow cytometry provides a direct assessment of apoptosis by detecting phosphatidylserine exposure on the cell surface, indicative of early apoptotic events (Vermes et al., 1995). The divergence in results from these assays underscores the complex interplay of cisplatin-induced cell death mechanisms, suggesting that impacts on cell viability stem not solely from apoptosis but from a broad spectrum of death pathways (Sazonova et al., 2022). This nuanced understanding is pivotal for interpreting the differential sensitivity and responses of the cell lines to cisplatin treatment, emphasizing the necessity for a holistic approach in drug efficacy evaluation.

Research into head and neck squamous cell carcinoma (HNSCC) has focused on understanding the chemoresistance mechanisms of various cell lines, including H357 and FaDu, which are derived from human oral and hypopharyngeal squamous cell carcinomas, respectively (Lamperska et al., 2017; Prime et al., 1990). Studies have shown that the H357 cell line exhibits a complex response to chemotherapeutic agents, influenced by a side population of stem-like cells expressing ABCG2 and ABCC1 multidrug transporters and displaying heightened Hoechst 33342 efflux, this phenomenon is associated with resistance to chemotherapy, which can be counteracted by the application of ABC transport inhibitors such as verapamil, thereby sensitizing both parent and side population cells to chemotherapy (Loebinger et al., 2008). Additionally, H357 cells have demonstrated resistance to cisplatin, a resistance further enhanced by co-culturing with cancer stem cell-derived extracellular vesicles (CSC-EVs). The mechanisms underpinning this resistance involve the modulation of apoptotic or necroptotic cell death pathways and the inhibition of inhibitor of apoptosis proteins (IAP) (Hu et al., 2023). Furthermore, low levels of caspase-8 in H357 cells, associated with poor prognosis in HNSCC, indicate a cell line-specific sensitivity to therapeutic agents like TRAIL and Smac-164 (SM), with SM treatment leading to caspase-10 activation and suggesting potential biomarkers for patient selection (Raulf et al., 2014).

Similarly, the FaDu cell line has been characterized by its resistance to a range of chemotherapeutic drugs including cisplatin, 5-fluorouracil (5-FU), doxorubicin, and vincristine. The resistance is notably higher in the FaDu/T-200 nM variant, indicating a generalized cross-resistance across FaDu/T cells to these agents (Raulf et al., 2014). Investigations into the role of let-7d microRNA expression have revealed its significant influence on the chemosensitivity of the FaDu cell line, with varying expression levels affecting the response to chemotherapy and radiotherapy (Lamperska et al., 2017). Notably, specific models within the FaDu line showed differential resistance to cisplatin, 5-FU, and doxorubicin, highlighting the impact of let-7d levels on drug resistance (Lamperska et al., 2017). The interaction between FaDu cells and cancer-associated fibroblasts (CAFs) further complicates the resistance landscape, co-culture with chemoresistant CAFs (rCAFs) increased FaDu cells' resistance to chemotherapeutic agents, a process mediated through TGF α -EGFR paracrine signalling, which could

be mitigated by cetuximab treatment, restoring chemosensitivity in co-injected tumour models (Su et al., 2023).

These investigations underscore the multifaceted nature of chemoresistance in HNSCC cell lines, pointing to the significant roles played by stem-like cell populations, microRNA expression, and the tumour microenvironment. Understanding these complex mechanisms is crucial for developing targeted therapies and selecting suitable treatments for HNSCC, thereby improving patient outcomes.

Hence, these findings, in conjunction with existing literature, accentuate the multifaceted mechanisms through which cisplatin achieves its cytotoxic effects. This study emphasizes the critical importance of considering both cell-specific factors and the comprehensive spectrum of cell death pathways in the development of more effective chemotherapeutic strategies. By acknowledging these complexities, they can be better understand the variability in drug responses among different cell lines, paving the way for tailored therapeutic approaches that can significantly enhance treatment outcomes for patients with head and neck cancer.

3.4.3 Characterisation of extracellular particle release in HNC cell lines in response to cisplatin treatment

The exploration of EPs, especially EVs, has become a focal point in cancer research. Their pivotal role in intercellular communication and their potential as both biomarkers and therapeutic targets have been extensively documented (Kim et al., 2002 ; Zhao et al., 2022). In the current study, It was embarked on characterization of EPs released from HNC cell lines H357 and FaDu, with a specific focus on the influence of cisplatin treatment.

Utilizing NTA, the results revealed a differential response in the release of EPs from the H357 and FaDu cell lines following cisplatin treatment. Notably, the H357 cell line demonstrated a pronounced increase in particle release at the 28 μ M cisplatin concentration.

In contrast, the FaDu cell line's response remained relatively consistent across all tested concentrations. This observation contrasts with prior studies indicating an augmented EV secretion from tumour cells after chemotherapy, which is associated with tumour progression (Bandari et al.,

2018; Pascucci et al., 2014). For instance, Lv et al. observed an increase in the levels of HepG2-derived exosomes following treatment with various chemotherapeutic agents (Lv et al., 2012). Similarly, increased levels of EVs have been linked to treatment failure and disease progression in breast cancer patients undergoing neoadjuvant chemotherapy (König et al., 2017).

Further validation of these particles was achieved through western blot analysis, targeting specific markers such as TSG101 and CD63. The consistent presence of these markers across different cisplatin concentrations suggests a potential interaction between cisplatin treatment and the release or composition of these cellular particles. This aligns with Shi et al. (2019), who emphasized the role of EVs in modulating drug resistance mechanisms.

The differential response of the H357 and FaDu cell lines to cisplatin might be attributed to distinct resistance mechanisms. It has been postulated that the molecular signature defining the resistant phenotype varies between tumours (Siddik, 2003). In this context, the H357 cell line might possess a unique molecular signature predisposing it to an increased release of EVs upon cisplatin exposure, as opposed to the FaDu cell line.

In addition, oxidative stress plays a pivotal role in the regulation of EV release. Excessive reactive oxygen species (ROS) can influence cellular signalling by modifying the number and molecular cargo of EVs (Chiaradia et al., 2021). Cisplatin has been shown to stimulate the release of multiple EVs from tumour cells during chemotherapy, potentially due to its induced increase in oxidative stress levels (Wysoczynski & Ratajczak, 2009). Xia et al. demonstrated that cisplatin-induced endoplasmic reticulum (ER) stress led to the release of exosomes encapsulating ER-resident protein 44 (ERp44) from nasopharyngeal carcinoma cells, thereby promoting drug resistance (Xia et al., 2021).

Moreover, oxidative stress brought on by cisplatin affects the functionality, distribution, and clustering of proteins that are deleterious to cell health. In response to this damage from toxic proteins, cells activate their protein quality control systems to diminish the build-up of these detrimental proteins (Yadav et al., 2019). The significant expulsion of EVs by tumour cells stressed with cisplatin may act as a defensive strategy to mitigate oxidative harm by eliminating drugs and oxidatively modified proteins. Nonetheless, these vesicles, laden with proteotoxic substances, can be transported to adjacent or remote cells, instigating oxidative stress reactions between cells (Malik et al., 2013).

In conclusion, the study underscores the intricate relationship between cisplatin treatment and the release of extracellular particles in HNC cell lines. The differential response observed between the H357 and FaDu cell lines emphasizes the heterogeneity in drug resistance mechanisms and underscores the inherent differences between HNC cell lines.

Chapter 4 Effect of blocking extracellular particle release on cisplatin sensitivity.

4.1 Introduction:

Extracellular particles, particularly EVs, have emerged as pivotal players in the intricate landscape of cell-to-cell communication. These particles carry a diverse array of biomolecules, including proteins, lipids, and nucleic acids, which can be transferred to recipient cells, influencing their behaviour and function (Lucotti et al., 2022). One of the most significant revelations in recent cancer research is the role of these particles in mediating drug resistance. For instance, exosomes, have been shown to contribute to chemoresistance by sequestering chemotherapeutic agents and facilitating their efflux from cancer cells (Bach et al., 2017). This mechanism acts as a cellular defence, allowing tumour cells to expel drugs and evade their cytotoxic effects. Furthermore, EVs can transfer drug resistance-conferring molecules, such as specific miRNAs or proteins, to drug-sensitive cells, thereby propagating a resistant phenotype within the tumour's microenvironment (Santos & Almeida, 2020).

Vault particles, on the other hand, are lesser known but equally intriguing. These protein-shelled structures (composed mainly of MVP) have been implicated in multidrug resistance, although the exact mechanisms remain under investigation. Previous studies suggest that vaults might protect cells from drugs by sequestering them or by modulating cellular pathways that counteract drug-induced stress (Mossink et al., 2003). Very recently it was shown that vault particles are present in the extracellular space, which raises the possibility that they too may be involved in efflux of drugs from cells (Jeppesen et al., 2019).

The blockade of EP release, therefore, represents a promising strategy to counteract these resistance mechanisms. By inhibiting the release of EVs or vault particles, one could potentially prevent the efflux of drugs from cancer cells, ensuring higher intracellular drug concentrations and enhanced cytotoxicity. Additionally, blocking the release of these particles could disrupt the transfer of resistance-conferring molecules, preventing the spread of drug resistance within the tumour (Musi & Bongiovanni, 2023).

In this chapter, it aims to delve deeper into this concept by utilising two CRISPR Cas9 edited cell lines recently created by members of our research group that are EV (H357 Δ HGS) and vault particle deficient (H357 Δ MVP). HGS, a member of the ESCRT, is a master regulator of EV biogenesis, in particular those derived from multivesicular bodies (i.e. exosomes) (Bache et al., 2003). MVP is the main structural component of the vault particle and is required for their assembly (Stephen et al., 2001). By blocking the release of EVs and vault particles, it is hypothesised that cells would exhibit heightened sensitivity to cisplatin.

4.2 Aim of this chapter:

This chapter aims to determine the sensitivity of the H357 cell line to cisplatin treatment following the blockade of EV and vault particle release, achieved by depleting the HGS (H357 Δ HGS) and MVP (H357 Δ MVP) proteins, respectively. To achieve this the following objectives will be addressed:

- Validate the cell lines using qPCR and western blotting to ensure the knockout of HGS and MVP proteins.
- Conduct a doubling time test for both cell lines to evaluate the growth rate and compare it with the parent cell line.
- Assess extracellular particle release in response to cisplatin treatment by NTA and western blotting.
- Compare the proportion of live, apoptotic and dead cells post-cisplatin treatment between the edited cell lines and the parent cell line by flow cytometry.

4.3 Results

4.3.1 Validation of HGS knockout in H357 cell line by qPCR and western blotting

Prior to conducting experiments to test the main hypothesis, it is sought to validate the successful knockout of HGS in the H357 cell line at the transcript and protein level by qPCR and western blotting, respectively. There was no significant difference in HGS transcript expression between the knockout and WT cell lines (Figure 4.1, A). However, western blotting showed that the HGS protein was not detectable in H357 Δ HGS cell line compared to the WT, confirming successful HGS knockout at the protein level (Figure 4.1, B/C).

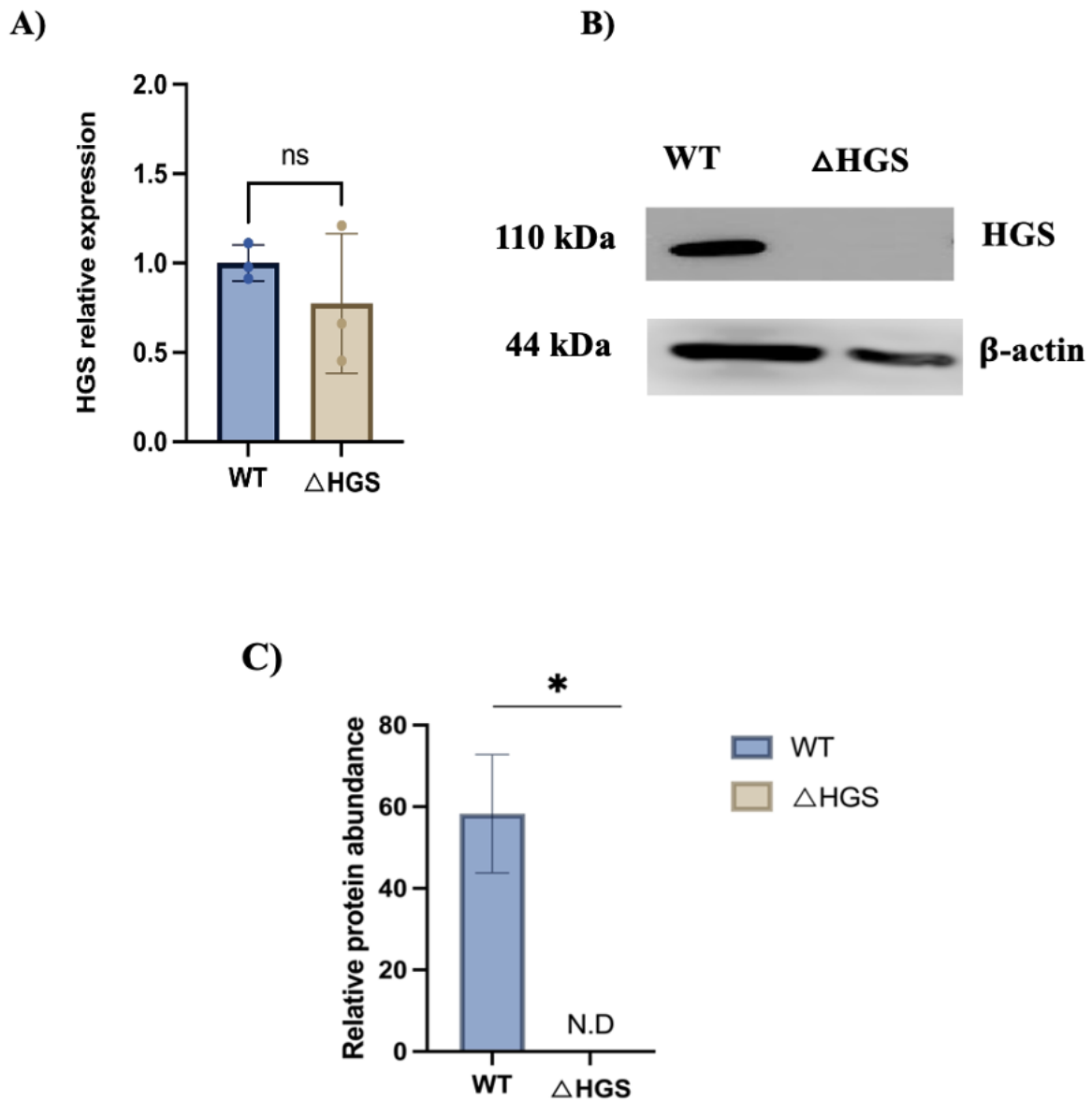


Figure 4.1 Evaluating the successful knockout of HGS protein from the H357 cell line.

(A) RNA was extracted from 2.5×10^5 cells/well seeded in 6-well plates and converted to cDNA before qPCR analysis. HGS transcript expression was normalised to GAPDH endogenous control expression and is presented relative to the WT cell line. The data represents the average from three biological repeats \pm SD. (B) Protein was extracted from 2.5×10^5 cell/well seeded in 6-well plates and was quantified by BCA assay. Equal quantities of protein 20 μ g were separated by SDS-PAGE, before western blotting to determine HGS and β -actin protein levels. Blots representative of three independent repeats are shown. (C) Densitometry analysis of HGS protein levels relative to β -actin levels. The data represents the average from three biological replicates \pm SD. NS = not significant and * indicates $p < 0.01$, as determined by unpaired t-test. ND = not detected.

4.3.2 Evaluating the growth rate and doubling time of WT and Δ HGS cell lines

The initial analysis is assessed the growth rate of both the WT and Δ HGS cell lines (Figure 4.2). An equal number of cells were seeded into 6-well plates and cell number was determined every 24 hours. At the 48, 72 and 96-hour time points, there were significantly more WT than Δ HGS cells ($p < 0.0001$) (Figure 4.2, A). Moreover, the Δ HGS cells took 25 hours to double in quantity, whereas the WT cells required only 21 hours. This represents a significant 1.2-fold increase in the doubling duration for the Δ HGS cells ($p < 0.0001$). (Figure 4.2, B). These observations underscore a consistent pattern wherein the Δ HGS cells manifest a diminished growth rate relative to the WT cells across the evaluated time intervals.

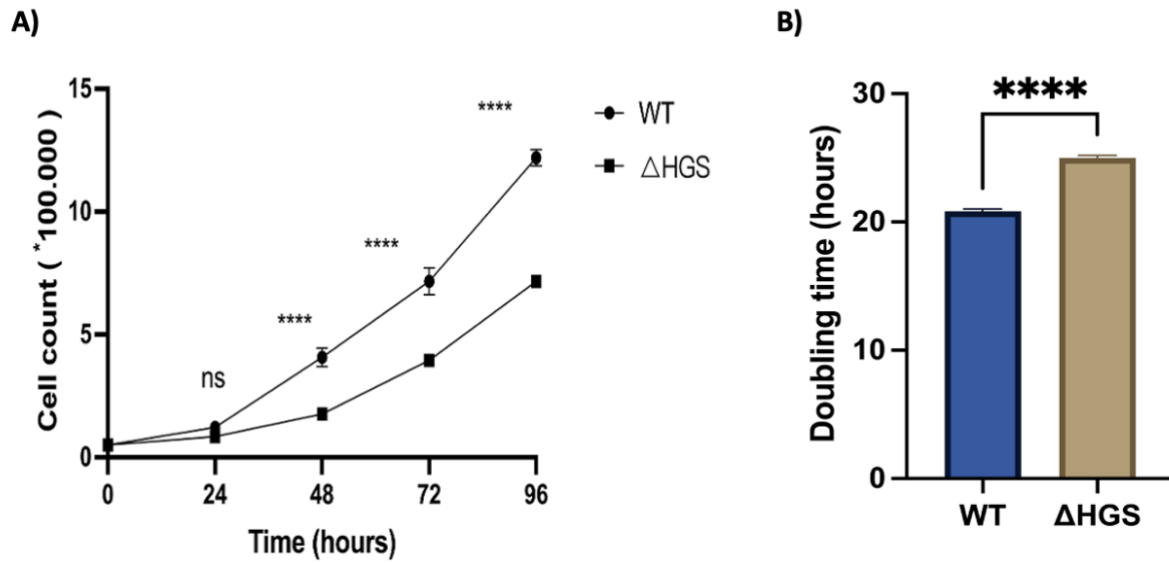


Figure 4.2 Growth curve of H357 WT and Δ HGS cell lines.

5×10^4 WT and Δ HGS cells were cultured in 6-well plates, at specific time points 24, 48, 72 and 96 hours, respectively. (A) cells from individual wells were harvested and counted to establish a growth rate. (B) At the 96-hour timepoint cell numbers were used to calculate the doubling time. The presented data is an average derived from three biological repeats \pm SEM. Where ns indicates no significant, and **** indicates $p < 0.0001$ as determined by a two-way ANOVA test and Student's t-test.

4.2.3 The impact of HGS depletion on cisplatin-induced extracellular particle release

Following successful validation of the H357 Δ HGS cell line (Section 4.2.1), It is sought to elucidate the impact of HGS depletion on EP release post cisplatin treatment, utilising the previously established IC50 value for cisplatin (Table 3.5).

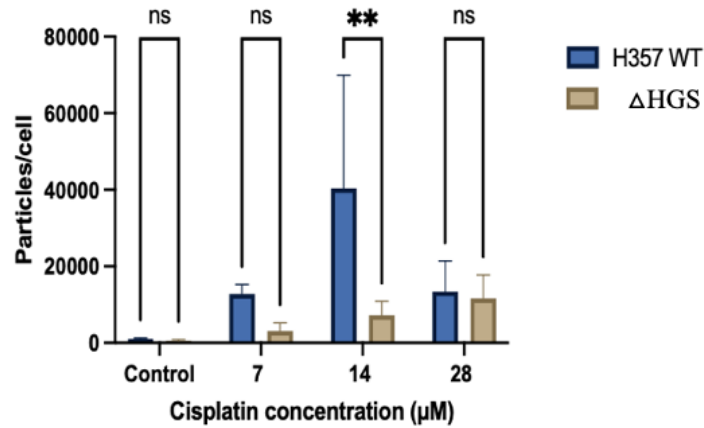
Cells were seeded at a density of 2.5×10^5 per well of a 6-well plate and allowed to adhere overnight. Following this, both H357 WT and Δ HGS cells were exposed to increasing concentrations of cisplatin: 7 μ M, 14 μ M, and 28 μ M. Treatment with 0.9% NaCl served as a vehicle control. After a 24-hour incubation period, the medium was substituted for medium supplemented with UF-dFBS for another 24 hours. Upon completion of the treatment regimen, the conditioned medium from each well was analysed using NTA to quantify the small particles. To account for potential variations in cell density, particle number was normalized based on the cell count in each well.

For the WT cell line, EP release was 1.12×10^3 particles per cell, 1.28×10^4 particles per cell, 4.03×10^4 particles per cell and 1.34×10^4 particles per cell for the vehicle control, 7 μ M, 14 μ M, and 28 μ M cisplatin, respectively (Figure 4.3, A). For the Δ HGS cell line, EP release remained much lower at 5.78×10^2 particles per cell, 3.11×10^3 particles per cell, 7.24×10^3 particles per cell and 1.17×10^4 particles per cell for the vehicle control, 7 μ M, 14 μ M, and 28 μ M cisplatin, respectively (Figure 4.3A). Following treatment with 14 μ M cisplatin, H357 WT released 6-fold more particles compared to H357 Δ HGS (Figure 4.3, A). This difference was exclusive to the 14 μ M concentration and there were no statistically significant differences for any of the other cisplatin doses tested.

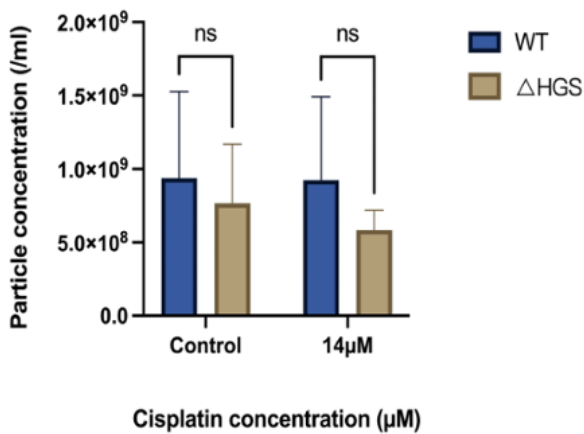
Following the observation of a significant difference in particle release into conditioned medium post-treatment with 14 μ M cisplatin, the next step was to pellet the EPs by ultracentrifugation to characterize their concentration and size. Cells were seeded at 2×10^6 cells per T75, allowed to adhere and then treated with either 14 μ M cisplatin or 0.9% NaCl vehicle control for 24 hours. Following this medium was substituted for medium supplemented with UF-dFBS for 24 hours. Conditioned medium was harvested and EPs isolation by ultracentrifugation. NTA revealed no significant difference in the concentration of the pelleted EPs (Figure 4.3, B) or their size (Figure 4.3, C).

Regarding the differential outcomes observed in this experiment regarding particle release, it is imperative to distinguish between the two-quantification metrics employed, particles / cell and particles /ml. The utilization of particles per cell as a metric in the initial experiment served a pivotal role in normalizing the data for variations in cell density, thereby facilitating a direct comparison of the impact of cisplatin treatment on a per-cell basis. This normalization is crucial, as it allows for an assessment of individual cellular responses to the treatment, accounting for any discrepancies in cell numbers arising from differential rates of proliferation or death induced by the treatment regimen. Conversely, the employment of particles / ml in this subsequent experiment provided invaluable insights into the overall yield of extracellular particles (EPs) from the conditioned medium. This metric is particularly relevant when evaluating the collective efficiency of EPs production and release into the medium, independent of the cell count. Such a measure is essential for measuring the scale at which vesicle release occurs in response to treatment, offering a broader perspective on the culture's extracellular dynamics.

A)



B)



C)

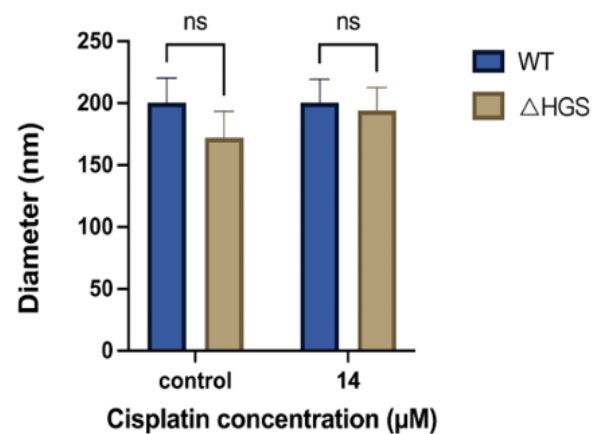


Figure 4.3 Effect of HGS depletion on EP release post cisplatin treatment.

Cells were seeded at 2.5×10^5 cells per well in 6-well plates, allowed to adhere overnight and then treated with 7 μM , 14 μM and 28 μM cisplatin or 0.9% NaCl vehicle control (control) for 24 hours. Medium was replaced with medium supplemented with EV-depleted FBS for 24 hours. Particle concentrations in the conditioned medium were quantified using NTA and subsequently normalized based on cell counts (A). Alternatively, cells were seeded at 2×10^6 cells per T75, allowed to adhere overnight and then treated with 14 μM cisplatin or vehicle control for 24 hours. Medium was substituted as above for 24 hours. EPs present in conditioned medium were pelleted by ultracentrifugation and concentration (B) and size (C) was determined by NTA. The presented data represent the average of three biological replicates, with error bars indicating the standard deviation (SD). Statistical significance was determined using two-way ANOVA, with ns=not significant and ** indicating $P < 0.01$.

The next step involved attempting to identify the EPs present in ultracentrifugation pellets using western blotting. EP pellets were prepared as for the NTA experiment above, except for the resulting pellets were solubilized in RIPA buffer for subsequent western blot analysis. TSG101 was chosen as a commonly used marker for EVs (Yoshioka et al., 2013). MVP was chosen as a marker for vault particles as it is the major structural component (Esfandiary et al., 2009). For this experiment, H357 WT and Δ HGS cell lines were exposed to the full range of predetermined cisplatin concentrations (Table 3.5). EP pellets derived from the WT cell line were positive for TSG101 and MVP (Figure 4.4). Conversely, these markers were conspicuously absent in the Δ HGS derived EP pellets across all treatments (Figure 4.4).

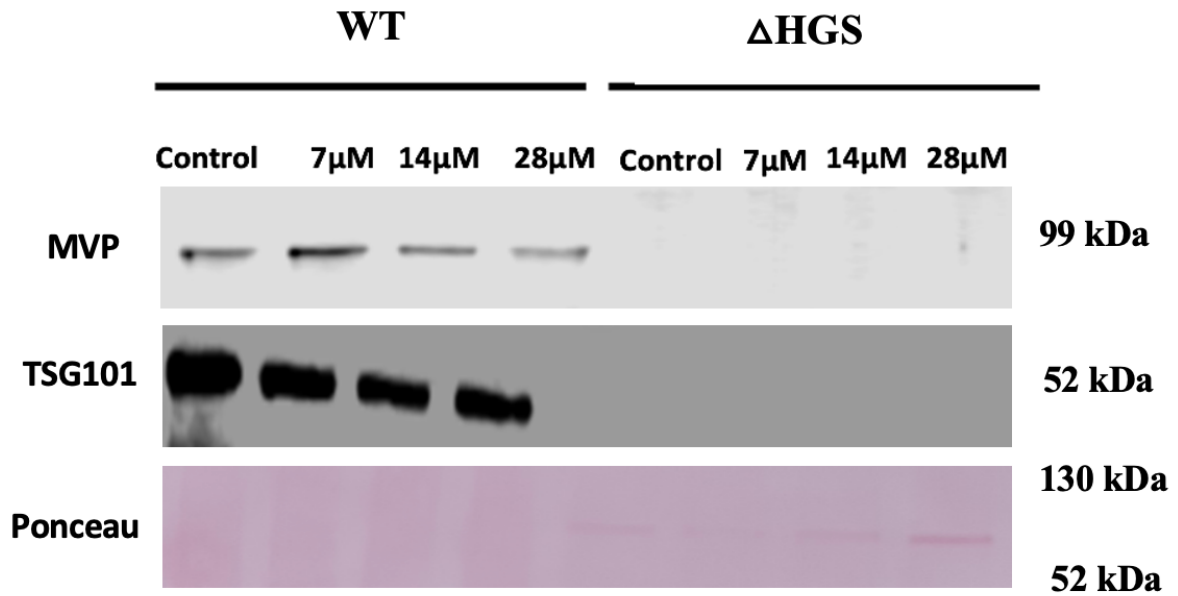


Figure 4.4 Detection of EV and vault particle markers present in EP pellets post cisplatin treatment.

Cells were seeded at 2×10^6 cells per T75 flask, allowed to adhere overnight and then treated with 7 μ M, 14 μ M and 28 μ M cisplatin or 0.9% NaCl vehicle control (control) for 24 hours. Medium was substituted for medium supplemented with EV-depleted FBS for 24 hours. EPs were pelleted by ultracentrifugation. The resulting EP pellets were then solubilised with RIPA buffer for subsequent western blotting analysis. Blocked membranes were probed with anti-MVP or anti-TSG101 antibodies for 24 hours at 4°C, followed by washing and then incubation with appropriate HRP-conjugated secondary antibodies at room temperature for 1 hour. Membranes were incubated with ECL reagent before exposure to x-ray film or digital image capture.

4.3.3 Determining live, apoptotic, and dead cells in response to cisplatin treatment after depletion of HGS

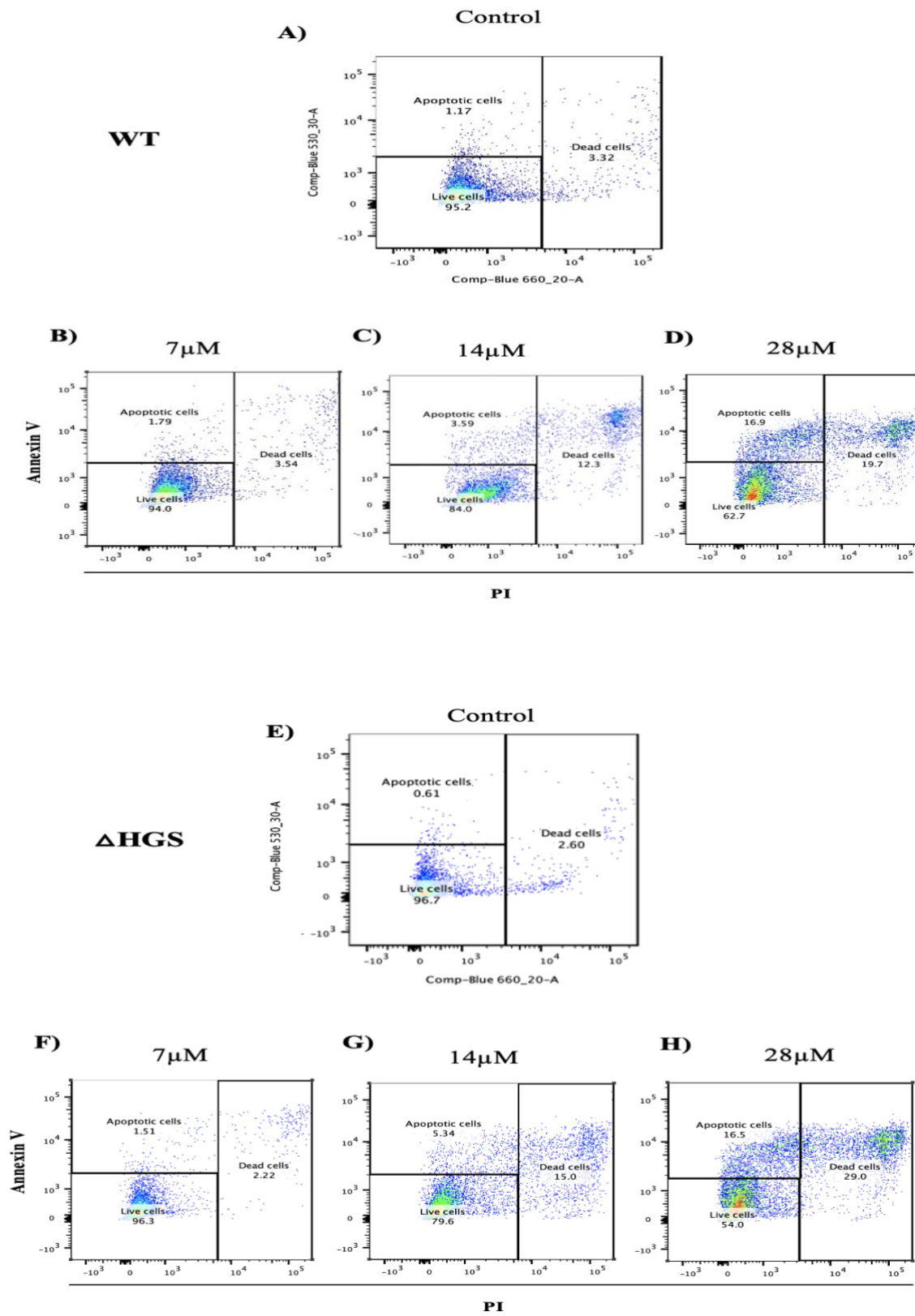
As previously described (Section 3.3), the proportion of live, apoptotic and dead cells following cisplatin treatment was determined by flow cytometry, utilising dual labelling with Annexin V-FITC and PI. This approach was applied to both WT and H357 Δ HGS cell lines. The data above (Section 4.2.3) demonstrated that depletion of HGS protein caused reduced release of EPs. The hypothesis was that the Δ HGS cell line would therefore have heightened sensitivity to cisplatin relative to the H357 WT due to impaired drug export.

Both cell lines were seeded in 6-well plates at a density of 2.5×10^5 cells per well and allowed an overnight period for adherence. Following this, the cells were exposed to cisplatin concentrations determined previously (Table 3.5): 7 μ M, 14 μ M, and 28 μ M. A vehicle control group was treated with a 0.9% NaCl solution. Post 24-hour cisplatin exposure, flow cytometry was used to assess the proportion of live, apoptotic, and dead cells.

As expected, A dose-dependent increase in apoptotic and dead cells was observed in H357 WT cells treated with cisplatin. (Figure 4.5, A-D). The mean live cell percentages in WT cells treated with the control (0.9% NaCl), was 95.47 % \pm 0.38 %, while for cisplatin concentrations of 7 μ M, 14 μ M, and 28 μ M, the percentages were 94.10% \pm 0.10%, 85.10% \pm 4.06%, and 51.53% \pm 12.91%, respectively. The mean apoptotic cell percentages were 1.01% \pm 0.20% for the control (0.9%NaCl), while for cisplatin concentrations of 7 μ M, 14 μ M, and 28 μ M were 1.54% \pm 0.24%, 6.09% \pm 5.51% and 27.20% \pm 8.94%, respectively. The mean dead cell percentages were 3.35% \pm 0.38% for the control (0.9%NaCl), while for cisplatin concentrations of 7 μ M, 14 μ M, and 28 μ M were 4.0% \pm 0.46%, 8.25% \pm 3.79% and 20.30% \pm 9.81%, respectively. Moreover, A dose-dependent increase in apoptotic and dead cells was observed in Δ HGS cells treated with cisplatin. (Figure 4.5, E-H). The mean live cell percentages in Δ HGS cells that treated with the control (0.9% NaCl), was 96.90 % \pm 2.01 %, while for cisplatin concentrations of 7 μ M, 14 μ M, and 28 μ M, the percentages were 97.03% \pm 0.64%, 85.73% \pm 5.52%, and 51.20% \pm 5.74%, respectively. The mean apoptotic cell percentage were 0.83% \pm 0.48% for the control (0.9%NaCl), while for cisplatin concentrations of 7 μ M, 14 μ M, and 28 μ M were 1.04%

$\pm 0.41\%$, $5.54\% \pm 0.98\%$ and $21.17\% \pm 5.83\%$, respectively. The mean dead cell percentages were $2.17\% \pm 1.52\%$ for the control (0.9% NaCl), while for cisplatin concentrations of $7\ \mu\text{M}$, $14\ \mu\text{M}$, and $28\ \mu\text{M}$ were $1.84\% \pm 0.33\%$, $8.55\% \pm 5.61\%$ and $27.27\% \pm 2.05\%$, respectively.

Contrary to this study's hypothesis, there were no significant differences in the proportions of live, apoptotic, or dead cells between the H357 WT and ΔHGS (Figure 4.5, I, J and K) cell lines.



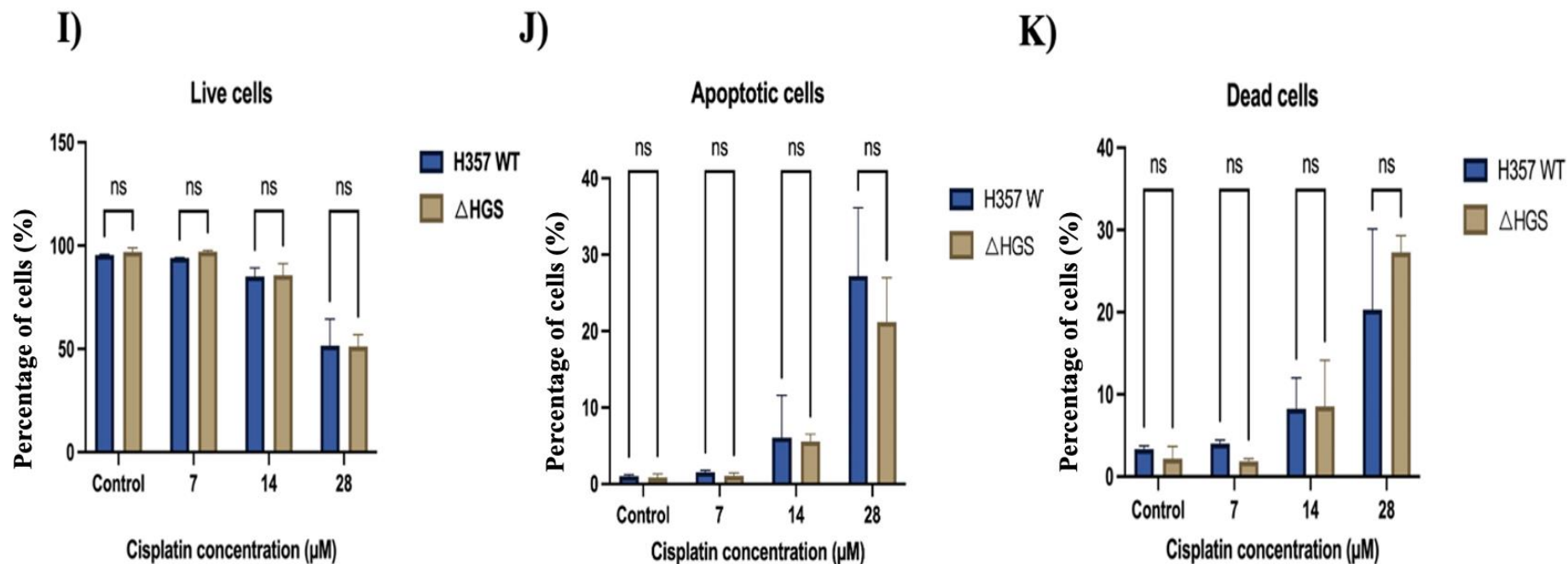


Figure 4.5 Flow cytometry analysis of cisplatin-induced responses in H357WT and ΔHGS cell lines.

The proportions of live, apoptotic and dead cells were quantified using flow cytometry, post-staining with Annexin V-FITC and PI. 2.5×10^5 cells were seeded per well of a 6-well plate, allowed to adhere for 24 hours and treated with different concentration of cisplatin for 24 hours. Representative scatter plots showcasing PI (X-axis) against Annexin V (Y-axis) are shown for WT (A-D) and ΔHGS (E-H). The percentages of viable, apoptotic, and dead cells for WT and ΔHGS cell lines are presented in I, J, and K. The percentage of live, apoptotic and dead cells within each individual sample was calculated following gating to select single cells. The presented values represent the average from three biological replicates \pm SD. There was no statistically significant difference between cells across all the concentrations by two-way ANOVA.

4.3.4 Validation of MVP knockout in H357 cell line by qPCR and western blotting

Prior to conducting experiments with the H357 Δ MVP cell line, The successful knockout of MVP at the transcript and protein levels was validated by qPCR and western blotting, respectively. There was no significant difference in MVP transcript expression between the knockout and WT cell lines (Figure 4.6, A.B). However, western blotting showed that the MVP protein was not detectable in H357 Δ MVP cell line compared to the WT, confirming successful MVP knockout at the protein level (Figure 4.6, C).

Published studies have previously shown that depletion of MVP can affect the abundance of other vault particle components (Esfandiary et al., 2009; C.-L. Zheng et al., 2004). Therefore, The expression of other vault components, specifically vtRNA1-1, TEP1, and PARP4, in the Δ MVP cell line was assessed. (Figure 4.6, D, E and F). There was no significant difference in expression of these transcripts between the H357 WT and H357 Δ MVP cell lines, taking into account that there are observable variations in transcript levels, particularly for the MVP, and considering the variation between different biological replicates.

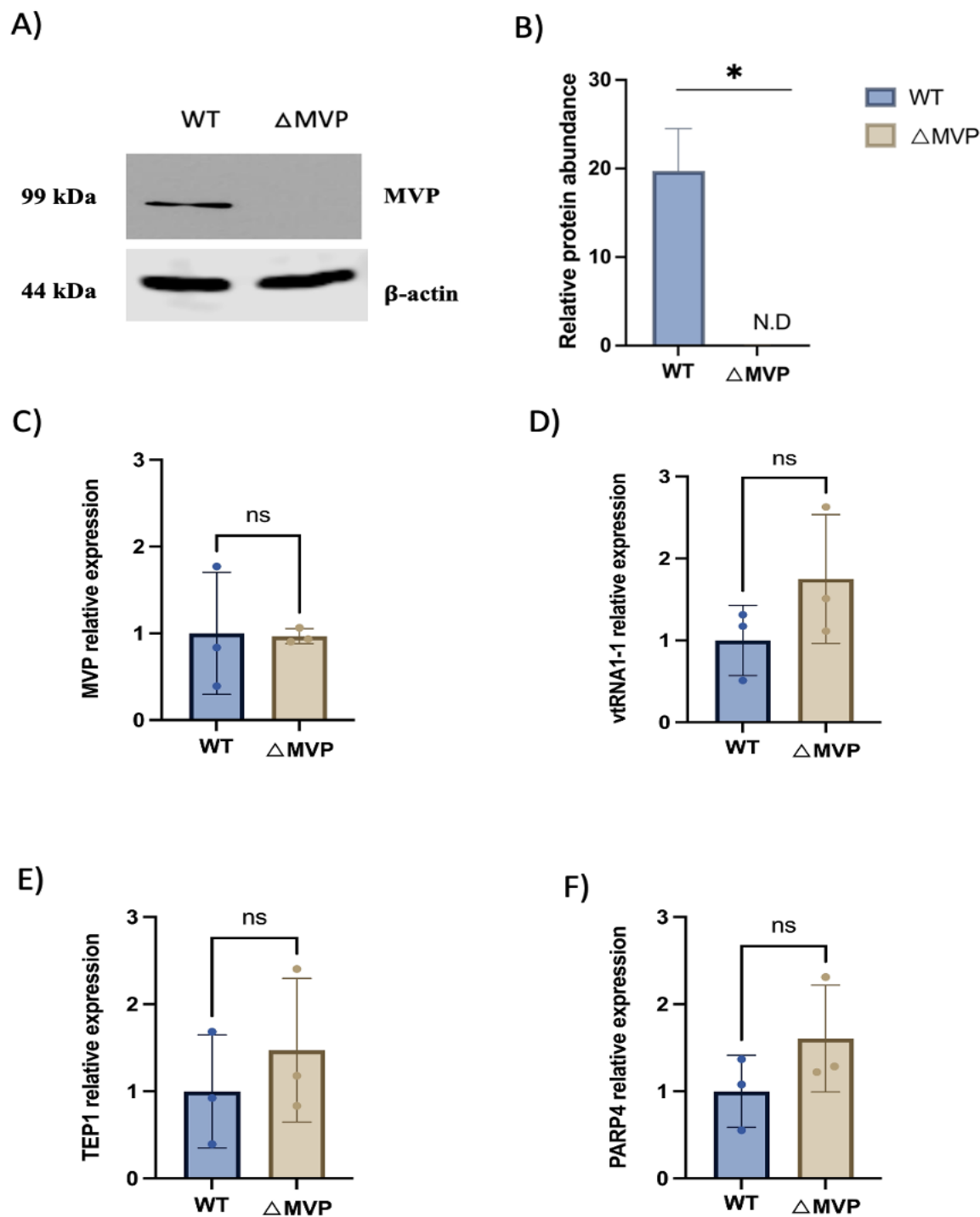


Figure 4.6 Evaluating the successful knockout of MVP protein from the H357 cell line.

(A) Protein was extracted from 2.5×10^5 cell/well seeded in 6-well plates and was quantified by BCA assay. Equal quantities of protein 20 μ g were separated by SDS-PAGE, before western blotting to determine MVP and β -actin protein levels. Blots representative of three independent repeats are shown. (B) Densitometry analysis of MVP protein levels relative to β -actin levels. (C) RNA was extracted from 2.5×10^5 cells/well seeded in 6-well plates and converted to cDNA before qPCR analysis. MVP, vtRNA1-1, TEP1 and PARP4 transcripts expression was normalised to GAPDH endogenous control expression and is presented relative to the WT cell line. The data represents the average from three biological repeats \pm SD. The data represents the average from three biological replicates \pm SD. NS = not significant and * indicates $p < 0.01$, as determined by unpaired t-test. ND = not detected.

4.3.5 Evaluating the growth rate and doubling time of WT and Δ MVP cell lines

The initial analysis was assessed the growth rate of both the WT and Δ MVP cell lines (Figure 4.7). An equal number of cells were seeded into 6-well plates and cell number was determined every 24 hours. There were significantly more WT than Δ MVP cells at the 48 ($p < 0.001$), 72 ($p < 0.05$) and 96-hour ($p < 0.0001$) time points (Figure 4.7, A). Moreover, the Δ MVP cells took 23 hours to double in quantity, whereas the WT cells required only 21 hours. This represents a significant 1.1-fold increase in the doubling duration for the Δ MVP cells ($p < 0.001$). (Figure 4.7, B). These observations underscore a consistent pattern wherein the Δ MVP cells manifest a diminished growth rate relative to the WT cells across the evaluated time intervals.

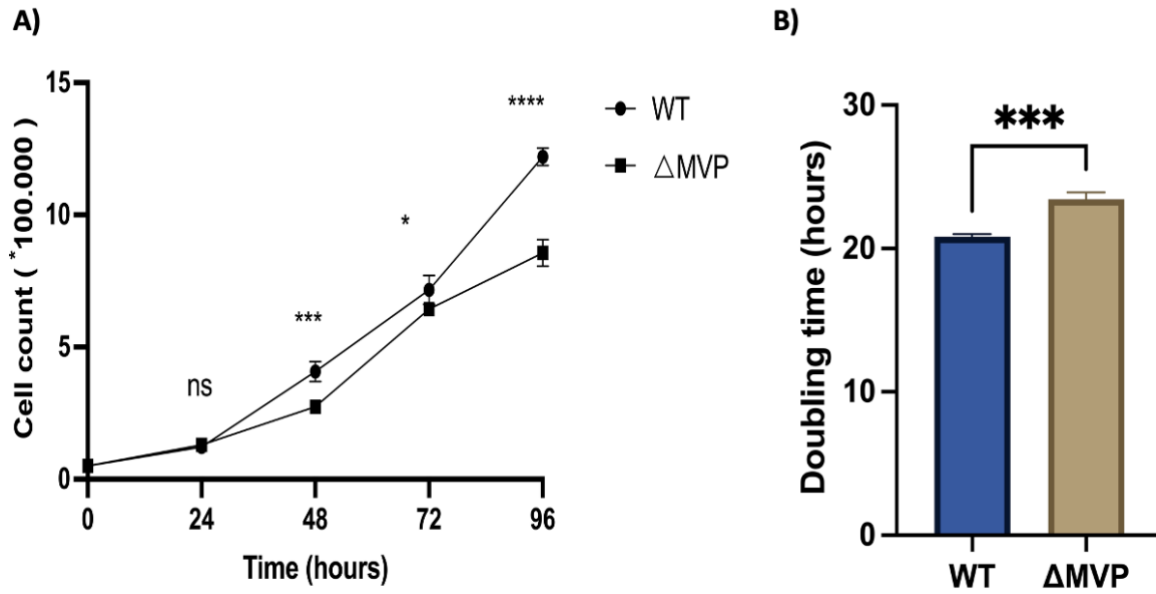


Figure 4.7 Growth curve of H357 WT and Δ MVP cell lines.

5×10^4 WT and Δ MVP cells were cultured in 6-well plates, at specific time points 24, 48, 72 and 96 hours, respectively. (A) cells from individual wells were harvested and counted to establish a growth rate. (B) At the 96-hour timepoint cell numbers were used to calculate the doubling time. The presented data is an average derived from three biological repeats \pm SEM. Where ns indicates no significant, * indicates $p < 0.05$, *** indicates $p < 0.001$ and **** indicates $p < 0.0001$ as determined by a two-way ANOVA test and Student's t-test.

4.3.6 The impact of MVP depletion on cisplatin-induced extracellular particle release

Following successful validation of the H357 Δ MVP cell line (Section 4.2.5), The impact of MVP depletion on extracellular particle release post cisplatin treatment was elucidated, utilizing the previously established IC50 value for cisplatin (Table 3.5). Cells were seeded at a density of 2.5×10^5 per well of a 6-well plate and allowed to adhere overnight. Following this, both H357 WT and Δ MVP cells were exposed to increasing concentrations of cisplatin: 7 μ M, 14 μ M, and 28 μ M. Treatment with 0.9% NaCl served as a vehicle control. After a 24-hour incubation period, the medium was substituted for medium supplemented with UF-dFBS for another 24 hours. Upon completion of the treatment regimen, the conditioned medium from each well was analysed using NTA to quantify the small particles. To account for potential variations in cell density, particle number was normalized based on the cell count in each well.

For the WT cell line, EP release was 1.12×10^3 particles per cell, 1.28×10^4 particles per cell, 4.03×10^4 particles per cell and 1.34×10^4 particles per cell for the vehicle control, 7 μ M, 14 μ M, and 28 μ M cisplatin, respectively (Figure 4.8, A). For the Δ MVP cell line, EP release remained much lower at 3.70×10^2 particles per cell, 8.15×10^3 particles per cell, 2.14×10^3 particles per cell and 3.32×10^3 particles per cell for the vehicle control, 7 μ M, 14 μ M, and 28 μ M cisplatin, respectively (Figure 4.8, A). Following treatment with 14 μ M cisplatin, H357 WT released 19-fold more particles per cell compared to H357 Δ MVP (Figure 4.8, A). This difference was exclusive to the 14 μ M concentration and there were no statistically significant differences for any of the other cisplatin doses tested.

Following the observation of a significant difference in particle release into conditioned medium post-treatment with 14 μ M cisplatin. Next, the EPs were pelleted by ultracentrifugation to characterize their concentration and size. Cells were seeded at 2×10^6 cells per T75, allowed to adhere and then treated with either 14 μ M cisplatin or 0.9% NaCl vehicle control for 24 hours. Following this medium was substituted for medium supplemented with UF-dFBS for 24 hours. Conditioned medium was harvested and EPs isolation by ultracentrifugation. NTA revealed no significant difference in the concentration of the pelleted EPs (Figure 4.8, B) or their size, taking into consideration that there are

variations in particle size range that can be attributed to differences between biological replicates.
(Figure 4.8, C).

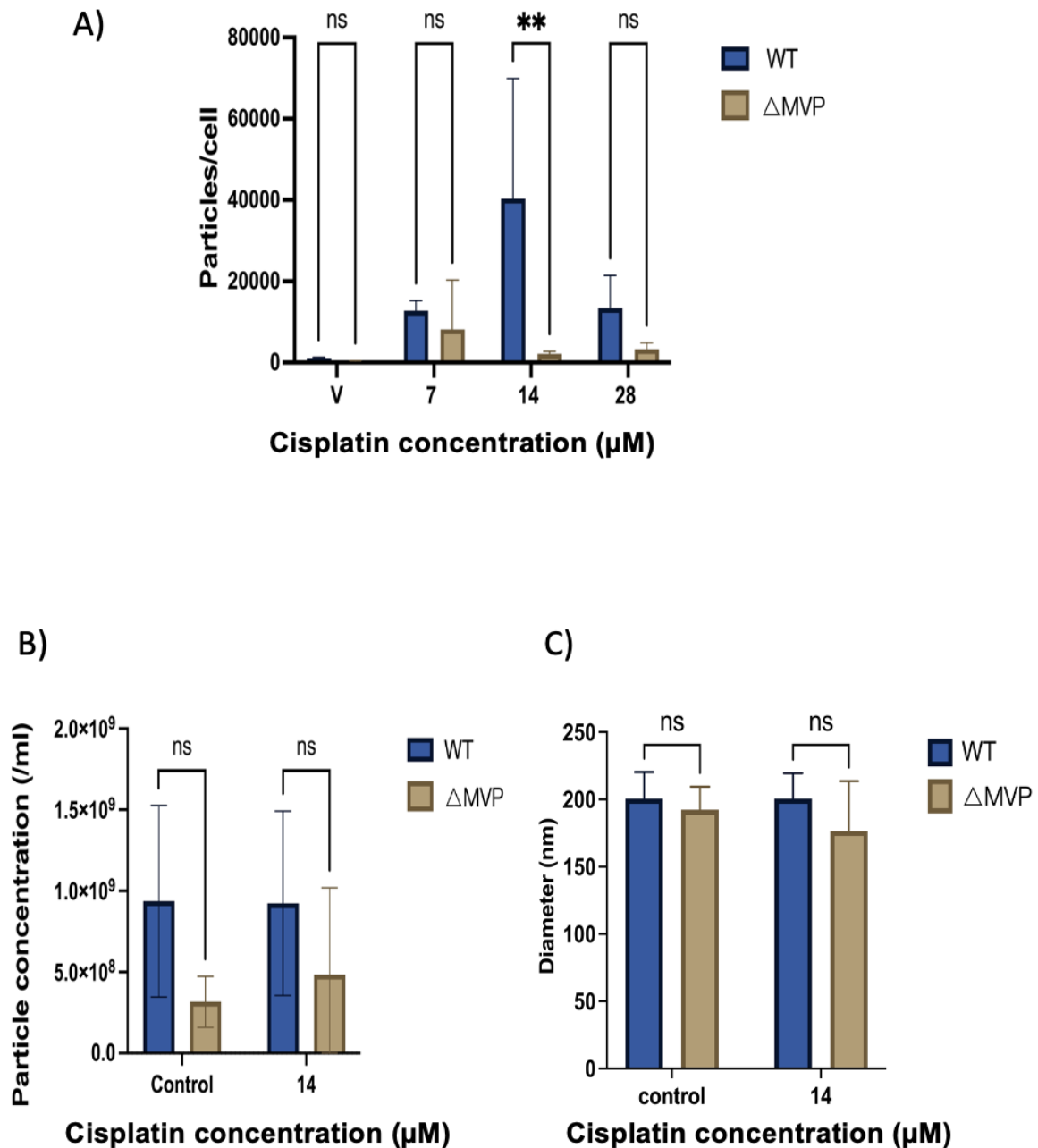


Figure 4.8 Effect of MVP depletion on EP release post cisplatin treatment.

Cells were seeded at 2.5×10^5 cells per well in 6-well plates, allowed to adhere overnight and then treated with 7 μ M, 14 μ M and 28 μ M cisplatin or 0.9% NaCl vehicle control (control) for 24 hours. Medium was replaced with medium supplemented with EV-depleted FBS for 24 hours. Particle concentrations in the conditioned medium were quantified using NTA and subsequently normalized based on cell counts (A). Alternatively, cells were seeded at 2×10^6 cells per T75, allowed to adhere overnight and then treated with 14 μ M cisplatin or vehicle control for 24 hours. Medium was substituted as above for 24 hours. EPs present in conditioned medium were pelleted by ultracentrifugation and concentration (B) and size (C) was determined by NTA. The presented data represent the average of three biological replicates, with error bars indicating the standard deviation (SD). Statistical significance was determined using two-way ANOVA, with ns=not significant and ** indicating $P < 0.01$.

Next, an attempt was made to identify the EPs present in ultracentrifugation pellets by western blotting. EP pellets were prepared as for the NTA experiment above, except for the resulting pellets was solubilized in RIPA buffer for subsequent western blot analysis. TSG101 and MVP was chosen as markers for EVs and vault particles, respectively. For this experiment, H357 WT and Δ MVP cell lines were exposed to the full range of predetermined cisplatin concentrations (Table 3.5). EP pellets derived from the WT cell line were positive for TSG101 and MVP (Figure 4.9). Conversely, these markers were conspicuously absent in the Δ MVP derived EP pellets across all treatments except for a faint TSG101 band was noticeable in the control (Figure 4.9).

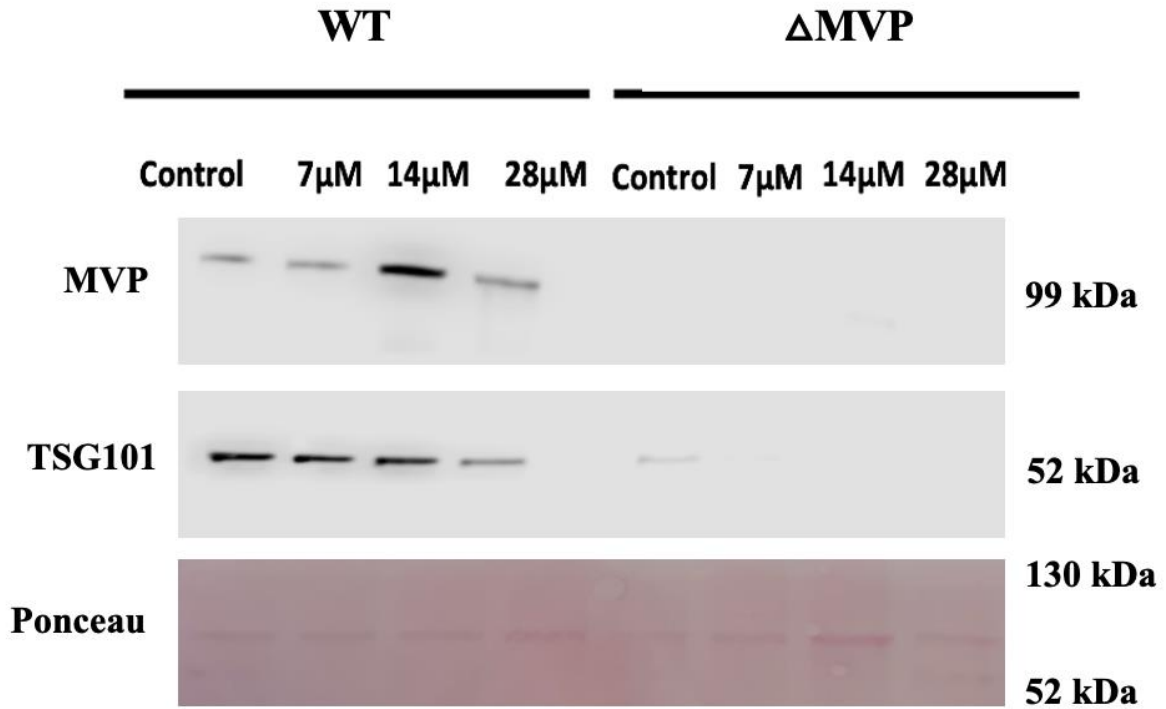


Figure 4.9 Detection of EV and vault particle markers present in EP pellets post cisplatin treatment.

Cells were seeded at 2×10^6 cells per T75 flask, allowed to adhere overnight and then treated with 7 μ M, 14 μ M and 28 μ M cisplatin or 0.9% NaCl vehicle control (control) for 24 hours. Medium was substituted for medium supplemented with EV-depleted FBS for 24 hours. EPs were pelleted by ultracentrifugation. The resulting EP pellets were then solubilised with RIPA buffer for subsequent western blotting analysis. Blocked membranes were probed with anti-MVP or anti-TSG101 antibodies for 24 hours at 4°C, followed by washing and then incubation with appropriate HRP-conjugated secondary antibodies at room temperature for 1 hour. Membranes were incubated with ECL reagent before exposure to x-ray film or digital image capture.

4.3.7 Determining live, apoptotic, and dead cells in response to cisplatin treatment after depletion of MVP

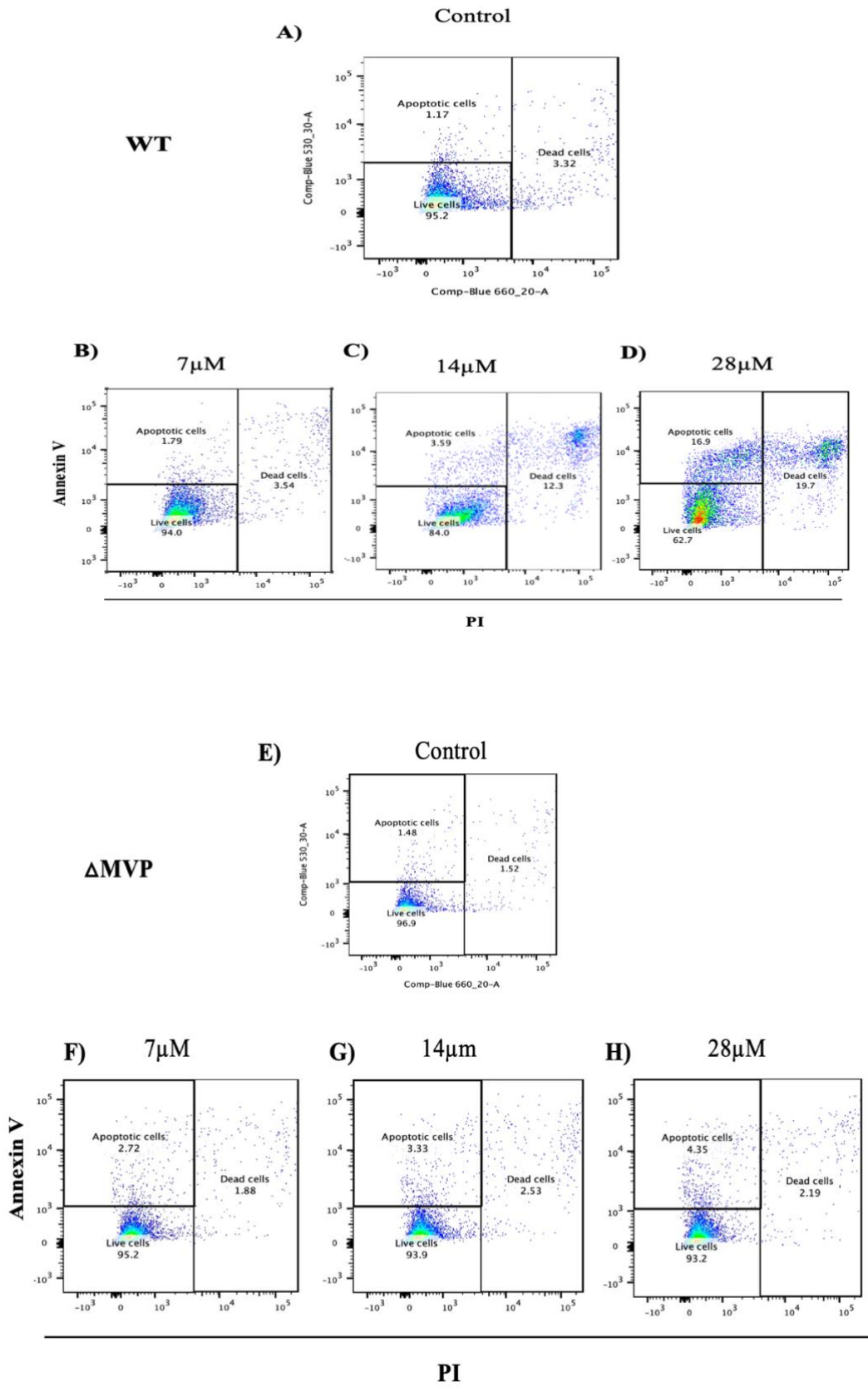
As previously described (Section 3.3), the proportion of live, apoptotic, and dead cells following cisplatin treatment was determined by flow cytometry, utilising dual labelling with Annexin V-FITC and PI. This approach was applied to both H357 WT and H357 Δ MVP cell lines. The data above (Section 4.2.7) demonstrated that depletion of MVP protein caused reduced release of EPs. The hypothesis was that Δ MVP cell line would therefore have heightened sensitivity to cisplatin relative to the H357 WT due to impaired drug export.

Both cell lines were seeded in 6-well plates at a density of 2.5×10^5 cells per well and allowed an overnight period for adherence. Following this, the cells were exposed to cisplatin concentrations determined previously (Table 3.5): 7 μ M, 14 μ M, and 28 μ M. A vehicle control group was treated with a 0.9% NaCl solution. Post 24-hour cisplatin exposure, flow cytometry was used to assess the proportion of live, apoptotic, and dead cells.

As expected, A dose-dependent increase in apoptotic and dead cells was observed in H357 WT treated with cisplatin. (Figure 4.10, A-D). The mean live cell percentages in WT cells that treated with the control (0.9% NaCl), was $95.47 \% \pm 0.38 \%$, while for cisplatin concentrations of 7 μ M, 14 μ M, and 28 μ M, the percentages were $94.10\% \pm 0.10\%$, $85.10\% \pm 4.06\%$, and $51.53\% \pm 12.91\%$, and for the mean apoptotic cell percentage were $1.01\% \pm 0.20\%$ for the control (0.9%NaCl), while for cisplatin concentrations of 7 μ M, 14 μ M, and 28 μ M were $1.54\% \pm 0.24\%$, $6.09\% \pm 5.51\%$ and $27.20\% \pm 8.94\%$, respectively. The mean dead cell percentage were $3.35\% \pm 0.38\%$ for the control (0.9%NaCl), while for cisplatin concentrations of 7 μ M, 14 μ M, and 28 μ M were $4.0\% \pm 0.46\%$, $8.25\% \pm 3.79\%$ and $20.30\% \pm 9.81\%$, respectively. There was no dose-dependent increase in apoptotic and dead cells in Δ MVP treated with cisplatin (Figure 4.10, E-H). The mean live cell percentages in Δ MVP cells that treated with the control (0.9% NaCl), was $96.57 \% \pm 0.55 \%$, while for cisplatin concentrations of 7 μ M, 14 μ M, and 28 μ M, the percentages were $93.93\% \pm 2.64\%$, $93.10\% \pm 2.50\%$, and $93.93\% \pm 2.19\%$. The mean apoptotic cell percentages were $1.30\% \pm 0.16\%$ for the control (0.9%NaCl), while for cisplatin concentrations of 7 μ M, 14 μ M, and 28 μ M were $2.52\% \pm 0.27\%$, $2.38\% \pm 0.83\%$ and 2.56%

$\pm 1.55\%$, respectively. The mean dead cell percentages were $1.91\% \pm 0.62\%$ for the control (0.9%NaCl), while for cisplatin concentrations of $7 \mu\text{M}$, $14 \mu\text{M}$, and $28 \mu\text{M}$ were $3.24\% \pm 2.25\%$, $4.21\% \pm 2.48\%$ and $3.18\% \pm 1.87\%$, respectively.

Contrary to this study's hypothesis, the ΔMVP cell line exhibited increased resistance to the $28 \mu\text{M}$ cisplatin treatment (Figure 4.10, I, J and K).



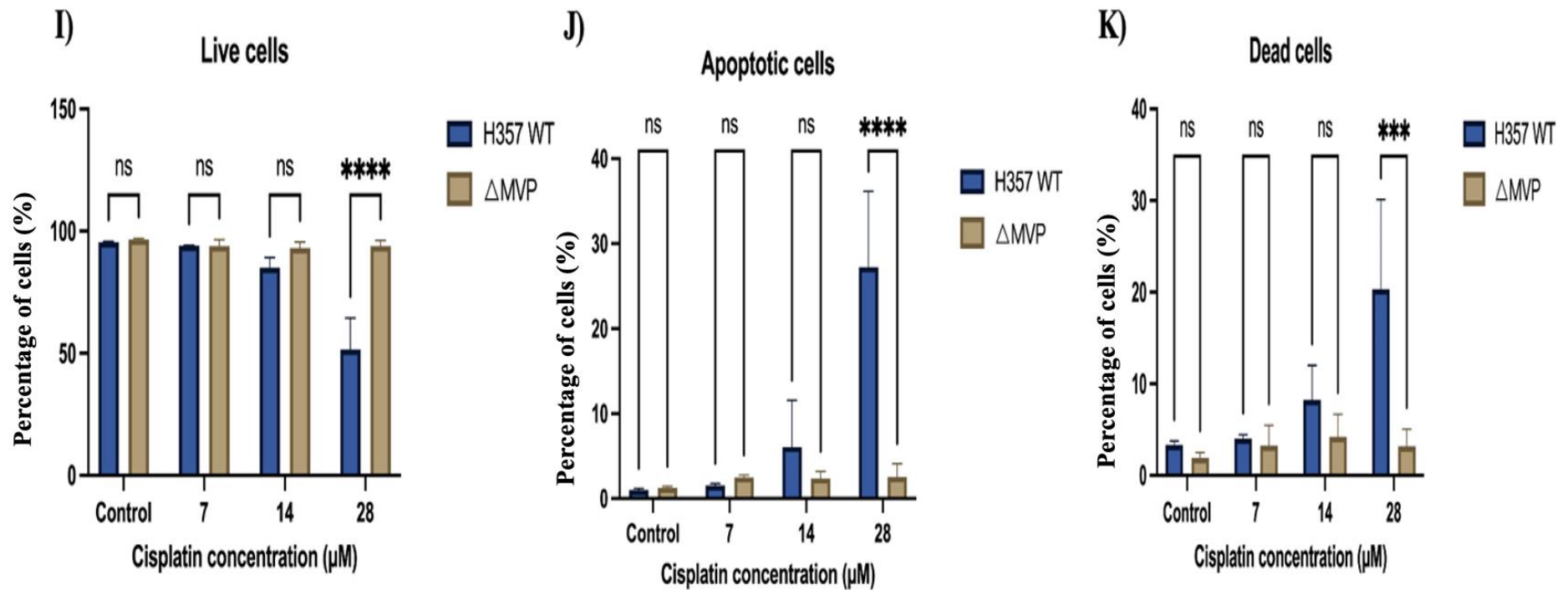


Figure 4.10 Flow cytometry analysis of cisplatin-induced responses in H357 WT and Δ MVP cell lines.

The proportions of live, apoptotic, and dead cells were quantified using flow cytometry, post-staining with Annexin V-FITC and PI. 2.5×10^5 cells were seeded per well of a 6-well plate, allowed to adhere for 24 hours and treated with different concentration of cisplatin for 24 hours. Representative scatter plots showcasing PI (X-axis) against Annexin V (Y-axis) are shown for WT (A-D) and Δ MVP (E-H). The percentages of viable, apoptotic, and dead cells for WT and Δ MVP cell lines are presented in I, J, and K. The percentage of live, apoptotic and dead cells within each individual sample was calculated following gating to select single cells. The presented values represent the average from three biological replicates \pm SD. Statistical significance was determined using two-way ANOVA, with *** $P < 0.0001$, **** $P < 0.00001$.

4.3.8 vtRNA1-1 antisense knockdown in Δ MVP cell line

Due to the findings above, which were contrary to the initial hypothesis, The study aimed to uncover the underlying mechanism of enhanced cisplatin resistance in the Δ MVP cell line. vtRNA1-1 (one of the vault particle components) has been shown to modulate resistance to apoptosis independent of the vault particle (Amort et al., 2015; Bracher et al., 2020). Loss of assembled vault particles in the Δ MVP cell line may result in enhanced resistance to apoptosis due to more ‘free’ vtRNA1-1 within the cell. To this end, The experiment was initiated to knock down vtRNA 1-1 and assess any resultant changes in drug sensitivity. For this experiment, H357 cells were seeded in a 24-well plate and subjected to transfection with increasing concentrations of antisense oligonucleotide (ASO) ranging from 0 to 200 nM. The 0 nM treatment served as a ‘mock transfected’ control, whereas the ‘control’ treatment was a ‘no transfection’ control. Following transfection, cells were incubated for 24 and 48 hours and then RNA was extracted for subsequent qPCR analysis.

The expected dose-dependent knockdown of vtRNA1-1 expression was not observed. There was a decrease in vtRNA1-1 expression in the 0 nM (mock transfection) compared to the control group (no transfection), suggesting that the transfection reagent alone caused a decrease in vtRNA1-1 expression (Figure 4.11). The data for 200 nM ASO (the highest concentration tested) was very similar to that of the 0 nM group, indicating that the knockdown experiment had not worked (Figure 4.11). Given that this was a preliminary experiment, it was conducted in technical duplicate (duplicate wells), which prevented any robust statistical analysis. Regrettably, due to time constraints, the experiment could not be repeated to carry out optimization and troubleshooting.

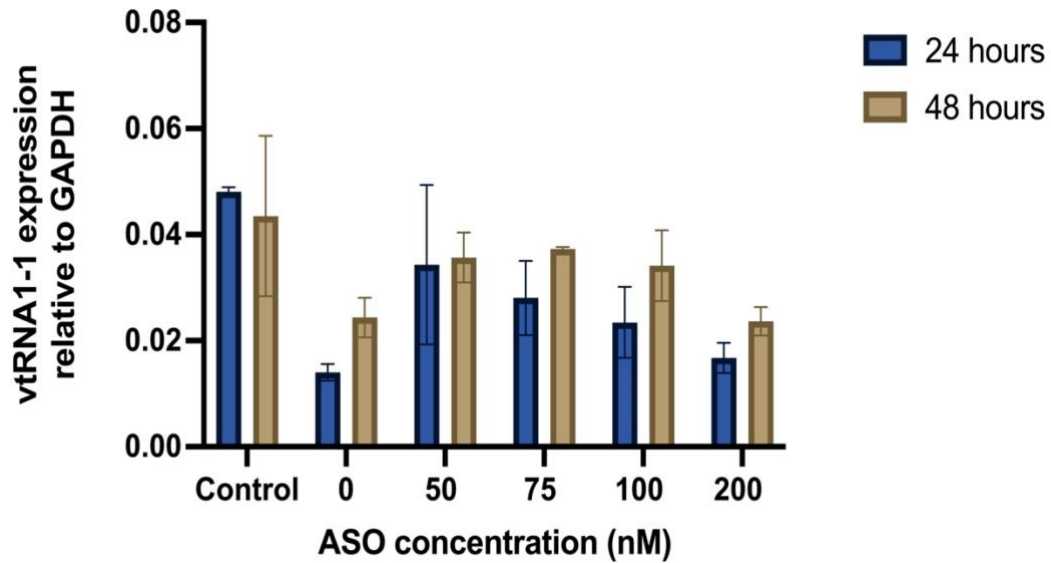


Figure 4.11 Preliminary experiment to test efficiency of antisense oligonucleotide knockdown of vtRNA1-1 expression.

H357 cells were seeded in a 24-well plate at 1×10^5 cells/well and transfected with increasing concentrations of antisense oligonucleotide (ASO) (0-200 nM). The control represents cells that were not subjected to transfection. After 24 and 48 hours of incubation post-transfection, RNA was extracted for qPCR analysis. vtRNA1-1 expression was normalised to GAPDH expression. Data are presented as mean values from duplicate transfected wells as part of one experiment.

4.4 Discussion

4.4.1 Characterisation of Δ HGS and Δ MVP cell lines

In this chapter, the aim was to delve deeper into the role that EVs play in cisplatin resistance, utilizing two CRISPR Cas9 edited cell lines recently created by members of the research group that are EV (H357 Δ HGS) and vault particle deficient (H357 Δ MVP). HGS, a member of the ESCRT, is a master regulator of EV biogenesis, in particular those derived from multivesicular bodies (i.e. exosomes) (Bache et al., 2003). MVP is the main structural component of the vault particle and is required for their assembly (Stephen et al., 2001). By blocking the release of EVs and vault particles. It was hypothesized that cells would exhibit heightened sensitivity to cisplatin. The initial step involved validating the successful knockout of HGS and MVP in the H357 cell line at the transcript and protein level, using qPCR and western blotting, respectively. Neither cell line showed a significant reduction in transcript expression. However, both HGS and MVP were silenced at the protein level.

This observation of transcripts without corresponding protein expression can be largely attributed to the effects of frameshift mutations induced by the CRISPR/Cas9 editing process. Such mutations, resulting from insertions or deletions (indels) at the genomic editing site, can disrupt the gene's reading frame and potentially introduce premature stop codons. These premature stop codons may trigger nonsense-mediated decay (NMD), a cellular mechanism designed to degrade mRNAs containing early termination codons, thus preventing the translation of truncated, potentially harmful proteins. Alternatively, even if these transcripts escape immediate degradation, the premature stop codons can halt translation prematurely, leading to the production of incomplete, non-functional proteins that the cell quickly degrades (Feser et al., 2023; Smargon et al., 2022).

The cell growth rate in the HGS and MVP knockout cells was next examined and found to be slower compared to WT cells. Evidence is lacking regarding the effect of HGS depletion on proliferation. However, several investigations have indicated that the depletion of ESCRT components leads to programmed cell death. For instance, the temporary reduction of HGS expression was found to compromise cell survival in hepatoblastoma and colorectal cancer cell lines (Canal et al., 2015). Similarly, diminishing levels of the ESCRT-I component TSG101 were associated with apoptosis in

cells from breast cancer, as documented by Zhu and colleagues in 2004. Furthermore, the downregulation of ESCRT-II components, specifically Vps22, Vps25, and Vps36, has been linked to increased cell mortality (Herz et al., 2006; Woodfield et al., 2013).

Regarding Δ MVP, again there is no published link between depletion and reduced proliferation, but others have shown a significant decrease in viability of Δ MVP-HAP1 cells compared to parental cells PAR-HAP1. In addition, contrasting with this observation, U2OS- Δ MVP cell line did not observe any proliferation abnormality compared with its parental cell line U2OS (Pietras et al., 2021).

4.4.2 Impact cisplatin treatment on Δ HGS and Δ MVP cell lines

Following the successful validation of HGS and MVP depletion in the H357 cell line, the examination of EPs released post-treatment of Δ HGS and Δ MVP, in comparison with WT cells using varying cisplatin concentrations, was then conducted. The NTA analysis revealed fewer particles were released from Δ HGS and Δ MVP when treated with the IC50 dose of cisplatin (14 μ M). Such findings align with existing literature which indicates that the absence of ESCRT-0 subunits leads to a decline in exosome release across diverse cell types (Hoshino *et al.*, 2013, Colombo *et al.*, 2013). This observed reduction in EV release can likely be attributed to compromised MVB formation, as documented by other researchers (Schmidt & Teis, 2012; Zheng et al., 2004). Furthermore, while HGS depletion has been previously linked to a decrease in exosome size in colorectal cancer cells as observed through TEM (Sun et al., 2016). The NTA results did not reflect a change in particle size. This discrepancy might arise from NTA's limitations in detecting particles smaller than 70 nm, unlike other methods such as TEM and nanoparticle flow cytometry, which can detect smaller particles.

Cisplatin, a platinum-based chemotherapy drug, is widely recognized for its effectiveness against various cancers, including ovarian, testicular, and head and neck cancers. Its mechanism involves entering cells and undergoing aquation reactions that replace chloride ions with water molecules, making the drug more reactive and capable of forming covalent bonds with DNA. This disrupts the cell's DNA replication and repair processes, leading to cell death (L. Wang et al., 2021). However, cancer cells can develop resistance to cisplatin through mechanisms like packaging the drug

into EVs and exporting it out of the cell, thus reducing its intracellular concentration and cytotoxic effects (Maleki et al., 2021). This method of drug sequestration and expulsion via EVs represents a form of drug resistance that enables cancer cells to survive despite chemotherapy treatment. The sequestration of cisplatin into EVs, thereby evading its cytotoxic effects, not only compromises the efficacy of cisplatin in resistant cells but also enables the spread of resistance by transferring drug resistance factors through EVs (Fontana et al., 2021).

In tackling the issue of cisplatin packaging into EVs, research has identified potential avenues to inhibit the formation and release of EVs. One such strategy involves the use of GW4869, a neutral sphingomyelinase inhibitor, which can block the formation of intraluminal vesicles (ILVs), thus preventing exosome production. By inhibiting EV biogenesis, there is potential to prevent the packaging of cisplatin into these vesicles, maintaining a higher concentration of the drug within the cancer cells and enhancing its cytotoxic effects (Catalano & O'Driscoll., 2019). This approach, targeting the resistance mechanism itself rather than merely attempting to prevent the release of EVs already containing cisplatin, offers a promising strategy to combat cisplatin resistance, presenting a novel means to bolster the therapeutic efficacy of cisplatin against resistant cancer types.

Western blotting was utilized to detect the presence of the EV marker TSG101 and the vault particle marker MVP. The MISEV guidelines recommend the use of at least one membrane-bound and one cytosolic protein for EV characterization (Lötvald et al., 2014; Théry et al., 2018). However, due to time constraints, the study could only proceed with one EV marker. It's well-documented that ESCRT-0 recruits the downstream ESCRT-I subunit TSG101 on early endosomes via PtdIns (3) P regulation, orchestrating various MVB biogenesis-related events, including viral budding, ubiquitinated cargo sorting, and endocytic trafficking (Colombo et al., 2013; Cvjetkovic et al., 2016; Q. Lu et al., 2003; Razi & Futter, 2006; Strickland et al., 2022). Moreover, TSG101's significant role in membrane dynamics, which modulates endosome fission and fusion, has been highlighted (Stuffers et al., 2009). Consequently, It was hypothesized that the absence of HGS would result in a reduction in the production of TSG101-positive EVs. This supposition was validated in this research, as the TSG101 protein was

notably missing in the Δ HGS-derived EPs when compared to the WT. An additional EV marker, such as CD63, would have been useful for detecting EVs produced via ESCRT-independent biogenesis.

Several independent studies have identified MVP in EV preparations derived from cancer cells, with many findings indicating its enrichment in exosomes or small EVs relative to the originating cells (Peinado et al., 2012; Welton et al., 2010; Xu et al., 2015). As expected, the western blotting results revealed a complete absence of MVP in the Δ MVP-derived EPs. However, the depletion of TSG101 in Δ MVP-derived EPs (with exception of a faint band in the control) was unexpected. There is no clear explanation for this, but there are some studies suggest a link between MVP/vault particles and the formation of EVs (Teng et al., 2017). Additionally, MVP has been observed to co-localize with the lysosomal marker CD63. This marker is not only prevalent in late endosomes (multivesicular bodies) but is also widely acknowledged as a standard marker for EVs (Berger et al., 2000; Schroeijers et al., 2002). Based on these previous studies, this might be a potential explanation of absence of MVP in Δ HGS cell line. It is tempting to speculate that vault particles may be exported in endosome-like structures in a similar manner to EVs. Currently, there is a complete lack of published research exploring the mechanism(s) of vault particle export from the cell, which warrants further investigation.

Despite there being a reduction in the EPs released by Δ HGS cells, flow cytometry data did not indicate any significant variances in the ratios of apoptotic and dead cells between WT and Δ HGS cells, which was contrary to the initial hypothesis. EPs aside, several studies have highlighted that the absence of ESCRT subunits can induce cellular apoptosis. For instance, the temporary suppression of HGS has been linked to reduced cell viability in hepatoblastoma and colorectal cancer cells (Canal et al., 2015), and the downregulation of the ESCRT-I subunit TSG101 was associated with apoptosis in breast cancer cells (G. Zhu et al., 2004). Additionally, the diminished expression of ESCRT-II subunits like Vps22, Vps25, and Vps36 has been implicated in cell death (Herz et al., 2006; Woodfield et al., 2013). The previous studies contrast with the finding as there was no difference in basal apoptotic proportion in Δ HGS cell line compared with WT cell line.

When comparing the Δ MVP cell line with WT, a notable difference was observed in the proportion of live, apoptotic, and dead cells upon treatment with double the IC_{50} concentration (28 μ M).

The Δ MVP cell line exhibited increased resistance to cisplatin, which was contrary to the hypothesis. MVP has been implicated in a wide array of cellular roles. It is associated with apoptotic resistance in aging human diploid fibroblasts (HDFs), where the suppression of MVP considerably decreased the levels of the anti-apoptotic proteins such as B-cell lymphoma 2 (Bcl-2) while amplifying c-Jun levels in these cells (Ryu et al., 2008). Additionally, a robust connection exists between MVP and cellular demise, demonstrated by the fact that diminishing MVP levels led to apoptosis in various cell types, including macrophages, human airway smooth muscle cells, as well as cells from hepatocellular carcinoma (HCC) and breast cancer lines (Ben et al., 2013; H. M. Lee et al., 2017; Pasillas et al., 2015). Another study, revealed that not only MVP might play a role in drug resistance, vtRNA1-1 is pivotal in imparting resistance to various cancer cells against chemotherapeutic agents (Chen et al., 2018). In addition, many research studies suggest a connection between telomerase and the responsiveness of cancer cells to treatment. This link is further supported by observations that heightened telomerase expression in cancer cells is associated with drug resistance in rectal cancer (Shin et al., 2012). Another study showed that inhibition TEPI activity leads to heightened sensitivity of certain cancer cells, such as breast cancer, to doxorubicin (DOX) (Dong et al., 2009). The alternative hypothesis was that ablation of MVP protein (and therefore vault particles) would release the other vault particle components to carry out alternative processes in the cell, which might be linked to resistance to apoptosis. So, the motivation to suppress vtRNA1-1 in the Δ MVP cell line in this study was to assess its potential to mediate resistance to cisplatin. Regrettably, this approach was unsuccessful, and so it remains a potential avenue for future research.

The main aim of this chapter was to ascertain whether the blockade of EVs and vault particles via deletion of HGS and MVP proteins in H357 would cause increased sensitivity to cisplatin. The results indicated that the Δ HGS cell line did not display a significant change in sensitivity to cisplatin. In contrast, the Δ MVP cell line showed a notable increase in cisplatin resistance compared to the WT.

Chapter 5 Are extracellular particles mediators of cisplatin resistance in head and neck cancer?

5.1 Introduction

Cisplatin, a platinum-based chemotherapeutic agent, has been a cornerstone in the treatment of various malignancies, including HNC (Siddik, 2003). Its cytotoxic mechanism primarily involves the formation of DNA adducts, leading to DNA damage and subsequent apoptosis. However, the emergence of cisplatin resistance in tumour cells poses a significant challenge to effective cancer therapy (Jordan & Carmo-Fonseca, 2000).

Recent studies have highlighted the role of EPs, particularly EVs, in mediating drug resistance (Jin et al., 2022). EVs contain a myriad of bioactive molecules, including proteins, lipids, and nucleic acids. They play a pivotal role in cell-to-cell communication and have been implicated in various pathological processes, including tumour progression and drug resistance (Jella et al., 2018).

A crucial cellular mechanism underlying cisplatin resistance involves alterations in drug transport. The copper transporter 1 (CTR1) is responsible for cisplatin influx into the cells, while ATP7A and ATP7B proteins mediate the efflux of cisplatin, leading to reduced intracellular drug concentrations and decreased cytotoxicity (Zisowsky et al., 2007). Several studies have delved into the molecular intricacies of cisplatin resistance in HNC. For instance, Yamano et al. (2010) focused on the identification of cisplatin-resistance-related genes. Their research provided insights into the molecular intricacies of cisplatin resistance, emphasizing the importance of global gene analysis in understanding the underlying mechanisms (Yamano et al., 2010). Another study by Bauer et al. (2007) revealed that HNC cell lines selected for cisplatin resistance exhibited wild-type p53 and high levels of Bcl-xL, suggesting the potential involvement of these factors in the resistance mechanism (Bauer et al., 2007).

There are many studies focusing on the cellular machinery involved in cisplatin resistance. However, the role that EPs play in cisplatin resistance in HNC remains to be fully elucidated. In this chapter, The study aimed to determine if EPs released by cisplatin-resistant HNC cells could bestow cisplatin resistance on naïve cells. Aim of this chapter:

This chapter aims to determine if EPs from a cisplatin resistant cell line can transfer resistance to naïve cells. To achieve this the following objectives will be addressed:

- Generate a cisplatin resistant (cisplatin^R) HNC cell line by prolonged incubation with gradually increasing cisplatin concentrations.
- Evaluate morphology, growth rate and doubling time of the cisplatin^R cell line compared to the parent cell line.
- Confirm cisplatin resistance by viability/metabolic activity assay (MTT) and analysis of apoptosis by flow cytometry.
- Assess impact of cisplatin treatment on the cell cycle of cisplatin^R cell line compared to the parent cell line by flow cytometry.
- Assess cellular mechanisms of resistance by western blotting of known mediators of cisplatin resistance (ATP7A, ATP7B, RRBP1, MVP and CTR1).
- Assess particle concentration in the conditioned medium of cisplatin^R and parent cells following cisplatin treatment by NTA.
- Isolate EPs from cisplatin^R and parent cells by ultracentrifugation and characterise them by NTA and western blotting.
- Isolate extracellular particles from cisplatin^R cell line and incubate with naïve cells to test if they can transfer cisplatin resistance.

5.2 Results:

5.2.1 Generation of a cisplatin resistant HNC cell line

In the endeavour to understand the mechanisms underlying cisplatin resistance in HNC, a systematic approach was employed to induce resistance in the H357 cell line. The cell line was subjected to a prolonged treatment regimen with cisplatin, spanning over 18 months. The initial treatment commenced with a sub-lethal dose of 0.5 μM cisplatin, a concentration chosen to ensure cell survival while introducing a selective pressure. Cells were routinely cultured in the presence of cisplatin and once confluent the dose was gradually increased, to ultimately reach the 24 hour IC50 concentration of 14 μM . Once this was achieved, the cells were used for further experiments.

5.2.2 Characterisation of the cisplatin resistant cell line

5.2.2.1 Cisplatin^R cell morphology and growth characteristics

Upon microscopic examination, both the WT and cisplatin^R cell lines appeared largely similar, with no consistent morphological changes evident. However, a notable observation was the presence of some spindle-shaped cells in the cisplatin^R cell line, a feature less prominent in the WT (Figure 5.1, A/B).

The growth rate of both the WT and cisplatin-resistant cell lines was next assessed (Figure 5.1, C/D). An equal number of cells were seeded into 6-well plates and cell number was determined every 24 hours. There were significantly more WT than cisplatin^R cells at the 24 ($p < 0.01$), 48 ($p < 0.0001$), 72 ($p < 0.0001$) and 96 hour ($p < 0.0001$) time points (Figure 5.1, C). Moreover, the cisplatin^R cells took 56 hours to double in quantity, whereas the WT cells required only 21 hours. This represents a significant 2.7-fold increase in the doubling time for the cisplatin^R cells ($p < 0.0001$). (Figure 5.1, D). These observations underscore a consistent pattern wherein the cisplatin^R cells manifest a diminished growth rate relative to the WT cells across the evaluated time intervals.

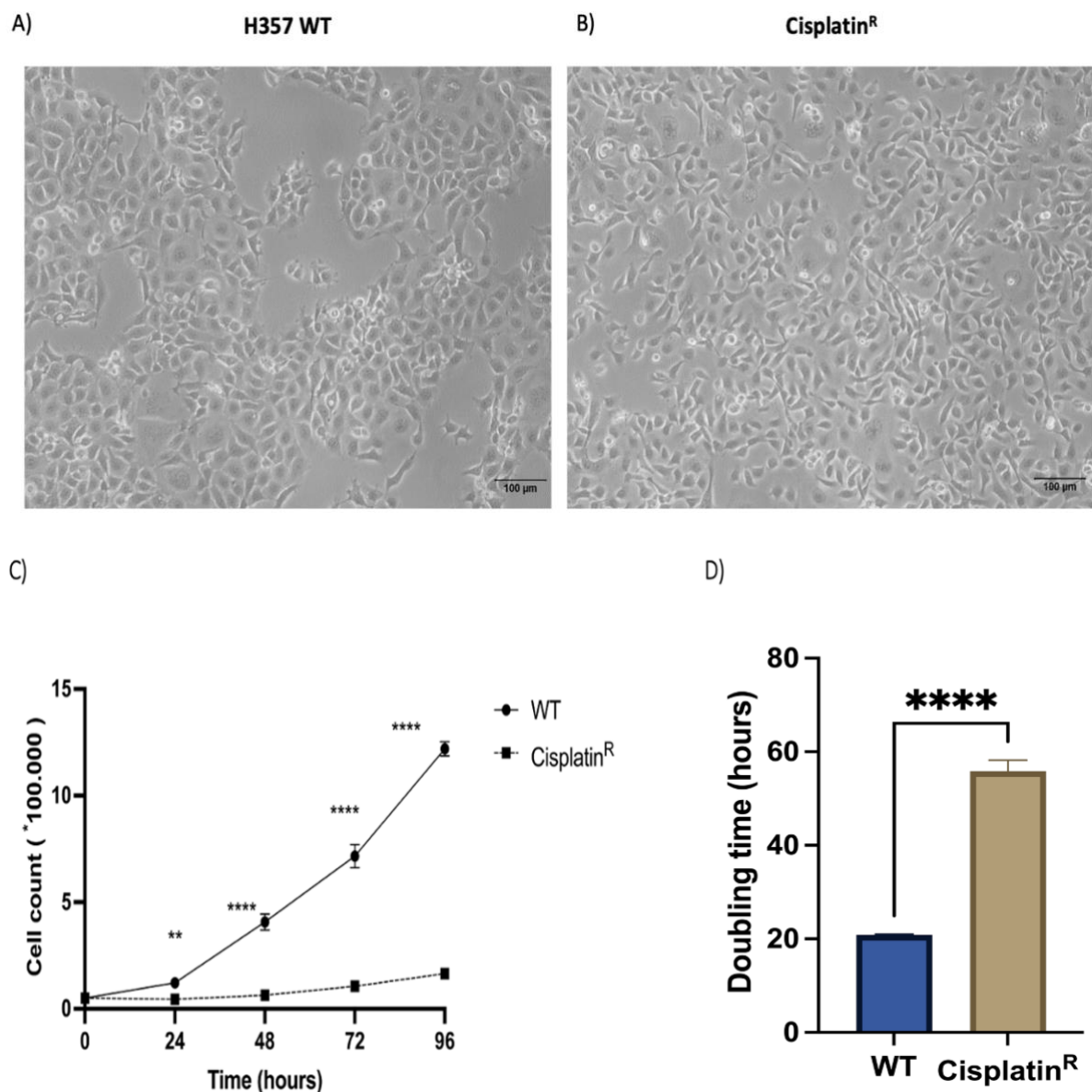


Figure 5.1 Morphology and growth characteristics of H357 WT and cisplatin^R cell lines.

H357 WT (A) and cisplatin^R (B) cell lines were cultured until ~70% confluent and then observed by light microscopy at 10X magnification. Scale bar denotes 100 μm . C) 5×10^4 cells were seeded in 6-well plates and counted at specific time points (24, 48, 72 and 96 hours) to determine growth rate. D) At the 96-hour timepoint cell numbers were used to calculate the doubling time. The data is an average derived from three biological repeats \pm SEM. Where ** indicates $p < 0.01$, **** indicates $p < 0.0001$ as determined by a two-way ANOVA test for growth rate and Student's t-test for doubling time.

5.2.2.2 Viability of cisplatin^R and WT cell lines following cisplatin exposure

To validate the phenotype of the cisplatin-resistant cell line, the MTT assay was employed to assess cellular metabolic activity, which can serve as an indirect measure of cell viability. Cells were seeded in a 96-well plate and after an overnight incubation, the cells were exposed to cisplatin concentrations based on the H357 WT IC₅₀ dose (7 μ M, 14 μ M, and 28 μ M). Concurrently, a control group was treated with 0.9% NaCl vehicle control. After 24 hours, MTT assay was used to calculate metabolic activity/viability.

There were pronounced differences in cell viability between the cisplatin^R and WT cells across the cisplatin concentrations tested (Figure 5.2). Specifically, for the WT cells subjected to 7 μ M, 14 μ M, and 28 μ M cisplatin, the average viabilities were $89.8\% \pm 6.4\%$, $69.9\% \pm 10.5\%$, and $45.3\% \pm 6.0\%$, respectively. In contrast, the cisplatin^R cells exhibited significant resistance to the same cisplatin concentrations, with viabilities of $110\% \pm 11.3\%$, $101\% \pm 9.2\%$, and $94.9\% \pm 4.5\%$, respectively (Figure 5.2).

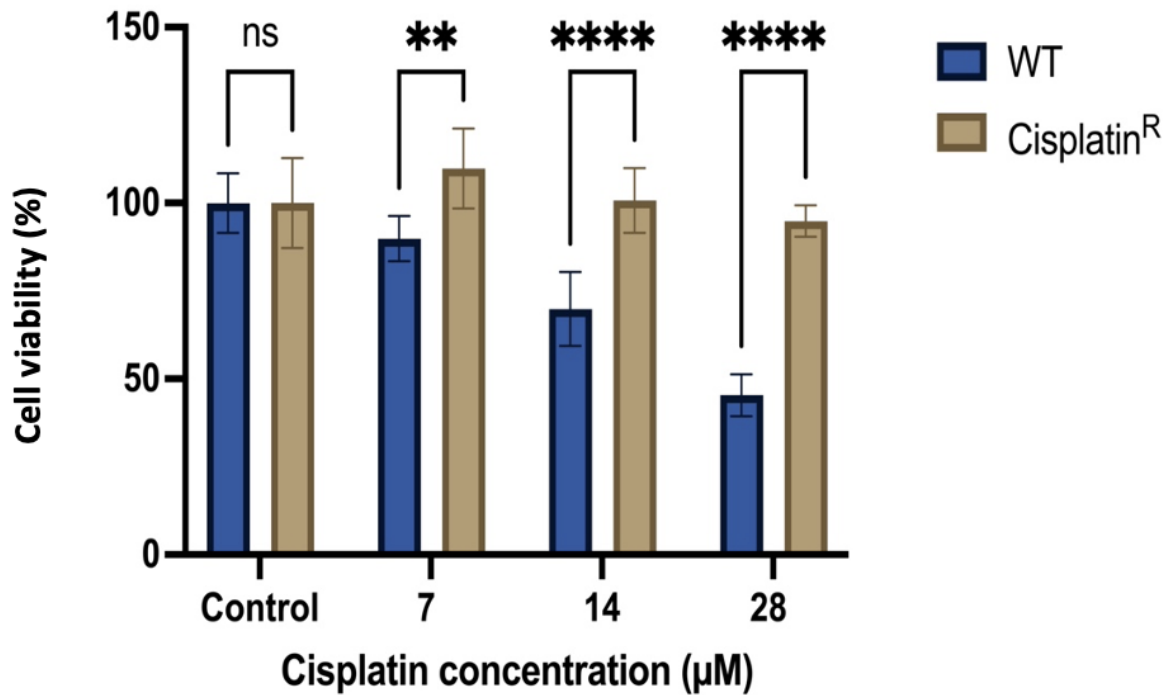


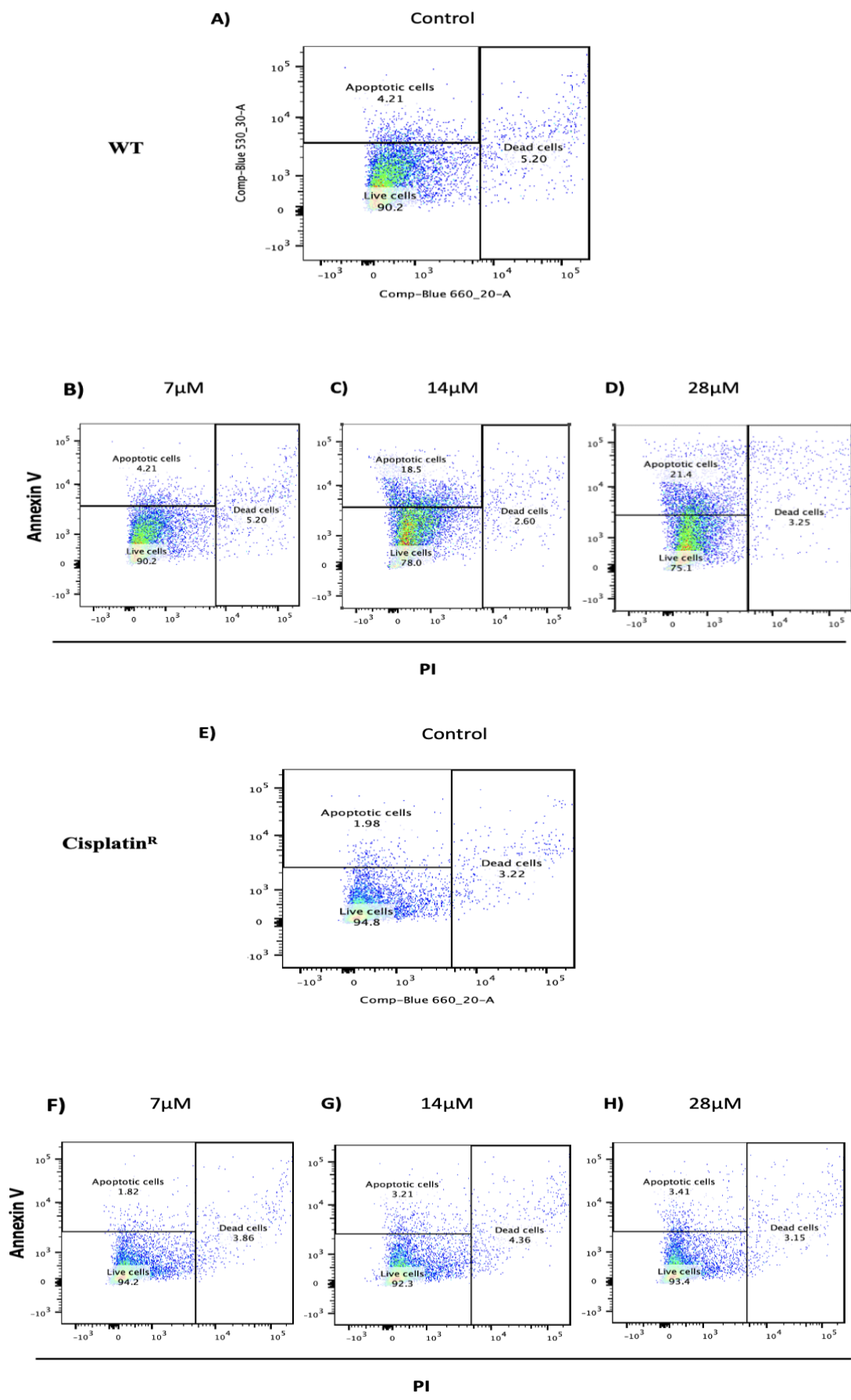
Figure 5.2 Metabolic activity/cell viability assessment of cisplatin^R and WT post cisplatin treatment.

For both H357 WT and cisplatinR cell lines, cell metabolic activity/viability was assessed using the MTT assay. Cells were seeded at a density of 1×10^4 cells per well in 96-well plates and allowed to adhere overnight. Following this, they were exposed to cisplatin for a 24-hour duration. The MTT assay was then conducted to assess cell viability. Percentage cell survival was calculated relative to the vehicle control. The data is an average derived from three biological replicates, with each having six technical repeats. Error bars signify the standard deviation. Significance levels are indicated as follows: ns=not significant, ** = $p < 0.01$, **** = $p < 0.0001$, determined via two-way ANOVA.

5.2.2.3 Comparing live, apoptotic, and dead cells in response to cisplatin treatment in Cisplatin^R and WT

To confirm the resistance of the cisplatin-resistant cell line to the pro-apoptotic action of cisplatin, flow cytometry, in conjunction with Annexin V-FITC and PI staining, was employed to determine the proportion of live, apoptotic, and dead cells following cisplatin treatment.

Illustrative scatter plots (Figure 5.3 panels A-H) depict the demarcation of these cellular populations. For the WT cells exposed to the control (0.9% NaCl), the average proportion of apoptotic cells was $2.2\% \pm 79.8\%$ (Figure 5.3. J). When treated with cisplatin at concentrations of 7 μM , 14 μM , and 28 μM , the apoptotic percentages were recorded as $13.6\% \pm 1.5\%$, $13.6\% \pm 2.7\%$, and $16.3\% \pm 4.5\%$, respectively (Figure 5.3. J). In contrast, the cisplatin^R cell line showed significantly fewer apoptotic cells: $1.6\% \pm 0.82\%$ (control), $2.1\% \pm 1.1\%$ (7 μM), $2.0\% \pm 1.60\%$ (14 μM), and $2.5\% \pm 1.5\%$ (28 μM) (Figure 5.3. J). There was a significant difference in the proportions of live (Annexin V⁻/PI⁻) and apoptotic (Annexin V⁺/PI⁻) cells between the cisplatin^R and WT lines was evident across all cisplatin concentrations (Figure 5.3. I and J). However, there was no statistical difference in the proportion of dead (PI⁺) cells across the concentrations (Figure 5.3. K).



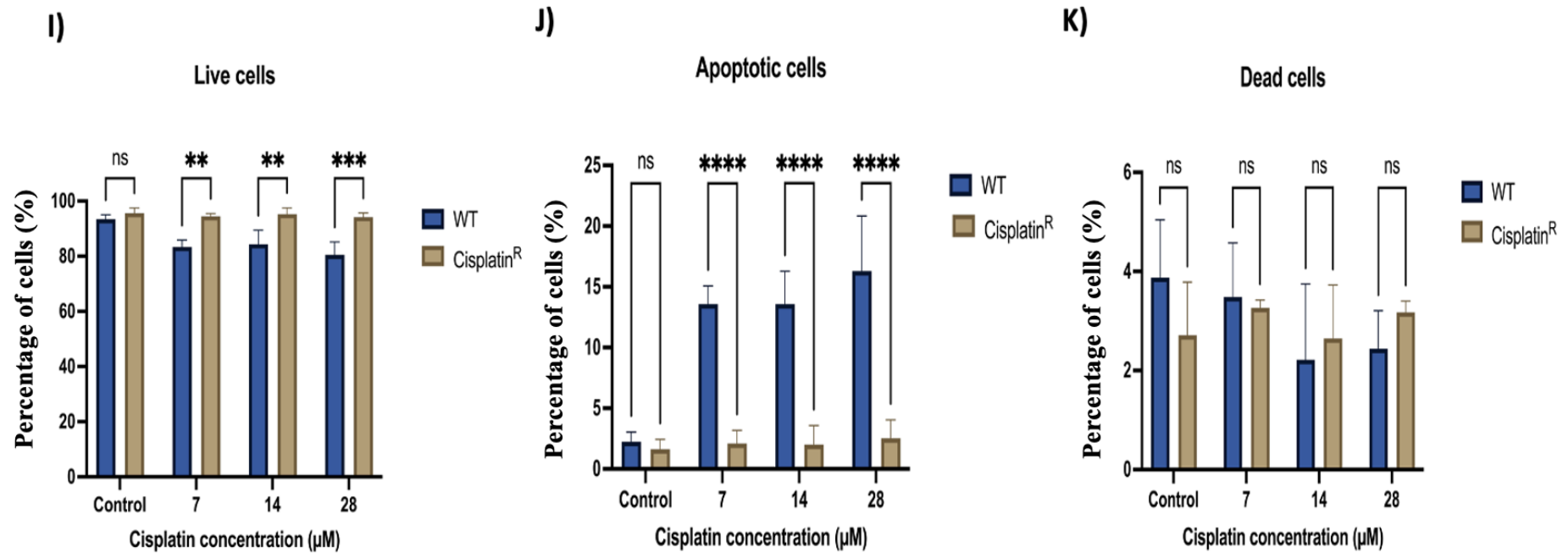


Figure 5.3 Flow cytometry analysis of cisplatin-induced apoptosis in WT and cisplatin^R cell lines.

The proportions of apoptotic and dead cells were determined using flow cytometry, post-staining with Annexin V-FITC and PI. WT panels (A-D) and cisplatin^R panels (E-H) cell lines. Cells were seeded at 2.5×10^5 cells/6-well and allowed to adhere overnight. Cells were treated with cisplatin for 24 hours before analysis by flow cytometry. Representative scatter plots showing PI (X-axis) against Annexin V (Y-axis) are depicted in panels A-H. The percentages of viable, apoptotic, and dead cells are presented in panels (I-K). The percentage of live, apoptotic and dead cells within each individual sample was calculated following gating to select single cells. The presented values represent the average from three biological replicates \pm SD. Significance levels are indicated as follows: ns=not significant, ** = $p < 0.01$, *** = $p < 0.001$, **** = $p < 0.0001$, determined via two-way ANOVA.

5.2.2.4 Analysis of cell cycle using flow cytometry

The cell cycle controls cellular growth and division. Moving through clear phases, G1, S, and G2, ending in mitosis, each phase is tightly controlled. The G1 phase focuses on cell growth and preparation for DNA replication, the S phase is for DNA synthesis, and the G2 phase makes sure the cell is ready for mitosis (Kamb, 1996). Cisplatin works mainly by causing DNA damage, which can then stop the cell cycle, giving cells a chance to either fix the damage or trigger apoptosis (Velma et al., 2016). The investigation then aimed to determine if there was a difference in the cell cycle of the Cisplatin^R cell line after cisplatin treatment compared to the WT.

The cell cycle distribution of the WT and Cisplatin^R was examined post a 24-hour exposure to 14 μ M of cisplatin. For comparative purposes, a control group was subjected to a 0.9% NaCl treatment. Post-treatment, cells were stained with PI and subsequently analysed via flow cytometry to determine the proportion of cells in the various cell cycle phases (Figure 5.4).

For untreated WT cells, 26% were in G1 phase, compared to 12.2% for cisplatin-treated WT cells. In comparison, the Cisplatin^R cell line showed 49.8% in G1 phase when not treated and 42.7% after cisplatin (Figure 5.6. E).

60.4% of untreated WT cells were in S phase, whereas 65.5% of cisplatin-treated WT cells were in S phase. The Cisplatin^R cell line showed 23.4% in S phase when not treated and 25.7% after cisplatin treatment (Figure 5.6.F).

Lastly, for the G2 phase, the untreated WT cells showed 10.8% in this phase and the treated WT cells had 21.5% in G2 phase. The Cisplatin^R cells showed 23.4% in G2 phase when not treated and 29.2% after treatment (Figure 5.6.G).

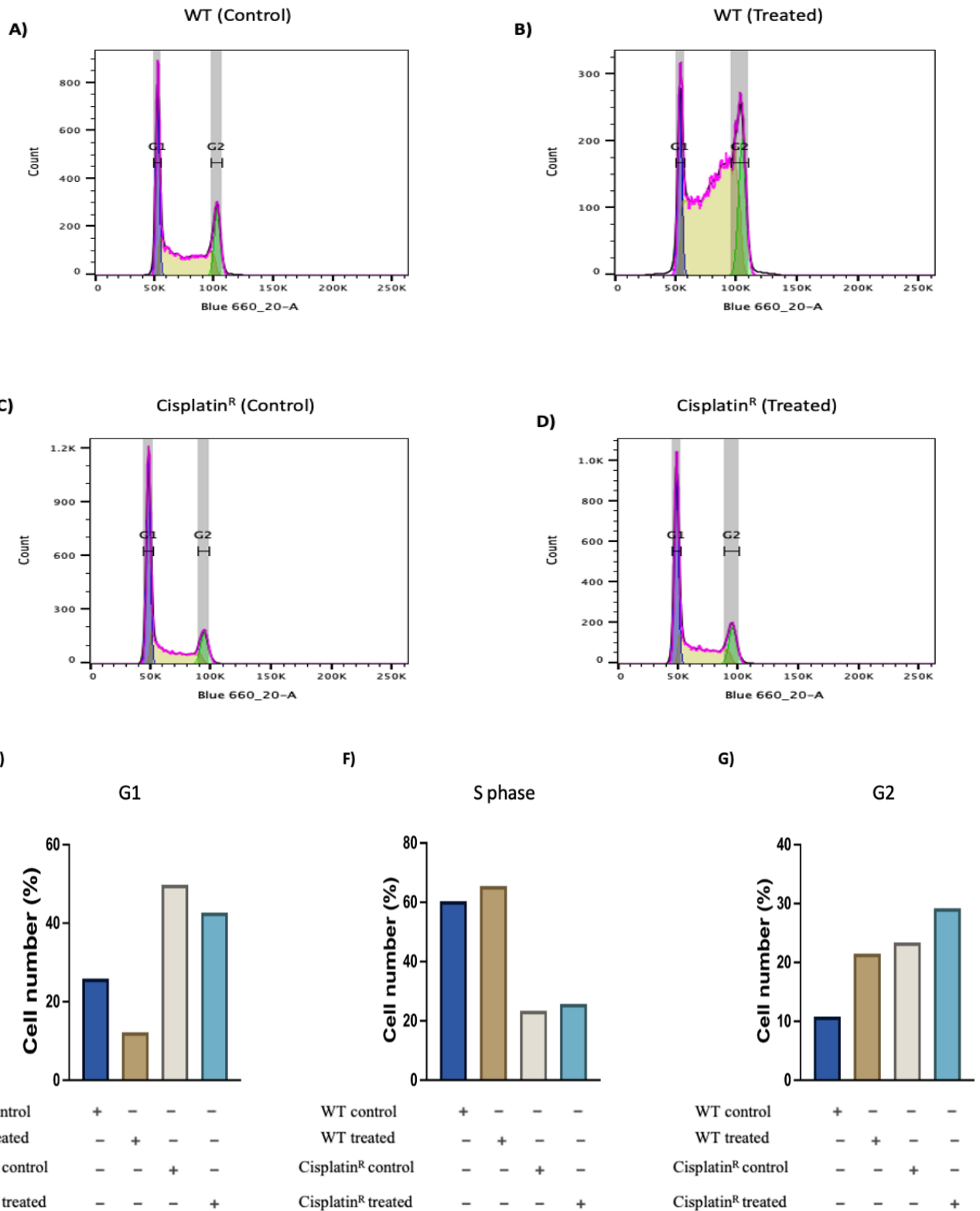


Figure 5.4 Cell cycle analysis for WT and cisplatin^R cell lines post cisplatin exposure.

Flow cytometry analysis of the cisplatin-induced variation in cell cycle distribution in H357 (WT) and cisplatin^R cell lines after 24 hours of cisplatin exposure panels (A-D). Cell cycle distribution in WT and cisplatin^R cell lines in response to 14 μ M of cisplatin in different cell cycle phases G1, S and G2 panels (E-G). This data is based on a single repeat n=1.

5.2.2.5 Cellular mechanisms of cisplatin resistance

The next step was to determine if there were cellular mechanisms that could explain the phenotype of the cisplatin^R cell line. As previously discussed, there are several proteins that are involved in cisplatin resistance, including drug efflux pumps (ATP7A and ATP7B) and drug influx pumps (CTR1). RRBP1 has previously been identified as a protein that is overexpressed in cisplatin resistant HNC cell lines (Shriwas et al., 2021), and MVP is frequently overexpressed in multidrug resistant cancer cells (Rimsza et al., 1999). Therefore, the expression of these proteins was assessed by western blotting.

Cells were cultured in normal growth medium and whole cell lysates were prepared for SDS-PAGE and subsequent western blotting. Despite loading 40 µg cell lysate per sample, no signal could be detected for ATP7A. Expression of ATP7B was very low and could only be detected by using Supernova ECL reagent. The other proteins were readily detected with standard ECL reagent (Figure 5.5A). The unglycosylated form of CTR1 (~25 kDa) was the most prominent form detected. However, overexposure of the blot revealed the presence of larger molecular weight protein:antibody complexes that could be glycosylated forms of CTR1 (Figure 5.5B). Densitometry analysis was performed to normalise target protein abundance to that of the β-actin loading control (Figure 5.5 C-G). The unglycosylated form of CTR1 was significantly reduced in the cisplatin^R cell line compared to the WT (Figure 5.5 F). There was no significant difference in the abundance of the other proteins examined.

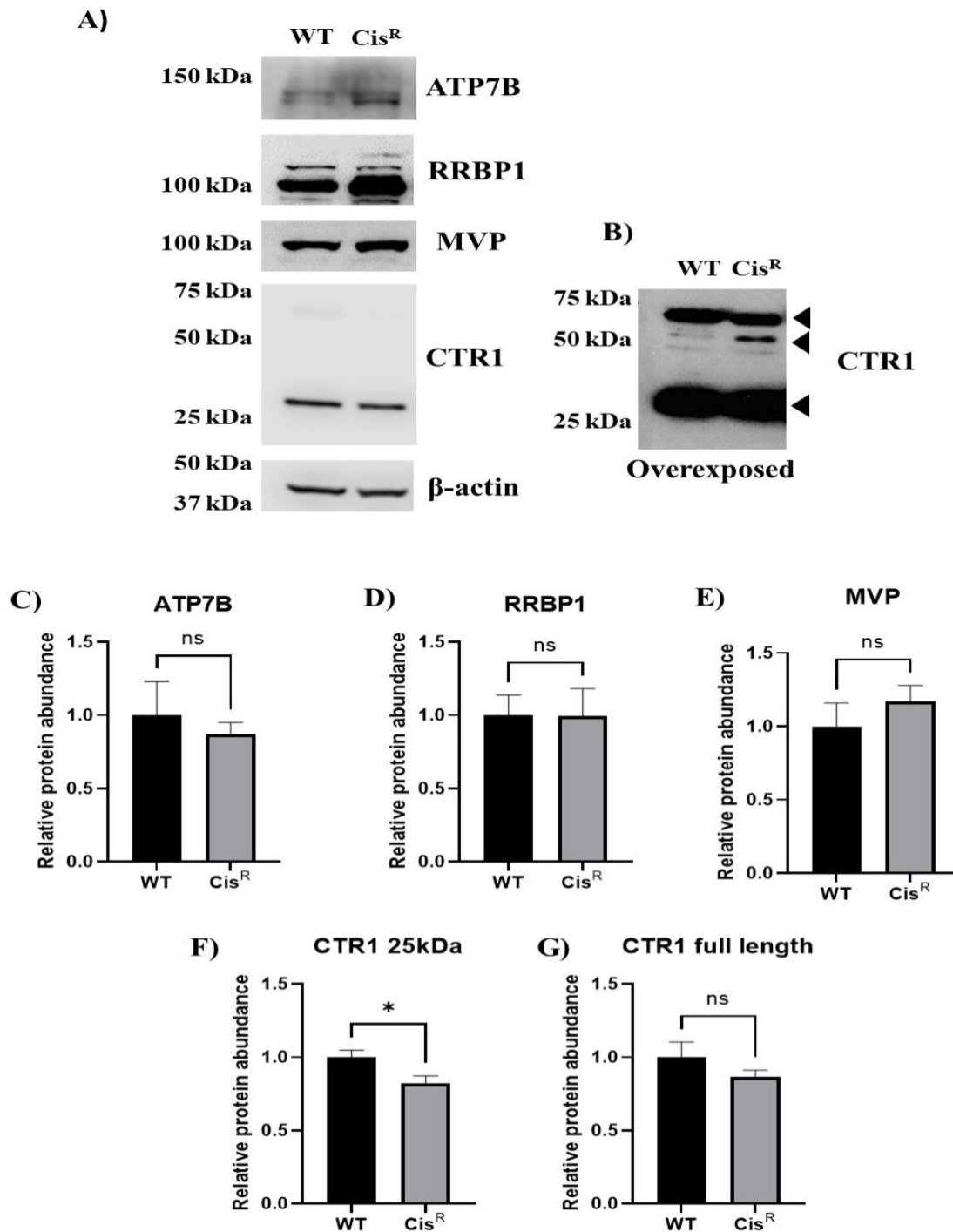


Figure 5.5 Detection of proteins involved in cisplatin resistance by western blotting.

Cells were seeded in a T25 flask at 1×10^6 cells per flask and allowed to adhere overnight. The following day, monolayers were washed in PBS and solubilised in RIPA buffer. Cell lysates were clarified by centrifugation. Protein concentration was determined by BCA assay and $40 \mu\text{g}$ lysate was separated by 12% SDS-PAGE before transfer to nitrocellulose membranes and subsequent western blotting. Representative western blots are shown (A/B). Densitometry was performed by ImageJ and target protein band intensity was normalised to the β -actin loading control. Normalised protein abundance is expressed relative to WT (C-G). Data represents the average of three biological repeats with error bars indicating standard deviation. ns= not significant and $*=p < 0.05$ by Students t-test.

5.2.2.6 Cellular expression of vault particle components and HGS

Despite not detecting a difference in the protein abundance of MVP (Figure 5.5 A/E). The transcript expression of the vault particle components was examined: MVP, vtRNA1-1, TEP1, and PARP4. Vault particle components (vtRNA1-1 in particular) have been linked to resistance to apoptosis and so their expression could mediate cisplatin resistance independent of the vault particle (Amort et al., 2015). Additionally, the expression of the HGS transcript was also assessed as an indication if ESCRT dependent EV biogenesis might be upregulated in the cisplatin^R cell line (Wang et al., 2023). Transcript expression was determined by qPCR with GAPDH serving as the internal control to normalize the expression data.

The findings revealed that the expression patterns of vtRNA1-1, TEP1, PARP4, and HGS were relatively consistent between the WT and cisplatin^R cell lines, with no statistically significant differences observed (Figure 5.6). However, a notable exception was observed in the expression of the MVP. The MVP transcript was found to be significantly downregulated in the cisplatin^R cell line compared to the WT cell line (p value < 0.05) (Figure 5.6.A).

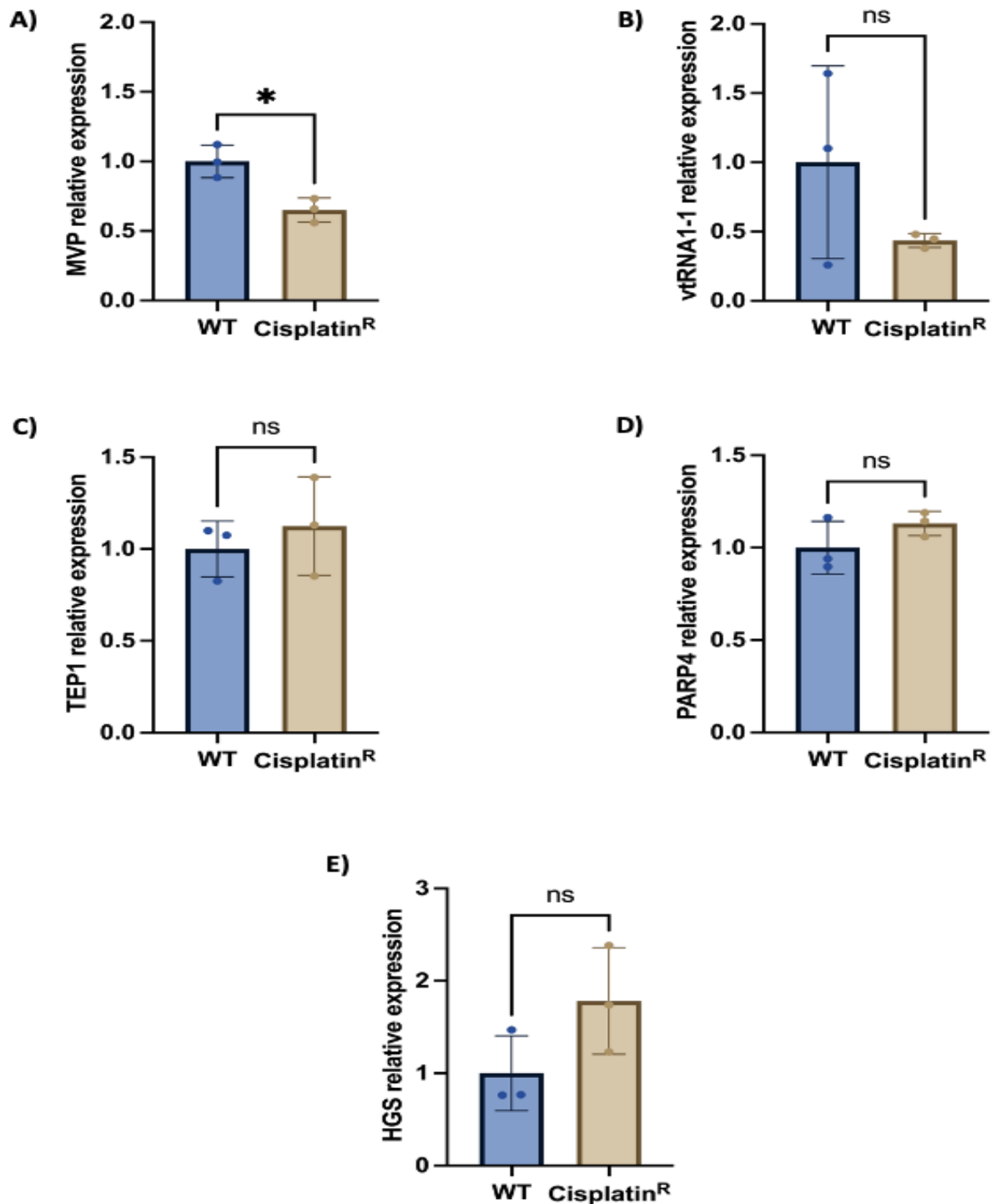


Figure 5.6 Cellular transcript expression of vault components and HGS.

Quantitative real-time PCR was performed using cDNA samples derived from the reverse transcription of 100 ng of total RNA, which was extracted from 2.5×10^5 cells cultured in 6-well plates. The relative expression changes of vault components (A-D) and HGS (E) were determined using TaqMan primers through a two-step protocol, with GAPDH serving as the internal reference panels (A-E). Results are presented as mean \pm SD, $n=3$, where ns indicates no significant difference, while * signifies $p < 0.05$ as determined by an unpaired t-test.

5.2.3 Impact of cisplatin treatment on EP release from WT and cisplatin^R cell lines

In the present investigation, the study aimed to elucidate the influence of cisplatin on the secretion of EPs in both WT and cisplatin^R cell lines. The foundation of the experimental approach was based on the previously identified IC₅₀ values for cisplatin (Table 3.5). Cells were seeded at 2.5×10^5 cells per 6-well and allowed to adhere overnight. Subsequently, both WT and cisplatin^R cells were incubated with cisplatin concentrations of 7 μM , 14 μM , and 28 μM or 0.9% NaCl vehicle control. After 24 hours of cisplatin exposure, the culture medium was replaced with medium supplemented with UF-dFBS for an additional 24-hour period. Post-treatment, the conditioned medium from each well was subjected to NTA for small particle quantification. To ensure consistency, these quantifications were adjusted based on the cell count of each respective well.

A dose-responsive increase in EP release was observed from the WT cell line, but this pattern was not evident in the cisplatin^R cell line. Notably, after 14 μM and 28 μM cisplatin treatment, the cisplatin^R cells released significantly fewer EPs, registering counts of $6.77 \times 10^2 \pm 8.43 \times 10^1$ particles per cell and $1.62 \times 10^3 \pm 8.39 \times 10^2$ particles per cell, respectively. This contrasted with the WT counts of $3.81 \times 10^4 \pm 3.18 \times 10^4$ particles per cell (14 μM) and in $5.67 \times 10^4 \pm 3.07 \times 10^4$ particles per cell (28 μM) (Figure 5.7.A). This significant difference was only observed at the 14 μM and 28 μM cisplatin concentrations, with no significant difference in EP release for the vehicle control or 7 μM cisplatin treatments (Figure 5.7A).

Cells were cultured on a larger scale (i.e. 2×10^6 cell per T75 flask) and treated with 14 μM cisplatin. EPs were pelleted by ultracentrifugation and analysed by NTA. There was no significant difference in the concentration or size of EPs that were enriched (Figure 5.7.B).

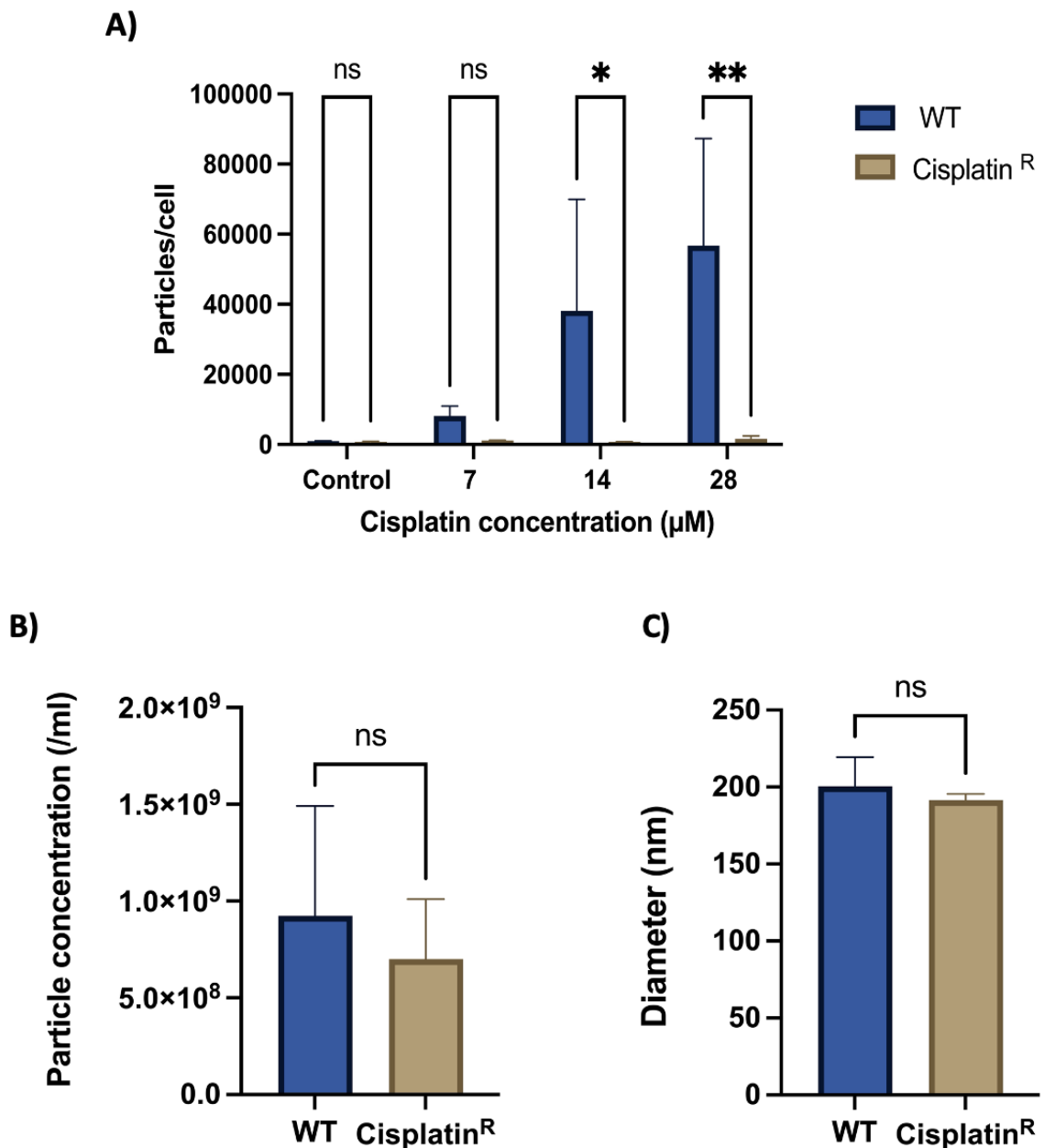


Figure 5.7 Impact of cisplatin treatment on EP release from cisplatin^R and WT cell lines.

Particle number in the conditioned medium from both WT and cisplatin^R cell lines was evaluated using NTA. For this assessment, 2.5×10^5 cells were seeded per well in a 6-well plate. The particle numbers were then normalized according to cell count (A). Cells were seeded at 2×10^6 per T75 to generate 24 hour conditioned medium for ultracentrifugation. Following this, the concentration of particles in the EP pellet was determined for both the WT and cisplatin^R cell lines (B). Additionally, the size of the particles in the pellet after cisplatin exposure was ascertained for both cell lines (C). The presented data is an average of three distinct biological repetitions, with the standard deviation (SD) depicted as error bars. To identify statistical differences, two-way ANOVA and Student's t-test were employed. In the results, "ns" indicates not significant, * indicates $p < 0.05$, and ** signifies $p < 0.01$.

In an attempt to identify the EPs released in the conditioned medium post cisplatin treatment, EP pellets (enriched by ultracentrifugation) were solubilized in RIPA buffer for western blot analysis. Lysates were probed for the abundance of TSG101 (a common marker associated with EVs) and MVP (a vault particle marker).

Both the WT and cisplatin^R cell lines were incubated with increasing cisplatin concentrations, based on the WT IC50 value (Table 3.5). Western blot analyses of the EP lysates highlighted the presence of specific markers. Notably, markers representative of EVs, such as TSG101, and those indicative of vault particles, like MVP, were detectable across all cisplatin concentrations (Figure 5.8).

A closer examination revealed a more intense MVP band in EP lysates derived from the WT cell line, particularly evident after cisplatin treatments of 7, 14, and 28 μM . In contrast, the cisplatin^R cell line did not show an increase in MVP band intensity following cisplatin treatment. In fact, the MVP band intensity decreased as cisplatin concentration increased (Figure 5.8). Regarding TSG101, the WT samples exhibited heightened band intensities at control, 7 μM , and 28 μM concentrations. However, TSG101 protein abundance was much lower in the cisplatin^R samples across all treatments. The western blot data is in broad agreement with NTA data that the cisplatin^R cell line releases fewer EPs (EVs and vaults) than the WT cell line after cisplatin treatment.

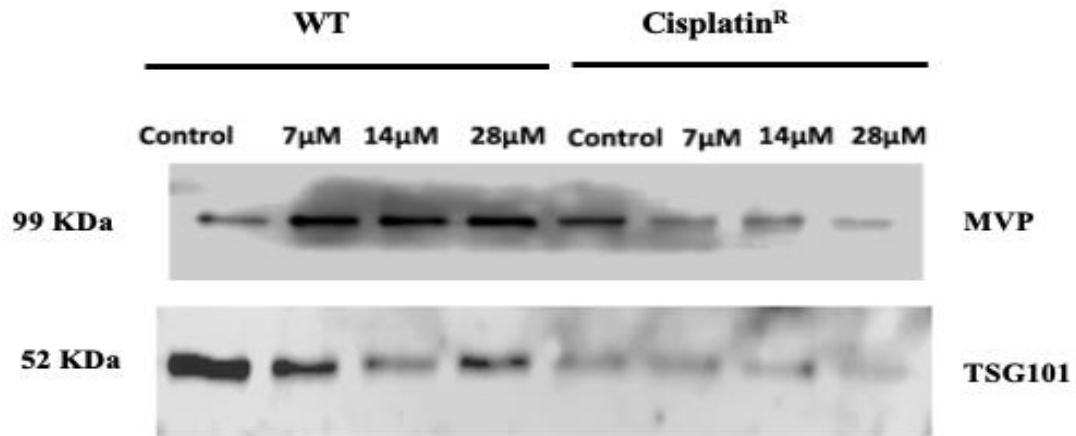


Figure 5.8 Detection of EV and vault particle markers derived from WT and cisplatin^R cells following cisplatin treatment.

Cells were seeded at 2×10^6 cells/75 cm² flask and allowed to adhere. Monolayers were treated with cisplatin for 24 h and then medium was replaced to that supplemented with UF-dFBS and incubated for a further 24 h. EPs were pelleted by ultracentrifugation at 100,000 x g for 1 h, followed by washing in PBS and recentrifugation at 100,000 x g for 1 h. The resulting EP pellets were then solubilised in RIPA buffer. Equal volumes of EP lysate were separated by SDS-PAGE and subsequently transferred onto a nitrocellulose membrane in preparation for western blotting. After blocking, these membranes were incubated with primary antibodies overnight at 4°C. Following a series of washes, the membranes were exposed to HRP-linked secondary antibodies at room temperature for 1h. After a brief 5-minute incubation with a luminescent substrate, the membranes were exposed to X-ray film.

5.2.4 Can EPs derived from cisplatin^R HNC cells transfer cisplatin resistance?

The aim here was to determine if EPs can transfer cisplatin resistance between HNC cancer cells. 2×10^6 cisplatin^R cells were seeded in T75 tissue culture flasks and allowed to adhere overnight, before incubating in growth medium supplemented with UF-dFBS for 24 hours. EPs were enriched from conditioned medium by ultracentrifugation and NTA used to enumerate EPs. Naïve H357 WT cells (i.e. cells not previously exposed to cisplatin) were seeded at a density of 2.5×10^5 cells per well in a 6-well plate and allowed to adhere overnight. These cells were then incubated with either 0.9% NaCl vehicle, 14 μ M cisplatin only, or 14 μ M cisplatin and 10 μ l of isolated EPs that equated to 8×10^9 particles. After a 24-hour incubation period, the proportion of live, apoptotic and dead cells was determined by flow cytometry in conjunction with dual Annexin V-FITC and PI labelling. Representative scatter plots are shown to illustrate how cell populations were selected (Figure 5.9 A-C).

When cells were exposed to the 0.9% NaCl vehicle control, cells exhibited a live percentage of $95.1\% \pm 0.757\%$ (Figure 5.9). Upon exposure to 14 μ M cisplatin, the viability decreased to $63.8\% \pm 6.41\%$. However, the concurrent administration of cisplatin and EPs partially restored live cell percentage to $80.4\% \pm 2.66\%$.

The proportion of apoptotic cells was $1.82\% \pm 0.51\%$ in the vehicle control. This proportion increased to $22.4\% \pm 5.37\%$ when cells were treated with 14 μ M cisplatin. The combined treatment of cisplatin and EPs reduced the proportion of apoptotic cells by half to $11.5\% \pm 2.36\%$ (Figure 5.9. D).

The proportion of dead cells was $2.92\% \pm 0.31\%$ in the vehicle control and increased to $12.7\% \pm 3.02\%$ when cells were treated with 14 μ M cisplatin. The combined treatment of cisplatin and EPs did not significantly decrease the proportion of dead cells which was $7.54\% \pm 0.58\%$ (Figure 5.9 D).

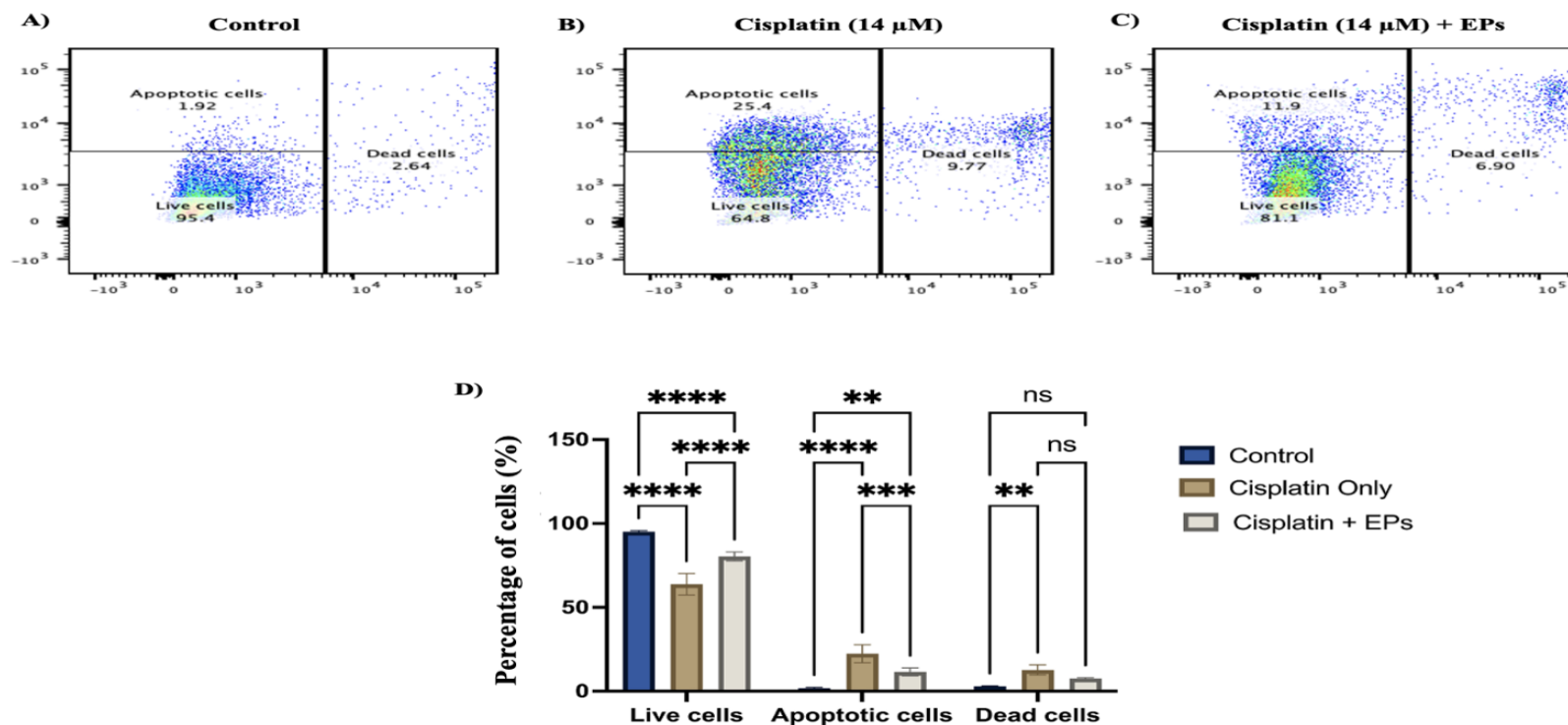


Figure 5.9 Investigation of role of extracellular particles in mediating cisplatin resistance.

The proportions of live, apoptotic, and dead cells were ascertained using flow cytometry, post-staining with Annexin V-FITC and PI. WT cells were incubated for 24 hours with either 0.9% NaCl vehicle control, 14 μM of cisplatin and cisplatin plus EPs. Scatter plots showcasing PI (X-axis) against Annexin V (Y-axis) are depicted for naïve cells (A-C). The percentages of viable, apoptotic, and dead cells are presented in (D). The percentage of live, apoptotic and dead cells within each individual sample was calculated following gating to select single cells. The presented values represent the average from three biological replicates ± SD. Statistical differences were identified using two-way ANOVA, where ns=not significant, * = p< 0.05 ** = p< 0.01 *** = p< 0.001 **** = p< 0.0001.

5.3 Discussion

5.3.1 Cisplatin^R cells show reduced proliferation rate

The reduced growth rate observed in the cisplatin^R cell line parallels findings from other research, such as the study by Duan et al. (2017), which documented a similar decrease in the HeLa/ddp, HGC27/ddp and AGS/ddp resistant cell lines (G. Duan et al., 2017). This trend of slowed proliferation in cisplatin-resistant cell lines is further corroborated by Walker et al. (1990), who noted that both the RT112-CP bladder carcinoma and SuSa-CP testicular tumour cell lines exhibited longer doubling times compared to their WT counterparts (Walker et al., 1990). The study, along with these corroborative findings, consistently points to a notable difference in growth rate and doubling time between cisplatin^R and its WT. The slower growth rate observed in cisplatin-resistant cell lines compared to their WT counterparts may be due to the energy and resources these cells expend on activating resistance mechanisms, such as enhanced DNA repair processes or drug efflux pumps, which could detract from their proliferative capacity.

To discern the impact of cisplatin resistance on cellular division, Preliminary cell cycle analysis was performed to compare the H357 WT and its cisplatin-resistant derivative. The analysis post-cisplatin exposure shed light on the differential responses of the WT and Cisplatin^R cells, with noticeable variations in the G1, S, and G2 phases. WT cells demonstrated a decrease in G1 phase following cisplatin treatment, but potentially increased cell cycle arrest in G2 phase. Even in the presence of cisplatin, WT cells entered S phase. Whereas a higher proportion of the cisplatin^R cell remained in G1 phase and did not enter S phase. It has been suggested that arrest in G1 phase is a protective mechanism against cisplatin treatment, allowing activation of repair mechanisms capable of correcting cisplatin-induced DNA damage (Mueller et al., 2006). Thus, the reduced proliferation rate and increased G1 arrest of the cisplatin^R cell line may be part of the cisplatin resistance mechanism. However, Caution must be exercised when interpreting the cell cycle data presented here, as it represents the findings from a single experiment. Further repeats with statistical analysis are required to make firm conclusions, but due to time constraints this was not possible.

5.3.2 Cisplatin^R cell line has reduced sensitivity to cisplatin and reduced expression of CTR1 influx pump

The MTT assay, a proxy for cellular viability, showed that cisplatin^R cells were significantly more resistant to cisplatin treatment than WT. This was further confirmed by flow cytometry showing a reduction in apoptosis in cisplatin^R cells. Such resistance to apoptosis is a hallmark of cancer cell survival and has been observed across various studies, such as those by Ji-Youn Han et al. (1999), corroborating the notion that evasion of programmed cell death is a cornerstone of cisplatin resistance (Han et al., 1999). Furthermore, a study by Yoon et al. (2001) established a cisplatin-resistant model using the H460 HNC cell line and deduced that alterations in apoptotic gene expressions might be instrumental in conferring drug resistance (Yoon et al., 2001).

It is already known that the balance between the influx and efflux of cisplatin, mediated by transporters such as CTR1, ATP7A, and ATP7B, is crucial in determining the drug's intracellular concentration and cytotoxicity (Zisowsky et al., 2007). The mechanistic underpinnings of this resistance phenotype are multifaceted. The western blot analyses indicate a significant reduction in the unglycosylated form of CTR1 in cisplatin^R cells. This finding is pivotal given the role of CTR1 as a key mediator of cisplatin uptake. The study by Öhrvik et al. (2013) sheds light on the complexity of CTR1 regulation and its influence on cisplatin transport, suggesting that the observed reduction in CTR1 may be a strategic adaptation to limit cisplatin influx (Öhrvik et al., 2013). The implications are twofold: on one hand, it highlights a potential resistance mechanism through altered drug uptake; on the other, it opens avenues for targeting the biogenesis and function of CTR1 to restore cisplatin sensitivity.

The roles of ATP7A and ATP7B in chemoresistance are well-established, as these copper-transporting proteins contribute to the efflux of platinum-based drugs, such as cisplatin, from cells. Typically, their upregulation is associated with reduced drug accumulation and diminished chemosensitivity (Barr et al., 2013). However, the undetectable expression of ATP7A and the low levels of ATP7B observed in the study in the cisplatin^R cell line suggest that other mechanisms may be more critical in conferring resistance in this context. This challenges the conventional view that emphasizes the dominance of efflux pumps in drug resistance, particularly in HNC, and calls for a broader

examination of the molecular adaptations that enable cancer cells to evade the cytotoxic effects of chemotherapy.

The discovery of proteins such as RRBPI and MVP, implicated in cisplatin resistance in other HNC cell lines (Kickhoefer et al., 1998; Shriwas et al., 2021), underscores the complexity of resistance mechanisms. RRBPI's upregulation has been linked to chemoresistance in OSCC, marking its potential as a target for overcoming drug resistance (Shriwas et al., 2021). Contrasting findings from the western blot study, however, reveal no significant change in RRBPI levels between cisplatin-resistant and WT H357 cell lines. This is difficult to consolidate because Shirwas et al. (2021) generated a cisplatin-resistant H357 cell line, which showed overexpression of RRBPI. However, they cultured H357 in 15 μM cisplatin for 5 months, until normal cell growth returned. The cisplatin^R cell line generated in the current study did not undergo such lengthy culture in the maximal cisplatin IC50 dose (14 μM) and still displayed reduced proliferation rate. In addition, when comparing the expression of proteins involved in cisplatin resistance, the cells were not treated with cisplatin, potentially obscuring any changes in protein expression that might occur in response to the drug. If the cisplatin-resistant cells had been exposed to cisplatin during the experiment, it might expect to see distinct upregulation or downregulation of certain proteins as part of the resistance mechanism. However, the presence of cisplatin in the experimental conditions would have resulted in significant cell death of the WT cell line. Due to the cytotoxic effects of cisplatin on WT cells, it is not feasible to expose them to the same concentration of cisplatin (14 μM) used for the resistant cells without a significant loss of cell viability, but lower sub-lethal cisplatin concentrations could have been used.

5.3.3 Cisplatin^R cells release fewer EPs after cisplatin treatment

The observations demonstrated that cisplatin^R H357 cells release fewer EPs post-treatment with 14 μM and 28 μM cisplatin compared to the WT. This contrasts with Khoo et al. (2019) who reported that there was a heightened release of EVs in both inherently resistant (H314) and adaptively resistant (H103/cisD2) OSCC cell lines compared to cisplatin-sensitive H103 cells.

Intriguingly, the data revealed a heightened MVP band intensity in EPs from the WT cell line specifically at cisplatin concentrations of 7, 14, and 28 μM . This contrasts with the cisplatin^R cell line

where more MVP was detected in control-treated samples compared to cisplatin-treated samples. MVP has been implicated in mediating nucleus-cytoplasm translocation of chemotherapeutic drugs (Meschini et al., 2002). Therefore, the cisplatin^R cell line may retain MVP/vault particles, rather than export them, to aid with cisplatin sequestration. It would be interesting to compare the amount of intracellular and extracellular MVP/vaults in WT and cisplatin^R cell lines following cisplatin treatment to determine any difference in retention or export. The increased abundance of MVP in the WT-derived EPs following cisplatin treatment suggests that MVP/vaults might mediate export of cisplatin from the cell. Furthermore, recent studies have highlighted the potential role of MVP in vesicular trafficking and selective cargo sorting, especially in exosomal cargo sorting in colon cancer cells (Teng et al., 2017). Therefore, MVP might be involved in the selective sorting of cisplatin or other cellular components into these vesicles. This could be particularly pertinent in the context of drug resistance, where cells might employ MVP-mediated vesicular sequestration to mitigate the cytotoxic effects of cisplatin.

5.3.4 EPs from cisplatin^R HNC cells can transfer cisplatin resistance

The findings highlight the protective effects conferred by EPs against cisplatin-induced cytotoxicity. Specifically, naïve cells treated with both cisplatin and EPs demonstrated a significant reduction in the proportion of apoptotic cells compared to cells exposed to cisplatin alone. Regrettably there was insufficient time to explore the mechanism underlying this protective effect. However, recent studies have shed light on the role of EVs in mediating drug resistance. EVs have been recognized as important vectors in the transfer of drug resistance features among cancer cells. These features include the transfer of drug efflux transporters like P-glycoprotein and MRP1/ABCC1, which have been shown to move from drug-resistant cells to their more sensitive counterparts, potentially spreading resistance (Levchenko et al., 2005; Lu et al., 2013; Lv et al., 2014; Zhang et al., 2012). Additionally, miRNAs that are selectively incorporated into EVs by resistant cells can, upon uptake by other cells, alter gene expression patterns and affect the cells' response to chemotherapy (Chen et al., 2014; Jaiswal et al., 2012). For instance, exosomes derived from cisplatin-resistant lung cancer cells have been shown to transfer miR-100-5p to recipient cells, leading to increased cisplatin resistance by targeting mTOR (Qin et al., 2017). Proteins such as Annexin A3, TRPC5, and inhibitors of apoptosis proteins are also among

the molecular cargo that can be shuttled via EVs, thereby disseminating resistance mechanisms (Ma et al., 2014; Yin et al., 2012).

The lipid content within EVs is another factor that contributes to the drug resistance phenotype. For example, EVs rich in sphingomyelinase have been implicated in conferring resistance characteristics to susceptible multiple myeloma cells (Faict et al., 2019). Moreover, gefitinib-resistant lung cancer cell lines have been observed to release EVs with distinct phospholipid compositions compared to those from sensitive parental lines, suggesting that the lipid makeup of EVs may influence drug responsiveness (Jung et al., 2015).

External factors like the acidity of the TME and hypoxia also play significant roles in modulating EV release and therapeutic outcomes, underscoring the influence of the TME on cancer behaviour and resistance (Logozzi et al., 2018; Parolini et al., 2009; Xavier et al., 2020). Tumour cell-induced acidification of the TME has been shown to stimulate EV secretion across various cancer types, which can be mitigated by neutralizing the acidity (Boussadia et al., 2018; Logozzi et al., 2018; Parolini et al., 2009). Similarly, hypoxic conditions have been found to increase the release of EVs in cancer cells such as NSCLC and glioblastoma, carrying miRNAs like miR-21 and miR-301a that are linked to enhanced drug resistance (Dong et al., 2019). In ovarian cancer models, hypoxic cells not only secreted more EVs but also extruded higher amounts of cisplatin through these vesicles, thereby bolstering their resistance to the drug (Dorayappan et al., 2018). When EVs from these hypoxic cells were combined with cisplatin-sensitive ovarian cancer cells, an increase in resistance to cisplatin treatment was observed (Dorayappan et al., 2018).

Chapter 6 General Discussion:

6.1 Extracellular particles and chemotherapy resistance

The role of extracellular particles EPs, particularly EVs, in mediating chemotherapy resistance has garnered significant attention in recent years. These vesicles, which are secreted by cells and contain a variety of molecular cargoes, including proteins, lipids, and nucleic acids, have been implicated in a range of cellular processes, from intercellular communication to the modulation of the tumour microenvironment (Xavier et al., 2020). In the context of chemotherapy resistance, two primary mechanisms have been proposed, the transfer of molecular messages that convey drug resistance and the direct export of chemotherapeutic drugs (Luqmani, 2005).

The molecular cargo of EPs can be transferred between cells, potentially conferring drug resistance to recipient cells. Samuels et al. (2022) emphasized the role of EVs in this context, suggesting that they might carry molecular signals that activate resistance pathways in recipient cells (Samuels et al., 2022). EPs might directly sequester and export chemotherapeutic agents from tumour cells, reducing the intracellular concentration of the drug and thereby diminishing its cytotoxic effects (Khoo et al., 2019). This mechanism could be particularly relevant during the initial exposure of naïve cells to a drug before they develop intrinsic resistance mechanisms. This is supported by data in the current study showing that naïve H357 WT cells release increased EPs in response cisplatin treatment, but cisplatin^R H357 cells did not respond in this way. The other possibility is that naïve cells release EPs as part of the apoptotic process, but cisplatin^R cells do not release these EPs as they can resist cisplatin-induced apoptosis.

It is likely that both mechanisms play a role in chemotherapy resistance, but their relative importance might vary depending on the stage of cancer and the specific tumour type. Initially, when naïve cells are first exposed to a drug, the direct export of the drug via EPs might be a dominant resistance mechanism. As cells become more chronically exposed to the drug and develop intrinsic resistance mechanisms, the transfer of molecular messages via EPs might become more prominent, helping to spread resistance to neighbouring or distant cells.

In conclusion, the multifaceted role of EPs in mediating chemotherapy resistance underscores the complexity of tumour biology and the challenges associated with cancer treatment. A deeper understanding of the mechanisms by which EPs contribute to resistance will be crucial for the development of more effective therapeutic strategies. Personalized therapeutic approaches, considering the specific resistance mechanisms employed by individual tumours, might be the key to improving treatment outcomes for patients with HNC and other malignancies.

6.2 Extracellular particles as targets to resensitize chemotherapy-resistant cells

The emergence of chemotherapy resistance remains a significant barrier to effective cancer treatment, leading to treatment failure and recurrence. In this context, the evolving understanding of the role of EPs provides a promising avenue for developing innovative therapeutic strategies (Maleki et al., 2021). Previous literature has implicated exosomes in sequestering chemotherapeutic agents, consequently facilitating their efflux from cancer cells. By blocking this efflux, it might be possible to increase the intracellular concentration of the drug, amplifying its cytotoxic effects and potentially resensitizing resistant cells to chemotherapy (Milman et al., 2019).

Another intriguing aspect of EPs is their potential role in transferring drug resistance-conferring molecules between cells. This capacity to educate previously drug-sensitive cells presents a dynamic interplay within the TME, propagating a resistant phenotype (Xavier et al., 2022). By inhibiting the release of these vesicles, the spread of drug resistance within a tumour could potentially be halted. The blockade of vault particles, which are lesser-known but intriguing, further complements this strategy, given their proposed role in drug resistance (Fontana et al., 2021).

While the idea of targeting EPs is promising, the findings illustrate the complexity of this approach. For instance, the absence of a significant change in sensitivity to cisplatin in the Δ HGS cell line demonstrates that identifying the correct EPs for targeting will be essential, and the involvement of other mechanisms that may complement or override the effects of blocking EPs should be considered. Identifying the specific EPs released by a patient's tumour could guide therapeutic strategies. By targeting the release or uptake of these specific EPs, personalized strategies to counteract chemotherapy

resistance could be formulated, tailoring treatments based on an individual's unique tumour biology. Additionally, considering the heterogeneous nature of tumours, a multi-targeted approach inhibiting multiple EPs release pathways may be more effective than targeting a singular pathway.

In summary, EPs have emerged as potential central players in the mechanism of chemotherapy resistance. Targeting them could provide a novel approach to counteract resistance mechanisms, offering hope for improved cancer treatment outcomes. However, this endeavour requires a comprehensive understanding, meticulous targeting strategies, and a multidisciplinary approach to fully exploit the therapeutic potential of EPs in the battle against cancer.

6.3 Monitoring cancer through circulating EVs

The landscape of cancer diagnostics and monitoring is undergoing a paradigm shift with the advent of liquid biopsies and the burgeoning interest in EVs as biomarkers. Circulating EVs, comprising a heterogeneous group of membrane-bound vesicles such as exosomes, microvesicles, and apoptotic bodies, are shed by various cell types into bodily fluids (Choi et al., 2019). Their presence in blood, saliva, urine, amniotic fluids, breast milk, seminal fluid and other biofluids provides a treasure trove of biological information that mirrors the physiological or pathological state of their cells of origin (An et al., 2015; Lane et al., 2018). EVs encapsulate an array of biomolecules including nucleic acids, proteins, and lipids, which can influence recipient cells and modulate biological processes (Colombo et al., 2014; Lane et al., 2018; Willms et al., 2018). Their role in intercellular communication has been implicated in numerous physiological processes and pathological conditions, including cancer, where they can contribute to tumour progression, metastasis, and the emergence of drug resistance (König et al., 2017; Vinik et al., 2020).

As a deeper understanding of EVs is developed, their significance in biofluids becomes increasingly apparent. They traverse the circulatory system, acting as vectors of molecular information, potentially revealing the molecular underpinnings of cancer (Stevic et al., 2020). The detection and analysis of EVs in various biofluids have emerged as a promising approach for non- or minimally-invasive cancer monitoring, enabling the detection of tumour-derived signatures and providing a real-

time snapshot of tumour behaviour. This has laid the foundation for exploiting circulating EVs as biomarkers for early detection, prognosis, treatment stratification, and monitoring of therapeutic response, representing a frontier in precision cancer (König et al., 2017). Here are some instances illustrating the function of circulating extracellular vesicles in different cancers:

In breast cancer, the most common cancer among women globally, EVs present in biofluids have been identified as potential harbingers of response to neoadjuvant chemotherapy (NACT) (Gralow et al., 2008). The presence of specific molecular signatures within these vesicles correlates with tumour response and the likelihood of a pathologic complete response (pCR). A lack of certain EV biomarkers has been linked to an incomplete therapeutic response, heralding a higher risk of recurrence and a less favourable prognosis.

HNSCC is the predominant type of epithelial cancer within head and neck malignancies. One of numerous studies has demonstrated that EVs play a crucial role in modulating biological functions, including the modulation of therapeutic responses, positioning them as potential markers for tracking treatment efficacy (Colombo et al., 2014). In the context of HNSCC, there is a significant focus on the analysis of EV-associated proteins. Rodrigues-Junior and colleagues conducted a study analysing the proteomic profiles of plasma EVs from HNSCC patients who either did or did not respond to chemoradiation therapy (CRT), highlighting the differences between these two groups (Rodrigues-Junior et al., 2019).

Glioblastoma (GBM) is the most prevalent central nervous system tumour, and treatment typically involves surgery, chemotherapy, and radiotherapy (D. R. Johnson & O'Neill, 2012; Stupp et al., 2005). EVs are gaining recognition for their potential in GBM research and patient management. Skog et al. identified GBM-specific RNA signatures in serum EVs, suggesting their use in non-invasive diagnostics (Skog, Würdinger, van Rijn, Meijer, Gainche, Curry, et al., 2008). Ricklefs et al. reported higher EV levels in GBM patients, a finding mirrored in mouse models (Ricklefs et al., 2019). Osti et al. noted a decrease in EVs after surgical removal of GBM and an increase at relapse, with a distinctive protein signature in these EVs, underscoring their role in tracking tumour dynamics and aiding in the management of GBM patients (Osti et al., 2019).

In conclusion, EVs in various bodily fluids provide a comprehensive snapshot of a patient's health status and serve as potent instruments for cancer screening, diagnosis, and treatment monitoring. EVs are particularly valuable in liquid biopsy methodologies due to their capacity to encapsulate and preserve cancer-specific molecules from degradation (Stevic et al., 2020). Despite this, the field of EV research faces challenges with the lack of a standardized nomenclature and consistent protocols for EV isolation and analysis, an issue the international society for extracellular vesicles (ISEV) has been addressing. The ISEV has introduced the Minimal Information for Studies of Extracellular Vesicles "MISEV" guidelines to establish a baseline for EV research.

Emerging research corroborates that EVs contain unique cancer-associated alterations in nucleic acids and proteins, and these molecular patterns in EVs mirror the changes in tumour cells during treatment as seen in patient blood samples (Skog, Würdinger, van Rijn, Meijer, Gainche, Curry, et al., 2008). The potential of EVs as a marker for cancer-associated components is undeniable. Consequently, the ongoing discussions around terminology and standardization of isolation practices should not overshadow the promising role of EVs in revolutionizing liquid biopsy techniques, which could significantly transform cancer management and surveillance.

6.4 Limitations and future work

6.4.1 Limitations

The COVID-19 pandemic affected the whole world and altered many plans. Due to the complete lockdown from March 2020 to August 2020 and limited lab access with maximum 10 hours per week from August 2020 to April 2021, some of the planned objectives of this project were not able to be completed.

Additional western blot EP markers would have been desirable to add rigor and to identify subpopulation of particles, especially EVs. MISEV2018 guidelines recommend that for the characterisation of protein content in EVs, it is advisable to utilize at least two proteins, encompassing one of membrane bound and one of cytosolic protein, but EP westerns are not always suitable for stripping and reprobing (due to the small amount of protein transferred to the membrane). Due to time

constraints, it was not possible to conduct additional repeats of experiments for additional protein markers.

An unbiased approach to identify the EPs present may have been preferable to blotting for markers. The pattern in the EP markers chosen was not always consistent with the NTA data suggesting that other types of EPs may be present. Mass spectrometry could have been used to identify proteins present in EP pellets and then validated by western blotting. Given that cisplatin causes apoptosis, an increase in apoptotic EV release might have been expected, suggesting that TSG101/CD63 might not have been the most suitable EV markers to use. MISEV2018 guidelines recommend that single particle characterisation such as transmission electron microscopy should be used to confirm the presence of EVs in preparations. This was attempted in collaboration with TUoS Electron Microscopy Facility, but unfortunately did not yield usable images. Due to time constraints, it was not possible to perform further troubleshooting and optimisation experiments.

Characterisation of the cisplatin-resistant cell line should have also been carried out in the presence of cisplatin, even if a low concentration (such as 0.5x IC₅₀). This may have heightened differences in the cellular machinery involved in cisplatin-resistance, which may have been more evident in western blot analysis.

6.4.2 Future work

Future work should focus on the comprehensive characterisation of the EPs released by H357 in response to cisplatin treatment, either using mass spectrometry or additional western blotting. If the latter, additional markers would be needed such as GM130 to determine if intracellular vesicles are being released, markers of apoptotic EVs, and markers of other cell compartments such as lysosomal markers. There is evidence in the literature that cisplatin is sequestered in lysosomes and then released. Cryoelectron microscopy would be an unbiased way to visualise the EPs being released. Further characterisation of the Δ MVP cell line is required to determine why it is more resistant to cisplatin treatment. Troubleshooting and optimisation of the ASO experiment is required to successfully

silence vtRNA to determine if vtRNA1-1 is part of the mechanism. Western blotting of ATP7B, CTR1, RRBP1 could determine if there is compensation in drug efflux/influx mechanisms in the Δ MVP cell line, which account for increased resistance.

Proteomics (mass spectrometry) characterisation of the cisplatin-resistant H357 cell line would determine proteins up and down regulated that may be involved in the cisplatin-resistant phenotype. This may identify novel regulators rather than just using western blotting of known proteins. Comprehensive characterisation of EPs released by the cisplatin-resistant H357 cell line by proteomics and/or small RNA sequencing to determine protein and RNA cargo, respectively. This would allow determination of likely mechanisms involved in transfer of cisplatin resistance. Creating a FaDu cisplatin resistant cell line would also allow comparison of mechanisms between HNC from different anatomical site.

Chapter 7 References:

- Abbondanza, C., Rossi, V., Roscigno, A., Gallo, L., Belsito, A., Piluso, G., Medici, N., Nigro, V., Molinari, A. M., Moncharmont, B., & Puca, G. A. (1998). Interaction of Vault Particles with Estrogen Receptor in the MCF-7 Breast Cancer Cell. *The Journal of Cell Biology*, *141*(6), 1301–1310.
- Abedini, M. R., Muller, E. J., Bergeron, R., Gray, D. A., & Tsang, B. K. (2010). Akt promotes chemoresistance in human ovarian cancer cells by modulating cisplatin-induced, p53-dependent ubiquitination of FLICE-like inhibitory protein. *Oncogene*, *29*(1), 11–25. <https://doi.org/10.1038/onc.2009.300>
- Admyre, C., Grunewald, J., Thyberg, J., Gripenbäck, S., Tornling, G., Eklund, A., Scheynius, A., & Gabrielsson, S. (2003). Exosomes with major histocompatibility complex class II and co-stimulatory molecules are present in human BAL fluid. *European Respiratory Journal*, *22*(4), 578–583. <https://doi.org/10.1183/09031936.03.00041703>
- Admyre, C., Johansson, S. M., Qazi, K. R., Filén, J.-J., Lahesmaa, R., Norman, M., Neve, E. P. A., Scheynius, A., & Gabrielsson, S. (2007). Exosomes with immune modulatory features are present in human breast milk. *Journal of Immunology (Baltimore, Md.: 1950)*, *179*(3), 1969–1978. <https://doi.org/10.4049/jimmunol.179.3.1969>
- Ahn, J.-H., Lee, H.-S., Lee, J.-S., Lee, Y.-S., Park, J.-L., Kim, S.-Y., Hwang, J.-A., Kunkeaw, N., Jung, S. Y., Kim, T. J., Lee, K.-S., Jeon, S. H., Lee, I., Johnson, B. H., Choi, J.-H., & Lee, Y. S. (2018). Nc886 is induced by TGF- β and suppresses the microRNA pathway in ovarian cancer. *Nature Communications*, *9*(1), 1166. <https://doi.org/10.1038/s41467-018-03556-7>

- Alberro, A., Iparraguirre, L., Fernandes, A., & Otaegui, D. (2021). Extracellular Vesicles in Blood: Sources, Effects, and Applications. *International Journal of Molecular Sciences*, 22(15), 8163. <https://doi.org/10.3390/ijms22158163>
- Aliotta, J. M., Sanchez-Guijo, F. M., Dooner, G. J., Johnson, K. W., Dooner, M. S., Greer, K. A., Greer, D., Pimentel, J., Kolankiewicz, L. M., Puente, N., Faradyan, S., Ferland, P., Bearer, E. L., Passero, M. A., Adedi, M., Colvin, G. A., & Quesenberry, P. J. (2007). Alteration of Marrow Cell Gene Expression, Protein Production, and Engraftment into Lung by Lung-Derived Microvesicles: A Novel Mechanism for Phenotype Modulation. *Stem Cells*, 25(9), 2245–2256. <https://doi.org/10.1634/stemcells.2007-0128>
- Almgren, M., Edwards, K., & Karlsson, G. (2000). Cryo transmission electron microscopy of liposomes and related structures. *Colloids and Surfaces A: Physicochemical and Engineering Aspects*, 174(1), 3–21. [https://doi.org/10.1016/S0927-7757\(00\)00516-1](https://doi.org/10.1016/S0927-7757(00)00516-1)
- Al-Nedawi, K., Meehan, B., Micallef, J., Lhotak, V., May, L., Guha, A., & Rak, J. (2008). Intercellular transfer of the oncogenic receptor EGFRvIII by microvesicles derived from tumour cells. *Nature Cell Biology*, 10(5), 619–624. <https://doi.org/10.1038/ncb1725>
- Amort, M., Nachbauer, B., Tuzlak, S., Kieser, A., Schepers, A., Villunger, A., & Polacek, N. (2015). Expression of the vault RNA protects cells from undergoing apoptosis. *Nature Communications*, 6(1), 7030. <https://doi.org/10.1038/ncomms8030>
- An, T., Qin, S., Xu, Y., Tang, Y., Huang, Y., Situ, B., Inal, J. M., & Zheng, L. (2015). Exosomes serve as tumour markers for personalized diagnostics owing to their important role in cancer metastasis. *Journal of Extracellular Vesicles*, 4, 10.3402/jev.v4.27522. <https://doi.org/10.3402/jev.v4.27522>

- Andreu, Z., & Yáñez-Mó, M. (2014). Tetraspanins in Extracellular Vesicle Formation and Function. *Frontiers in Immunology*, 5, 442.
<https://doi.org/10.3389/fimmu.2014.00442>
- Antonyak, M. A., Li, B., Boroughs, L. K., Johnson, J. L., Druso, J. E., Bryant, K. L., Holowka, D. A., & Cerione, R. A. (2011). Cancer cell-derived microvesicles induce transformation by transferring tissue transglutaminase and fibronectin to recipient cells. *Proceedings of the National Academy of Sciences*, 108(12), 4852–4857.
<https://doi.org/10.1073/pnas.1017667108>
- Arck, P. C., & Hecher, K. (2013). Fetomaternal immune cross-talk and its consequences for maternal and offspring's health. *Nature Medicine*, 19(5), 548–556.
<https://doi.org/10.1038/nm.3160>
- Au Yeung, C. L., Co, N.-N., Tsuruga, T., Yeung, T.-L., Kwan, S.-Y., Leung, C. S., Li, Y., Lu, E. S., Kwan, K., Wong, K.-K., Schmandt, R., Lu, K. H., & Mok, S. C. (2016). Exosomal transfer of stroma-derived miR21 confers paclitaxel resistance in ovarian cancer cells through targeting APAF1. *Nature Communications*, 7(1), 11150.
<https://doi.org/10.1038/ncomms11150>
- Aubrey, B. J., Kelly, G. L., Janic, A., Herold, M. J., & Strasser, A. (2018). How does p53 induce apoptosis and how does this relate to p53-mediated tumour suppression? *Cell Death & Differentiation*, 25(1), Article 1. <https://doi.org/10.1038/cdd.2017.169>
- Babst, M., Katzmann, D. J., Estepa-Sabal, E. J., Meerloo, T., & Emr, S. D. (2002). Escrt-III: An endosome-associated heterooligomeric protein complex required for mvb sorting. *Developmental Cell*, 3(2), 271–282. [https://doi.org/10.1016/S1534-5807\(02\)00220-4](https://doi.org/10.1016/S1534-5807(02)00220-4)
- Bach, D.-H., Hong, J.-Y., Park, H. J., & Lee, S. K. (2017). The role of exosomes and miRNAs in drug-resistance of cancer cells. *International Journal of Cancer*, 141(2), 220–230. <https://doi.org/10.1002/ijc.30669>

- Bache, K. G., Brech, A., Mehlum, A., & Stenmark, H. (2003). Hrs regulates multivesicular body formation via ESCRT recruitment to endosomes. *The Journal of Cell Biology*, *162*(3), 435–442. <https://doi.org/10.1083/jcb.200302131>
- Bai, H., Wang, C., Qi, Y., Xu, J., Li, N., Chen, L., Jiang, B., Zhu, X., Zhang, H., Li, X., Yang, Q., Ma, J., Xu, Y., Ben, J., & Chen, Q. (2019). Major vault protein suppresses lung cancer cell proliferation by inhibiting STAT3 signaling pathway. *BMC Cancer*, *19*, 454. <https://doi.org/10.1186/s12885-019-5665-6>
- Bandari, S. K., Purushothaman, A., Ramani, V. C., Brinkley, G. J., Chandrashekar, D. S., Varambally, S., Mobley, J. A., Zhang, Y., Brown, E. E., Vlodaysky, I., & Sanderson, R. D. (2018). Chemotherapy induces secretion of exosomes loaded with heparanase that degrades extracellular matrix and impacts tumor and host cell behavior. *Matrix Biology: Journal of the International Society for Matrix Biology*, *65*, 104–118. <https://doi.org/10.1016/j.matbio.2017.09.001>
- Barilà, D., Rufini, A., Condò, I., Ventura, N., Dorey, K., Superti-Furga, G., & Testi, R. (2003). Caspase-Dependent Cleavage of c-Abl Contributes to Apoptosis. *Molecular and Cellular Biology*, *23*(8), 2790–2799. <https://doi.org/10.1128/MCB.23.8.2790-2799.2003>
- Barr, M. P., Gray, S. G., Hoffmann, A. C., Hilger, R. A., Thomale, J., O’Flaherty, J. D., Fennell, D. A., Richard, D., O’Leary, J. J., & O’Byrne, K. J. (2013). Generation and Characterisation of Cisplatin-Resistant Non-Small Cell Lung Cancer Cell Lines Displaying a Stem-Like Signature. *PLOS ONE*, *8*(1), e54193. <https://doi.org/10.1371/journal.pone.0054193>
- Basu, A., & Krishnamurthy, S. (2010). Cellular responses to Cisplatin-induced DNA damage. *Journal of Nucleic Acids*, *2010*, 201367. <https://doi.org/10.4061/2010/201367>

- Batey, R. T., Rambo, R. P., Lucast, L., Rha, B., & Doudna, J. A. (2000). Crystal Structure of the Ribonucleoprotein Core of the Signal Recognition Particle. *Science*.
<https://doi.org/10.1126/science.287.5456.1232>
- Batista, B. S., Eng, W. S., Pilobello, K. T., Hendricks-Muñoz, K. D., & Mahal, L. K. (2011). Identification of a Conserved Glycan Signature for Microvesicles. *Journal of Proteome Research*, *10*(10), 4624–4633. <https://doi.org/10.1021/pr200434y>
- Bauer, J. A., Kumar, B., Cordell, K. G., Prince, M. E., Tran, H. H., Wolf, G. T., Chepeha, D. B., Teknos, T. N., Wang, S., Eisbruch, A., Tsien, C. I., Urban, S. G., Worden, F. P., Lee, J., Griffith, K. A., Taylor, J. M. G., D'Silva, N., Wang, S. J., Wolter, K. G., ... Bradford, C. R. (2007). Targeting Apoptosis to Overcome Cisplatin Resistance: A Translational Study in Head and Neck Cancer. *International Journal of Radiation Oncology, Biology, Physics*, *69*(2 Suppl), S106–S108.
<https://doi.org/10.1016/j.ijrobp.2007.05.080>
- Becker, A., Thakur, B. K., Weiss, J. M., Kim, H. S., Peinado, H., & Lyden, D. (2016). Extracellular vesicles in cancer: Cell-to-cell mediators of metastasis. *Cancer Cell*, *30*(6), 836–848. <https://doi.org/10.1016/j.ccell.2016.10.009>
- Bellingham, S. A., Coleman, B. M., & Hill, A. F. (2012). Small RNA deep sequencing reveals a distinct miRNA signature released in exosomes from prion-infected neuronal cells. *Nucleic Acids Research*, *40*(21), 10937–10949.
<https://doi.org/10.1093/nar/gks832>
- Ben, J., Zhang, Y., Zhou, R., Zhang, H., Zhu, X., Li, X., Zhang, H., Li, N., Zhou, X., Bai, H., Yang, Q., Li, D., Xu, Y., & Chen, Q. (2013). Major vault protein regulates class A scavenger receptor-mediated tumor necrosis factor- α synthesis and apoptosis in macrophages. *The Journal of Biological Chemistry*, *288*(27), 20076–20084.
<https://doi.org/10.1074/jbc.M112.449538>

- Berckmans, R. J., Sturk, A., van Tienen, L. M., Schaap, M. C. L., & Nieuwland, R. (2011). Cell-derived vesicles exposing coagulant tissue factor in saliva. *Blood*, *117*(11), 3172–3180. <https://doi.org/10.1182/blood-2010-06-290460>
- Berger, W., Elbling, L., & Micksche, M. (2000). Expression of the major vault protein LRP in human non-small-cell lung cancer cells: Activation by short-term exposure to antineoplastic drugs. *International Journal of Cancer*, *88*(2), 293–300.
- Berger, W., Steiner, E., Grusch, M., Elbling, L., & Micksche, M. (2009). Vaults and the major vault protein: Novel roles in signal pathway regulation and immunity. *Cellular and Molecular Life Sciences: CMLS*, *66*(1), 43–61. <https://doi.org/10.1007/s00018-008-8364-z>
- Bhome, R., Del Vecchio, F., Lee, G.-H., Bullock, M. D., Primrose, J. N., Sayan, A. E., & Mirnezami, A. H. (2018). Exosomal microRNAs (exomiRs): Small molecules with a big role in cancer. *Cancer Letters*, *420*, 228–235. <https://doi.org/10.1016/j.canlet.2018.02.002>
- Blatt, S., Krüger, M., Ziebart, T., Sagheb, K., Schiegnitz, E., Goetze, E., Al-Nawas, B., & Pabst, A. M. (2017). Biomarkers in diagnosis and therapy of oral squamous cell carcinoma: A review of the literature. *Journal of Cranio-Maxillofacial Surgery*, *45*(5), 722–730. <https://doi.org/10.1016/j.jcms.2017.01.033>
- Blot, W. J., McLaughlin, J. K., Winn, D. M., Austin, D. F., Greenberg, R. S., Preston-Martin, S., Bernstein, L., Schoenberg, J. B., Stemhagen, A., & Fraumeni, J. F. (1988). Smoking and drinking in relation to oral and pharyngeal cancer. *Cancer Research*, *48*(11), 3282–3287.
- Boussadia, Z., Lamberti, J., Mattei, F., Pizzi, E., Puglisi, R., Zanetti, C., Pasquini, L., Fratini, F., Fantozzi, L., Felicetti, F., Fecchi, K., Raggi, C., Sanchez, M., D'Atri, S., Carè, A., Sargiacomo, M., & Parolini, I. (2018). Acidic microenvironment plays a key role in

- human melanoma progression through a sustained exosome mediated transfer of clinically relevant metastatic molecules. *Journal of Experimental & Clinical Cancer Research: CR*, 37(1), 245. <https://doi.org/10.1186/s13046-018-0915-z>
- Bracher, L., Ferro, I., Pulido-Quetglas, C., Ruepp, M.-D., Johnson, R., & Polacek, N. (2020). Human vtRNA1-1 Levels Modulate Signaling Pathways and Regulate Apoptosis in Human Cancer Cells. *Biomolecules*, 10(4), 614. <https://doi.org/10.3390/biom10040614>
- Bray, F., Ferlay, J., Soerjomataram, I., Siegel, R. L., Torre, L. A., & Jemal, A. (2018). Global cancer statistics 2018: GLOBOCAN estimates of incidence and mortality worldwide for 36 cancers in 185 countries. *CA: A Cancer Journal for Clinicians*, 68(6), 394–424. <https://doi.org/10.3322/caac.21492>
- Brouwers, J. F., Aalberts, M., Jansen, J. W. A., van Niel, G., Wauben, M. H., Stout, T. A. E., Helms, J. B., & Stoorvogel, W. (2013). Distinct lipid compositions of two types of human prostasomes. *Proteomics*, 13(10–11), 1660–1666. <https://doi.org/10.1002/pmic.201200348>
- Buschow, S. I., Nolte-'t Hoen, E. N. M., van Niel, G., Pols, M. S., ten Broeke, T., Lauwen, M., Ossendorp, F., Melief, C. J. M., Raposo, G., Wubbolts, R., Wauben, M. H. M., & Stoorvogel, W. (2009). MHC II in dendritic cells is targeted to lysosomes or T cell-induced exosomes via distinct multivesicular body pathways. *Traffic (Copenhagen, Denmark)*, 10(10), 1528–1542. <https://doi.org/10.1111/j.1600-0854.2009.00963.x>
- Canal, F., Anthony, E., Lescure, A., Del Nery, E., Camonis, J., Perez, F., Ragazzon, B., & Perret, C. (2015). A kinome siRNA screen identifies HGS as a potential target for liver cancers with oncogenic mutations in CTNNB1. *BMC Cancer*, 15, 1020. <https://doi.org/10.1186/s12885-015-2037-8>

- Castellana, D., Zobairi, F., Martinez, M. C., Panaro, M. A., Mitolo, V., Freyssinet, J.-M., & Kunzelmann, C. (2009). Membrane Microvesicles as Actors in the Establishment of a Favorable Prostatic Tumoral Niche: A Role for Activated Fibroblasts and CX3CL1-CX3CR1 Axis. *Cancer Research*, 69(3), 785–793. <https://doi.org/10.1158/0008-5472.CAN-08-1946>
- Catalano, M., & O’Driscoll, L. (n.d.). Inhibiting extracellular vesicles formation and release: A review of EV inhibitors. *Journal of Extracellular Vesicles*, 9(1), 1703244. <https://doi.org/10.1080/20013078.2019.1703244>
- Chaturvedi, P., Kalani, A., Medina, I., Familtseva, A., & Tyagi, S. C. (2015). Cardiosome mediated regulation of MMP9 in diabetic heart: Role of mir29b and mir455 in exercise. *Journal of Cellular and Molecular Medicine*, 19(9), 2153–2161. <https://doi.org/10.1111/jcmm.12589>
- Chen, B.-Y., Sung, C. W.-H., Chen, C., Cheng, C.-M., Lin, D. P.-C., Huang, C.-T., & Hsu, M.-Y. (2019). Advances in exosomes technology. *Clinica Chimica Acta; International Journal of Clinical Chemistry*, 493, 14–19. <https://doi.org/10.1016/j.cca.2019.02.021>
- Chen, J., OuYang, H., An, X., & Liu, S. (2018). Vault RNAs partially induces drug resistance of human tumor cells MCF-7 by binding to the RNA/DNA-binding protein PSF and inducing oncogene GAGE6. *PloS One*, 13(1), e0191325. <https://doi.org/10.1371/journal.pone.0191325>
- Chen, W., Cai, Y., Lv, M., Chen, L., Zhong, S., Ma, T., Zhao, J., & Tang, J. (2014). Exosomes from docetaxel-resistant breast cancer cells alter chemosensitivity by delivering microRNAs. *Tumor Biology*, 35(10), 9649–9659. <https://doi.org/10.1007/s13277-014-2242-0>

- Chen, Y.-W., Chen, Y.-C., & Wang, J.-S. (2013). Absolute hypoxic exercise training enhances in vitro thrombin generation by increasing procoagulant platelet-derived microparticles under high shear stress in sedentary men. *Clinical Science (London, England: 1979)*, *124*(10), 639–649. <https://doi.org/10.1042/CS20120540>
- Cheng, S. H., Lam, W., Lee, A. S., Fung, K. P., Wu, R. S., & Fong, W. F. (2000). Low-level doxorubicin resistance in benzo[a]pyrene-treated KB-3-1 cells is associated with increased LRP expression and altered subcellular drug distribution. *Toxicology and Applied Pharmacology*, *164*(2), 134–142. <https://doi.org/10.1006/taap.2000.8903>
- Chiaradia, E., Tancini, B., Emiliani, C., Delo, F., Pellegrino, R. M., Tognoloni, A., Urbanelli, L., & Buratta, S. (2021). Extracellular Vesicles under Oxidative Stress Conditions: Biological Properties and Physiological Roles. *Cells*, *10*(7), 1763. <https://doi.org/10.3390/cells10071763>
- Choi, D., Montermini, L., Jeong, H., Sharma, S., Meehan, B., & Rak, J. (2019). Mapping Subpopulations of Cancer Cell-Derived Extracellular Vesicles and Particles by Nano-Flow Cytometry. *ACS Nano*, *13*(9), 10499–10511. <https://doi.org/10.1021/acsnano.9b04480>
- Chow, L. Q. M. (2020). Head and Neck Cancer. *The New England Journal of Medicine*, *382*(1), 60–72. <https://doi.org/10.1056/NEJMra1715715>
- Chowdhury, R., Webber, J. P., Gurney, M., Mason, M. D., Tabi, Z., & Clayton, A. (2014). Cancer exosomes trigger mesenchymal stem cell differentiation into pro-angiogenic and pro-invasive myofibroblasts. *Oncotarget*, *6*(2), 715–731.
- Chua, S., Wilkins, T., Sargent, I., & Redman, C. (1991). Trophoblast deportation in pre-eclamptic pregnancy. *British Journal of Obstetrics and Gynaecology*, *98*(10), 973–979. <https://doi.org/10.1111/j.1471-0528.1991.tb15334.x>

- Chugani, D. C., Rome, L. H., & Kedersha, N. L. (1993). Evidence that vault ribonucleoprotein particles localize to the nuclear pore complex. *Journal of Cell Science*, *106 (Pt 1)*, 23–29. <https://doi.org/10.1242/jcs.106.1.23>
- Ciravolo, V., Huber, V., Ghedini, G. C., Venturelli, E., Bianchi, F., Campiglio, M., Morelli, D., Villa, A., Mina, P. D., Menard, S., Filipazzi, P., Rivoltini, L., Tagliabue, E., & Pupa, S. M. (2012). Potential role of HER2-overexpressing exosomes in countering trastuzumab-based therapy. *Journal of Cellular Physiology*, *227(2)*, 658–667. <https://doi.org/10.1002/jcp.22773>
- Cocucci, E., Racchetti, G., & Meldolesi, J. (2009). Shedding microvesicles: Artefacts no more. *Trends in Cell Biology*, *19(2)*, 43–51. <https://doi.org/10.1016/j.tcb.2008.11.003>
- Colombo, M., Moita, C., van Niel, G., Kowal, J., Vigneron, J., Benaroch, P., Manel, N., Moita, L. F., Théry, C., & Raposo, G. (2013). Analysis of ESCRT functions in exosome biogenesis, composition and secretion highlights the heterogeneity of extracellular vesicles. *Journal of Cell Science*, *126(Pt 24)*, 5553–5565. <https://doi.org/10.1242/jcs.128868>
- Colombo, M., Raposo, G., & Théry, C. (2014). Biogenesis, secretion, and intercellular interactions of exosomes and other extracellular vesicles. *Annual Review of Cell and Developmental Biology*, *30*, 255–289. <https://doi.org/10.1146/annurev-cellbio-101512-122326>
- Conde-Vancells, J., Gonzalez, E., Lu, S. C., Mato, J. M., & Falcon-Perez, J. M. (2010). Overview of Extracellular Microvesicles in Drug Metabolism. *Expert Opinion on Drug Metabolism & Toxicology*, *6(5)*, 543–554. <https://doi.org/10.1517/17425251003614766>
- Conde-Vancells, J., Rodriguez-Suarez, E., Embade, N., Gil, D., Matthiesen, R., Valle, M., Elortza, F., Lu, S. C., Mato, J. M., & Falcon-Perez, J. M. (2008). Characterization and

- comprehensive proteome profiling of exosomes secreted by hepatocytes. *Journal of Proteome Research*, 7(12), 5157–5166. <https://doi.org/10.1021/pr8004887>
- Corcoran, C., Rani, S., O'Brien, K., O'Neill, A., Prencipe, M., Sheikh, R., Webb, G., McDermott, R., Watson, W., Crown, J., & O'Driscoll, L. (2012). Docetaxel-resistance in prostate cancer: Evaluating associated phenotypic changes and potential for resistance transfer via exosomes. *PloS One*, 7(12), e50999. <https://doi.org/10.1371/journal.pone.0050999>
- Costa-Silva, B., Aiello, N. M., Ocean, A. J., Singh, S., Zhang, H., Thakur, B. K., Becker, A., Hoshino, A., Mark, M. T., Molina, H., Xiang, J., Zhang, T., Theilen, T.-M., García-Santos, G., Williams, C., Ararso, Y., Huang, Y., Rodrigues, G., Shen, T.-L., ... Lyden, D. (2015). Pancreatic cancer exosomes initiate pre-metastatic niche formation in the liver. *Nature Cell Biology*, 17(6), 816–826. <https://doi.org/10.1038/ncb3169>
- Crescitelli, R., Lässer, C., Szabó, T. G., Kittel, A., Eldh, M., Dianzani, I., Buzás, E. I., & Lötval, J. (2013). Distinct RNA profiles in subpopulations of extracellular vesicles: Apoptotic bodies, microvesicles and exosomes. *Journal of Extracellular Vesicles*, 2(1), 20677. <https://doi.org/10.3402/jev.v2i0.20677>
- Cvjetkovic, A., Jang, S. C., Konečná, B., Höög, J. L., Sihlbom, C., Lässer, C., & Lötval, J. (2016). Detailed Analysis of Protein Topology of Extracellular Vesicles-Evidence of Unconventional Membrane Protein Orientation. *Scientific Reports*, 6, 36338. <https://doi.org/10.1038/srep36338>
- Davies, M. S., Berners-Price, S. J., & Hambley, T. W. (2000). Slowing of cisplatin aquation in the presence of DNA but not in the presence of phosphate: Improved understanding of sequence selectivity and the roles of mono-aquated and diaquated species in the binding of cisplatin to DNA. *Inorganic Chemistry*, 39(25), 5603–5613. <https://doi.org/10.1021/ic000847w>

- de Gassart, A., Géminard, C., Février, B., Raposo, G., & Vidal, M. (2003). Lipid raft-associated protein sorting in exosomes. *Blood*, *102*(13), 4336–4344.
<https://doi.org/10.1182/blood-2003-03-0871>
- Depraetere, V. (2000). “Eat me” signals of apoptotic bodies. *Nature Cell Biology*, *2*(6), E104–E104. <https://doi.org/10.1038/35014098>
- Dong, C., Liu, X., Wang, H., Li, J., Dai, L., Li, J., & Xu, Z. (2019). Hypoxic non-small-cell lung cancer cell-derived exosomal miR-21 promotes resistance of normoxic cell to cisplatin. *Oncotargets and Therapy*, *12*, 1947–1956.
<https://doi.org/10.2147/OTT.S186922>
- Dong, X., Liu, A., Zer, C., Feng, J., Zhen, Z., Yang, M., & Zhong, L. (2009). siRNA inhibition of telomerase enhances the anti-cancer effect of doxorubicin in breast cancer cells. *BMC Cancer*, *9*, 133. <https://doi.org/10.1186/1471-2407-9-133>
- Dorayappan, K. D. P., Wanner, R., Wallbillich, J. J., Saini, U., Zingarelli, R., Suarez, A. A., Cohn, D. E., & Selvendiran, K. (2018). Hypoxia-induced exosomes contribute to a more aggressive and chemoresistant ovarian cancer phenotype: A novel mechanism linking STAT3/Rab proteins. *Oncogene*, *37*(28), Article 28.
<https://doi.org/10.1038/s41388-018-0189-0>
- D’Souza-Schorey, C., & Clancy, J. W. (2012). Tumor-derived microvesicles: Shedding light on novel microenvironment modulators and prospective cancer biomarkers. *Genes & Development*, *26*(12), 1287–1299. <https://doi.org/10.1101/gad.192351.112>
- Duan, G., Tang, Q., Yan, H., Xie, L., Wang, Y., Zheng, X. E., Zhuge, Y., Shen, S., Zhang, B., Zhang, X., Wang, J., Wang, W., & Zou, X. (2017). A Strategy to Delay the Development of Cisplatin Resistance by Maintaining a Certain Amount of Cisplatin-Sensitive Cells. *Scientific Reports*, *7*(1), Article 1. <https://doi.org/10.1038/s41598-017-00422-2>

- Duan, M., Ulibarri, J., Liu, K. J., & Mao, P. (2020). Role of Nucleotide Excision Repair in Cisplatin Resistance. *International Journal of Molecular Sciences*, *21*(23), 9248. <https://doi.org/10.3390/ijms21239248>
- Duray, A., Descamps, G., Decaestecker, C., Rimmelink, M., Sirtaine, N., Lechien, J., Ernoux-Neufcoeur, P., Bletard, N., Somja, J., Depuydt, C. E., Delvenne, P., & Saussez, S. (2012). Human papillomavirus DNA strongly correlates with a poorer prognosis in oral cavity carcinoma. *The Laryngoscope*, *122*(7), 1558–1565. <https://doi.org/10.1002/lary.23298>
- Eastman, A. (1991). Mechanisms of resistance to cisplatin. In R. F. Ozols (Ed.), *Molecular and Clinical Advances in Anticancer Drug Resistance* (pp. 233–249). Springer US. https://doi.org/10.1007/978-1-4615-3872-1_11
- Eichholtz-Wirth, H., & Hietel, B. (1986). The relationship between cisplatin sensitivity and drug uptake into mammalian cells in vitro. *British Journal of Cancer*, *54*(2), 239–243.
- EL Andaloussi, S., Mäger, I., Breakefield, X. O., & Wood, M. J. A. (2013). Extracellular vesicles: Biology and emerging therapeutic opportunities. *Nature Reviews Drug Discovery*, *12*(5), 347–357. <https://doi.org/10.1038/nrd3978>
- Elliott, M. R., Chekeni, F. B., Tramont, P. C., Lazarowski, E. R., Kadl, A., Walk, S. F., Park, D., Woodson, R. I., Ostankovich, M., Sharma, P., Lysiak, J. J., Harden, T. K., Leitinger, N., & Ravichandran, K. S. (2009). Nucleotides released by apoptotic cells act as a find-me signal to promote phagocytic clearance. *Nature*, *461*(7261), 282–286. <https://doi.org/10.1038/nature08296>
- Escola, J. M., Kleijmeer, M. J., Stoorvogel, W., Griffith, J. M., Yoshie, O., & Geuze, H. J. (1998). Selective enrichment of tetraspan proteins on the internal vesicles of multivesicular endosomes and on exosomes secreted by human B-lymphocytes. *The*

Journal of Biological Chemistry, 273(32), 20121–20127.

<https://doi.org/10.1074/jbc.273.32.20121>

Esfandiary, R., Kickhoefer, V. A., Rome, L. H., Joshi, S. B., & Middaugh, C. R. (2009).

Structural stability of vault particles. *Journal of Pharmaceutical Sciences*, 98(4), 1376–1386. <https://doi.org/10.1002/jps.21508>

Faict, S., Oudaert, I., D’Auria, L., Dehairs, J., Maes, K., Vlummens, P., De Veirman, K., De

Bruyne, E., Fostier, K., Vande Broek, I., Schots, R., Vanderkerken, K., Swinnen, J. V., & Menu, E. (2019). The Transfer of Sphingomyelinase Contributes to Drug Resistance in Multiple Myeloma. *Cancers*, 11(12), Article 12.

<https://doi.org/10.3390/cancers11121823>

Feser, C. J., Williams, J. M., Lammers, D. T., Bingham, J. R., Eckert, M. J., Tolar, J., &

Osborn, M. J. (2023). Engineering Human Cells Expressing CRISPR/Cas9-Synergistic Activation Mediators for Recombinant Protein Production. *International Journal of Molecular Sciences*, 24(10), Article 10.

<https://doi.org/10.3390/ijms24108468>

Floros, K. V., Thomadaki, H., Lallas, G., Katsaros, N., Talieri, M., & Scorilas, A. (2003).

Cisplatin-induced apoptosis in HL-60 human promyelocytic leukemia cells: Differential expression of BCL2 and novel apoptosis-related gene BCL2L12. *Annals of the New York Academy of Sciences*, 1010, 153–158.

<https://doi.org/10.1196/annals.1299.025>

Fontana, F., Carollo, E., Melling, G. E., & Carter, D. R. F. (2021). Extracellular Vesicles:

Emerging Modulators of Cancer Drug Resistance. *Cancers*, 13(4), 749.

<https://doi.org/10.3390/cancers13040749>

- Fraval, H. N. A., & Roberts, J. J. (1979). Excision Repair of cis-Diamminedichloroplatinum(II)-induced Damage to DNA of Chinese Hamster Cells. *Cancer Research*, *39*(5), 1793–1797.
- Friedl, P., Vischer, P., & Freyberg, M. A. (2002). The role of thrombospondin-1 in apoptosis. *Cellular and Molecular Life Sciences: CMLS*, *59*(8), 1347–1357.
<https://doi.org/10.1007/s00018-002-8512-9>
- Galluzzi, L., Vitale, I., Aaronson, S. A., Abrams, J. M., Adam, D., Agostinis, P., Alnemri, E. S., Altucci, L., Amelio, I., Andrews, D. W., Annicchiarico-Petruzzelli, M., Antonov, A. V., Arama, E., Baehrecke, E. H., Barlev, N. A., Bazan, N. G., Bernassola, F., Bertrand, M. J. M., Bianchi, K., ... Kroemer, G. (2018). Molecular mechanisms of cell death: Recommendations of the Nomenclature Committee on Cell Death 2018. *Cell Death and Differentiation*, *25*(3), 486–541. <https://doi.org/10.1038/s41418-017-0012-4>
- Gauvreau, M.-É., Côté, M.-H., Bourgeois-Daigneault, M.-C., Rivard, L.-D., Xiu, F., Brunet, A., Shaw, A., Steimle, V., & Thibodeau, J. (2009). Sorting of MHC Class II Molecules into Exosomes through a Ubiquitin-Independent Pathway. *Traffic*, *10*(10), 1518–1527. <https://doi.org/10.1111/j.1600-0854.2009.00948.x>
- Gillison, M. L., D'Souza, G., Westra, W., Sugar, E., Xiao, W., Begum, S., & Viscidi, R. (2008). Distinct risk factor profiles for human papillomavirus type 16-positive and human papillomavirus type 16-negative head and neck cancers. *Journal of the National Cancer Institute*, *100*(6), 407–420. <https://doi.org/10.1093/jnci/djn025>
- Goldenberg, D., Lee, J., Koch, W. M., Kim, M. M., Trink, B., Sidransky, D., & Moon, C.-S. (2004). Habitual risk factors for head and neck cancer. *Otolaryngology--Head and Neck Surgery: Official Journal of American Academy of Otolaryngology-Head and Neck Surgery*, *131*(6), 986–993. <https://doi.org/10.1016/j.otohns.2004.02.035>

- Golec, E., Lind, L., Qayyum, M., Blom, A. M., & King, B. C. (2019). The Noncoding RNA nc886 Regulates PKR Signaling and Cytokine Production in Human Cells. *Journal of Immunology (Baltimore, Md.: 1950)*, 202(1), 131–141.
<https://doi.org/10.4049/jimmunol.1701234>
- Golub, E. E. (2009). Role of matrix vesicles in biomineralization. *Biochimica Et Biophysica Acta*, 1790(12), 1592–1598. <https://doi.org/10.1016/j.bbagen.2009.09.006>
- Gopinath, S. C. B., Matsugami, A., Katahira, M., & Kumar, P. K. R. (2005). Human vault-associated non-coding RNAs bind to mitoxantrone, a chemotherapeutic compound. *Nucleic Acids Research*, 33(15), 4874–4881. <https://doi.org/10.1093/nar/gki809>
- Gopinath, S. C. B., Wadhwa, R., & Kumar, P. K. R. (2010). Expression of noncoding vault RNA in human malignant cells and its importance in mitoxantrone resistance. *Molecular Cancer Research: MCR*, 8(11), 1536–1546. <https://doi.org/10.1158/1541-7786.MCR-10-0242>
- Gralow, J. R., Burstein, H. J., Wood, W., Hortobagyi, G. N., Gianni, L., von Minckwitz, G., Buzdar, A. U., Smith, I. E., Symmans, W. F., Singh, B., & Winer, E. P. (2008). Preoperative therapy in invasive breast cancer: Pathologic assessment and systemic therapy issues in operable disease. *Journal of Clinical Oncology: Official Journal of the American Society of Clinical Oncology*, 26(5), 814–819.
<https://doi.org/10.1200/JCO.2007.15.3510>
- Gupta, P., Miller, A., Olayanju, A., Madhuri, T. K., & Velliou, E. (2022). A Systematic Comparative Assessment of the Response of Ovarian Cancer Cells to the Chemotherapeutic Cisplatin in 3D Models of Various Structural and Biochemical Configurations—Does One Model Type Fit All? *Cancers*, 14(5), 1274.
<https://doi.org/10.3390/cancers14051274>

- György, B., Szabó, T. G., Turiák, L., Wright, M., Herczeg, P., Lédeczi, Z., Kittel, Á., Polgár, A., Tóth, K., Dérfalvi, B., Zelenák, G., Böröcz, I., Carr, B., Nagy, G., Vékey, K., Gay, S., Falus, A., & Buzás, E. I. (2012). Improved Flow Cytometric Assessment Reveals Distinct Microvesicle (Cell-Derived Microparticle) Signatures in Joint Diseases. *PLoS ONE*, 7(11), e49726. <https://doi.org/10.1371/journal.pone.0049726>
- Han, J. Y., Chung, Y. J., Park, S. W., Kim, J. S., Rhyu, M. G., Kim, H. K., & Lee, K. S. (1999). The relationship between cisplatin-induced apoptosis and p53, bcl-2 and bax expression in human lung cancer cells. *The Korean Journal of Internal Medicine*, 14(1), 42–52. <https://doi.org/10.3904/kjim.1999.14.1.42>
- Harding, C. V., Heuser, J. E., & Stahl, P. D. (2013). Exosomes: Looking back three decades and into the future. *The Journal of Cell Biology*, 200(4), 367–371. <https://doi.org/10.1083/jcb.201212113>
- Hauser, P., Wang, S., & Didenko, V. V. (2017). Apoptotic Bodies: Selective Detection in Extracellular Vesicles. *Methods in Molecular Biology (Clifton, N.J.)*, 1554, 193–200. https://doi.org/10.1007/978-1-4939-6759-9_12
- Hazlehurst, L. A., & Dalton, W. S. (2001). Mechanisms Associated with cell Adhesion Mediated Drug Resistance (CAM-DR) in Hematopoietic Malignancies. *Cancer and Metastasis Reviews*, 20(1), 43–50. <https://doi.org/10.1023/A:1013156407224>
- He, Y., Zhu, Q., Chen, M., Huang, Q., Wang, W., Li, Q., Huang, Y., & Di, W. (2016). The changing 50% inhibitory concentration (IC50) of cisplatin: A pilot study on the artifacts of the MTT assay and the precise measurement of density-dependent chemoresistance in ovarian cancer. *Oncotarget*, 7(43), 70803–70821. <https://doi.org/10.18632/oncotarget.12223>

Head and neck cancers statistics. (2017, February 8). Cancer Research UK.

<https://www.cancerresearchuk.org/health-professional/cancer-statistics/statistics-by-cancer-type/head-and-neck-cancers>

Heijnen, H. F. G., Schiel, A. E., Fijnheer, R., Geuze, H. J., & Sixma, J. J. (1999). Activated Platelets Release Two Types of Membrane Vesicles: Microvesicles by Surface Shedding and Exosomes Derived From Exocytosis of Multivesicular Bodies and α -Granules. *Blood*, *94*(11), 3791–3799. <https://doi.org/10.1182/blood.V94.11.3791>

Henke, E., Nandigama, R., & Ergün, S. (2020). Extracellular Matrix in the Tumor Microenvironment and Its Impact on Cancer Therapy. *Frontiers in Molecular Biosciences*, *6*. <https://doi.org/10.3389/fmolb.2019.00160>

Herlevsen, M., Oxford, G., Owens, C. R., Conaway, M., & Theodorescu, D. (2007). Depletion of major vault protein increases doxorubicin sensitivity and nuclear accumulation and disrupts its sequestration in lysosomes. *Molecular Cancer Therapeutics*, *6*(6), 1804–1813. <https://doi.org/10.1158/1535-7163.MCT-06-0372>

Herrmann, C., Kellner, R., & Volkandt, W. (1998). Major vault protein of electric ray is a phosphoprotein. *Neurochemical Research*, *23*(1), 39–46. <https://doi.org/10.1023/a:1022445302710>

Herrmann, C., Volkandt, W., Wittich, B., Kellner, R., & Zimmermann, H. (1996). The major vault protein (MVP100) is contained in cholinergic nerve terminals of electric ray electric organ. *The Journal of Biological Chemistry*, *271*(23), 13908–13915. <https://doi.org/10.1074/jbc.271.23.13908>

Herz, H.-M., Chen, Z., Scherr, H., Lackey, M., Bolduc, C., & Bergmann, A. (2006). Vps25 mosaics display non-autonomous cell survival and overgrowth, and autonomous apoptosis. *Development (Cambridge, England)*, *133*(10), 1871–1880. <https://doi.org/10.1242/dev.02356>

- Hinshaw, D. C., & Shevde, L. A. (2019). The Tumor Microenvironment Innately Modulates Cancer Progression. *Cancer Research*, 79(18), 4557–4566.
<https://doi.org/10.1158/0008-5472.CAN-18-3962>
- Hong, J.-Y., Kim, G.-H., Kim, J.-W., Kwon, S.-S., Sato, E. F., Cho, K.-H., & Shim, E. B. (2012). Computational modeling of apoptotic signaling pathways induced by cisplatin. *BMC Systems Biology*, 6, 122. <https://doi.org/10.1186/1752-0509-6-122>
- Horos, R., Büscher, M., Kleinendorst, R., Alleaume, A.-M., Tarafder, A. K., Schwarzl, T., Dziuba, D., Tischer, C., Zielonka, E. M., Adak, A., Castello, A., Huber, W., Sachse, C., & Hentze, M. W. (2019). The Small Non-coding Vault RNA1-1 Acts as a Riboregulator of Autophagy. *Cell*, 176(5), 1054-1067.e12.
<https://doi.org/10.1016/j.cell.2019.01.030>
- Horos, R., Büscher, M., Sachse, C., & Hentze, M. W. (2019). Vault RNA emerges as a regulator of selective autophagy. *Autophagy*, 15(8), 1463–1464.
<https://doi.org/10.1080/15548627.2019.1609861>
- Hu, H., Li, B., Wang, J., Tan, Y., Xu, M., Xu, W., & Lu, H. (2023). New advances into cisplatin resistance in head and neck squamous carcinoma: Mechanisms and therapeutic aspects. *Biomedicine & Pharmacotherapy*, 163, 114778.
<https://doi.org/10.1016/j.biopha.2023.114778>
- Huo, Y., Zheng, Z., Chen, Y., Wang, Q., Zhang, Z., & Deng, H. (2016). Downregulation of vimentin expression increased drug resistance in ovarian cancer cells. *Oncotarget*, 7(29), 45876–45888. <https://doi.org/10.18632/oncotarget.9970>
- Hussain, S., Sajini, A. A., Blanco, S., Dietmann, S., Lombard, P., Sugimoto, Y., Paramor, M., Gleeson, J. G., Odom, D. T., Ule, J., & Frye, M. (2013). NSun2-mediated cytosine-5 methylation of vault noncoding RNA determines its processing into regulatory small RNAs. *Cell Reports*, 4(2), 255–261. <https://doi.org/10.1016/j.celrep.2013.06.029>

- Ikeda, R., Iwashita, K. ichi, Sumizawa, T., Beppu, S. ichi, Tabata, S., Tajitsu, Y., Shimamoto, Y., Yoshida, K., Furukawa, T., Che, X. F., Yamaguchi, T., Ushiyama, M., Miyawaki, A., Takeda, Y., Yamamoto, M., Zhao, H. Y., Shibayama, Y., Yamada, K., & Akiyama, S. ichi. (2008). Hyperosmotic stress up-regulates the expression of major vault protein in SW620 human colon cancer cells. *Experimental Cell Research*, 314(16), 3017–3026. <https://doi.org/10.1016/j.yexcr.2008.07.001>
- Ishikawa, T. (1992). The ATP-dependent glutathione S-conjugate export pump. *Trends in Biochemical Sciences*, 17(11), 463–468. [https://doi.org/10.1016/0968-0004\(92\)90489-v](https://doi.org/10.1016/0968-0004(92)90489-v)
- Ita, M., & Murakami, T. (1998). [Study of cell death in squamous cell carcinoma cell line KM-1 treated by cisplatin]. *Human Cell*, 11(1), 13–20.
- Jaiswal, R., Gong, J., Sambasivam, S., Combes, V., Mathys, J.-M., Davey, R., Grau, G. E. R., & Bebawy, M. (2012). Microparticle-associated nucleic acids mediate trait dominance in cancer. *The FASEB Journal*, 26(1), 420–429. <https://doi.org/10.1096/fj.11-186817>
- Jella, K. K., Nasti, T. H., Li, Z., Malla, S. R., Buchwald, Z. S., & Khan, M. K. (2018). Exosomes, Their Biogenesis and Role in Inter-Cellular Communication, Tumor Microenvironment and Cancer Immunotherapy. *Vaccines*, 6(4), 69. <https://doi.org/10.3390/vaccines6040069>
- Jeppesen, D. K., Fenix, A. M., Franklin, J. L., Higginbotham, J. N., Zhang, Q., Zimmerman, L. J., Liebler, D. C., Ping, J., Liu, Q., Evans, R., Fissell, W. H., Patton, J. G., Rome, L. H., Burnette, D. T., & Coffey, R. J. (2019). Reassessment of Exosome Composition. *Cell*, 177(2), 428-445.e18. <https://doi.org/10.1016/j.cell.2019.02.029>
- Jiang, S., & Dong, Y. (2017). Human papillomavirus and oral squamous cell carcinoma: A review of HPV-positive oral squamous cell carcinoma and possible strategies for

- future. *Current Problems in Cancer*, 41(5), 323–327.
<https://doi.org/10.1016/j.currproblcancer.2017.02.006>
- Jin, Y., Xing, J., Xu, K., Liu, D., & Zhuo, Y. (2022). Exosomes in the tumor microenvironment: Promoting cancer progression. *Frontiers in Immunology*, 13, 1025218. <https://doi.org/10.3389/fimmu.2022.1025218>
- Johnson, D. E., Burtneess, B., Leemans, C. R., Lui, V. W. Y., Bauman, J. E., & Grandis, J. R. (2020). Head and neck squamous cell carcinoma. *Nature Reviews Disease Primers*, 6(1), 1–22. <https://doi.org/10.1038/s41572-020-00224-3>
- Johnson, D. R., & O’Neill, B. P. (2012). Glioblastoma survival in the United States before and during the temozolomide era. *Journal of Neuro-Oncology*, 107(2), 359–364. <https://doi.org/10.1007/s11060-011-0749-4>
- Johnstone, R. M. (2006). Exosomes biological significance: A concise review. *Blood Cells, Molecules & Diseases*, 36(2), 315–321. <https://doi.org/10.1016/j.bcmed.2005.12.001>
- Johnstone, R. M., Adam, M., Hammond, J. R., Orr, L., & Turbide, C. (1987). Vesicle formation during reticulocyte maturation. Association of plasma membrane activities with released vesicles (exosomes). *Journal of Biological Chemistry*, 262(19), 9412–9420. [https://doi.org/10.1016/S0021-9258\(18\)48095-7](https://doi.org/10.1016/S0021-9258(18)48095-7)
- Jordan, P., & Carmo-Fonseca, M. (2000). Molecular mechanisms involved in cisplatin cytotoxicity. *Cellular and Molecular Life Sciences: CMLS*, 57(8–9), 1229–1235. <https://doi.org/10.1007/pl00000762>
- Jung, J. H., Lee, M. Y., Choi, D.-Y., Lee, J. W., You, S., Lee, K. Y., Kim, J., & Kim, K. P. (2015). Phospholipids of tumor extracellular vesicles stratify gefitinib-resistant nonsmall cell lung cancer cells from gefitinib-sensitive cells. *PROTEOMICS*, 15(4), 824–835. <https://doi.org/10.1002/pmic.201400243>

- Kahlert, C., & Kalluri, R. (2013). Exosomes in tumor microenvironment influence cancer progression and metastasis. *Journal of Molecular Medicine*, *91*(4), 431–437.
<https://doi.org/10.1007/s00109-013-1020-6>
- Kalayda, G. V., Wagner, C. H., & Jaehde, U. (2012). Relevance of copper transporter 1 for cisplatin resistance in human ovarian carcinoma cells. *Journal of Inorganic Biochemistry*, *116*, 1–10. <https://doi.org/10.1016/j.jinorgbio.2012.07.010>
- Kamb, A. C. (1996). A Cell Cycle Regulator and Cancer. In J. J. Li, S. A. Li, J.-Å. Gustafsson, S. Nandi, & L. I. Sekely (Eds.), *Hormonal Carcinogenesis II* (pp. 59–67). Springer. https://doi.org/10.1007/978-1-4612-2332-0_6
- Kaminagakura, E., Villa, L. L., Andreoli, M. A., Sobrinho, J. S., Vartanian, J. G., Soares, F. A., Nishimoto, I. N., Rocha, R., & Kowalski, L. P. (2012). High-risk human papillomavirus in oral squamous cell carcinoma of young patients. *International Journal of Cancer*, *130*(8), 1726–1732. <https://doi.org/10.1002/ijc.26185>
- Kanno, Y., Chen, C.-Y., Lee, H.-L., Chiou, J.-F., & Chen, Y.-J. (2021). Molecular Mechanisms of Chemotherapy Resistance in Head and Neck Cancers. *Frontiers in Oncology*, *11*, 640392. <https://doi.org/10.3389/fonc.2021.640392>
- Kaufmann, S. H., & Earnshaw, W. C. (2000). Induction of Apoptosis by Cancer Chemotherapy. *Experimental Cell Research*, *256*(1), 42–49.
<https://doi.org/10.1006/excr.2000.4838>
- Kedersha, N. L., Heuser, J. E., Chugani, D. C., & Rome, L. H. (1991). Vaults. III. Vault ribonucleoprotein particles open into flower-like structures with octagonal symmetry. *The Journal of Cell Biology*, *112*(2), 225–235. <https://doi.org/10.1083/jcb.112.2.225>
- Kedersha, N. L., Miquel, M. C., Bittner, D., & Rome, L. H. (1990). Vaults. II. Ribonucleoprotein structures are highly conserved among higher and lower

eukaryotes. *The Journal of Cell Biology*, 110(4), 895–901.

<https://doi.org/10.1083/jcb.110.4.895>

- Kedersha, N. L., & Rome, L. H. (1986). Isolation and characterization of a novel ribonucleoprotein particle: Large structures contain a single species of small RNA. *The Journal of Cell Biology*, 103(3), 699–709. <https://doi.org/10.1083/jcb.103.3.699>
- Khoo, X.-H., Paterson, I. C., Goh, B.-H., & Lee, W.-L. (2019). Cisplatin-Resistance in Oral Squamous Cell Carcinoma: Regulation by Tumor Cell-Derived Extracellular Vesicles. *Cancers*, 11(8), 1166. <https://doi.org/10.3390/cancers11081166>
- Kickhoefer, V. A., Liu, Y., Kong, L. B., Snow, B. E., Stewart, P. L., Harrington, L., & Rome, L. H. (2001). The Telomerase/Vault-Associated Protein Tep1 Is Required for Vault RNA Stability and Its Association with the Vault Particle. *The Journal of Cell Biology*, 152(1), 157–164.
- Kickhoefer, V. A., Poderycki, M. J., Chan, E. K. L., & Rome, L. H. (2002). The La RNA-binding protein interacts with the vault RNA and is a vault-associated protein. *The Journal of Biological Chemistry*, 277(43), 41282–41286. <https://doi.org/10.1074/jbc.M206980200>
- Kickhoefer, V. A., Rajavel, K. S., Scheffer, G. L., Dalton, W. S., Scheper, R. J., & Rome, L. H. (1998). Vaults are up-regulated in multidrug-resistant cancer cell lines. *The Journal of Biological Chemistry*, 273(15), 8971–8974. <https://doi.org/10.1074/jbc.273.15.8971>
- Kickhoefer, V. A., Siva, A. C., Kedersha, N. L., Inman, E. M., Ruland, C., Streuli, M., & Rome, L. H. (1999). The 193-Kd Vault Protein, Vparp, Is a Novel Poly(Adp-Ribose) Polymerase. *The Journal of Cell Biology*, 146(5), 917–928.

- Kickhoefer, V. A., Stephen, A. G., Harrington, L., Robinson, M. O., & Rome, L. H. (1999). Vaults and Telomerase Share a Common Subunit, TEP1 *. *Journal of Biological Chemistry*, 274(46), 32712–32717. <https://doi.org/10.1074/jbc.274.46.32712>
- Kickhoefer, V. A., Vasu, S. K., & Rome, L. H. (1996). Vaults are the answer, what is the question? *Trends in Cell Biology*, 6(5), 174–178. [https://doi.org/10.1016/0962-8924\(96\)10014-3](https://doi.org/10.1016/0962-8924(96)10014-3)
- Kim, C. W., Lee, H. M., Lee, T. H., Kang, C., Kleinman, H. K., & Gho, Y. S. (2002). Extracellular membrane vesicles from tumor cells promote angiogenesis via sphingomyelin. *Cancer Research*, 62(21), 6312–6317.
- Kim, S.-Y., Cordeiro, M. H., Serna, V. A., Ebbert, K., Butler, L. M., Sinha, S., Mills, A. A., Woodruff, T. K., & Kurita, T. (2013). Rescue of platinum-damaged oocytes from programmed cell death through inactivation of the p53 family signaling network. *Cell Death and Differentiation*, 20(8), 987–997. <https://doi.org/10.1038/cdd.2013.31>
- Kitazono, M., Okumura, H., Ikeda, R., Sumizawa, T., Furukawa, T., Nagayama, S., Seto, K., Aikou, T., & Akiyama, S. (2001). Reversal of LRP-associated drug resistance in colon carcinoma SW-620 cells. *International Journal of Cancer*, 91(1), 126–131. [https://doi.org/10.1002/1097-0215\(20010101\)91:1<126::aid-ijc1018>3.0.co;2-8](https://doi.org/10.1002/1097-0215(20010101)91:1<126::aid-ijc1018>3.0.co;2-8)
- Knepper, M. A., & Pisitkun, T. (2007). Exosomes in urine: Who would have thought...? *Kidney International*, 72(9), 1043–1045. <https://doi.org/10.1038/sj.ki.5002510>
- Kong, L. B., Siva, A. C., Kickhoefer, V. A., Rome, L. H., & Stewart, P. L. (2000). RNA location and modeling of a WD40 repeat domain within the vault. *RNA (New York, N.Y.)*, 6(6), 890–900. <https://doi.org/10.1017/s1355838200000157>
- Kong, L. B., Siva, A. C., Rome, L. H., & Stewart, P. L. (1999). Structure of the vault, a ubiquitous cellular component. *Structure (London, England: 1993)*, 7(4), 371–379. [https://doi.org/10.1016/s0969-2126\(99\)80050-1](https://doi.org/10.1016/s0969-2126(99)80050-1)

- König, L., Kasimir-Bauer, S., Bittner, A.-K., Hoffmann, O., Wagner, B., Santos Manvailer, L. F., Kimmig, R., Horn, P. A., & Rebmann, V. (2017). Elevated levels of extracellular vesicles are associated with therapy failure and disease progression in breast cancer patients undergoing neoadjuvant chemotherapy. *Oncoimmunology*, 7(1), e1376153. <https://doi.org/10.1080/2162402X.2017.1376153>
- Korita, P. V., Wakai, T., Shirai, Y., Matsuda, Y., Sakata, J., Takamura, M., Yano, M., Sanpei, A., Aoyagi, Y., Hatakeyama, K., & Ajioka, Y. (2010). Multidrug resistance-associated protein 2 determines the efficacy of cisplatin in patients with hepatocellular carcinoma. *Oncology Reports*, 23(4), 965–972. https://doi.org/10.3892/or_00000721
- Kornilov, R., Puhka, M., Mannerström, B., Hiidenmaa, H., Peltoniemi, H., Siljander, P., Seppänen-Kaijansinkko, R., & Kaur, S. (2018). Efficient ultrafiltration-based protocol to deplete extracellular vesicles from fetal bovine serum. *Journal of Extracellular Vesicles*, 7(1), 1422674. <https://doi.org/10.1080/20013078.2017.1422674>
- Kosaka, N., Iguchi, H., Hagiwara, K., Yoshioka, Y., Takeshita, F., & Ochiya, T. (2013). Neutral Sphingomyelinase 2 (nSMase2)-dependent Exosomal Transfer of Angiogenic MicroRNAs Regulate Cancer Cell Metastasis *. *Journal of Biological Chemistry*, 288(15), 10849–10859. <https://doi.org/10.1074/jbc.M112.446831>
- Kotzerke, K., Mempel, M., Aung, T., Wulf, G. G., Urlaub, H., Wenzel, D., Schön, M. P., & Braun, A. (2013). Immunostimulatory activity of murine keratinocyte-derived exosomes. *Experimental Dermatology*, 22(10), 650–655. <https://doi.org/10.1111/exd.12230>
- Kouketsu, A., Sato, I., Abe, S., Oikawa, M., Shimizu, Y., Takahashi, T., & Kumamoto, H. (2016). Detection of human papillomavirus infection in oral squamous cell carcinoma: A cohort study of Japanese patients. *Journal of Oral Pathology & Medicine: Official Publication of the International Association of Oral Pathologists*

and the American Academy of Oral Pathology, 45(8), 565–572.

<https://doi.org/10.1111/jop.12416>

Lamperska, K. M., Kolenda, T., Teresiak, A., Kowalik, A., Kruszyna-Mochalska, M., Jackowiak, W., Bliźniak, R., Przybyła, W., Kapalczyńska, M., & Kozłowski, P. (2017). Different levels of let-7d expression modulate response of FaDu cells to irradiation and chemotherapeutics. *PLoS ONE*, 12(6), e0180265.

<https://doi.org/10.1371/journal.pone.0180265>

Lane, R. E., Korbie, D., Hill, M. M., & Trau, M. (2018). Extracellular vesicles as circulating cancer biomarkers: Opportunities and challenges. *Clinical and Translational Medicine*, 7(1), 14. <https://doi.org/10.1186/s40169-018-0192-7>

Lässer, C., Alikhani, V. S., Ekström, K., Eldh, M., Paredes, P. T., Bossios, A., Sjöstrand, M., Gabrielsson, S., Lötvall, J., & Valadi, H. (2011). Human saliva, plasma and breast milk exosomes contain RNA: Uptake by macrophages. *Journal of Translational Medicine*, 9, 9. <https://doi.org/10.1186/1479-5876-9-9>

Lässer, C., Shelke, G. V., Yeri, A., Kim, D.-K., Crescitelli, R., Raimondo, S., Sjöstrand, M., Gho, Y. S., Van Keuren Jensen, K., & Lötvall, J. (2016). Two distinct extracellular RNA signatures released by a single cell type identified by microarray and next-generation sequencing. *RNA Biology*, 14(1), 58–72.

<https://doi.org/10.1080/15476286.2016.1249092>

Lee, H. M., Joh, J. W., Seo, S.-R., Kim, W.-T., Kim, M. K., Choi, H. S., Kim, S. Y., Jang, Y.-J., Sinn, D. H., Choi, G. S., Kim, J. M., Kwon, C. H. D., Chang, H. J., Kim, D. S., & Ryu, C. J. (2017). Cell-surface major vault protein promotes cancer progression through harboring mesenchymal and intermediate circulating tumor cells in hepatocellular carcinomas. *Scientific Reports*, 7(1), 13201.

<https://doi.org/10.1038/s41598-017-13501-1>

- Lee, S.-O., Masyuk, T., Splinter, P., Banales, J. M., Masyuk, A., Stroope, A., & Larusso, N. (2008). MicroRNA15a modulates expression of the cell-cycle regulator Cdc25A and affects hepatic cystogenesis in a rat model of polycystic kidney disease. *The Journal of Clinical Investigation*, *118*(11), 3714–3724. <https://doi.org/10.1172/JCI34922>
- Lehuédé, C., Li, X., Dauvillier, S., Vaysse, C., Franchet, C., Clement, E., Esteve, D., Longué, M., Chaltiel, L., Le Gonidec, S., Lazar, I., Geneste, A., Dumontet, C., Valet, P., Nieto, L., Fallone, F., & Muller, C. (2019). Adipocytes promote breast cancer resistance to chemotherapy, a process amplified by obesity: Role of the major vault protein (MVP). *Breast Cancer Research*, *21*(1), 7. <https://doi.org/10.1186/s13058-018-1088-6>
- Leidal, A. M., & Debnath, J. (2020). LC3-dependent extracellular vesicle loading and secretion (LDELS). *Autophagy*, *16*(6), 1162–1163. <https://doi.org/10.1080/15548627.2020.1756557>
- Levchenko, A., Mehta, B. M., Niu, X., Kang, G., Villafania, L., Way, D., Polycarpe, D., Sadelain, M., & Larson, S. M. (2005). Intercellular transfer of P-glycoprotein mediates acquired multidrug resistance in tumor cells. *Proceedings of the National Academy of Sciences*, *102*(6), 1933–1938. <https://doi.org/10.1073/pnas.0401851102>
- Li, F., Chen, Y., Zhang, Z., Ouyang, J., Wang, Y., Yan, R., Huang, S., Gao, G. F., Guo, G., & Chen, J.-L. (2015). Robust expression of vault RNAs induced by influenza A virus plays a critical role in suppression of PKR-mediated innate immunity. *Nucleic Acids Research*, *43*(21), 10321–10337. <https://doi.org/10.1093/nar/gkv1078>
- Li, I., & Nabet, B. Y. (2019). Exosomes in the tumor microenvironment as mediators of cancer therapy resistance. *Molecular Cancer*, *18*(1), 32. <https://doi.org/10.1186/s12943-019-0975-5>

- Li, J. Y., Volknandt, W., Dahlstrom, A., Herrmann, C., Blasi, J., Das, B., & Zimmermann, H. (1999). Axonal transport of ribonucleoprotein particles (vaults). *Neuroscience*, *91*(3), 1055–1065. [https://doi.org/10.1016/s0306-4522\(98\)00622-8](https://doi.org/10.1016/s0306-4522(98)00622-8)
- Liu, Y., Snow, B. E., Hande, M. P., Baerlocher, G., Kickhoefer, V. A., Yeung, D., Wakeham, A., Itie, A., Siderovski, D. P., Lansdorp, P. M., Robinson, M. O., & Harrington, L. (2000). Telomerase-Associated Protein TEP1 Is Not Essential for Telomerase Activity or Telomere Length Maintenance In Vivo. *Molecular and Cellular Biology*, *20*(21), 8178–8184.
- Llorente, A., Skotland, T., Sylvänne, T., Kauhanen, D., Róg, T., Orłowski, A., Vattulainen, I., Ekroos, K., & Sandvig, K. (2013). Molecular lipidomics of exosomes released by PC-3 prostate cancer cells. *Biochimica Et Biophysica Acta*, *1831*(7), 1302–1309. <https://doi.org/10.1016/j.bbaliip.2013.04.011>
- Lloret, M., Lara, P. C., Bordón, E., Fontes, F., Rey, A., Pinar, B., & Falcón, O. (2009). Major vault protein may affect nonhomologous end-joining repair and apoptosis through Ku70/80 and bax downregulation in cervical carcinoma tumors. *International Journal of Radiation Oncology, Biology, Physics*, *73*(4), 976–979. <https://doi.org/10.1016/j.ijrobp.2008.11.013>
- Loebinger, M. R., Giangreco, A., Groot, K. R., Prichard, L., Allen, K., Simpson, C., Bazley, L., Navani, N., Tibrewal, S., Davies, D., & Janes, S. M. (2008). Squamous cell cancers contain a side population of stem-like cells that are made chemosensitive by ABC transporter blockade. *British Journal of Cancer*, *98*(2), 380–387. <https://doi.org/10.1038/sj.bjc.6604185>
- Logozzi, M., Milito, A. D., Lugini, L., Borghi, M., Calabrò, L., Spada, M., Perdicchio, M., Marino, M. L., Federici, C., Iessi, E., Brambilla, D., Venturi, G., Lozupone, F., Santinami, M., Huber, V., Maio, M., Rivoltini, L., & Fais, S. (2009). High Levels of

- Exosomes Expressing CD63 and Caveolin-1 in Plasma of Melanoma Patients. *PLOS ONE*, 4(4), e5219. <https://doi.org/10.1371/journal.pone.0005219>
- Logozzi, M., Mizzoni, D., Angelini, D. F., Di Raimo, R., Falchi, M., Battistini, L., & Fais, S. (2018). Microenvironmental pH and Exosome Levels Interplay in Human Cancer Cell Lines of Different Histotypes. *Cancers*, 10(10), Article 10. <https://doi.org/10.3390/cancers10100370>
- Lorch, J. H., Goloubeva, O., Haddad, R. I., Cullen, K., Sarlis, N., Tishler, R., Tan, M., Fasciano, J., Sammartino, D. E., & Posner, M. R. (2011). Induction chemotherapy with cisplatin and fluorouracil alone or in combination with docetaxel in locally advanced squamous-cell cancer of the head and neck: Long-term results of the TAX 324 randomised phase 3 trial. *The Lancet Oncology*, 12(2), 153–159. [https://doi.org/10.1016/S1470-2045\(10\)70279-5](https://doi.org/10.1016/S1470-2045(10)70279-5)
- Lötvall, J., Hill, A. F., Hochberg, F., Buzás, E. I., Di Vizio, D., Gardiner, C., Ghossein, Y. S., Kurochkin, I. V., Mathivanan, S., Quesenberry, P., Sahoo, S., Tahara, H., Wauben, M. H., Witwer, K. W., & Théry, C. (2014). Minimal experimental requirements for definition of extracellular vesicles and their functions: A position statement from the International Society for Extracellular Vesicles. *Journal of Extracellular Vesicles*, 3, 10.3402/jev.v3.26913. <https://doi.org/10.3402/jev.v3.26913>
- Lu, J. F., Luk, F., Gong, J., Jaiswal, R., Grau, G. E. R., & Bebawy, M. (2013). Microparticles mediate MRP1 intercellular transfer and the re-templating of intrinsic resistance pathways. *Pharmacological Research*, 76, 77–83. <https://doi.org/10.1016/j.phrs.2013.07.009>
- Lu, Q., Hope, L. W., Brasch, M., Reinhard, C., & Cohen, S. N. (2003). TSG101 interaction with HRS mediates endosomal trafficking and receptor down-regulation. *Proceedings*

- of the National Academy of Sciences of the United States of America*, 100(13), 7626–7631. <https://doi.org/10.1073/pnas.0932599100>
- Lucchetti, D., Calapà, F., Palmieri, V., Fanali, C., Carbone, F., Papa, A., De Maria, R., De Spirito, M., & Sgambato, A. (2017). Differentiation Affects the Release of Exosomes from Colon Cancer Cells and Their Ability to Modulate the Behavior of Recipient Cells. *The American Journal of Pathology*, 187(7), 1633–1647. <https://doi.org/10.1016/j.ajpath.2017.03.015>
- Lucotti, S., Kenific, C. M., Zhang, H., & Lyden, D. (2022). Extracellular vesicles and particles impact the systemic landscape of cancer. *The EMBO Journal*, 41(18), e109288. <https://doi.org/10.15252/emboj.2021109288>
- Luga, V., Zhang, L., Vilorio-Petit, A. M., Ogunjimi, A. A., Inanlou, M. R., Chiu, E., Buchanan, M., Hosein, A. N., Basik, M., & Wrana, J. L. (2012). Exosomes mediate stromal mobilization of autocrine Wnt-PCP signaling in breast cancer cell migration. *Cell*, 151(7), 1542–1556. <https://doi.org/10.1016/j.cell.2012.11.024>
- Lunavat, T. R., Cheng, L., Kim, D.-K., Bhadury, J., Jang, S. C., Lässer, C., Sharples, R. A., López, M. D., Nilsson, J., Gho, Y. S., Hill, A. F., & Lötvall, J. (2015). Small RNA deep sequencing discriminates subsets of extracellular vesicles released by melanoma cells—Evidence of unique microRNA cargos. *RNA Biology*, 12(8), 810–823. <https://doi.org/10.1080/15476286.2015.1056975>
- Lunt, S. J., Chaudary, N., & Hill, R. P. (2009). The tumor microenvironment and metastatic disease. *Clinical & Experimental Metastasis*, 26(1), 19–34. <https://doi.org/10.1007/s10585-008-9182-2>
- Luqmani, Y. A. (2005). Mechanisms of drug resistance in cancer chemotherapy. *Medical Principles and Practice: International Journal of the Kuwait University, Health Science Centre*, 14 Suppl 1, 35–48. <https://doi.org/10.1159/000086183>

- Lv, L.-H., Wan, Y.-L., Lin, Y., Zhang, W., Yang, M., Li, G.-L., Lin, H.-M., Shang, C.-Z., Chen, Y.-J., & Min, J. (2012). Anticancer drugs cause release of exosomes with heat shock proteins from human hepatocellular carcinoma cells that elicit effective natural killer cell antitumor responses in vitro. *The Journal of Biological Chemistry*, *287*(19), 15874–15885. <https://doi.org/10.1074/jbc.M112.340588>
- Lv, M., Zhu, X., Chen, W., Zhong, S., Hu, Q., Ma, T., Zhang, J., Chen, L., Tang, J., & Zhao, J. (2014). Exosomes mediate drug resistance transfer in MCF-7 breast cancer cells and a probable mechanism is delivery of P-glycoprotein. *Tumour Biology: The Journal of the International Society for Oncodevelopmental Biology and Medicine*, *35*(11), 10773–10779. <https://doi.org/10.1007/s13277-014-2377-z>
- Ma, X., Chen, Z., Hua, D., He, D., Wang, L., Zhang, P., Wang, J., Cai, Y., Gao, C., Zhang, X., Zhang, F., Wang, T., Hong, T., Jin, L., Qi, X., Chen, S., Gu, X., Yang, D., Pan, Q., ... Yao, X. (2014). Essential role for TrpC5-containing extracellular vesicles in breast cancer with chemotherapeutic resistance. *Proceedings of the National Academy of Sciences*, *111*(17), 6389–6394. <https://doi.org/10.1073/pnas.1400272111>
- Maleki, S., Jabalee, J., & Garnis, C. (2021). The Role of Extracellular Vesicles in Mediating Resistance to Anticancer Therapies. *International Journal of Molecular Sciences*, *22*(8), 4166. <https://doi.org/10.3390/ijms22084166>
- Malik, Z. A., Kott, K. S., Poe, A. J., Kuo, T., Chen, L., Ferrara, K. W., & Knowlton, A. A. (2013). Cardiac myocyte exosomes: Stability, HSP60, and proteomics. *American Journal of Physiology. Heart and Circulatory Physiology*, *304*(7), H954-965. <https://doi.org/10.1152/ajpheart.00835.2012>
- Malkin, E. Z., & Bratman, S. V. (2020). Bioactive DNA from extracellular vesicles and particles. *Cell Death & Disease*, *11*(7), 584. <https://doi.org/10.1038/s41419-020-02803-4>

- Mandic, R., Schamberger, C. J., Müller, J. F., Geyer, M., Zhu, L., Carey, T. E., Grénman, R., Dünne, A. A., & Werner, J. A. (2005). Reduced cisplatin sensitivity of head and neck squamous cell carcinoma cell lines correlates with mutations affecting the COOH-terminal nuclear localization signal of p53. *Clinical Cancer Research: An Official Journal of the American Association for Cancer Research*, *11*(19 Pt 1), 6845–6852. <https://doi.org/10.1158/1078-0432.CCR-05-0378>
- Martínez, M. C., & Freyssinet, J. M. (2001). Deciphering the plasma membrane hallmarks of apoptotic cells: Phosphatidylserine transverse redistribution and calcium entry. *BMC Cell Biology*, *2*, 20. <https://doi.org/10.1186/1471-2121-2-20>
- Marzesco, A.-M., Janich, P., Wilsch-Bräuninger, M., Dubreuil, V., Langenfeld, K., Corbeil, D., & Huttner, W. B. (2005). Release of extracellular membrane particles carrying the stem cell marker prominin-1 (CD133) from neural progenitors and other epithelial cells. *Journal of Cell Science*, *118*(13), 2849–2858. <https://doi.org/10.1242/jcs.02439>
- Matsuo, H., Chevallier, J., Mayran, N., Le Blanc, I., Ferguson, C., Fauré, J., Blanc, N. S., Matile, S., Dubochet, J., Sadoul, R., Parton, R. G., Vilbois, F., & Gruenberg, J. (2004). Role of LBPA and Alix in multivesicular liposome formation and endosome organization. *Science (New York, N.Y.)*, *303*(5657), 531–534. <https://doi.org/10.1126/science.1092425>
- Medina, A., & Ghahary, A. (2010). Transdifferentiated circulating monocytes release exosomes containing 14-3-3 proteins with matrix metalloproteinase-1 stimulating effect for dermal fibroblasts. *Wound Repair and Regeneration: Official Publication of the Wound Healing Society [and] the European Tissue Repair Society*, *18*(2), 245–253. <https://doi.org/10.1111/j.1524-475X.2010.00580.x>
- Mehanna, H., Beech, T., Nicholson, T., El-Hariry, I., McConkey, C., Paleri, V., & Roberts, S. (2013). Prevalence of human papillomavirus in oropharyngeal and nonoropharyngeal

- head and neck cancer—Systematic review and meta-analysis of trends by time and region. *Head & Neck*, 35(5), 747–755. <https://doi.org/10.1002/hed.22015>
- Meschini, S., Marra, M., Calcabrini, A., Monti, E., Gariboldi, M., Dolfini, E., & Arancia, G. (2002). Role of the lung resistance-related protein (LRP) in the drug sensitivity of cultured tumor cells. *Toxicology in Vitro: An International Journal Published in Association with BIBRA*, 16(4), 389–398. [https://doi.org/10.1016/s0887-2333\(02\)00035-8](https://doi.org/10.1016/s0887-2333(02)00035-8)
- Michalke, B. (2010). Platinum speciation used for elucidating activation or inhibition of Pt-containing anti-cancer drugs. *Journal of Trace Elements in Medicine and Biology: Organ of the Society for Minerals and Trace Elements (GMS)*, 24(2), 69–77. <https://doi.org/10.1016/j.jtemb.2010.01.006>
- Milane, L., Singh, A., Mattheolabakis, G., Suresh, M., & Amiji, M. M. (2015). Exosome mediated communication within the tumor microenvironment. *Journal of Controlled Release*, 219, 278–294. <https://doi.org/10.1016/j.jconrel.2015.06.029>
- Milman, N., Ginini, L., & Gil, Z. (2019). Exosomes and their role in tumorigenesis and anticancer drug resistance. *Drug Resistance Updates: Reviews and Commentaries in Antimicrobial and Anticancer Chemotherapy*, 45, 1–12. <https://doi.org/10.1016/j.drup.2019.07.003>
- Minciacchi, V. R., Freeman, M. R., & Di Vizio, D. (2015). Extracellular Vesicles in Cancer: Exosomes, Microvesicles and the Emerging Role of Large Oncosomes. *Seminars in Cell & Developmental Biology*, 40, 41–51. <https://doi.org/10.1016/j.semcdb.2015.02.010>
- Mineo, M., Garfield, S. H., Taverna, S., Flugy, A., De Leo, G., Alessandro, R., & Kohn, E. C. (2012). Exosomes released by K562 chronic myeloid leukemia cells promote

angiogenesis in a Src-dependent fashion. *Angiogenesis*, 15(1), 33–45.

<https://doi.org/10.1007/s10456-011-9241-1>

Mirnikjoo, B., Balasubramanian, K., & Schroit, A. J. (2009). Mobilization of Lysosomal Calcium Regulates the Externalization of Phosphatidylserine during Apoptosis. *The Journal of Biological Chemistry*, 284(11), 6918–6923.

<https://doi.org/10.1074/jbc.M805288200>

Mohapatra, P., Shriwas, O., Mohanty, S., Ghosh, A., Smita, S., Kaushik, S. R., Arya, R., Rath, R., Das Majumdar, S., Muduly, D. K., Raghav, S., Nanda, R. K., & Dash, R. (2021). CMTM6 drives cisplatin resistance by regulating Wnt signaling through ENO-1/AKT/GSK3 β axis. *JCI Insight*. <https://doi.org/10.1172/jci.insight.143643>

Mossink, M. H., van Zon, A., Fränzel-Luiten, E., Schoester, M., Kickhoefer, V. A., Scheffer, G. L., Scheper, R. J., Sonneveld, P., & Wiemer, E. A. C. (2002). Disruption of the murine major vault protein (MVP/LRP) gene does not induce hypersensitivity to cytostatics. *Cancer Research*, 62(24), 7298–7304.

Mossink, M. H., van Zon, A., Scheper, R. J., Sonneveld, P., & Wiemer, E. A. (2003). Vaults: A ribonucleoprotein particle involved in drug resistance? *Oncogene*, 22(47), Article 47. <https://doi.org/10.1038/sj.onc.1206947>

Mueller, S., Schittenhelm, M., Honecker, F., Malenke, E., Lauber, K., Wesselborg, S., Hartmann, J. T., Bokemeyer, C., & Mayer, F. (2006). Cell-cycle progression and response of germ cell tumors to cisplatin in vitro. *International Journal of Oncology*, 29(2), 471–479.

Muralidharan-Chari, V., Clancy, J. W., Sedgwick, A., & D'Souza-Schorey, C. (2010). Microvesicles: Mediators of extracellular communication during cancer progression. *Journal of Cell Science*, 123(Pt 10), 1603–1611. <https://doi.org/10.1242/jcs.064386>

- Musi, A., & Bongiovanni, L. (2023). Extracellular Vesicles in Cancer Drug Resistance: Implications on Melanoma Therapy. *Cancers*, *15*(4), 1074.
<https://doi.org/10.3390/cancers15041074>
- Nahar, N. N., Missana, L. R., Garimella, R., Tague, S. E., & Anderson, H. C. (2008). Matrix vesicles are carriers of bone morphogenetic proteins (BMPs), vascular endothelial growth factor (VEGF), and noncollagenous matrix proteins. *Journal of Bone and Mineral Metabolism*, *26*(5), 514–519. <https://doi.org/10.1007/s00774-008-0859-z>
- Nolte-'t Hoen, E. N. M., Buermans, H. P. J., Waasdorp, M., Stoorvogel, W., Wauben, M. H. M., & 't Hoen, P. A. C. (2012). Deep sequencing of RNA from immune cell-derived vesicles uncovers the selective incorporation of small non-coding RNA biotypes with potential regulatory functions. *Nucleic Acids Research*, *40*(18), 9272–9285.
<https://doi.org/10.1093/nar/gks658>
- Öhrvik, H., Nose, Y., Wood, L. K., Kim, B.-E., Gleber, S.-C., Ralle, M., & Thiele, D. J. (2013). Ctr2 regulates biogenesis of a cleaved form of mammalian Ctr1 metal transporter lacking the copper- and cisplatin-binding ecto-domain. *Proceedings of the National Academy of Sciences*, *110*(46), E4279–E4288.
<https://doi.org/10.1073/pnas.1311749110>
- Okoye, I. S., Coomes, S. M., Pelly, V. S., Czieso, S., Papayannopoulos, V., Tolmachova, T., Seabra, M. C., & Wilson, M. S. (2014). MicroRNA-containing T-regulatory-cell-derived exosomes suppress pathogenic T helper 1 cells. *Immunity*, *41*(1), 89–103.
<https://doi.org/10.1016/j.immuni.2014.05.019>
- Osti, D., Del Bene, M., Rappa, G., Santos, M., Matafora, V., Richichi, C., Faletti, S., Beznoussenko, G. V., Mironov, A., Bachi, A., Fornasari, L., Bongetta, D., Gaetani, P., DiMeco, F., Lorico, A., & Pelicci, G. (2019). Clinical Significance of Extracellular Vesicles in Plasma from Glioblastoma Patients. *Clinical Cancer Research: An*

Official Journal of the American Association for Cancer Research, 25(1), 266–276.

<https://doi.org/10.1158/1078-0432.CCR-18-1941>

Palanisamy, V., Sharma, S., Deshpande, A., Zhou, H., Gimzewski, J., & Wong, D. T. (2010).

Nanostructural and Transcriptomic Analyses of Human Saliva Derived Exosomes.

PLoS ONE, 5(1), e8577. <https://doi.org/10.1371/journal.pone.0008577>

Parolini, I., Federici, C., Raggi, C., Lugini, L., Palleschi, S., De Milito, A., Coscia, C., Iessi,

E., Logozzi, M., Molinari, A., Colone, M., Tatti, M., Sargiacomo, M., & Fais, S.

(2009). Microenvironmental pH Is a Key Factor for Exosome Traffic in Tumor Cells*. *Journal of Biological Chemistry*, 284(49), 34211–34222.

<https://doi.org/10.1074/jbc.M109.041152>

Pascucci, L., Coccè, V., Bonomi, A., Ami, D., Ceccarelli, P., Ciusani, E., Viganò, L.,

Locatelli, A., Sisto, F., Doglia, S. M., Parati, E., Bernardo, M. E., Muraca, M.,

Alessandri, G., Bondiolotti, G., & Pessina, A. (2014). Paclitaxel is incorporated by mesenchymal stromal cells and released in exosomes that inhibit in vitro tumor growth: A new approach for drug delivery. *Journal of Controlled Release: Official Journal of the Controlled Release Society*, 192, 262–270.

<https://doi.org/10.1016/j.jconrel.2014.07.042>

Pasillas, M. P., Shields, S., Reilly, R., Strnadel, J., Behl, C., Park, R., Yates, J. R., Klemke,

R., Gonias, S. L., & Coppinger, J. A. (2015). Proteomic analysis reveals a role for

Bcl2-associated athanogene 3 and major vault protein in resistance to apoptosis in senescent cells by regulating ERK1/2 activation. *Molecular & Cellular Proteomics: MCP*,

14(1), 1–14. <https://doi.org/10.1074/mcp.M114.037697>

Peinado, H., Alečković, M., Lavotshkin, S., Matei, I., Costa-Silva, B., Moreno-Bueno, G.,

Hergueta-Redondo, M., Williams, C., García-Santos, G., Nitadori-Hoshino, A.,

Hoffman, C., Badal, K., Garcia, B. A., Callahan, M. K., Yuan, J., Martins, V. R.,

- Skog, J., Kaplan, R. N., Brady, M. S., ... Lyden, D. (2012). Melanoma exosomes educate bone marrow progenitor cells toward a pro-metastatic phenotype through MET. *Nature Medicine*, *18*(6), 883–891. <https://doi.org/10.1038/nm.2753>
- Perdomo, S., Martin Roa, G., Brennan, P., Forman, D., & Sierra, M. S. (2016). Head and neck cancer burden and preventive measures in Central and South America. *Cancer Epidemiology*, *44 Suppl 1*, S43–S52. <https://doi.org/10.1016/j.canep.2016.03.012>
- Persson, H., Kvist, A., Vallon-Christersson, J., Medstrand, P., Borg, A., & Rovira, C. (2009). The non-coding RNA of the multidrug resistance-linked vault particle encodes multiple regulatory small RNAs. *Nature Cell Biology*, *11*(10), 1268–1271. <https://doi.org/10.1038/ncb1972>
- Petti, S. (2009). Lifestyle risk factors for oral cancer. *Oral Oncology*, *45*(4), 340–350. <https://doi.org/10.1016/j.oraloncology.2008.05.018>
- Pietras, P., Leśniczak-Staszak, M., Kasprzak, A., Andrzejewska, M., Jopek, K., Sowiński, M., Rucinski, M., Lyons, S. M., Ivanov, P., & Szaflarski, W. (2021). MVP Expression Facilitates Tumor Cell Proliferation and Migration Supporting the Metastasis of Colorectal Cancer Cells. *International Journal of Molecular Sciences*, *22*(22), 12121. <https://doi.org/10.3390/ijms222212121>
- Poderycki, M. J., Rome, L. H., Harrington, L., & Kickhoefer, V. A. (2005). The p80 homology region of TEP1 is sufficient for its association with the telomerase and vault RNAs, and the vault particle. *Nucleic Acids Research*, *33*(3), 893–902. <https://doi.org/10.1093/nar/gki234>
- Posner, M. R. (2005). Paradigm Shift in the Treatment of Head and Neck Cancer: The Role of Neoadjuvant Chemotherapy. *The Oncologist*, *10*(S3), 11–19. <https://doi.org/10.1634/theoncologist.10-90003-11>

- Prime, S. S., Nixon, S. V., Crane, I. J., Stone, A., Matthews, J. B., Maitland, N. J., Remnant, L., Powell, S. K., Game, S. M., & Scully, C. (1990). The behaviour of human oral squamous cell carcinoma in cell culture. *The Journal of Pathology*, *160*(3), 259–269. <https://doi.org/10.1002/path.1711600313>
- Qin, X., Yu, S., Zhou, L., Shi, M., Hu, Y., Xu, X., Shen, B., Liu, S., Yan, D., & Feng, J. (2017). Cisplatin-resistant lung cancer cell-derived exosomes increase cisplatin resistance of recipient cells in exosomal miR-100-5p-dependent manner. *International Journal of Nanomedicine*, *12*, 3721–3733. <https://doi.org/10.2147/IJN.S131516>
- Rangan, S. R. (1972). A new human cell line (FaDu) from a hypopharyngeal carcinoma. *Cancer*, *29*(1), 117–121. [https://doi.org/10.1002/1097-0142\(197201\)29:1<117::aid-cncr2820290119>3.0.co;2-r](https://doi.org/10.1002/1097-0142(197201)29:1<117::aid-cncr2820290119>3.0.co;2-r)
- Raposo, G., Nijman, H. W., Stoorvogel, W., Liejendekker, R., Harding, C. V., Melief, C. J., & Geuze, H. J. (1996). B lymphocytes secrete antigen-presenting vesicles. *The Journal of Experimental Medicine*, *183*(3), 1161–1172. <https://doi.org/10.1084/jem.183.3.1161>
- Ratajczak, J., Wysoczynski, M., Hayek, F., Janowska-Wieczorek, A., & Ratajczak, M. Z. (2006). Membrane-derived microvesicles: Important and underappreciated mediators of cell-to-cell communication. *Leukemia*, *20*(9), 1487–1495. <https://doi.org/10.1038/sj.leu.2404296>
- Raulf, N., El-Attar, R., Kulms, D., Lecis, D., Delia, D., Walczak, H., Papenfuss, K., Odell, E., & Tavassoli, M. (2014). Differential response of head and neck cancer cell lines to TRAIL or Smac mimetics is associated with the cellular levels and activity of caspase-8 and caspase-10. *British Journal of Cancer*, *111*(10), 1955–1964. <https://doi.org/10.1038/bjc.2014.521>

- Ravichandran, K. S. (2010). Find-me and eat-me signals in apoptotic cell clearance: Progress and conundrums. *Journal of Experimental Medicine*, 207(9), 1807–1817.
<https://doi.org/10.1084/jem.20101157>
- Razi, M., & Futter, C. E. (2006). Distinct Roles for Tsg101 and Hrs in Multivesicular Body Formation and Inward Vesiculation. *Molecular Biology of the Cell*, 17(8), 3469–3483.
<https://doi.org/10.1091/mbc.e05-11-1054>
- Rezaee, M., Sanche, L., & Hunting, D. J. (2013). Cisplatin enhances the formation of DNA single- and double-strand breaks by hydrated electrons and hydroxyl radicals. *Radiation Research*, 179(3), 323–331. <https://doi.org/10.1667/RR3185.1>
- Rezende, T. M. B., Freire, M. de S., & Franco, O. L. (2010). Head and neck cancer. *Cancer*, 116(21), 4914–4925. <https://doi.org/10.1002/cncr.25245>
- Richards, K. E., Zeleniak, A. E., Fishel, M. L., Wu, J., Littlepage, L. E., & Hill, R. (2017). Cancer-associated fibroblast exosomes regulate survival and proliferation of pancreatic cancer cells. *Oncogene*, 36(13), 1770–1778.
<https://doi.org/10.1038/onc.2016.353>
- Ricklefs, F. L., Maire, C. L., Reimer, R., Dührsen, L., Kolbe, K., Holz, M., Schneider, E., Rissiek, A., Babayan, A., Hille, C., Pantel, K., Krasemann, S., Glatzel, M., Heiland, D. H., Flitsch, J., Martens, T., Schmidt, N. O., Peine, S., Breakefield, X. O., ... Lamszus, K. (2019). Imaging flow cytometry facilitates multiparametric characterization of extracellular vesicles in malignant brain tumours. *Journal of Extracellular Vesicles*, 8(1), 1588555.
<https://doi.org/10.1080/20013078.2019.1588555>
- Ried, M., Lehle, K., Neu, R., Diez, C., Bednarski, P., Sziklavari, Z., & Hofmann, H.-S. (2015). Assessment of cisplatin concentration and depth of penetration in human lung

- tissue after hyperthermic exposure†. *European Journal of Cardio-Thoracic Surgery*, 47(3), 563–566. <https://doi.org/10.1093/ejcts/ezu217>
- Rimsza, L. M., Campbell, K., Dalton, W. S., Salmon, S., Willcox, G., & Grogan, T. M. (1999). The major vault protein (MVP), a new multidrug resistance associated protein, is frequently expressed in multiple myeloma. *Leukemia & Lymphoma*, 34(3–4), 315–324. <https://doi.org/10.3109/10428199909050956>
- Roberts, J. J., & Friedlos, F. (1987). Quantitative estimation of cisplatin-induced DNA interstrand cross-links and their repair in mammalian cells: Relationship to toxicity. *Pharmacology & Therapeutics*, 34(2), 215–246. [https://doi.org/10.1016/0163-7258\(87\)90012-x](https://doi.org/10.1016/0163-7258(87)90012-x)
- Roberts, J. J., & Thomson, A. J. (1979). The Mechanism of Action of Antitumor Platinum Compounds. In W. E. Cohn (Ed.), *Progress in Nucleic Acid Research and Molecular Biology* (Vol. 22, pp. 71–133). Academic Press. [https://doi.org/10.1016/S0079-6603\(08\)60799-0](https://doi.org/10.1016/S0079-6603(08)60799-0)
- Rodrigues-Junior, D. M., Tan, S. S., de Souza Viana, L., Carvalho, A. L., Lim, S. K., Iyer, N. G., & Vettore, A. L. (2019). A preliminary investigation of circulating extracellular vesicles and biomarker discovery associated with treatment response in head and neck squamous cell carcinoma. *BMC Cancer*, 19(1), 373. <https://doi.org/10.1186/s12885-019-5565-9>
- Rome, L., Kedersha, N., & Chugani, D. (1991). Unlocking vaults: Organelles in search of a function. *Trends in Cell Biology*, 1(2–3), 47–50. [https://doi.org/10.1016/0962-8924\(91\)90088-q](https://doi.org/10.1016/0962-8924(91)90088-q)
- Royo, F., Schlangen, K., Palomo, L., Gonzalez, E., Conde-Vancells, J., Berisa, A., Aransay, A. M., & Falcon-Perez, J. M. (2013). Transcriptome of extracellular vesicles released by hepatocytes. *PloS One*, 8(7), e68693. <https://doi.org/10.1371/journal.pone.0068693>

- Ryu, S. J., An, H. J., Oh, Y. S., Choi, H. R., Ha, M. K., & Park, S. C. (2008). On the role of major vault protein in the resistance of senescent human diploid fibroblasts to apoptosis. *Cell Death and Differentiation*, *15*(11), 1673–1680.
<https://doi.org/10.1038/cdd.2008.96>
- Safaei, R., Katano, K., Larson, B. J., Samimi, G., Holzer, A. K., Naerdemann, W., Tomioka, M., Goodman, M., & Howell, S. B. (2005). Intracellular localization and trafficking of fluorescein-labeled cisplatin in human ovarian carcinoma cells. *Clinical Cancer Research: An Official Journal of the American Association for Cancer Research*, *11*(2 Pt 1), 756–767.
- Saito, T., Matsuda, Y., Suzuki, T., Hayashi, A., Yuan, X., Saito, M., Nakayama, J., Hori, T., & Ishikawa, F. (1997). Comparative gene mapping of the human and mouse TEP1 genes, which encode one protein component of telomerases. *Genomics*, *46*(1), 46–50.
<https://doi.org/10.1006/geno.1997.5005>
- Sajini, A. A., Choudhury, N. R., Wagner, R. E., Bornelöv, S., Selmi, T., Spanos, C., Dietmann, S., Rappsilber, J., Michlewski, G., & Frye, M. (2019). Loss of 5-methylcytosine alters the biogenesis of vault-derived small RNAs to coordinate epidermal differentiation. *Nature Communications*, *10*(1), Article 1.
<https://doi.org/10.1038/s41467-019-10020-7>
- Samuels, M., Cilibrasi, C., Papanastasopoulos, P., & Giamas, G. (2022). Extracellular Vesicles as Mediators of Therapy Resistance in the Breast Cancer Microenvironment. *Biomolecules*, *12*(1), 132. <https://doi.org/10.3390/biom12010132>
- Santos, P., & Almeida, F. (2020). Role of Exosomal miRNAs and the Tumor Microenvironment in Drug Resistance. *Cells*, *9*(6), 1450.
<https://doi.org/10.3390/cells9061450>

- Sato, S., Zhu, X. L., & Sly, W. S. (1990). Carbonic anhydrase isozymes IV and II in urinary membranes from carbonic anhydrase II-deficient patients. *Proceedings of the National Academy of Sciences*, 87(16), 6073–6076.
<https://doi.org/10.1073/pnas.87.16.6073>
- Savill, J. (1997). Recognition and phagocytosis of cells undergoing apoptosis. *British Medical Bulletin*, 53(3), 491–508.
<https://doi.org/10.1093/oxfordjournals.bmb.a011626>
- Sazonova, E. V., Chesnokov, M. S., Zhivotovsky, B., & Kopeina, G. S. (2022). Drug toxicity assessment: Cell proliferation versus cell death. *Cell Death Discovery*, 8(1), 1–11.
<https://doi.org/10.1038/s41420-022-01207-x>
- Scheffer, G. L., Wijngaard, P. L., Flens, M. J., Izquierdo, M. A., Slovak, M. L., Pinedo, H. M., Meijer, C. J., Clevers, H. C., & Scheper, R. J. (1995). The drug resistance-related protein LRP is the human major vault protein. *Nature Medicine*, 1(6), 578–582.
<https://doi.org/10.1038/nm0695-578>
- Scheper, R. J., Broxterman, H. J., Scheffer, G. L., Kaaijk, P., Dalton, W. S., van Heijningen, T. H., van Kalken, C. K., Slovak, M. L., de Vries, E. G., & van der Valk, P. (1993). Overexpression of a M(r) 110,000 vesicular protein in non-P-glycoprotein-mediated multidrug resistance. *Cancer Research*, 53(7), 1475–1479.
- Schmidt, O., & Teis, D. (2012). The ESCRT machinery. *Current Biology*, 22(4), R116–R120.
<https://doi.org/10.1016/j.cub.2012.01.028>
- Schmidt, W., & Chaney, S. G. (1993). Role of carrier ligand in platinum resistance of human carcinoma cell lines. *Cancer Research*, 53(4), 799–805.
- Schroeijers, A. B., Reurs, A. W., Scheffer, G. L., Stam, A. G. M., de Jong, M. C., Rustemeyer, T., Wiemer, E. A. C., de Gruijl, T. D., & Scheper, R. J. (2002). Up-regulation of drug resistance-related vaults during dendritic cell development. *Journal*

of Immunology (Baltimore, Md.: 1950), 168(4), 1572–1578.

<https://doi.org/10.4049/jimmunol.168.4.1572>

Schroeijers, A. B., Siva, A. C., Scheffer, G. L., de Jong, M. C., Bolick, S. C., Dukers, D. F., Slootstra, J. W., Meloen, R. H., Wiemer, E., Kickhoefer, V. A., Rome, L. H., & Scheper, R. J. (2000). The Mr 193,000 vault protein is up-regulated in multidrug-resistant cancer cell lines. *Cancer Research*, 60(4), 1104–1110.

Segura, E., Amigorena, S., & Théry, C. (2005). Mature dendritic cells secrete exosomes with strong ability to induce antigen-specific effector immune responses. *Blood Cells, Molecules & Diseases*, 35(2), 89–93. <https://doi.org/10.1016/j.bcmed.2005.05.003>

Shang, C., Feng, L., Gu, Y., Hong, H., Hong, L., & Hou, J. (2021). Impact of Multidisciplinary Team Management on the Survival Rate of Head and Neck Cancer Patients: A Cohort Study Meta-analysis. *Frontiers in Oncology*, 11.

<https://www.frontiersin.org/articles/10.3389/fonc.2021.630906>

Sherman-Baust, C. A., Weeraratna, A. T., Rangel, L. B. A., Pizer, E. S., Cho, K. R., Schwartz, D. R., Shock, T., & Morin, P. J. (2003). Remodeling of the extracellular matrix through overexpression of collagen VI contributes to cisplatin resistance in ovarian cancer cells. *Cancer Cell*, 3(4), 377–386. [https://doi.org/10.1016/S1535-6108\(03\)00058-8](https://doi.org/10.1016/S1535-6108(03)00058-8)

Shin, J.-S., Foo, T., Hong, A., Zhang, M., Lum, T., Solomon, M. J., & Lee, C. S. (2012). Telomerase expression as a predictive marker of radiotherapy response in rectal cancer. *Pathology*, 44(3), 209–215. <https://doi.org/10.1097/PAT.0b013e3283511cd5>

Shriwas, O., Arya, R., Mohanty, S., Mohapatra, P., Kumar, S., Rath, R., Kaushik, S. R., Pahwa, F., Murmu, K. C., Majumdar, S. K. D., Muduly, D. K., Dixit, A., Prasad, P., Nanda, R. K., & Dash, R. (2021). RRBPI rewires cisplatin resistance in oral

- squamous cell carcinoma by regulating Hippo pathway. *British Journal of Cancer*, 124(12), 2004–2016. <https://doi.org/10.1038/s41416-021-01336-7>
- Shurtleff, M. J., Yao, J., Qin, Y., Nottingham, R. M., Temoche-Diaz, M. M., Schekman, R., & Lambowitz, A. M. (2017). Broad role for YBX1 in defining the small noncoding RNA composition of exosomes. *Proceedings of the National Academy of Sciences*, 114(43), E8987–E8995. <https://doi.org/10.1073/pnas.1712108114>
- Siddik, Z. H. (2003). Cisplatin: Mode of cytotoxic action and molecular basis of resistance. *Oncogene*, 22(47), Article 47. <https://doi.org/10.1038/sj.onc.1206933>
- Siegel, R. L., Miller, K. D., & Jemal, A. (2016). Cancer statistics, 2016. *CA: A Cancer Journal for Clinicians*, 66(1), 7–30. <https://doi.org/10.3322/caac.21332>
- Sieuwert, A. M., Klijn, J. G., Peters, H. A., & Foekens, J. A. (1995). The MTT tetrazolium salt assay scrutinized: How to use this assay reliably to measure metabolic activity of cell cultures in vitro for the assessment of growth characteristics, IC50-values and cell survival. *European Journal of Clinical Chemistry and Clinical Biochemistry: Journal of the Forum of European Clinical Chemistry Societies*, 33(11), 813–823. <https://doi.org/10.1515/cclm.1995.33.11.813>
- Skog, J., Würdinger, T., van Rijn, S., Meijer, D. H., Gainche, L., Curry, W. T., Carter, B. S., Krichevsky, A. M., & Breakefield, X. O. (2008). Glioblastoma microvesicles transport RNA and proteins that promote tumour growth and provide diagnostic biomarkers. *Nature Cell Biology*, 10(12), Article 12. <https://doi.org/10.1038/ncb1800>
- Skriner, K., Adolph, K., Jungblut, P. R., & Burmester, G. R. (2006). Association of citrullinated proteins with synovial exosomes. *Arthritis and Rheumatism*, 54(12), 3809–3814. <https://doi.org/10.1002/art.22276>

- Smargon, A. A., Madrigal, A. A., Yee, B. A., Dong, K. D., Mueller, J. R., & Yeo, G. W. (2022). Crosstalk between CRISPR-Cas9 and the human transcriptome. *Nature Communications*, *13*, 1125. <https://doi.org/10.1038/s41467-022-28719-5>
- Son, B., Lee, S., Youn, H., Kim, E., Kim, W., & Youn, B. (2016). The role of tumor microenvironment in therapeutic resistance. *Oncotarget*, *8*(3), 3933–3945. <https://doi.org/10.18632/oncotarget.13907>
- Sorenson, C. M., Barry, M. A., & Eastman, A. (1990). Analysis of events associated with cell cycle arrest at G2 phase and cell death induced by cisplatin. *Journal of the National Cancer Institute*, *82*(9), 749–755. <https://doi.org/10.1093/jnci/82.9.749>
- Sousa, D., Lima, R. T., & Vasconcelos, M. H. (2015). Intercellular Transfer of Cancer Drug Resistance Traits by Extracellular Vesicles. *Trends in Molecular Medicine*, *21*(10), 595–608. <https://doi.org/10.1016/j.molmed.2015.08.002>
- Squadrito, M. L., Baer, C., Burdet, F., Maderna, C., Gilfillan, G. D., Lyle, R., Ibberson, M., & De Palma, M. (2014). Endogenous RNAs modulate microRNA sorting to exosomes and transfer to acceptor cells. *Cell Reports*, *8*(5), 1432–1446. <https://doi.org/10.1016/j.celrep.2014.07.035>
- Sridevi, P., Nhiayi, M. K., & Wang, J. Y. J. (2013). Genetic disruption of Abl nuclear import reduces renal apoptosis in a mouse model of cisplatin-induced nephrotoxicity. *Cell Death and Differentiation*, *20*(7), 953–962. <https://doi.org/10.1038/cdd.2013.42>
- Stachowiak, J. C., Schmid, E. M., Ryan, C. J., Ann, H. S., Sasaki, D. Y., Sherman, M. B., Geissler, P. L., Fletcher, D. A., & Hayden, C. C. (2012). Membrane bending by protein–protein crowding. *Nature Cell Biology*, *14*(9), 944–949. <https://doi.org/10.1038/ncb2561>
- Stadler, P. F., Chen, J. J.-L., Hackermüller, J., Hoffmann, S., Horn, F., Khaitovich, P., Kretzschmar, A. K., Mosig, A., Prohaska, S. J., Qi, X., Schutt, K., & Ullmann, K.

- (2009). Evolution of vault RNAs. *Molecular Biology and Evolution*, 26(9), 1975–1991. <https://doi.org/10.1093/molbev/msp112>
- Steinbichler, T. B., Dudás, J., Skvortsov, S., Ganswindt, U., Riechelmann, H., & Skvortsova, I.-I. (2019). Therapy resistance mediated by exosomes. *Molecular Cancer*, 18(1), 58. <https://doi.org/10.1186/s12943-019-0970-x>
- Stephen, A. G., Raval-Fernandes, S., Huynh, T., Torres, M., Kickhoefer, V. A., & Rome, L. H. (2001). Assembly of vault-like particles in insect cells expressing only the major vault protein. *The Journal of Biological Chemistry*, 276(26), 23217–23220. <https://doi.org/10.1074/jbc.C100226200>
- Stevic, I., Buescher, G., & Ricklefs, F. L. (2020). Monitoring Therapy Efficiency in Cancer through Extracellular Vesicles. *Cells*, 9(1), 130. <https://doi.org/10.3390/cells9010130>
- Street, J. M., Barran, P. E., Mackay, C. L., Weidt, S., Balmforth, C., Walsh, T. S., Chalmers, R. T., Webb, D. J., & Dear, J. W. (2012). Identification and proteomic profiling of exosomes in human cerebrospinal fluid. *Journal of Translational Medicine*, 10(1), 5. <https://doi.org/10.1186/1479-5876-10-5>
- Strickland, M., Watanabe, S., Bonn, S. M., Camara, C. M., Starich, M. R., Fushman, D., Carter, C. A., & Tjandra, N. (2022). Tsg101/ESCRT-I recruitment regulated by the dual binding modes of K63-linked diubiquitin. *Structure (London, England: 1993)*, 30(2), 289-299.e6. <https://doi.org/10.1016/j.str.2021.09.006>
- Stuffers, S., Sem Wegner, C., Stenmark, H., & Brech, A. (2009). Multivesicular Endosome Biogenesis in the Absence of ESCRTs. *Traffic*, 10(7), 925–937. <https://doi.org/10.1111/j.1600-0854.2009.00920.x>
- Stupp, R., Mason, W. P., van den Bent, M. J., Weller, M., Fisher, B., Taphoorn, M. J. B., Belanger, K., Brandes, A. A., Marosi, C., Bogdahn, U., Curschmann, J., Janzer, R. C., Ludwin, S. K., Gorlia, T., Allgeier, A., Lacombe, D., Cairncross, J. G., Eisenhauer,

- E., Mirimanoff, R. O., ... National Cancer Institute of Canada Clinical Trials Group. (2005). Radiotherapy plus concomitant and adjuvant temozolomide for glioblastoma. *The New England Journal of Medicine*, 352(10), 987–996. <https://doi.org/10.1056/NEJMoa043330>
- Su, L., Wu, S., Huang, C., Zhuo, X., Chen, J., Jiang, X., Kong, X., Lv, C., Xu, Q., Han, P., Huang, X., & Wong, P.-P. (2023). Chemoresistant fibroblasts dictate neoadjuvant chemotherapeutic response of head and neck cancer via TGF α -EGFR paracrine signaling. *Npj Precision Oncology*, 7(1), 1–17. <https://doi.org/10.1038/s41698-023-00460-2>
- Suades, R., Padró, T., Vilahur, G., & Badimon, L. (2012). Circulating and platelet-derived microparticles in human blood enhance thrombosis on atherosclerotic plaques. *Thrombosis and Haemostasis*, 108(6), 1208–1219. <https://doi.org/10.1160/TH12-07-0486>
- Sullivan, R., Saez, F., Girouard, J., & Frenette, G. (2005). Role of exosomes in sperm maturation during the transit along the male reproductive tract. *Blood Cells, Molecules & Diseases*, 35(1), 1–10. <https://doi.org/10.1016/j.bcmed.2005.03.005>
- Sun, Y., Zheng, W., Guo, Z., Ju, Q., Zhu, L., Gao, J., Zhou, L., Liu, F., Xu, Y., Zhan, Q., Zhou, Z., Sun, W., & Zhao, X. (2016). A novel TP53 pathway influences the HGS-mediated exosome formation in colorectal cancer. *Scientific Reports*, 6, 28083. <https://doi.org/10.1038/srep28083>
- Szaflarski, W., Sujka-Kordowska, P., Pula, B., Jaszczyńska-Nowinka, K., Andrzejewska, M., Zawierucha, P., Dziegiel, P., Nowicki, M., Ivanov, P., & Zabel, M. (2013). Expression profiles of vault components MVP, TEP1 and vPARP and their correlation to other multidrug resistance proteins in ovarian cancer. *International Journal of Oncology*, 43(2), 513–520. <https://doi.org/10.3892/ijo.2013.1975>

- Takizawa, F., Tsuji, S., & Nagasawa, S. (1996). Enhancement of macrophage phagocytosis upon iC3b deposition on apoptotic cells. *FEBS Letters*, *397*(2–3), 269–272.
[https://doi.org/10.1016/s0014-5793\(96\)01197-0](https://doi.org/10.1016/s0014-5793(96)01197-0)
- Tauro, B. J., Greening, D. W., Mathias, R. A., Mathivanan, S., Ji, H., & Simpson, R. J. (2013). Two Distinct Populations of Exosomes Are Released from LIM1863 Colon Carcinoma Cell-derived Organoids *. *Molecular & Cellular Proteomics*, *12*(3), 587–598. <https://doi.org/10.1074/mcp.M112.021303>
- Taylor, R. C., Cullen, S. P., & Martin, S. J. (2008). Apoptosis: Controlled demolition at the cellular level. *Nature Reviews. Molecular Cell Biology*, *9*(3), 231–241.
<https://doi.org/10.1038/nrm2312>
- Tchoryk, A., Taresco, V., Argent, R. H., Ashford, M., Gellert, P. R., Stolnik, S., Grabowska, A., & Garnett, M. C. (2019). Penetration and Uptake of Nanoparticles in 3D Tumor Spheroids. *Bioconjugate Chemistry*, *30*(5), 1371–1384.
<https://doi.org/10.1021/acs.bioconjchem.9b00136>
- Teng, Y., Ren, Y., Hu, X., Mu, J., Samykutty, A., Zhuang, X., Deng, Z., Kumar, A., Zhang, L., Merchant, M. L., Yan, J., Miller, D. M., & Zhang, H.-G. (2017). MVP-mediated exosomal sorting of miR-193a promotes colon cancer progression. *Nature Communications*, *8*(1), Article 1. <https://doi.org/10.1038/ncomms14448>
- Théry, C., Boussac, M., Véron, P., Ricciardi-Castagnoli, P., Raposo, G., Garin, J., & Amigorena, S. (2001). Proteomic Analysis of Dendritic Cell-Derived Exosomes: A Secreted Subcellular Compartment Distinct from Apoptotic Vesicles1. *The Journal of Immunology*, *166*(12), 7309–7318. <https://doi.org/10.4049/jimmunol.166.12.7309>
- Théry, C., Witwer, K. W., Aikawa, E., Alcaraz, M. J., Anderson, J. D., Andriantsitohaina, R., Antoniou, A., Arab, T., Archer, F., Atkin-Smith, G. K., Ayre, D. C., Bach, J.-M., Bachurski, D., Baharvand, H., Balaj, L., Baldacchino, S., Bauer, N. N., Baxter, A. A.,

- Bebawy, M., ... Zuba-Surma, E. K. (2018). Minimal information for studies of extracellular vesicles 2018 (MISEV2018): A position statement of the International Society for Extracellular Vesicles and update of the MISEV2014 guidelines. *Journal of Extracellular Vesicles*, 7(1), 1535750.
<https://doi.org/10.1080/20013078.2018.1535750>
- Théry, C., Zitvogel, L., & Amigorena, S. (2002). Exosomes: Composition, biogenesis and function. *Nature Reviews. Immunology*, 2(8), 569–579. <https://doi.org/10.1038/nri855>
- Trajkovic, K., Hsu, C., Chiantia, S., Rajendran, L., Wenzel, D., Wieland, F., Schwille, P., Brügger, B., & Simons, M. (2008). Ceramide Triggers Budding of Exosome Vesicles into Multivesicular Endosomes. *Science*, 319(5867), 1244–1247.
<https://doi.org/10.1126/science.1153124>
- Trams, E. G., Lauter, C. J., Salem, N., & Heine, U. (1981). Exfoliation of membrane ectoenzymes in the form of micro-vesicles. *Biochimica Et Biophysica Acta*, 645(1), 63–70. [https://doi.org/10.1016/0005-2736\(81\)90512-5](https://doi.org/10.1016/0005-2736(81)90512-5)
- Truman, L. A., Ford, C. A., Pasikowska, M., Pound, J. D., Wilkinson, S. J., Dumitriu, I. E., Melville, L., Melrose, L. A., Ogden, C. A., Nibbs, R., Graham, G., Combadiere, C., & Gregory, C. D. (2008). CX3CL1/fractalkine is released from apoptotic lymphocytes to stimulate macrophage chemotaxis. *Blood*, 112(13), 5026–5036.
<https://doi.org/10.1182/blood-2008-06-162404>
- Usanova, S., Piée-Staffa, A., Sied, U., Thomale, J., Schneider, A., Kaina, B., & Köberle, B. (2010). Cisplatin sensitivity of testis tumour cells is due to deficiency in interstrand-crosslink repair and low ERCC1-XPF expression. *Molecular Cancer*, 9, 248.
<https://doi.org/10.1186/1476-4598-9-248>
- Valadi, H., Ekström, K., Bossios, A., Sjöstrand, M., Lee, J. J., & Lötval, J. O. (2007). Exosome-mediated transfer of mRNAs and microRNAs is a novel mechanism of

- genetic exchange between cells. *Nature Cell Biology*, 9(6), 654–659.
<https://doi.org/10.1038/ncb1596>
- van Balkom, B. W. M., Pisitkun, T., Verhaar, M. C., & Knepper, M. A. (2011). Exosomes and the kidney: Prospects for diagnosis and therapy of renal diseases. *Kidney International*, 80(11), 1138–1145. <https://doi.org/10.1038/ki.2011.292>
- van Niel, G., Raposo, G., Candalh, C., Boussac, M., Hershberg, R., Cerf-Bensussan, N., & Heyman, M. (2001). Intestinal epithelial cells secrete exosome-like vesicles. *Gastroenterology*, 121(2), 337–349. <https://doi.org/10.1053/gast.2001.26263>
- van Zon, A., Mossink, M. H., Schoester, M., Houtsmuller, A. B., Scheffer, G. L., Scheper, R. J., Sonneveld, P., & Wiemer, E. A. C. (2003). The formation of vault-tubes: A dynamic interaction between vaults and vault PARP. *Journal of Cell Science*, 116(Pt 21), 4391–4400. <https://doi.org/10.1242/jcs.00749>
- van Zon, A., Mossink, M. H., Schoester, M., Scheffer, G. L., Scheper, R. J., Sonneveld, P., & Wiemer, E. A. (2001). Multiple human vault RNAs. Expression and association with the vault complex. *The Journal of Biological Chemistry*, 276(40), 37715–37721. <https://doi.org/10.1074/jbc.M106055200>
- Velma, V., Dasari, S. R., & Tchounwou, P. B. (2016). Low Doses of Cisplatin Induce Gene Alterations, Cell Cycle Arrest, and Apoptosis in Human Promyelocytic Leukemia Cells. *Biomarker Insights*, 11, 113–121. <https://doi.org/10.4137/BMI.S39445>
- Vermes, I., Haanen, C., Steffens-Nakken, H., & Reutelingsperger, C. (1995). A novel assay for apoptosis. Flow cytometric detection of phosphatidylserine expression on early apoptotic cells using fluorescein labelled Annexin V. *Journal of Immunological Methods*, 184(1), 39–51. [https://doi.org/10.1016/0022-1759\(95\)00072-i](https://doi.org/10.1016/0022-1759(95)00072-i)
- Vidal, M., Sainte-Marie, J., Philippot, J. R., & Bienvenue, A. (1989). Asymmetric distribution of phospholipids in the membrane of vesicles released during in vitro

maturation of guinea pig reticulocytes: Evidence precluding a role for ‘aminophospholipid translocase’. *Journal of Cellular Physiology*, *140*(3), 455–462.
<https://doi.org/10.1002/jcp.1041400308>

- Villarroya-Beltri, C., Gutiérrez-Vázquez, C., Sánchez-Cabo, F., Pérez-Hernández, D., Vázquez, J., Martín-Cofreces, N., Martínez-Herrera, D. J., Pascual-Montano, A., Mittelbrunn, M., & Sánchez-Madrid, F. (2013). Sumoylated hnRNP A2B1 controls the sorting of miRNAs into exosomes through binding to specific motifs. *Nature Communications*, *4*(1), 2980. <https://doi.org/10.1038/ncomms3980>
- Vinik, Y., Ortega, F. G., Mills, G. B., Lu, Y., Jurkowicz, M., Halperin, S., Aharoni, M., Gutman, M., & Lev, S. (2020). Proteomic analysis of circulating extracellular vesicles identifies potential markers of breast cancer progression, recurrence, and response. *Science Advances*, *6*(40), eaba5714. <https://doi.org/10.1126/sciadv.aba5714>
- Vlaeminck-Guillem, V. (2018). Extracellular Vesicles in Prostate Cancer Carcinogenesis, Diagnosis, and Management. *Frontiers in Oncology*, *8*.
<https://doi.org/10.3389/fonc.2018.00222>
- Walker, M. C., Povey, S., Parrington, J. M., Riddle, P. N., Knuechel, R., & Masters, J. R. (1990). Development and characterization of cisplatin-resistant human testicular and bladder tumour cell lines. *European Journal of Cancer (Oxford, England: 1990)*, *26*(6), 742–747. [https://doi.org/10.1016/0277-5379\(90\)90133-e](https://doi.org/10.1016/0277-5379(90)90133-e)
- Wang, J., Liu, Q., Zhao, Y., Fu, J., & Su, J. (2023). Tumor Cells Transmit Drug Resistance via Cisplatin-Induced Extracellular Vesicles. *International Journal of Molecular Sciences*, *24*(15), Article 15. <https://doi.org/10.3390/ijms241512347>
- Wang, L., Zhao, X., Fu, J., Xu, W., & Yuan, J. (2021). The Role of Tumour Metabolism in Cisplatin Resistance. *Frontiers in Molecular Biosciences*, *8*.
<https://www.frontiersin.org/articles/10.3389/fmolb.2021.691795>

- Wang, W., Wu, M., Wu, D., Wang, L., Li, H., Lin, Z., & Li, J. (2021). Calculating the dose of cisplatin that is actually utilized in hyperthermic intraperitoneal chemotherapy among ovarian cancer patients. *Journal of Ovarian Research*, *14*, 9. <https://doi.org/10.1186/s13048-021-00764-6>
- Wang, W., Xiong, L., Wang, P., Wang, F., & Ma, Q. (2020). Major vault protein plays important roles in viral infection. *Iubmb Life*, *72*(4), 624–631. <https://doi.org/10.1002/iub.2200>
- Webber, J. P., Spary, L. K., Sanders, A. J., Chowdhury, R., Jiang, W. G., Steadman, R., Wymant, J., Jones, A. T., Kynaston, H., Mason, M. D., Tabi, Z., & Clayton, A. (2015). Differentiation of tumour-promoting stromal myofibroblasts by cancer exosomes. *Oncogene*, *34*(3), 290–302. <https://doi.org/10.1038/onc.2013.560>
- Welters, M. J., Fichtinger-Schepman, A. M., Baan, R. A., Flens, M. J., Scheper, R. J., & Braakhuis, B. J. (1998). Role of glutathione, glutathione S-transferases and multidrug resistance-related proteins in cisplatin sensitivity of head and neck cancer cell lines. *British Journal of Cancer*, *77*(4), 556–561. <https://doi.org/10.1038/bjc.1998.90>
- Welters, M. J., Fichtinger-Schepman, A. M., Baan, R. A., Hermsen, M. A., van der Vijgh, W. J., Cloos, J., & Braakhuis, B. J. (1997). Relationship between the parameters cellular differentiation, doubling time and platinum accumulation and cisplatin sensitivity in a panel of head and neck cancer cell lines. *International Journal of Cancer*, *71*(3), 410–415. [https://doi.org/10.1002/\(sici\)1097-0215\(19970502\)71:3<410::aid-ijc18>3.0.co;2-j](https://doi.org/10.1002/(sici)1097-0215(19970502)71:3<410::aid-ijc18>3.0.co;2-j)
- Welton, J. L., Khanna, S., Giles, P. J., Brennan, P., Brewis, I. A., Staffurth, J., Mason, M. D., & Clayton, A. (2010). Proteomics analysis of bladder cancer exosomes. *Molecular & Cellular Proteomics: MCP*, *9*(6), 1324–1338. <https://doi.org/10.1074/mcp.M000063-MCP201>

- Willms, E., Cabañas, C., Mäger, I., Wood, M. J. A., & Vader, P. (2018). Extracellular Vesicle Heterogeneity: Subpopulations, Isolation Techniques, and Diverse Functions in Cancer Progression. *Frontiers in Immunology*, 9, 738.
<https://doi.org/10.3389/fimmu.2018.00738>
- Wojtowicz, K., Januchowski, R., Nowicki, M., & Zabel, M. (2017). vPARP Adjusts MVP Expression in Drug-resistant Cell Lines in Conjunction with MDR Proteins. *Anticancer Research*, 37(6), 3015–3023. <https://doi.org/10.21873/anticancer.11656>
- Woodfield, S. E., Graves, H. K., Hernandez, J. A., & Bergmann, A. (2013). De-regulation of JNK and JAK/STAT signaling in ESCRT-II mutant tissues cooperatively contributes to neoplastic tumorigenesis. *PloS One*, 8(2), e56021.
<https://doi.org/10.1371/journal.pone.0056021>
- Wysoczynski, M., & Ratajczak, M. Z. (2009). Lung cancer secreted microvesicles: Underappreciated modulators of microenvironment in expanding tumors. *International Journal of Cancer*, 125(7), 1595–1603.
<https://doi.org/10.1002/ijc.24479>
- Xavier, C. P. R., Belisario, D. C., Rebelo, R., Assaraf, Y. G., Giovannetti, E., Kopecka, J., & Vasconcelos, M. H. (2022). The role of extracellular vesicles in the transfer of drug resistance competences to cancer cells. *Drug Resistance Updates: Reviews and Commentaries in Antimicrobial and Anticancer Chemotherapy*, 62, 100833.
<https://doi.org/10.1016/j.drug.2022.100833>
- Xavier, C. P. R., Caires, H. R., Barbosa, M. A. G., Bergantim, R., Guimarães, J. E., & Vasconcelos, M. H. (2020). The Role of Extracellular Vesicles in the Hallmarks of Cancer and Drug Resistance. *Cells*, 9(5), Article 5.
<https://doi.org/10.3390/cells9051141>

- Xia, T., Tian, H., Zhang, K., Zhang, S., Chen, W., Shi, S., & You, Y. (2021). Exosomal ERp44 derived from ER-stressed cells strengthens cisplatin resistance of nasopharyngeal carcinoma. *BMC Cancer*, *21*(1), 1003. <https://doi.org/10.1186/s12885-021-08712-9>
- Xiao, Y.-S., Zeng, D., Liang, Y.-K., Wu, Y., Li, M.-F., Qi, Y.-Z., Wei, X.-L., Huang, W.-H., Chen, M., & Zhang, G.-J. (2019). Major vault protein is a direct target of Notch1 signaling and contributes to chemoresistance in triple-negative breast cancer cells. *Cancer Letters*, *440–441*, 156–167. <https://doi.org/10.1016/j.canlet.2018.09.031>
- Xu, R., Greening, D. W., Rai, A., Ji, H., & Simpson, R. J. (2015). Highly-purified exosomes and shed microvesicles isolated from the human colon cancer cell line LIM1863 by sequential centrifugal ultrafiltration are biochemically and functionally distinct. *Methods (San Diego, Calif.)*, *87*, 11–25. <https://doi.org/10.1016/j.ymeth.2015.04.008>
- Yadav, K., Yadav, A., Vashistha, P., Pandey, V. P., & Dwivedi, U. N. (2019). Protein Misfolding Diseases and Therapeutic Approaches. *Current Protein & Peptide Science*, *20*(12), 1226–1245. <https://doi.org/10.2174/1389203720666190610092840>
- Yamano, Y., Uzawa, K., Saito, K., Nakashima, D., Kasamatsu, A., Koike, H., Kouzu, Y., Shinozuka, K., Nakatani, K., Negoro, K., Fujita, S., & Tanzawa, H. (2010). Identification of cisplatin-resistance related genes in head and neck squamous cell carcinoma. *International Journal of Cancer*, *126*(2), 437–449. <https://doi.org/10.1002/ijc.24704>
- Yamasaki, M., Makino, T., Masuzawa, T., Kurokawa, Y., Miyata, H., Takiguchi, S., Nakajima, K., Fujiwara, Y., Matsuura, N., Mori, M., & Doki, Y. (2011). Role of multidrug resistance protein 2 (MRP2) in chemoresistance and clinical outcome in oesophageal squamous cell carcinoma. *British Journal of Cancer*, *104*(4), 707–713. <https://doi.org/10.1038/sj.bjc.6606071>

- Yang, Z., Liao, J., Carter-Cooper, B. A., Lapidus, R. G., Cullen, K. J., & Dan, H. (2019). Regulation of cisplatin-resistant head and neck squamous cell carcinoma by the SRC/ETS-1 signaling pathway. *BMC Cancer*, *19*(1), 485. <https://doi.org/10.1186/s12885-019-5664-7>
- Yellon, D. M., & Davidson, S. M. (2014). Exosomes. *Circulation Research*, *114*(2), 325–332. <https://doi.org/10.1161/CIRCRESAHA.113.300636>
- Yeudall, W. A., Torrance, L. K., Elsegood, K. A., Speight, P., Scully, C., & Prime, S. S. (1993). Ras Gene point mutation is a rare event in premalignant tissues and malignant cells and tissues from oral mucosal lesions. *European Journal of Cancer Part B: Oral Oncology*, *29*(1), 63–67. [https://doi.org/10.1016/0964-1955\(93\)90012-4](https://doi.org/10.1016/0964-1955(93)90012-4)
- Yin, J., Yan, X., Yao, X., Zhang, Y., Shan, Y., Mao, N., Yang, Y., & Pan, L. (2012). Secretion of annexin A3 from ovarian cancer cells and its association with platinum resistance in ovarian cancer patients. *Journal of Cellular and Molecular Medicine*, *16*(2), 337–348. <https://doi.org/10.1111/j.1582-4934.2011.01316.x>
- Yoon, S. S., Ahn, K. S., Kim, S. H., Shim, Y. M., & Kim, J. (2001). In vitro establishment of cis-diammine-dichloroplatinum(II) resistant lung cancer cell line and modulation of apoptotic gene expression as a mechanism of resistant phenotype. *Lung Cancer (Amsterdam, Netherlands)*, *33*(2–3), 221–228. [https://doi.org/10.1016/s0169-5002\(01\)00205-7](https://doi.org/10.1016/s0169-5002(01)00205-7)
- Yoshida, K., Yamaguchi, T., Natsume, T., Kufe, D., & Miki, Y. (2005). JNK phosphorylation of 14-3-3 proteins regulates nuclear targeting of c-Abl in the apoptotic response to DNA damage. *Nature Cell Biology*, *7*(3), 278–285. <https://doi.org/10.1038/ncb1228>
- Yoshioka, Y., Konishi, Y., Kosaka, N., Katsuda, T., Kato, T., & Ochiya, T. (2013). Comparative marker analysis of extracellular vesicles in different human cancer

types. *Journal of Extracellular Vesicles*, 2, 10.3402/jev.v2i0.20424.

<https://doi.org/10.3402/jev.v2i0.20424>

Yuan, L., Zhao, N., Wang, J., Liu, Y., Meng, L., Guo, S., Wiemer, E. A. C., Chen, Q., Mao, Y., Ben, J., & Ma, J. (2021). Major vault protein (MVP) negatively regulates osteoclastogenesis via calcineurin-NFATc1 pathway inhibition. *Theranostics*, 11(15), 7247–7261. <https://doi.org/10.7150/thno.58468>

Zhang, B., Liu, M., Tang, H., Ma, H., Wang, C., Chen, X., & Huang, H. (2012). The expression and significance of MRP1, LRP, TOPOII β , and BCL2 in tongue squamous cell carcinoma. *Journal of Oral Pathology & Medicine: Official Publication of the International Association of Oral Pathologists and the American Academy of Oral Pathology*, 41(2), 141–148. <https://doi.org/10.1111/j.1600-0714.2011.01066.x>

Zhang, H., Freitas, D., Kim, H. S., Fabijanic, K., Li, Z., Chen, H., Mark, M. T., Molina, H., Martin, A. B., Bojmar, L., Fang, J., Rampersaud, S., Hoshino, A., Matei, I., Kenific, C. M., Nakajima, M., Mutvei, A. P., Sansone, P., Buehring, W., ... Lyden, D. (2018). Identification of distinct nanoparticles and subsets of extracellular vesicles by asymmetric-flow field-flow fractionation. *Nature Cell Biology*, 20(3), 332–343. <https://doi.org/10.1038/s41556-018-0040-4>

Zhang, J., Ye, Z., Tew, K. D., & Townsend, D. M. (2021). Cisplatin chemotherapy and renal function. *Advances in Cancer Research*, 152, 305–327. <https://doi.org/10.1016/bs.acr.2021.03.008>

Zhang, Q., Jeppesen, D. K., Higginbotham, J. N., Graves-Deal, R., Trinh, V. Q., Ramirez, M. A., Sohn, Y., Neining, A. C., Taneja, N., McKinley, E. T., Niitsu, H., Cao, Z., Evans, R., Glass, S. E., Ray, K. C., Fissell, W. H., Hill, S., Rose, K. L., Huh, W. J., ... Coffey, R. J. (2021). Supermeres are functional extracellular nanoparticles replete

- with disease biomarkers and therapeutic targets. *Nature Cell Biology*, 23(12), Article 12. <https://doi.org/10.1038/s41556-021-00805-8>
- Zhang, Y., Liu, Y., Liu, H., & Tang, W. H. (2019). Exosomes: Biogenesis, biologic function and clinical potential. *Cell & Bioscience*, 9(1), 19. <https://doi.org/10.1186/s13578-019-0282-2>
- Zhao, S., Mi, Y., Zheng, B., Wei, P., Gu, Y., Zhang, Z., Xu, Y., Cai, S., Li, X., & Li, D. (2022). Highly-metastatic colorectal cancer cell released miR-181a-5p-rich extracellular vesicles promote liver metastasis by activating hepatic stellate cells and remodelling the tumour microenvironment. *Journal of Extracellular Vesicles*, 11(1), e12186. <https://doi.org/10.1002/jev2.12186>
- Zheng, C.-L., Sumizawa, T., Che, X.-F., Tsuyama, S., Furukawa, T., Haraguchi, M., Gao, H., Gotanda, T., Jueng, H.-C., Murata, F., & Akiyama, S. (2004). Characterization of MVP and VPARP assembly into vault ribonucleoprotein complexes. *Biochemical and Biophysical Research Communications*, 326(1), 100–107. <https://doi.org/10.1016/j.bbrc.2004.11.006>
- Zheng, X., Chen, F., Zhang, J., Zhang, Q., & Lin, J. (2014). Exosome analysis: A promising biomarker system with special attention to saliva. *The Journal of Membrane Biology*, 247(11), 1129–1136. <https://doi.org/10.1007/s00232-014-9717-1>
- Zhu, G., Gilchrist, R., Borley, N., Chng, H. W., Morgan, M., Marshall, J. F., Camplejohn, R. S., Muir, G. H., & Hart, I. R. (2004). Reduction of TSG101 protein has a negative impact on tumor cell growth. *International Journal of Cancer*, 109(4), 541–547. <https://doi.org/10.1002/ijc.20014>
- Zhu, H., Luo, H., Zhang, W., Shen, Z., Hu, X., & Zhu, X. (2016). Molecular mechanisms of cisplatin resistance in cervical cancer. *Drug Design, Development and Therapy*, 10, 1885–1895. <https://doi.org/10.2147/DDDT.S106412>

- Zisowsky, J., Koegel, S., Leyers, S., Devarakonda, K., Kassack, M. U., Osmak, M., & Jaehde, U. (2007). Relevance of drug uptake and efflux for cisplatin sensitivity of tumor cells. *Biochemical Pharmacology*, *73*(2), 298–307.
<https://doi.org/10.1016/j.bcp.2006.10.003>
- Zomer, A., Maynard, C., Verweij, F. J., Kamermans, A., Schäfer, R., Beerling, E., Schiffelers, R. M., de Wit, E., Berenguer, J., Ellenbroek, S. I. J., Wurdinger, T., Pegtel, D. M., & van Rheenen, J. (2015). In Vivo imaging reveals extracellular vesicle-mediated phenocopying of metastatic behavior. *Cell*, *161*(5), 1046–1057.
<https://doi.org/10.1016/j.cell.2015.04.042>
- Züllig, S., Neukomm, L. J., Jovanovic, M., Charette, S. J., Lyssenko, N. N., Halleck, M. S., Reutelingsperger, C. P. M., Schlegel, R. A., & Hengartner, M. O. (2007). Aminophospholipid Translocase TAT-1 Promotes Phosphatidylserine Exposure during *C. elegans* Apoptosis. *Current Biology*, *17*(11), 994–999.
<https://doi.org/10.1016/j.cub.2007.05.024>
- zur Hausen, H., & de Villiers, E. M. (1994). Human papillomaviruses. *Annual Review of Microbiology*, *48*, 427–447. <https://doi.org/10.1146/annurev.mi.48.100194.002235>